HBRC Journal

Volume 3, Number 3, December 2007
ISSN: 1687-4048
DEP: 12479/2004

Contents

Technical Note

87 El-Tahrir St. Dokki 11511 P.O.BOX 1770 Cairo, EGYPT
Phone: 00202-37617062 Fax.: 00202-33367179
www.hbrc.edu.eg, journal@hbrc.edu.eg

Vol. 3 No. 3
December 2007
ISSN: 1687-4048
DEP: 12479/2004

HBRC Journal Vol. 3 No. 3 December 2007 ISSN: 1687-4048 DEP: 12479/2004

HBRC Journal

Housing & Building National Research Center

IMPROVING PLASTIC SHRINKAGE CRACKING OF CONCRETE USING RECYCLED WASTE RUBBER CRUMBS

Amany G. Botros Micheal
Lecturer, Structural Engineering Dept., Faculty of Engineering, Tanta University, EGYPT
Email: AG_Botros@yahoo.com

ABSTRACT

The objective of this study is to investigate a new technique to control plastic cracks due to concrete shrinkage by replacing a percentage of sand with fine crumbs of waste tires. This technique utilizes a waste material to achieve crack control, which subsequently improves concrete durability. Recycling used tires is another advantage, since they represent one of the most harmful waste materials causing a lot of pollution when recycled in an improper way. An experimental program is designed to study the effect of rubber-sand replacement ratio (R-SR) on plastic shrinkage of concrete. A total number of 20 specimens with different (R-SR) percentages are tested under different environmental conditions. Specimens are divided into four groups of five specimens each. Three percentages of (R-SR) of 3%, 5% and 7% by weight are used for the first three groups and the fourth one is the control group with no replacement. The five specimens within each group are subjected to five different environmental conditions, which are: indoor condition, outdoor environment, wind effect, hot temperature and curing by covering with plastic sheets. The study includes measurements of the first cracking time, crack width, percentage of cracking area and rate of evaporation. The results are compared with the previous results available in literature using other types of additives. Other 15.8-x15.8x15.8 cm cube specimens are tested to investigate the effect of rubber crumbs on concrete strength. Also, 15x30 cm cylinders are used to draw the stress-strain curve for all (R-SR) percentages and normal concrete.

Key Words: Plastic Shrinkage, Rubber Recycling, Additives, Hot Weather Concrete

INRTODUCTION

Plastic shrinkage cracking is the phenomenon within which random pattern of cracks are developed while concrete is still in its plastic state. It occurs within the first few hours after concrete has been placed. They may be observed after 4 to 6 hours of placing. Cracking occurs when the rate of evaporation of moisture from the surface exceeds the rate of moisturing it and due to the edge restrainment in concrete forms. They may grow parallel or in random distribution. They also extend and widen during drying shrinkage, which means a major loss in concrete durability. These cracks affect not only the concrete appearance but they also affect the physical properties of concrete. Mix proportions, additives, constituent's properties and weather conditions including high temperature, relative humidity, wind velocity all affect surface shrinkage.

REVIEW OF PLASTIC SHRINKAGE CRACKING STUDIES

Review on previous researches on controlling plastic shrinkage shows that increasing cement content leads to increase in plastic shrinkage of concrete while mixtures with high water content may suffer other causes of cracks as plastic settlement of aggregates. On the other hand, containing high dose of fine materials as silica fume may increase cracking due to lower bleeding potential. The ACI Committee 305 suggests a threshold of rate of evaporation of 1 kg / m2 / hr for the plastic shrinkage to occur [8-9]. Almusallam, Maslehuddin, Abdul-Waris & Khan

[4] studied the effect of mix proportions on the plastic shrinkage of concrete in hot weather. They showed that plastic shrinkage cracking occurs at lower rate of evaporation than the value proposed by ACI. They stated that the critical rate of evaporation varies from 0.2 to 0.7 kg / m2 /hr according to mixtures proportions. They also concluded that the stiff mixes result in earlier cracking than plastic ones, while the crack intensity is higher in high water content mixtures. Samman, Mizra, & Wafa [6] studied the plastic shrinkage cracking of both normal and high strength concrete under different weather conditions. They proved that both types of concrete behave differently concerning plastic shrinkage due to the different water cement ratios (W/C) and the existence of silica fume in the high strength mixes. The latter permits little water bleeding which initiates cracking. Also, for high strength concrete, cracking occurs at rates of evaporation less than 1kg / m2 / hr. They proved that wind blowing on concrete surface is the most severe condition and leads to early cracking and high cracking intensity.
Ma, Tan & Wu [1] studied the effect of adding polypropylene fibers with different geometry on plastic shrinkage cracking of cement mortar. They prove that the finer the fibers, the greater the reduction in the weighted crack values for the same fiber content. On the other hand, Branch, Rowling, Hannant & Mulheron [2] studied also the effect of polypropylene fibers on the plastic shrinkage of high strength concrete. They showed that fibers do not affect crack initiation but they can reduce cracking area up to 85% with 0.1% volume content.

CONCRETE INCORPORATING RUBBER

The rapid increase in the amount of scrap tires produced every year makes the development of a safer way to recycle tires an urgent need. For over 40 years the scrap tires have been used as an asphalt paving material. Serumgrad [10] demonstrated a technique of recycling waste rubber tires after they are prereacted with hot liquid asphalt cement for a specified period of time. The reacted mix can be used as a crack sealant in rehabilitation of the cracked pavement. In the past couple of years wide investigations have taken place to mobilize waste rubber crumbs in structural concrete. The researches cover compressive strength, splitting tension and flexural strength. Different techniques of replacing fine aggregate and coarse aggregate with waste rubber according to the size of the crumbs were presented. Reduction in concrete strength was observed while improvements in concrete ductility and flexibility were also observed. Researchers as Li, Li & Li [5] used particles of waste tire coated with cement paste to control reduction in strength and to have the advantage of high ductility. They used rubberized concrete to isolate a structural base, which can shift the fundamental frequency of the structure to a lower value.
Other attempt to improve cement mortar resistance to chemical attack was made by El-Sherbiny [3]. In this research sand was replaced by fine rubber crumbs with 3%, 7% and 10% by weight and 7x7x7 cm mortar cubes were tested against the attack of both hydrochloric and sulpheric acids. Soaked specimens in both sulpheric acid and hydrochloric acid showed increase in mortar resistance to acids attack for specimens, which contain rubber crumbs compared to specimens with no rubber. The results showed that best results were obtained using 7 % specimens.

RESEARCH PLAN

In this research crumbs of scrub tires were used as concrete additives to improve plastic shrinkage. Rubber was utilized as sand replacement with percentages 3%, 5% and 7% by weight. Concrete specimens were slabs of dimensions 300x 300 x 30 mm with span to depth ratio of 1/10. Other cube specimens were used to determine the 28 days concrete strength. Cylinders were also used to plot stress-strain curve of concrete. For each rubber percentage, five slabs were placed and subjected to different environmental conditions. These conditions were indoor condition, out-door condition, wind effect, high temperature and partial curing by covering with polyethylene sheets. Table (1) shows specimens coding according to their environmental condition. Five control specimens with no sand-rubber replacement were also placed and subjected to the same environmental conditions for comparison. Normal Portland cement type I was used for all specimens. Cement content was 350 kg / m^3 and W/C was maintained constant with value 0.48 for all specimens.

Table 1: Specimens Coding

Specimen Code	Description
ID	Indoor condition
OD	Outdoor condition
ODW	Outdoor with wind effect
IDH	Indoor and thermal effect
PCR	Partial Curing

Coarse aggregate was gravel with maximum nominal size of 9.5mm to fulfill the specifications of being 1/3 concrete slab thickness. Coarse aggregate with maximum nominal size of 19 mm was used for cube and cylinder specimens. Coarse aggregate, sand and rubber sieve analyses are given in Figure (1). Aggregate specific weight was 2.55 and its percentage of absorption was 0.5 %. The mixture proportions are given in Table (2).

Table 2: Mixture Proportions

Mixture	Cement kg/m^3	W/C	Gravel kg/m^3	Sand kg/m^3	Rubber kg/m^3
Control	350	0.48	1392	696	0.0
3% RS-R	350	0.48	1392	675	20.88
5% RS-R	350	0.48	1392	661	34.8
7% RS-R	350	0.48	1392	647	48.72

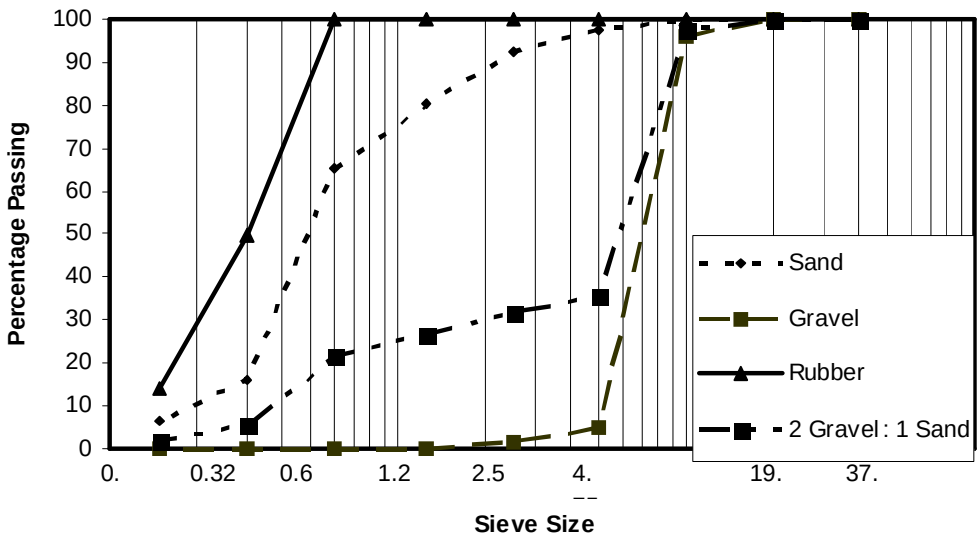

Fig. 1: Coarse and Fine Aggregate Grading

The moulds were of 18mm-ply wood and lined with aluminum foil to prevent any water absorption by moulds, which may affect readings. The indoor condition (ID) was at temperature of 25^{o}C and humidity of 55±5%. Compaction was performed using a vibrating table and the surface was finished and trawled to produce smooth surface. The outdoor condition (OD) was achieved by placing the specimens in the outdoor climate where temperature and humidity changed naturally. The wind effect (ODW) was applied using two electric fans at speed of 10m/sec and the specimens were not subjected to sunlight. High temperature specimens surfaces (IDT) were kept under constant temperature of 50^{o}C using electrical coil. This thermal

load resembles the environmental condition in the Middle East in summer months when temperature may reach high value of 55°C. The high temperature specimens were not subjected to other accompanied factors of wind or humidity.
The partially cured specimens (PCR) were kept outdoor and covered with polyethylene sheets to avoid moisture loss. All specimens were exposed to these environmental conditions for a period of four hours. The specimen's weights were recorded directly after placing and at the end of exposure to determine rate of evaporation. The specimens were checked every 10 to15 minutes to determine first cracking time. Measurements included rate of evaporation at the end of exposure, first cracking time, percentage of cracked area.
Moulds were removed after 24 hours and the specimens were kept indoor. Cracks were marked and their total length was measured using a flexible wire to account for curved and irregular shapes. Average width was measured after 24 hours of placing using an optical tool with accuracy .02 mm. Cubes and cylinders specimens were totally cured by immersing in water for 28 days and then tested in compression to determine cube strength and to plot the stress-strain curve.

RESULTS

Environmental Effect on Normal Concrete

Concrete in its plastic state is greatly affected by the environmental conditions which include many elements. Weather variables such as temperature, humidity, wind velocity have significant effect on concrete plastic shrinkage and consequently concrete durability. For the conditions investigated in this experimental program, both wind and high temperature prove to be the most severe conditions on concrete even if they do not occur simultaneously. The out door condition comes after them as the most harmful effect. For normal concrete panels with stiff mixes and no rubber content, the percentages of cracked area are shown in Figure (2).
ODW percentage of cracking area is about 0.0178 and for OD is about 0.0111. If such concrete slabs are subjected to both sunrays and wind effect the percentage of cracking is expected to

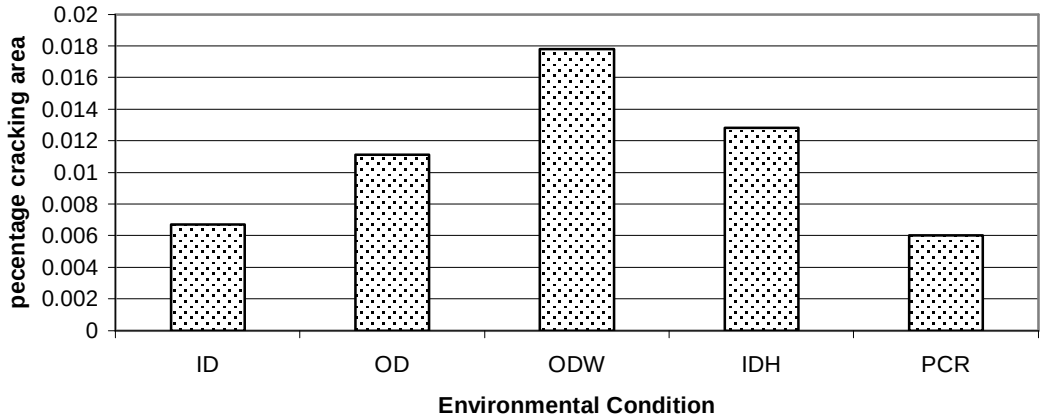

Fig. 2 : Percentage Cracking Area for Normal concrete

increase considerably. On the other hand, the percentage of cracking area after 24 hours of placing for IDH panel is 0.0128 %. In fact, the high value of percentage of cracked area for the panels under thermal load can be attributed to the tensile stresses generated during cooling down which exceeds the concrete tensile strength at this early age. The ID panel percentage cracking area is 0.0067%.
First cracking time for normal concrete is shown in Figure (3). The weather condition affects the results. Where concrete panel ODW cracks after 90 minutes, panel in open air takes 80 minutes to crack. The indoor normal concrete panel cracks appear after 105 minutes. Cracks due to high rate of evaporation resulting from high temperature in a relatively confined domain are observed later compared to the panels subjected to wind. The first cracking time for panels under thermal load is 120 minutes This observation confirms the fact that accompanying wind with high

temperature is the real problem to fresh concrete. The cured panels show no cracking during the observation period of four hours.

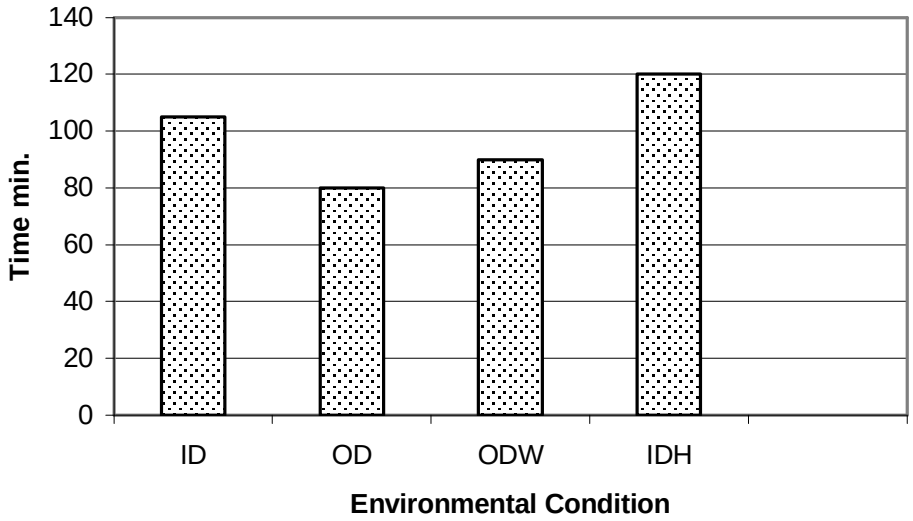

Fig. 3 : First Cracking Time Comparison for Normal Concrete

Results of Mixes with Rubber Additives

Unit Weight and Strength Comparison

Concrete unit weight comparison for all rubber percentages with normal concrete shows that a loss in concrete unit weight of 1.6% for 3% rubber replacement and 2.24% for 5% specimens and 4.54% for 7% specimens. The 28 days cube compressive strength is shown in Figure (4).

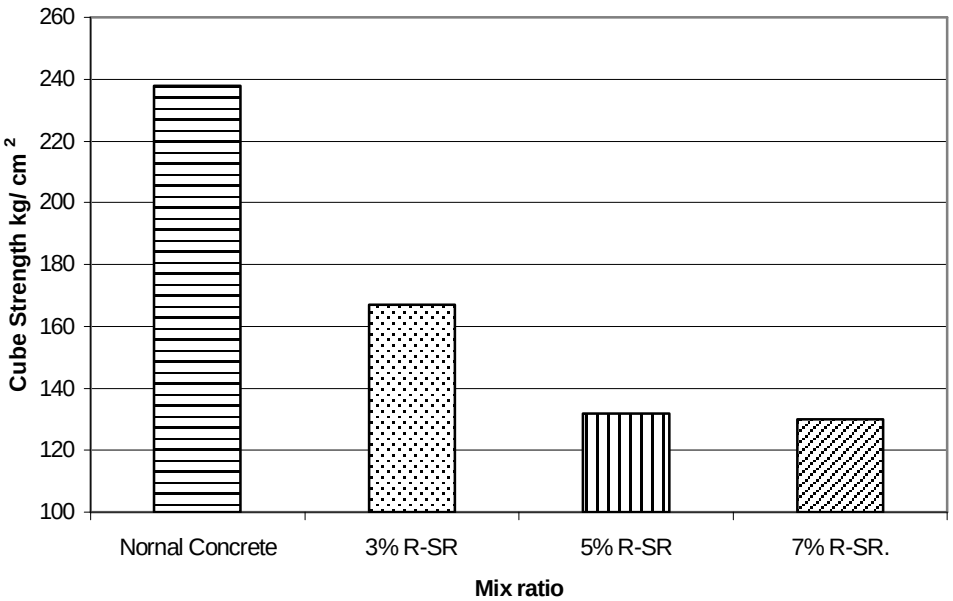

Fig. 4 : The 28 Days Compressive Strength Comparison

The results show 29% reduction in 28 days strength for 3% specimens and 44.5% reduction in strength for 5% replacement and 45.4% for 7% sand replacement with rubber. These results conform with the results published by other researchers [3] and [5]. The stress-strain curves for mixtures with different rubber percentages compared with the normal concrete curve are shown in Figure (5),

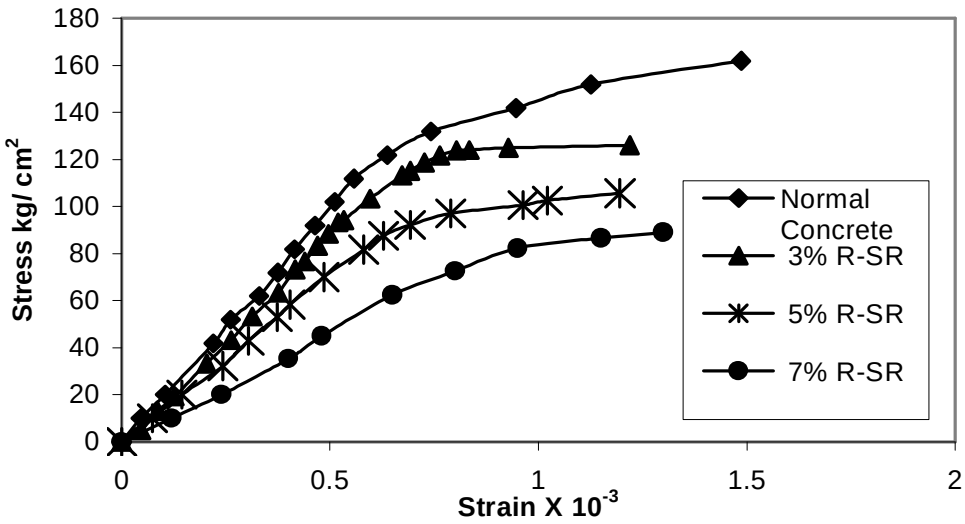

Fig. 5 : Stress Strain Curve for Concrete with Different R-SR

where the increase in concrete ductility is not quite obvious but reduction in elastic stiffness modulus is clear.

Rate of Evaporation

Rates of evaporation for all specimens are shown in Figure (6). It is clear that the maximum rate of evaporation occurs for specimens subjected to high temperature and the minimum rate of evaporation is for the partially cured specimens. For all environmental effects, the rate of evaporation is less than the threshold value of the ACI of 1 kg/m^2/hr and still cracks occur under different weather conditions.

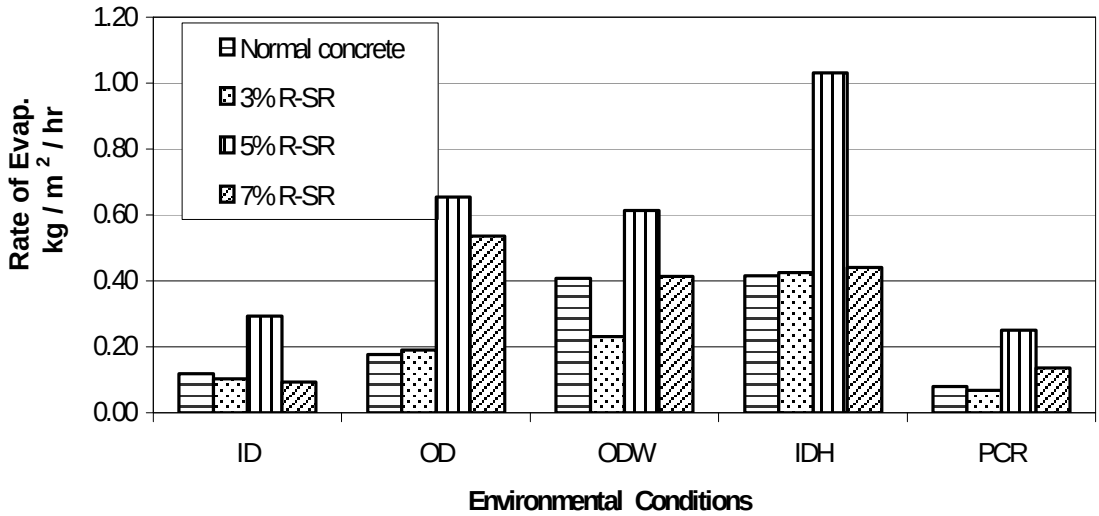

Fig. 6 : Rate of Evaporation Comparison

The rubber additive does not improve much the rate of evaporation since this additive cannot be considered very fine particles, which prevent water capillary rise as the other pozzolanic additives as silica fume. The rubber grading shown in Figure (1) shows that most of the shredded tire particles are of size 15 micron and this size is controlled by the commercial supply.

First Cracking Time

Figure (7) shows the first cracking time for all specimens. It is clear that wind effect is the case in which cracks appear faster. Under outdoor conditions, panel with no rubber additives cracks at time of 80 minutes and panels with 3%, 5% and 7% rubber crack after 120, 130, 135 minutes

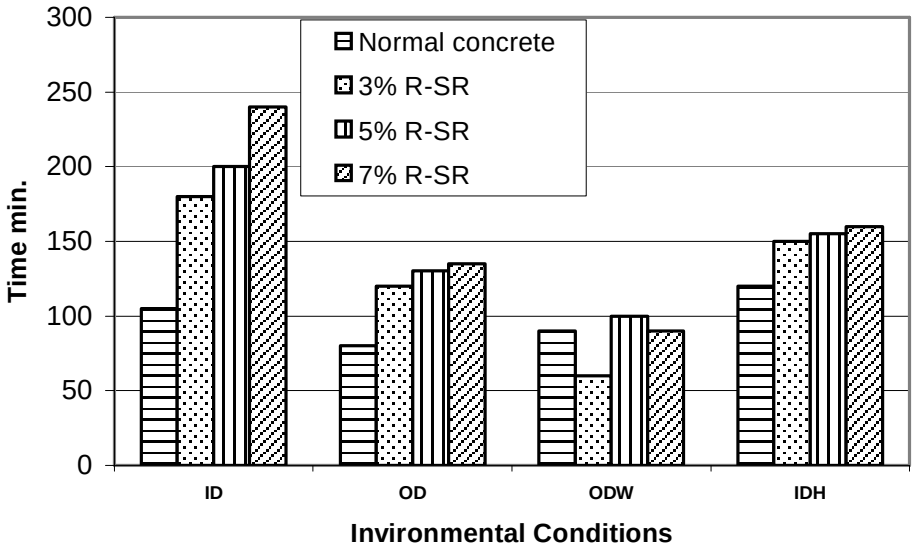

Fig. 7: First Cracking Time Comparison

respectively. The delay in cracking is clear. This observation is typical for all the environmental conditions except ODW.
First cracking time of ODW specimen is 90 minutes for normal concrete, 60 minutes for concrete with 3% sand replacement, 100 minutes for 5% specimens and 90 minutes for the 7% specimens. For partially cured specimens, no cracks are observed during the four hours of exposure. The first cracking time of these specimens is not plotted. The first cracking time of specimens which contain rubber additives and are subjected to thermal load, increases from 120 minutes for normal concrete to 150, 155, 160 minutes for 3%, 5% and 7% R-SR respectively. Cracks were too narrow and were hard to detect even after 24 hours of placing. This observation can be explained as high temperature is not -by itself- a severe condition for rubberized concrete if it is not accompanied by wind velocity. This observation meets with the hot weather concrete behavior found in literature.

Percentage of Cracking Area

The cracks are randomly oriented and their widths range from .2mm to .4 mm and lengths range from 5mm to 20mm. As the percentage of rubber- sand replacement increases, the cracks are less to form and harder to detect. For specimens with 7% rubber, cracks are hard to detect even after 24 hours of placing. Figure (8) shows a plot of cracking area as percentage of the total area of specimens. The percentage of cracking area for OD specimens are 0.0192%, 0.01211%, 0.0056% and 0.00378% for normal concrete, 3% R-SR, 5% R-SR and 7% R-SR respectively. The reduction in the percentage of cracking area is distinguished. The case of thermal condition shows this phenomenon as can not be clearer. The previously mentioned ratios for high temperature panels are .0125%, .06%, .004% and 0.002% in the same respect.

The improvement in concrete flexibility depicted in Figure (5) presents an explanation. It can be concluded that under same stress level concrete incorporated rubber crumbs exhibit more deformations than normal concrete. This phenomenon leads to more flexible behavior and subsequently less plastic cracking. The reduction in percentage of cracking area may also be attributed to the fact that the recycled rubber acts as an inclusion that arrest micro cracks and bridge across the cracks to restrain their widening [7].

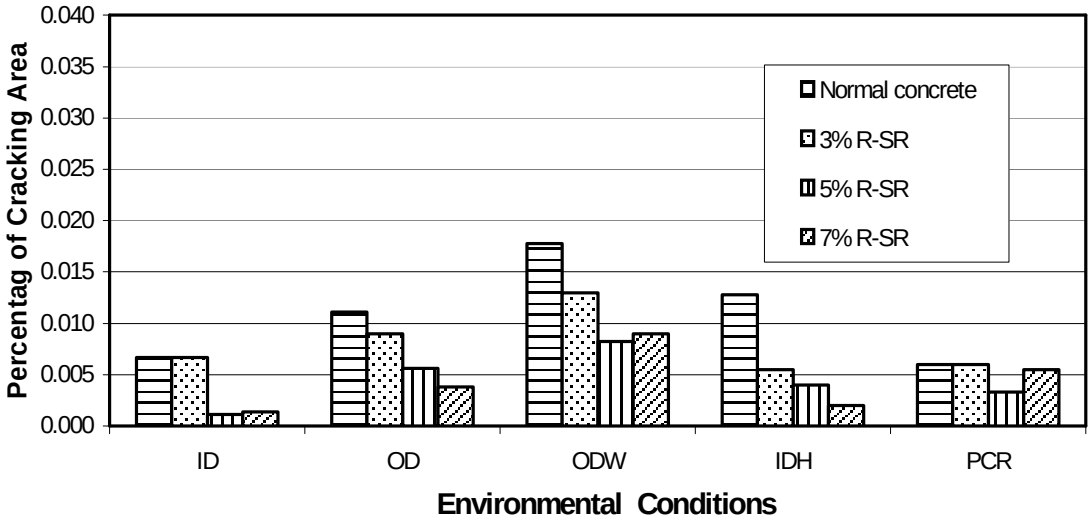

Fig. 8 : Percentage of Cracking Area

CONCLUSION

In this research the waste rubber tires are utilized in controlling concrete plastic cracking. The experimental program reveals that, under different weather conditions , including high temperature, and when using rubber crumbs as additive, we can get a significant delay in cracking. Also the percentage of cracking area decreases considerably. This is attributed to the increase in concrete flexibility characterizing concrete with rubber additives. The rate of evaporation differs slightly for rubberized concrete since the additive refinement is not enough to decrease capillary rise and it is controlled by the available commercial size. The loss in concrete strength may not be of great significance if this concrete is used in structures where delaying and reducing cracking are the major priorities such as concrete pavements, flooring, canal lining and other applications. Concrete which contains rubber crumbs, shows good plastic behavior under all weather conditions which nominates it as a suitable construction material for hot weather.

REFERENCES

1-Ma, Y., Tan, M. & Wu, K. (2002). Effect of different geometric polypropylene fibers on plastic shrinkage cracking of cement mortars, Materials and Structures 35 : 165-169.

2-Branch, J., Rawling, A., Hannant, D.J. & Mulheron, M. (2002). The effects of fibers on the plastic shrinkage cracking of high strength concrete, Materials and Structures 35 : 189-194.

3-El-Sherbiny, Sh. A. (2000). Chemical resistance of mortar containing waste rubber crumbs. M. Sc. Thesis, Faculty of Engineering, Cairo University.

4-Almusallam, A.A., Maslehuddin, M., Abdul-Waris, M. & Khan, M.M. (1998). Effect of mix properties on plastic shrinkage cracking of concrete in hot environment. Construction and Building Materials 12 : 353-358.

5-Li, Z., Li, F. & Li, J. S. L. (1998). Properties of concrete incorporating rubber tire particles Magazine of Concrete Research 50 : 297-304.

6-Samman, T.A., Mizra, W. H. & Wafa, F. F.(1996). Plastic shrinkage cracking of normal and high-strength concrete: A comparative study. ACI Material Journal : 36-40.
7-Soroushian, P., Eldarwish, A.I., Tlili, A. & Ostowari, K. (1999). Experimental investigation of the optimized use of plastic flakes in normal-weight concrete. Magazine of Concrete Research 51 : pp 27-33.
8- Carlson, M. , (2001). Hot weather concreting : problems & solutions. *Civil Engineering Dept. Iowa State University* :pp1-7.
9-ACI 305 (1989). *Hot Weather Concreting.*
10-Serumgrad, J.R. (1997). Municipal Solid Wastes: Problems and Solution . CRC Press : 127-132.

A STUDY ON THE PERFORMANCE OF LIGHTWEIGHT SELF-CONSOLIDATED CONCRETE

Dr. Gamal Elsayed Abdelaziz
Associate Professor, Faculty of Engineering in Shoubra, Banha University, Egypt
E-mail: abdelazizge@yahoo.co.uk

ABSTRACT

This paper presents a study on the fresh and hardened characteristics of lightweight aggregate concrete incorporating self-consolidated agent (LWSCC). Self-consolidated agent (a polycarboxylic-based superplasticizer in combination with a viscosity modifying admixture) and local-produced lightweight aggregate (LWA) produced from expanded clay type were utilized. Various LWSCC mixes made with different mix proportions, namely dosage of self-consolidated agent, water/cement ratio, LWA/Sand ratio and normal weight aggregate as a partial replacement of LWA, were prepared. The initial slump flow, rate of slump flow loss and air content were then performed to assess the fresh properties of LWSCC. Twenty-eight day compressive strength, ultrasonic pulse velocity, porosity and density were determined for investigating the hardened properties of LWSCC. The results reveal that, by using local-produced materials, it is possible to manufacture a structural lightweight aggregate concrete with low density and high self-consolidating characteristics (flowability, deformability and stability). Both fresh and hardened characteristics of LWSCC are mainly controlled by dosage of self-consolidated agent (SCA), where the flowability, self-compactability, strength, homogeneity and porosity of LWSCC can be enhanced with increasing SCA content up to certain dosage of SCA (≈0.80), at which all these characteristics would start to decline with increasing SCA content. However, LWSCC losses its fresh parameters rapidly with increasing the dosage of SCA and lightweight aggregate/sand ratio. The results also showed that the compressive strength, homogeneity and porosity of LWSCC could be significantly improved with reducing the ratio of w/c and LWA/Sand ratio, and utilizing normal weight aggregate in LWSCC mixes.

Keywords: Self-consolidated, Aggregate, Lightweight concrete, Admixtures.

INTRODUCTION

Lightweight aggregate concrete (LWAC) with closed structure has been used successfully for structural purposes since the late nineteenth century. The density of structural LWAC typically ranges from 1400 to 2000 kg/m^3 [1-2]. Lightweight aggregate concrete has obvious advantages of a higher strength/weight ratio, better strain capacity, lower coefficient of thermal expansion, and superior heat and sound insulation characteristics due to air voids existed in lightweight aggregate (LWA) [1-3]. Furthermore, Topcu [3] reported that the reduction in the dead weight of a building by the use of lightweight concrete could lead to a considerable decrease in the cross section of steel reinforced columns, beams, plates and foundation. It is also possible to reduce steel reinforcement and increase cost savings. LWAC may be produced by using either natural lightweight aggregates such as pumice, scoria, volcanic cinders, tuff and diatomite, or by using artificial lightweight aggregates, which can be produced by heating clay, shale, slate, diatomaceous shale, perlite, obsidian, and vermiculite. Industrial cinders and blast-furnace slag that has been specially cooled can also be used [1-4].

Despite of the above-mentioned advantageous and the increase demand of LWAC worldwide, there are still many difficulties facing such type of industry, which requires more efforts to be

tackled out. These difficulties mainly include segregation of coarse aggregate and compressive strength are not as great as ordinary concrete [5-6]. In practice, as lightweight aggregates often have lower particle densities than the density of the mortar matrix in concrete, upward segregation of the coarse aggregates may be sometimes experienced when the workability of the fresh concrete is not appropriate. This is in contrast to normal-weight aggregate concrete, in which coarse aggregate may sink to the bottom if the workability is not appropriate.

Chia and Zhang [5] studied the effect of a superplasticizer on the rheological behavior of fresh lightweight aggregate concrete and the stability of the concrete under vibration. Their results indicated that an increase in superplasticizer content in the concrete reduced the yield stress, but did not have a significant effect on the plastic viscosity. They also showed that the segregation resistance of LWAC was decreased with increasing the dosage of superplasticizer in LWAC mixes. Therefore, incorporating of water-reducing/high-range water reducing admixtures in such type of concrete (LWAC) requires a great attention, to attain all beneficial effects out of using these admixtures. Otherwise, an excessive segregation to concrete ingredients might take place.

One of the most advanced generations of water-reducing admixtures is self-consolidating admixture, also known as a self-compacting admixture. Admixing this type of admixture with viscosity modifying agent, occasionally, in concrete mixes could lead to producing a special concrete with high-fluidity, self-compactability and minimum water dilution and segregation, which nowadays known as self-compacting concrete or self-consolidating concrete (SCC) [6,7,8]. The Japanese developed this type of concrete in the early 1990s and it is now widely used in congested and non-congested members, complex formwork, deep sections and restricted areas [9-10].

RESEARCH SIGNIFICANCES

The approach of manufacturing of SCC was recently modified and developed to produce SCC with high performance and strength characteristics [11-12-13]. However, all previous efforts and attempts in the field of SCC were concerned and dealt with normal-weight aggregate concrete, and there is a lack of knowledge regarding the utilization of such innovative generation of self-compacting admixture in the field of manufacturing LWAC.

Generally, there is a great interest and tendency between researchers and concrete technologists to develop concretes with combining multi unique characteristics, which would not be attained in traditional normal-weight concrete. Therefore, an attempt was carried out herein to develop a concrete owing the main advantages of both LWAC and SCC together, called lightweight self-consolidated concrete (LWSCC). Local-produced materials will be adopted. This development aims to enhance the self-compactability and the other various fresh and hardened characteristics of LWAC, and to reduce the possibility of occurrence of segregation/floating of coarse LWA.

Consequently, an extensive experimental program was designated and conducted to achieve the following objectives:

1- To develop a lightweight aggregate self-compacting concrete (LWSCC) from local-produced materials (light expanded clay aggregate, LECA).
2- To assess the effect of self-consolidated agent content and the ratios of water/cement and lightweight aggregate/sand on fresh parameters, compressive strength, homogeneity, porosity and density of LWSCC. The assessed fresh parameters of LWSCC include flowability, deformability, self-compactability and rate of loss in fluidity.
3- To investigate the possibility of using normal weight aggregate as a partial replacement of LWA for improving the various fresh and hardened characteristics of LWSCC.

EXPERIMENTAL

Materials and Mix Proportions

Local ordinary Portland cement (OPC) complying with BS 12 (1978), ESS 373 (1991) and ASTM C618 (1992) was used. The chemical analysis of OPC is summarized in Table 1. Well-graded crushed limestone aggregate of maximum nominal size of 15 mm and washed natural desert sand were selected in accordance with ASTM C33 and ESS 1109/1971, used as a source of normal-weight aggregate. The coarse lightweight aggregate used in this study was locally produced from expanded clay type (LECA). The maximum nominal size of LECA was 15 mm. The sieve analysis of LECA is given in Table 2. The physical properties of the used coarse aggregate (normal weight and lightweight) and sand are presented in Table 3. In this study, the dry LECA was pre-soaked in water for 48 hours before mixing in concrete until steady weight of LECA was achieved, to ensure that all voids inside LECA particles are fully filled with water.

Table 1: Chemical Analysis of OPC.

Oxide,	SiO_2	Al_2O_3	Fe_2O_3	CaO	MgO	Na_2O	K_2O	SO_3	L.O.I.
%	22.4	4.85	3.9	61.7	2.23	0.43	0.24	2.48	1.70

Table 2: Sieve Analysis of Lightweight Aggregate (LECA).

Size, mm	14.0	10.0	5.0	3.35	2.0	pan
Passing, %	95.6	80.9	20.1	6.8	0.40	0.00

Table 3: Physical Properties of Coarse Aggregate and Sand.

	24-hour water absorption, %	Specific gravity	Fineness modulus	Unit weight, kg/m^3
Normal weight coarse aggregate (NWA)	0.98	2.60	-	1571
Lightweight coarse aggregate (LECA)	20.07	1.08	-	667
Sand	0.67	2.65	2.55	1585

A self-consolidated agent was utilized for producing the lightweight self-consolidated concrete mixes. The used self-consolidated agent (SCA) contains a polycarboxylic-based copolymer-based mixture and modified cellulose product to achieve the dual action effect of high-range water reducer and viscosity-modifying admixture, respectively. SCA was in a turbid liquid with a specific gravity of 1.11, and conforms to the requirements of ASTM-C-494 Types G and F.

Sixteen mixes of lightweight aggregate concrete (LWAC) and lightweight aggregate concrete incorporating self-consolidated agents (LWSCC) were prepared using the specific gravity factor method, as described elsewhere [4-5]. Various mix proportions such as water/cement ratio, dosage of self-consolidated agents (SCA), LWA/sand ratio, and contents of normal weight aggregate (% by weight of LECA) were regarded. The mix proportions of mixes considered in this program of study are shown in Table 4.

All aggregate types used in this study were weighed on a saturated-surface-dry (SSD) basis, to achieve good moisture control in the concrete mixes. The constituent materials were mixed in a pan mixer with a capacity of 0.08 m^3 and a mixing speed of 50 rev/min at ambient temperatures of about 22±2ºC. The self-consolidated agent was separately added into the concrete after about one minute of mixing. Mixing was continued for another two minutes before the mixture was left at rest for approximately 3 minutes.

Table 4: Mix Proportions of LWAC and LWSCC

Mix Code	OPC content, Kg/m^3	w/b ratio	SCA, % by weight of OPC	LWA/sand ratio	Normal-weight aggregate, % by weight of LWA
LWAC	450	0.30	-	1.50	-
LWSCC1	450	0.30	0.40	1.50	-
LWSCC2	450	0.30	0.50	1.50	-
LWSCC3	450	0.30	0.60	1.50	-
LWSCC4	450	0.30	0.80	1.50	-
LWSCC5	450	0.30	0.90	1.50	-
LWSCC6	450	0.30	1.00	1.50	-
LWSCC7	450	0.30	1.20	1.50	-
LWSCC8	450	0.35	0.80	1.50	-
LWSCC9	450	0.25	0.80	1.50	-
LWSCC10	450	0.30	0.80	2.00	-
LWSCC11	450	0.30	0.80	1.00	-
LWSCC12	450	0.30	0.80	1.50	35
LWSCC13	450	0.30	0.80	1.50	50
LWSCC14	450	0.30	0.80	1.50	65
LWSCC15	450	0.30	0.80	1.50	100

Test Methods

Immediately after mixing process, slump flow, and air content tests were performed. The slump flow test was carried out as described earlier in literature [9-12-14]. The diameter of flow measured with slump flow approach for LWSCC mixes was determined at different elapsed times from the end of mixing process, 0, 30, 60, 120 and 240 minutes, to assess the initial flowability and rate of slump flow loss of LWSCC. The air content of LWSCC was determined with according to the method B described in BS 1881: part 106: 1983 and ASTM- C 173. The analysis of air content of concrete was considered in this study to provide an indicative approach for measuring the degree of compactability of concrete. Immediately after mixing, five cubical concrete specimens (150x150x150 mm) made from each considered mix were prepared for measuring the hardened properties of LWAC and LWSCC. The specimens were stored in water curing tanks at 22±2°C until age of testing.

At the age of 28 days, the homogeneity of tested specimens was determined using ultra-sonic pulse velocity (UPV). The porosity of the concretes was also calculated based on the volume of the voids occupied by the absorbed water, as described earlier in literature [4]. This was followed by determining the compressive strength by crushing the five 150-mm cubes considered for each case of study, according to BS 1881: Part 116: 1983 and BS 1881: Part 121: 1883. An average of five measurement values was then obtained. Prior to compressive strength test, the cubes were used to test the SSD density by following BS 1881: Part 114: 1983.

RESULTS AND DISCUSSION

As a newly concrete type, lightweight self-consolidated concrete (LWSCC), it is vital to judge and understand its various characteristics in both fresh and hardened states. Clarifying the factors controlling the various characteristics of such concrete will be also essential. These factors include the dosage of self-compacting agent (SCA), w/c ratio, LWA/sand ratio and lightweight/normal weight coarse aggregate ratio. In this study, the fresh characteristics of LWSCC were evaluated in terms of slump flow, air content and rate of slump flow loss, while the hardened characteristics were assessed by investigating its pore structure, homogeneity and

compressive strength. Having a knowledge about these aspects can leads to develop the industry of LWAC and producing LWAC with unique properties.

Fresh Characteristics of LWSCC

Two approaches were considered to assess the fresh properties of LWSCC, Slump flow and air content. Slump flow technique is a commonly used approach in literature and recommended by Euro and Japanese standards for evaluating the main fresh parameters of self-compacting concrete, flowability and deformability [8-14]. It can also provide some information about stability of concrete mix, resistance against segregation of concrete ingredients [8]. On the other hand, determination of air content of LWSCC in its fresh state was considered to give an indicative measure for the degree of self-compactability of LWAC incorporating SCA, where the self-compactability is inversely proportionally with the amount of air content existed in fresh concrete. Moreover, the rates of loss in flowability and deformability characteristics of LWSCC were monitored at different elapsed periods from mixing, using slump flow approach.

Slump Flow and Air Content

To develop LWSCC, the effects of SCA on flowability and self-compactability of LWAC were initially investigated. The results are illustrated in Fig. 1, at which the measurements of slump flow and air content were plotted against SCA content. As clearly seen, the slump flow increase rapidly with increasing SCA content up to certain value (≈0.8). Beyond this dosage, slump flow measurements started to decrease with increasing the dosage of SCA in LWAC mix. An opposite trend was noted when the relationship between the amount of air content in fresh LWSCC and dosage of SCA was considered. Where, the air content decreased significantly with increasing SCA content up to 0.8% and then started to increase with increasing SCA dosage. These results reveal that increasing of SCA content in LWAC resulted in significant enhancements in its fresh parameters (flowability, deformability and self-compactability). The maximum enhancements were produced when a dosage of 0.80 % SCA was utilized in LWAC mix. However, beyond this dosage, the amount enhancements were declined.

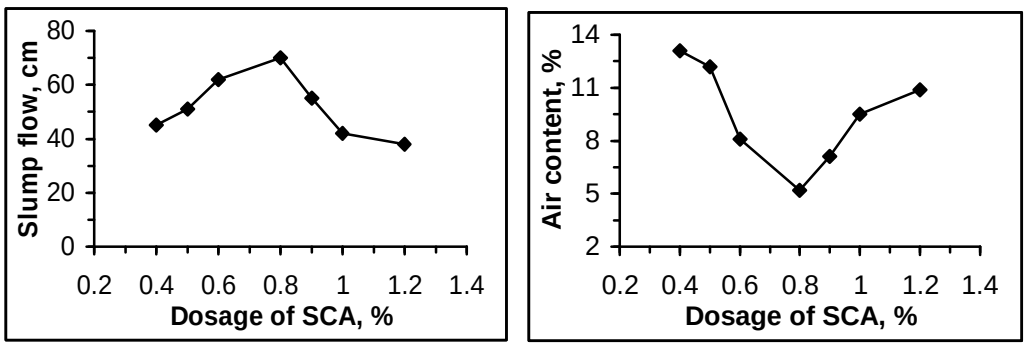

Fig. 1: Slump Flow and Air Content of LWSCC Made with Different Dosages of SCA, using Ratios of 1.50 LWA/Sand and 0.30 w/c.

Meanwhile, the stability of LWSCC mixes was examined visually to observe any possible segregation to their mix ingredients. The visual inspection of LWSCC mixes assured that despite of the high fluidity of such concrete, the uniformity of LWSCC made with 0.4, 0.5, 0.6 and 0.8 % SCA seemed to be very high, where no segregation to the ingredients of concrete mixes was noted. Whilst an opposite behavior was observed when 1.0 and 1.2% of SCA were utilized, where few particles of coarse aggregate were found on the edges of spread concrete. This agrees with the results shown in Fig. 1, where a substantial increase in the air content of fresh LWSCC was produced when a dosage of SCA of more than 0.80% was utilized.

The substantial improvement occurred to the main fresh parameters of LWSCC may be attributed to the physical effect of SCA. The incorporation of SCA affects the aqueous phase of cement phase where chains of water-soluble polymer present in SCA can absorb some of the

free water in the system, thus enhancing the viscosity of the cement phase. As a result, less free water can be available for bleeding and segregation of LWSCC mix ingredients [15]. The enhanced viscosity of LWSCC mix can lead to improving the capacity of paste to suspend the solid particles (LWA) and consequently enhancing the stability, deformability and degree of compactability of LWSCC. However, this physical effect may be affected by the dosage of SCA and amount of LWA in concrete mix, which led to altering the fresh parameters of LWSCC.

Another explanation can be provided, based on the assumption that the use of SCA resulted in a notable reduction in the amount of attractive forces between oppositely charged particles (deflocculating) and increasing the amount of inter-particle repulsive forces, due to the high negative charge conveyed to the particles by SCA. Therefore, the more SCA content, the more viscosity and negative charges in concrete mixture can be produced. However, increasing of SCA content beyond a certain dosage in LWAC mixes can also leads to a contradictory effect, where it may increase the possibility of segregation/floating of LWA, due to the excessive repulsive forces created by the higher dosages of SCA.

Rate of Slump Flow Loss

The rate of slump flow loss of LWSCC was investigated to provide a good understanding to the fresh properties during casting and placement state. The slump flow of LWAC mixes made with 0.60, 0.80, 1.00 and 1.20% SCA were monitored at different elapsed periods from mixing, 0, 30, 60, 120 and 240 min. The results are shown in Fig. 2, at which the relationships between the % of instant/initial slump flow of these mixes versus elapsed time from mixing were plotted. It can be seen the % of instant/initial slump of LWSCC are rapidly diminished with increasing elapsed period from mixing. Such diminishing effect significantly pronounced with increasing SCA content. After 120 min from mixing, LWSCC lost about 60, 65, 90 and 100 of its flowability due to inducing 0.60, 0.80, 1.00 and 1.20% SCA into LWAC mixes, respectively.

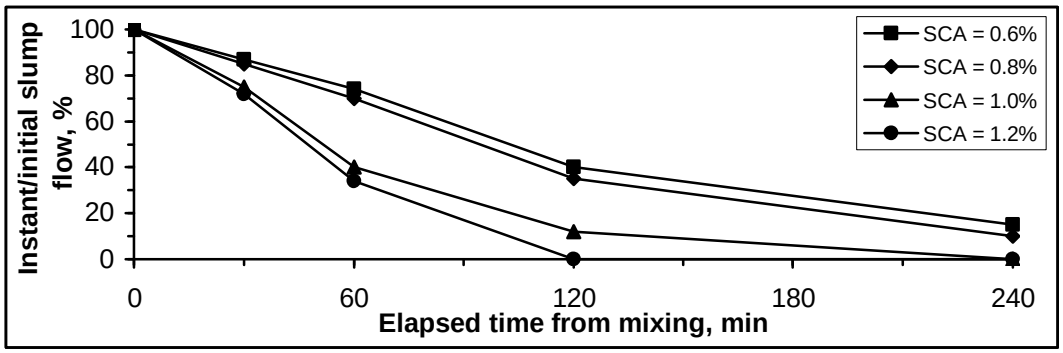

Fig. 2: Rate of Slump Flow Loss of LWSCC Made with Different Dosages of SCA, using Ratios of 1.50 LWA/Sand and 0.30 w/c .

The rapid loss in the slump flow of LWSCC indicates that the main mechanisms of SCA, necessary for improving the properties of fresh concrete, would be diminished with time. In other words, increasing of elapsed period from mixing can leads to a dramatic decrease in the viscosity and reduction in the amount of negative ions of LWSCC mixture, generated as a result of using SCA. Therefore, care is greatly important when casting and placing such type of concrete, to avoid the high losses in its fresh parameters.

Hardened Characteristics of LWSCC

After elucidating the performance of LWSCC during its fresh state, it is necessary to understand the performance of this type of concrete during its hardened state. So the 28 day-compressive strength, homogeneity, density and porosity of LWAC made with different dosages of SCA were assessed, see Fig. 3. In this study, the mechanical properties of LWSCC was investigated using compressive strength approach, while the porosity and homogeneity of LWSCC were examined by means of porosity and ultra-sonic pulse velocity (UPV) tests, respectively.

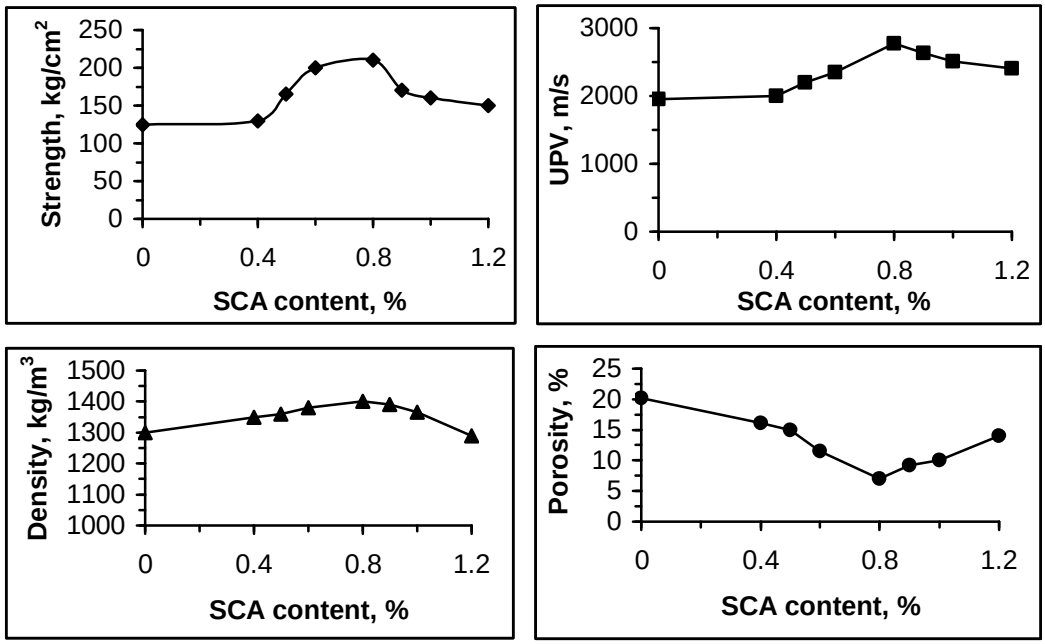

Fig. 3: Compressive Strength, Ultrasonic Pulse Velocity (UPV), Density and Porosity of LWSCC Made with Different Dosages of SCA.

As noted from the results demonstrated in Fig. 3 the compressive strength, UPV and saturated-surface dried density measurements reasonably increased with increasing the dosage SCA induced in LWAC mixes till a certain content of SCA (≈0.8%), at which these characteristics started to decline with increasing SCA. The maximum enhancements in the compressive strength and UPV reach about 60 and 40%, respectively, as a result of increasing the dosage of SCA from 0.00 to 0.80%. Whilst, the compressive strength and UPV measurements were reduced by about 40 and 15%, respectively, when the dosage of SCA was increased from 0.80 to 1.20%. In addition, the density of hardened concrete at saturated-surface dried (SSD) increased from 1250 to 1400 kg/m^3, as a result of inducing 0.80% SCA in LWAC mix, and then reduced to about 1350 kg/m^3, when 1.20% SCA was used.

On the other hand, an opposite effect for SCA content on the porosity of LWSCC was shown (see Fig. 3), compared to that noted effects of SCA on compressive strength, UPV and density. The porosity measurements was significantly affected by the content of SCA utilized in LWAC mixes, where the porosity of LWSCC decreased dramatically with increasing the dosage of SCA from 0.0 to 0.80 and then started to increase with increasing SCA content. The maximum achieved reduction in the porosity reached about 70%, when 0.80% SCA was utilized.

This means that SCA has significant effects on 28-day compressive strength, homogeneity, poosity and density of LWAC. These effects mainly dependent on the adopted dosage of SCA. The noted increase in the compressive strength and homogeneity of LWSCC when the dosage of SCA was increased from 0.40 to 0.80 may be attributed to the beneficial effect of this range of SCA dosages on the pore structure of LWAC. While the decline effect of increasing the dosage of SCA beyond 0.80% on compressive strength, homogeneity and density of LWSCC can be attributed to the increase in the porosity and slight segregation occurred to mix ingredients containing high dosages of SCA, as discussed above. Generally, it can be stated that, from the mechanical, homogeneity and porosity points of view, the optimum dosage of SCA to be induced in LWAC for producing LWSCC is 0.80.

Factors Affecting Fresh and Hardened Characteristics of LWSCC

It can be seen from the above discussion that it is possible to develop a concrete made from a local materials with the following characteristics; low density, high flowability and deformability, high self-compactability and high stability against separation of concrete ingredients. However, these advantages may be controlled by many factors such as dosage of self-consolidated agent, as explained above, concrete mix proportions (ratios of w/c and LWA/Sand) and inclusion of normal weight aggregate as a partial replacement of LWA. Therefore, this study was conducted to confirm such hypothesis, i.e. to investigate the influence of these factors on the various characteristics of LWSCC in its fresh and hardened state.

Effect of LWA/sand ratio

The slump flow and air content of LWSCC made with 0.30 w/c ratio, 0.80% SCA and different ratios of LWA/Sand (2.00, 1.50 and 1.00) were studied and the results are shown in Fig. 4. As seen, reducing the ratio of LWA/Sand has led to improve the various fresh parameters of LWSCC, flowability, deformability and self-compactability. Where, the slump flow measurements increased with decreasing the ratio of LWA/Sand and the amount of increase reached about 20% as a result of using LWA/Sand ratio of 1.0 instead of 2.0. On the other hand, the air content was significantly reduced with reducing LWA/Sand ratio. The lowest value of air content was obtained when a ratio of LWA/Sand of 1.0 was considered, at which the amount of reduction in air content reached about 60%, compared to the corresponding of that mixes made with LWA/Sand ratio of 2.0.

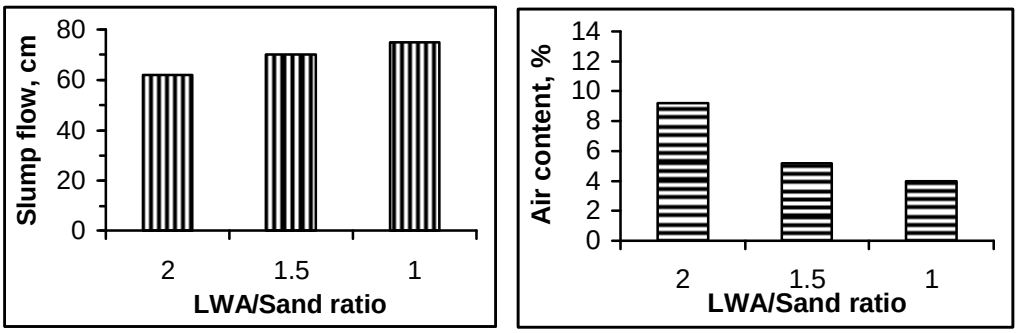

Fig. 4: Effect of LWA/Sand Ratio on the Slump Flow and Air Content of LWSCC, Made with 0.80% SCA and 0.30 w/c Ratio.

The effect of LWA/Sand ratio on the rate of flowability loss of LWSCC was also investigated and the results are shown in Fig. 5. It can be seen that increasing the ratio of LWA/Sand resulted in an increase in the rate of flowability loss, where the % of instant/initial slump flow at later ages (60, 120 and 240 min) was notably reduced with increasing the ratio of LWA/Sand from 1.50 to 2.0. After two hours from mixing, LWSCC lost about 60, 65 and 90 % of its fresh plasticity (flowability) when LWA/Sand ratios of 1.0, 1.50 and 2.0 were utilized in concrete mix. Despite of this notable effect, the rate of loss in slump flow of mixes made with 1.0 and 1.50 LWA/Sand ratio are slightly comparable.

The improvement in the fresh concrete properties due to reducing LWA/Sand ratio may be attributed to the decrease in the friction between concrete ingredients, which may be produced from the interlocking effect between coarse aggregate particles, thus leading to increase the degree of flowability and deformability of LWSCC. The amount of air content was reduced due to the enhancement occurred in the cohesion of concrete which might increase with increasing the amount of sand in LWSCC. Increasing LWA/Sand ratio can also increase the possibility of adsorption of water from concrete mix by LWA, thus reducing the instant slump flow measurements and consequently the rate of loss in slump flow of LWSCC.

Fig. 6 demonstrates the effects of LWA/Sand ratio on various hardened characteristics of LWSCC, 28-day compressive strength, UPV, SSD density and porosity. LWA/Sand ratio had

slight effects on both compressive strength and homogeny of LWSCC. The compressive strength and UPV increased from 205 kg/cm^2 to 220 kg/cm^2 and from 2700 to 2760 m/s, respectively, as a result of reducing the ratio of LWA/Sand from 2.0 to 1.0. The results plotted in Fig. 6 also show a significant increase in the SSD density of LWSCC due to reducing LWA/Sand ratio. The density increased from 1260 to 1550 kg/m^3 as a result of utilizing a ratio of LWA/Sand 1.0 instead of 2.0.

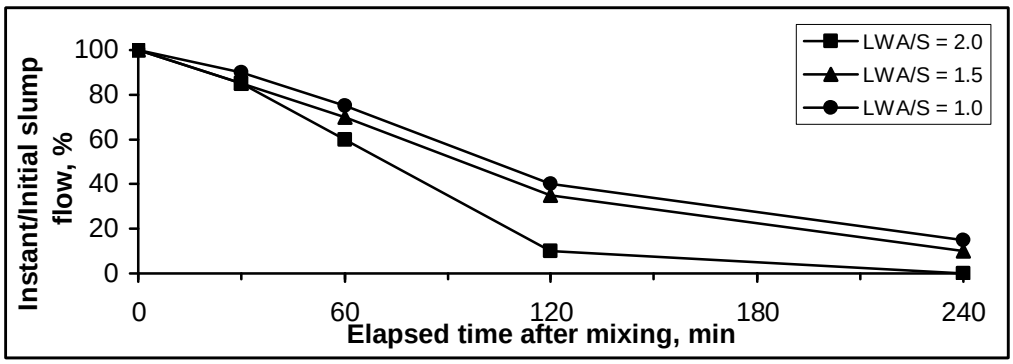

Fig. 5: Effect of LWA/Sand ratio on Rate of Slump Flow Loss of LWSCC.

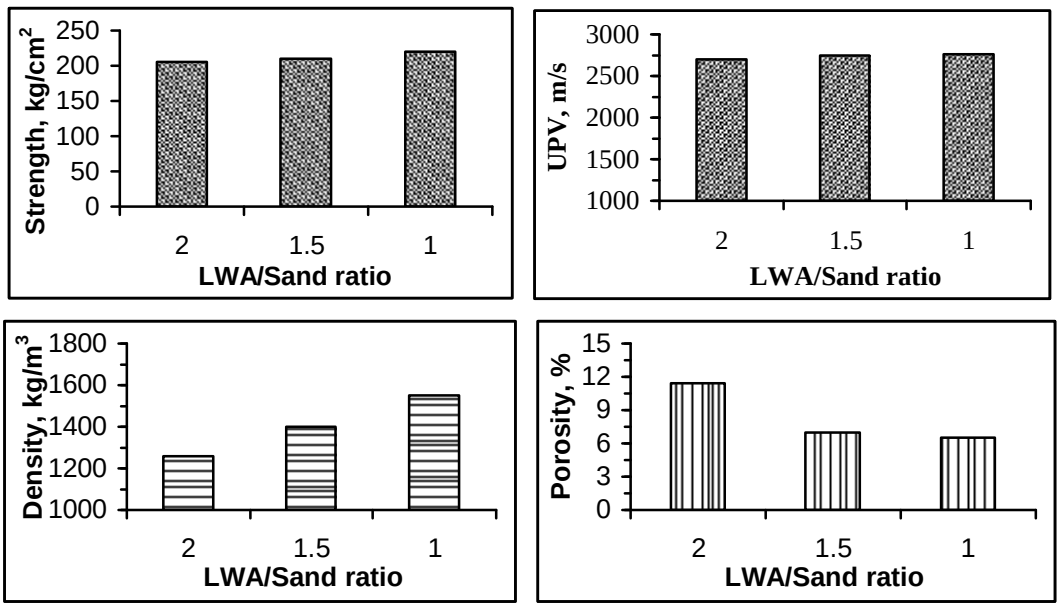

Fig. 6: Effect of LWA/Sand ratio on the Compressive Strength, Ultrasonic Pulse Velocity (UPV), Porosity and Density of LWSCC.

On the other hand, considerable reduction in the porosity of LWSCC with decreasing the ratio of LWA/Sand was produced. The amount of reduction reaches about 40% for concrete made with LWA/Sand of 1.50, compared to the corresponding of that made with LWA/Sand ratio of 2.0. The reduction in the porosity may be attributed to the increase in the packing effect of coarse aggregate, which increases with increasing the content of sand in LWAC, where reducing LWA/Sand ratio can lead to fill the voids with fine sand grains, hence decreasing the amount of pores in concrete. The amount of pores also decreased with decreasing the amount of LWA in OPC matrix, thus reducing the amount of pores (porosity) and increasing density. The reduction in the porosity is generally in agreement with the slight enhancement occurred in the compressive strength and UPV when the ratio of LWA/Sand was lowered.

Effect of w/c Ratio

The effects of w/c ratio on both fresh and hardened properties of LWSCC were also clarified and the results are listed in Tables 5 and 6, respectively. As seen from the results reported in Table 5 that, the amount air content in LWSCC was remarkably reduced with decreasing w/c ratio from 0.35 to 0.30 and the amount of reduction reached about 60%. While, reducing the w/c ratio from 0.30 to 0.25 resulted in a trivial reduction in the amount of air content (≈5%). On the other hand, the slump flow measurements seemed not to be affected by changing the w/c ratio of LWSCC mix.

Table 5: Effect of Water Cement Ratio on the Fresh Properties of LWSCC.

Water/cement ratio	Fresh properties	
	Slump flow (cm)	Air content (%)
0.35	69	12.3
0.30	70	5.2
0.25	72	4.8

Table 6: Effect of Water Cement Ratio on The Hardened Properties of LWSCC.

Water/cement ratio	Hardened properties			
	Strength (k/cm^2)	UPV (m/s)	Porosity (%)	Density (kg/m^3)
0.35	130	2600	14.5	1295
0.30	210	2750	7.0	1410
0.25	225	2795	5.4	1515

This means that w/c ratio has insignificant effect on the flowability and deformability of LWSCC mixes and considerable role on enhancing the self-compactability, especially when a range of 0.35 and 0.30 w/c ratio was utilized. In other words, the self-consolidation of LWSCC can be improved at low ranges of w/c ratio, which may be attributed to alterations occurred in cohesion and viscosity of concrete. However, there is a need for a further rheological study to confirm this explanation and the others discussed above concerning the fresh characteristics of LWSCC.

The results demonstrated in Table 6 emphasized that the w/c ratio had significant roles in enhancing the 28-day compressive strength and pore structure of LWSCC. Where the compressive strength increased with decreasing w/c ratio, while the values of porosity decreased with lowering w/c ratio. The amount of enhancements in compressive strength and porosity reached about 75 and 60%, respectively, as a result of lowering the w/c ratio from 0.35 to 0.25. Also, both homogeneity and unit weight of LWSCC were slightly increased with decreasing the ratio of w/c. These effects may be attributed to the significant effect of w/c on altering the porosity of LWSCC, thus leading to various alterations in concrete properties.

Effect of Partial Replacement of LWA with Normal Weight Aggregate

As an attempt for improving the hardened characteristics of LWSCC, especially compressive strength, the impacts of partial replacement of lightweight aggregate (LWA) with normal weight aggregate (NWA) on compressive strength, UPV and porosity were investigated, as demonstrated in Fig. 7. The SSD unit weight of concretes made with a combination of LWA and NWA was also noted down. As obviously seen, both compressive strength and UPV substantially increase with increasing the portion of NWA in LWSCC mix. The amount of increase in compressive strength reached by about 15, 30, 50 and 90%, when 35, 50, 60 and 100% NWA were used as a partial replacement of LWA.

This increase in strength is accompanied with a significant increase in the density of concrete, i.e. to enhance the mechanical properties of LWSCC using this approach, sacrificial increase in the density of concrete has to be regarded and accepted. Where, the density increased

dramatically with increasing the % of replacement of LWA with NWA and reached about 2230 kg/m^3 when LWA was fully replaced with NWA, normal weight concrete. However, the maximum content of LWA to be partially replaced by NWA in LWAC mixes should not exceed half of LWA content, to fulfill density criteria for manufacturing structural LWAC, as stated by ACI 211.2-81 [1].

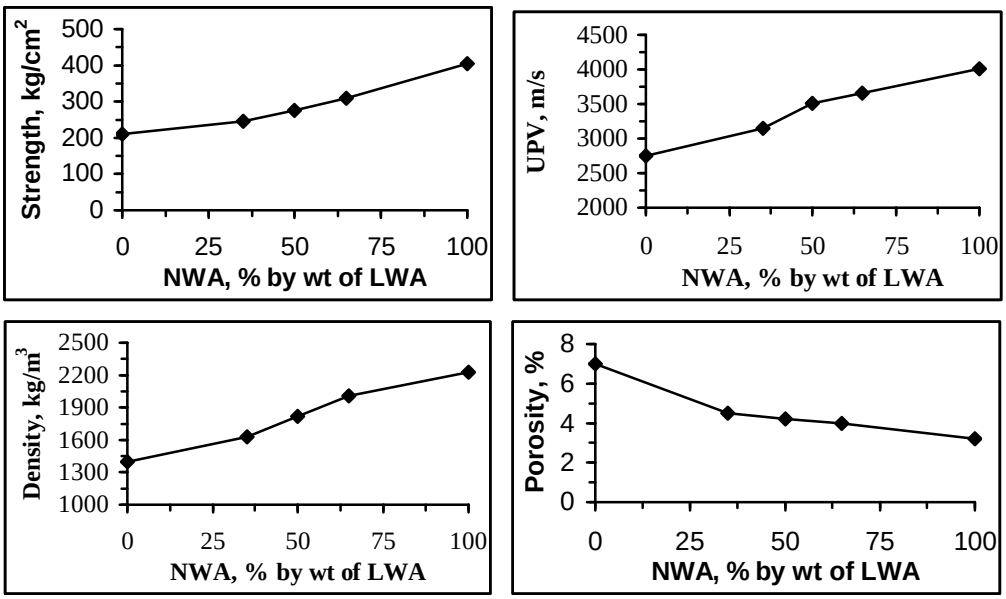

Fig. 7: Effect of Partial Replacement of LWA with NWA on Compressive Strength, Ultra-Sonic Pulse Velocity and Density of LWSCC, using Ratios of 1.50 LWA/Sand and 0.30 w/c, and 0.80% SCA.

The partial replacement of LWA with NWA also resulted in improvement in the porosity of LWSCC, where increasing the % NWA in LWAC mixes led to a notable reduction in its porosity results. The porosity of self-consolidated concrete made with 100% LWA is approximately twice of that concrete made with 100 % NWA. This reduction in the porosity agrees with the resulted improvements in compressive strength and UPV and can be attributed to decreasing the amount of pores as a result of inducing NWA in LWSCC.

To clarify the impact of utilizing NWA on the fresh properties of LWSCC, the slump flow, air content measurements were recorded for concrete mixes containing 0, 35, 50, 65 and 100 % NWA, by weight of LWA. The results are shown in Fig. 8. Obviously, both slump flow and air content measurements were remarkably with increasing the portion of NWA in LWSCC mix. This means that, despite the produced enhancement in the self-compactability, the LWSCC lost much of its flowability and deformability characteristics due to inclusion of NWA into LWSCC mixes. However, to overcome such problem, the proper dosage of SCA in such type of concrete, which incorporating of both NWA and LWA, has to be reviewed and adjusted.

Moreover, the rate of flowability loss of concrete made with both LWA and NWA was studied, as shown in Fig. 9. As seemed, the rate of slump flow loss of mixes made with 35% NWA is similar to the corresponding of that mixes made with 65% NWA. Both mixes however had lower rate of loss in their slump flow, compared to that made with 100% LWA. This again emphasize that the inclusion of NWA in LWSCC can improve the rate of loss in its fresh parameters as well as hardened properties of LWSCC.

The reduction in the amount of air due to increasing the portion of NWA in LWSCC may be attributed to the increase in the viscosity and cohesion of concrete mix, which can leads to improve the self-compactability of LWSCC. On the other hand, the resulted reduction in flowability and deformability of LWSCC with increasing the portion of NWA can be attributed to the amount of repulsive forces created by the considered dosage of SCA, which might decrease

with increasing NWA. Generally, a rheological study is required to find an explanation for such phenomena and the others discussed above, to understand the various fresh aspects of such newly concrete.

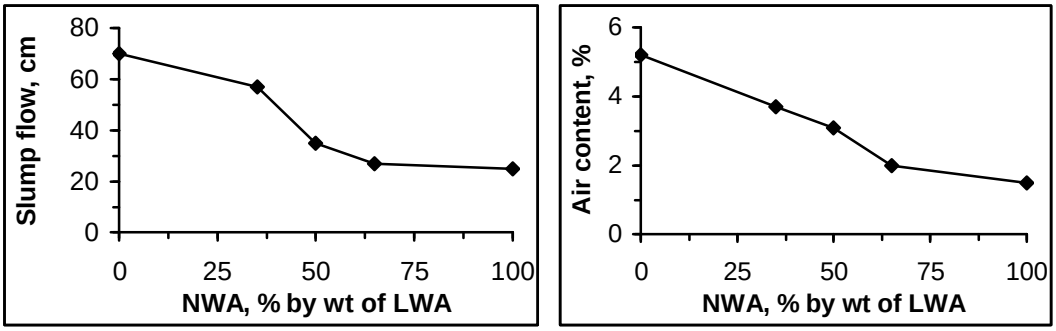

Fig. 8: Effect of Partial Replacement of LWA with NWA on Slump Flow and Air Content of LWSCC, Made With Ratios of 0.30 w/c and 1.50 LWA/Sand, and 0.80% SCA.

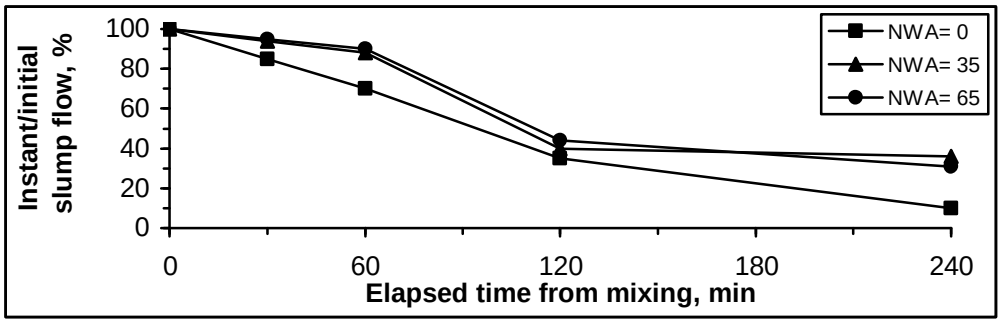

Fig. 9: Effect of Replacement of LWA with NWA on Rate of Flowability Loss of LWSCC.

CONCLUSIONS

Based on the results of this study, the following conclusions may be drawn.

1- It is possible to manufacture a structural lightweight aggregate concrete with low density and high self-consolidating characteristics (flowability, deformability, self-compactability and stability) using local-produced materials.

2- The fresh and hardened characteristics of lightweight self-consolidated concrete (LWSCC) are mainly controlled by dosage of self-consolidated agent (SCA), where the flowability, self-compactability, strength, homogeneity and porosity of LWSCC can be enhanced with increasing SCA content up to certain dosage of SCA (≈0.80), at which these characteristics started to decline with increasing SCA content.

3- LWSCC losses its fresh parameters (flowability and deformability) rapidly with increasing the dosage of SCA and lightweight aggregate/sand ratio. However, the rate of loss can be minimized with partially replacing lightweight aggregate with normal weight aggregate.

4- The compressive strength, homogeneity and porosity of LWSCC can be significantly improved with reducing the ratios of w/c and lightweight aggregate/sand, and utilizing normal weight aggregate in LWSCC mixes as a partial replacement of lightweight aggregate. However, increasing the portion of normal weight aggregate in LWSCC is accompanied with a substantial sacrificial increase in its unit weight.

5- SCA content and the ratio of lightweight aggregate/sand had a notable effect on the density of LWSCC, which increases with increasing the dosage of SCA up to 0.80% SCA and with reducing the ratio of lightweight/sand. On the other hand, w/c ratio had a trivial role on altering the unit weight of LWSCC.

ACKNOWLEDGEMENTS

The author would like to thank Prof. Assem Abdelalim for his helpful discussion. The author would like to acknowledge all staff members working in the laboratory of Quality Control Lab., Civil Engineering Department, Faculty of Engineering in Shoubra, Banha University, for their technical support.

REFERENCES

1- ACI 211.2-81 (1981), "Standard Practice for Selecting Proportions of Structural Lightweight Concrete".
2- Bamforth, P.B. (1987), "The Properties of High Strength Lightweight concrete", Concrete, Vol. 21, No. 4, pp. 8-9.
3- Topcu, I.B. (1997), "Semi-Lightweight Concretes produced by Volcanic Ash", Cement and Concrete Research, Vol. 27, pp. 15-21.
4- Bai, Y., Ibrahim, R. and Muhammed Basheer, P. A. (May 2004), "Properties of Lightweight Concrete Manufactured with Fly ash, Furnace Bottom Ash, and Lytag", International Workshop on Sustainable Development and Concrete Technology, Beijing, pp. 77-88.
5- Chia, K.S. and Zhang, M.H. (2004), "Effect of Chemical admixtures on Rheological Parameters and Stability of Fresh Lightweight Aggregate Concrete", Magazine of Concrete Research, Vol. 56, No. 8, pp. 465-473.
6- Khayat, K.H. and Guizani, Z. (1997), "Use of Viscosity-Modifying Admixtures to Enhance Stability of Fluid Concrete", ACI Materials Journal, Vol. 94, No. 4, pp. 332-340.
7- Okamura, H. (April 2003), "Self-Compacting Concrete", Journal of Advanced Concrete Technology, Vol. 1, No. 1, pp. 5-15.
8- Goodier, C.I. (2003), "Development of Self-Compacting Concrete", Structures and Buildings, Vol. 156, Issue 4, pp. 405-414.
9- Ozawa, K., Sakata, N. and Okamura, H. (1994), “Evaluation of Self-Compactability of Fresh Concrete Using the Funnel Test”, Proceedings, Japan Society of Civil Engineering, Vol. 23, No. 490, pp. 180-189.
10- Henderson, N. (April 2000), “Self-Compacting Concrete at Millennium Point”, Concrete, Vol. 37, No. 4, pp. 26-27.
11- Seleem, H.E.H. and Noval, N. (December 2004), "The Effect of Steel Fibers on Fresh and Hardened Self-Compacting Concrete Properties", International Conference: Future Vision and Challenges for Urban Development, Housing and Building Research Centre, Cairo, 13 pp.
12- Felekoglu, B., Turkel, S. and Baradan, B. (2007), "Effect of Water/Cement Ratio on the Fresh and Hardened Properties of Self-Compacting Concrete", Building and Environment, Vol. 42, Issue 4, pp. 1795-1802.
13- Sahmaran, M. and Yaman, O. (2007), "Hybrid Fiber Reinforced Self-Compacting Concrete with a High Volume Coarse Fly Ash", Construction and Building Materials, Vol. 21, Issue 1, pp. 150-156.
14- "The European Guidelines for Self-Compacting Concrete- Specification, Production and Use" (May 2005), 63 pp.
15- Sakata, N., Marruyama, K. and Minami, M. (1996), “Basic Properties and Effects of Welan Gum on Self-Consolidating Concrete”, RILEM Proceedings 32, Production Methods and Workability of Concrete, Paisely, Ed. Bartos, P.J.M., Marrs, D.L., and Cleland, D.J, pp. 237-253.

EFFECT OF FIRE ON THE DETERIORATION OF PORTLAND AND BLENDED CEMENTS

Hamdy El-Didamony
Chemistry Department, Faculty of Science Zagazig University, Zagazig, Egypt
M. Heikal
Chemistry Department, Faculty of Science, Benha University, Benha, Egypt
T.M.El-sokkary
Housing and Building National Research Center , Dokki,Cairo,Egypt
M. Abdallah Moustafa
Chemistry Dept., Faculty of Science, University of Gar Younis, Benghazi, Libya
E-Mail: tarek_elsokkary@yahoo.com, Tel.0020124556223, Fax.: +2-02-3351564

ABSTRACT

The effect of thermally treated temperature on ternary blended cement pastes containing ground blast furnace slag (WCS) and ground clay bricks (GCB) was studied. After moulding, the cement pastes were cured under tap-water for 28 days and dried at 105oC for 24 hours. The cubes were subjected to heat treatment at rate of 10oC/min and then kept for 3 hours at heating the peak exposure temperature to establish a stable temperature at 200, 300, 400, 500, 600 and 800oC, then cooled to room temperature in the furnace. The specimens were covered with plastic film and kept into desiccators in order to avoid the influence of humidity and the carbonization of thermally treated pastes. The weight loss of blended cement pastes is higher than OPC up to 400oC. As the heat treatment increases up to 500-800 oC, the weight loss of OPC increases. The compressive strength of blended cement pastes increase up to 400oC, then decreases. The OPC pastes are deteriorated after 600 oC. The micrograph of thermally treated blended cement pastes shows dense closed microstructure, displayed the absence of microcracks.

Keywords: Ternary blended cement system, microstructure, and thermally treated temperature.

INTRODUCTION

Fire is one of the hazards that attack the building. The damage occurring takes place due exposure to fire. Chemical processes stimulated by temperature increase on cement phases have a significant influence on the thermal deformation, cracking, spalling and compressive strength losses. Concrete subjected to elevated temperatures may suffer considerable loss in strength due to the development of microcracks or phase transformations in the matrix. The water loss, affects capillary and porosity as well as the microstructure to collapses C-S-H gel [1- 3]. Between temperature range (100–300oC), free water and bound water from C-S-H gel, reduction in strength in the range of 15-40%, whereas at 550oC, reduction in strength in the range 55-70%, due to the hydroxylation of Ca(OH)2 takes place to produce CaO.

Pozzolanic materials were used to enhance strength and reduce the permeability. The pozzolanic material depletes Ca(OH)2 liberated from the OPC phases to produce additional CSH, therefore, they enhance the fire resistance. Furthermore, pozzolanic materials are expected to play a significant role in the self-heating process of high strength concrete, when damaged through transformation of Ca(OH)2 deposited in cracks into CSH.

The effect of firing temperature on the hardened blended cement pastes cured at 28 days under tap water, dried for 24 hours at 105oC, then subjected to thermal treatment for 3 hours at 200, 300, 400, 500, 600 and 800oC, and cooled to room temperature in the

furnace, the weight loss, bulk density, total porosity and compressive strength were determined. The phase composition was determined by XRD as well as the microstructure was identified for the formed and decomposed phases. The results show that additional hydration of unhydrated phases, recrystallization, deformation and transformation of CSH phases were occurred [4]. The changes in physical state of cement paste were studied by measuring the deterioration in the compressive strength with temperature.

Poon et al. [5] prepared high strength concrete (HSC) incorporating 5, 10 and 20% MK and compared with the equivalent SF and FA mixes. It was found that the MK concrete possessed higher strength, lower permeability and less porosity as compared to the corresponding SF and FA concretes. It was observed that the fire resistance of concrete is highly dependent on its constituent materials, particularly the pozzolanas. A number of research studies indicated that the addition of SF highly densifies the pore structure of concrete, which can result in explosive spalling due to the build-up of pore pressure by steam. Since the evaporation of physically adsorbed water starts at 80°C which induces thermal cracks, such concretes may show inferior performance as compared to pure OPC concretes at elevated temperatures [6].

The change occurring in the phase composition and microstructure of MK cement pastes exposed to high temperatures was investigated [7]. The firing temperature varied from 100 to 600°C for 3hrs by increment of 100°C. The phase composition and microstructure were performed by DTA and SEM. The results show recrystallization and carbonation of Ca(OH)2 as well as deformation of C-S-H and C4AH13 phases.

Heikal [8] studied the effect of temperature on the phase composition and physico-mechanical properties of 10, 20 and 30% Homra blended cement pastes, fired for 3 hours without any load from 100 to 600oC by increment of 100oC. The results show that the replacement of OPC by 20% Homra improves the compressive strength by about 25.0%, but at 10 and 30% Homra, the strength increases by 4.0 and 8.5% at 600oC. As the temperature increases from 25oC to 600oC, the compressive strength of OPC and OPC-10% Homra decreases by 23.4% and 17.0% whereas the strength increases by 11.80% and 1.43% for 20 and 30%. The micrograph of cement pastes containing 20% homra at 300oC shows the formation of C-S-H as a result of consumption of hydrated lime by Homra, the C-S-H phases are deposited within the pore system, leading to high compressive strength as compared with those of OPC pastes. The microstructure at higher temperature (600°C) displayed the formation of dense masses of hydrated products having micro-and narrow pores. Therefore, the 20% Homra-blended cement pastes represents the most suitable fire resistance cement up to 600oC.

The work aimed to study the effect of thermally treated temperature on ternary blended cement system containing ground blast furnace slag and ground clay bricks.

Materials and Experimental Techniques

The materials used in this investigation were ground granulated blast-furnace slag (WCS), which provided from iron steel company, Helwan, Egypt, and ordinary Portland cement (OPC) from Suez cement Company; Homra (GCB) from Misr Brick (Helwan, Egypt). The chemical oxide compositions of each starting materials and surface area are given in Table (1).

Table 1: Chemical Composition of Starting Materials, Mass%.

Oxides / MATERIALS	SiO_2	Al_2O_3	Fe_2O_3	CaO	MgO	MnO	Na_2O	K_2O	BaO	SO_3	L.O.I	surface area, Cm^2/g
WCS	37.48	12.86	0.40	36.70	2.45	6.24	1.84	0.71	5.31	0.01	--	3500
OPC	21.51	5.07	4.39	65.21	2.00	0.15	0.23	0.29		0.25	0.40	3010
Homra	74.80	14.03	5.04	1.25	1.30	--	--	--	--	0.80	--	3000

The dry constituents of OPC, WCS, and GCB were mechanically mixed for one hour in a porcelain ball mill using three balls to attain complete homogeneity, then kept in airtight containers until the time of cement preparation. The mix compositions and W/C ratio and initial as well as final setting time are given in Table (2).

Table 2: The Mix Composition of Specimens, Water of Consistency and Initial as well as Final Setting Time of Cement Pastes.

	OPC	Slag	Homra	Standard water of consistency	Setting time (min)	
					Initial	Final
OPC	100	-	-	27.0	161	281
S_1	79	30	-	26.7	184	251
S_2	70	20	10	28.0	230	312
S_4	70	-	30	28.7	191	266

The mixing was carried out on the cement powder with the required water of standard consistency [9]. The blended cement was placed on a smooth non-absorbent surface and a crater was formed in the center. The required amount of water was poured into the crater by the aid of a trowel. The dry cement around the outside of the crater was slightly troweled over the remaining mixture to absorb the water for about one minute. The mixing operation was then completed by continuous vigorous mixing for about three minutes by means of ordinary gauging trowel. At the end of mixing, the paste was directly moulded in (2×2×2cm) Stainless steel moulds. Freshly prepared cement paste was placed in the moulds into two approximately equal layers, compacted and pressed until homogeneous specimen was obtained. The moulds were then vibrated for a few minutes to remove any air bubbles to give a better compaction of the paste, and then the moulds were cured in a humidity chamber at 100% relative humidity at constant temperature of 25 ± 1oC for the first 24 hours. The samples were cured under tap-water for 28 days and dried at 105oC for 24 hours. The cubes were heated at a rate of 10oC/min and then kept for 3 hours at the peak exposure temperature to establish a stable temperature [9]. The pastes were kept for 3 hours at 200, 300, 400, 500, 600 and 800oC, then cooled to room temperature in the furnace and taken out for testing. After cooling, the specimens were covered with plastic film and kept into desiccators in order to avoid the influence of humidity and the carbonization of thermally treated pastes. The total porosity of the cement pastes was determined according Egyptian specification. The compressive strength was carried out on four samples as described by ASTM Specifications [10].

X-ray diffraction technique was carried on some selected cement pastes. The samples were finely ground to pass through 200 mesh sieve. The samples were carried out using x-ray diffraction using a Philips diffractometer with a scanning speed 2q o/min. (Ni-filtered CuKa radiation). The identification of all samples were conformed by computer-aided search of the PDF data base obtained from joint committee on powder diffraction standards International Center for Diffraction Date (JCPDS-ICDD), 2001.

The microstructure of the selected samples was examined using a high-resolution scanning electron microscopy JEOL-JXA-840.

RESULTS AND DISCUSSION

Weight loss

The weight loss of hardened OPC and blended cement pastes (S1, S2 and S4) as a function of thermally treatment temperature up to 800oC are given in Figure 1. Generally, the weight loss increases with temperature due to the decomposition of some hydration products [10]. The free water was removed below 105 oC, partially decomposition of calcium silicate, calcium aluminate, calcium sulpho-aluminate and alumino-silicate hydrates takes place below 200 oC. The decomposition of gehlenite hydrate (C2ASH8) is occurred at 200-250oC. The decomposition of hydrogarnet hydrate is up to 400 oC and the dehydroxylation of Ca(OH)2 occurs at temperature of 420-520oC (7). The weight loss increases up to 400 oC, due to the decomposition of CSH, CAH and calcium sulphoaluminate hydrates as well as gehlenite and hydrogarnet hydrates. It was shown that S1 and S4 have weight loss higher than OPC up to 400oC.

As the heat treatment increases up to 500-600 oC, the weight loss of OPC increases, this is mainly due to the increase of the amount of Ca(OH)2 content in OPC pastes. The decrease of weight loss of blended cements at these temperature, is mainly due to the decrease of the amount of Ca(OH)2 as a result of pozzolanic reaction. Increase of the temperature up to 800oC the weight loss of OPC pastes shows the higher value due to the increase of the amount of Ca(OH)2 decomposed and some converted CaCO3. The blended cement pastes have lower amount of Ca(OH)2 as well as CaCO3 contents.

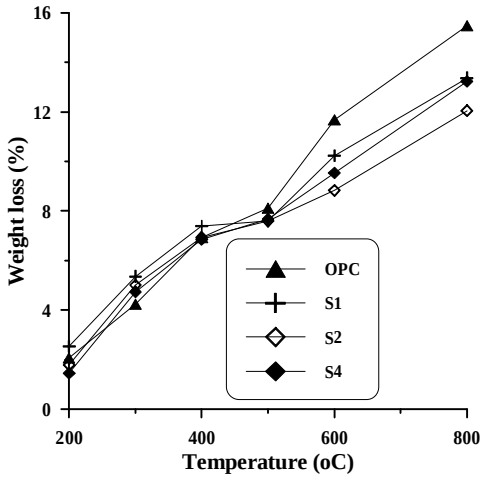

Fig. 1: Weight Loss of OPC and Blended Cement Pastes Containing (S1, S2 and S4) at Different Heat Treatment Temperature up to 800oC.

Total Porosity

The variation of porosity of OPC and blended cement pastes containing WCS and GCB cement pastes are graphically plotted as a function of treatment temperature were given in Figure 2. The porosity increases with treatment temperature. At 300oC it was shown that S2 has the lowest values of porosity than those of other blended cement as well as OPC cement pastes, this is due to the pozzolanic activity and internal or self-autoclaving [8]. This attributed to the filling role of pozzolanic products and its reactivity to react with lime to form more cementitious materials that fill the pores and then decrease the porosity.

Increase of the treatment temperature (400-600oC), the porosity of all blended cement has the lowest values than OPC pastes. The porosity increases slowly up to 600oC, then sharply increases up to 800oC for all blended cement. The OPC cement pastes destroyed completely at 800oC.

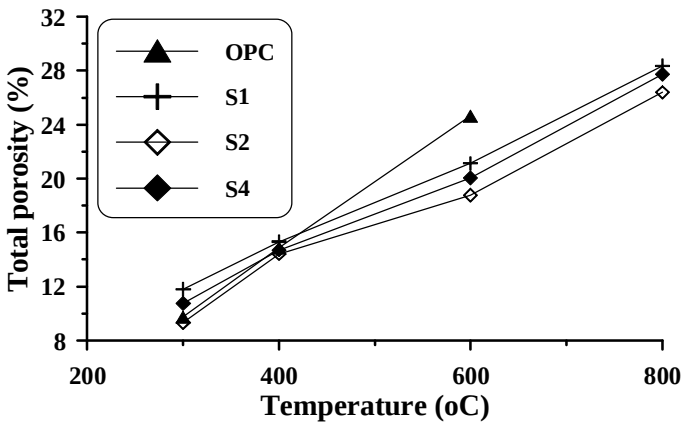

Fig. 2: Porosity of OPC and S1, S2 and S4 with Treatment Temperature up to 800oC.

Compressive Strength

The compressive strength of OPC and blended cement pastes namely S1, S2 and S4 as a function of thermally treated temperature are graphically represented in Figure 3. It illustrates the variations of compressive strength of different thermally treated blended cement pastes. The compressive strength of OPC pastes increases up to 300oC due to the self autoclaving of the cement pastes. The increase of temperature from 500 to 600oC decreases the compressive strength, but at 800oC, the OPC specimens were completely destroyed.

The temperature range between 100-300oC, leads to additional hydration products from the anhydrous cement grains. The compressive strength increases with the addition of WCS and GCB up to 400oC, then decreases. The higher compressive strength at 400oC is for the cement pastes containing 70% OPC + 20 WCS + 10% GCB (S2). This is due to the reaction of liberated lime with the pozzolanic materials to form additional amounts of calcium silicate, aluminate and alumino-silicate hydrates. These hydrates deposited within the pore system as shown in the SEM micrograph later. As the treatment temperature increases from 400oC to 800oC, the compressive strength of OPC was completely destroyed, where the blended cement S1, S2 and S4 decreases by 32.29, 27.21 and 24.15 respectively. Therefore, the blended cement containing only 30% GCB represented the most suitable fire resistance up to 800oC. This is mainly due to that the ground clay brick is composed only of aluminosilicate and has no calcium compounds. The aluminosilicate materials react with the decomposed Ca(OH)2 forming a strong ceramic material.

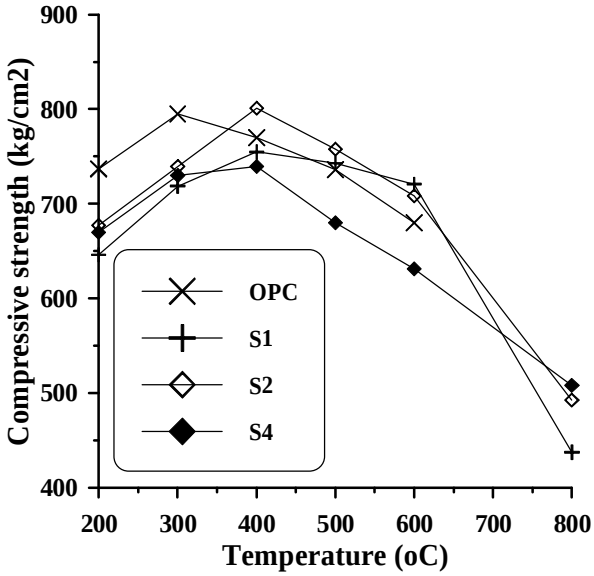

Figure 3: Compressive Strength of OPC and Blended Cement Pastes Containing S1, S2 and S4 with Treatment Temperature from 200 up to 800oC.

X-Ray Diffraction Studies

Figure 4 illustrates the XRD patterns of OPC pastes containing thermally treated at 105, 300, 500 and 800oC. The diffractograms of OPC at 105, 300, 500 and 800oC shows the main peaks of the anhydrous phases (C3S and C2S) and Ca(OH)2, CSH, ettringite which are found in sample at 105oC. After thermally treatment some reflections disappear as shown in Figure 4. A progressive reduction of the intensity of the peak of Ca(OH)2 is noticed. at 500oC. The presence of CaCO3 is detected and even increases up to 500oC. At higher temperature, 800oC, the reflection peaks of calcite practically disappears. Lime (CaO) is also well identified at 800oC, from the decomposition of Ca(OH)2 and CaCO3, C4AF is also present in all specimens heated and the same for C2S [11]. Increasing the heat above 500oC, the cement paste shows that Ca(OH)2 and calcite decompose into CaO. But by thermally treated up to 105-300oC an increase of Ca(OH)2 is found due to progress of hydration of residual anhydrous components. This hypothesis is sustained by the parallel increase in CSH, indicating higher content of C-S-H

gel. At 800oC C-S-H gel has completely disappeared, this is mainly replaced by crystalline phase with structure similar to C2S [11]. As shown in Figure 5 the main products of C-S-H decomposed was C2S consistent with previous reports [9].

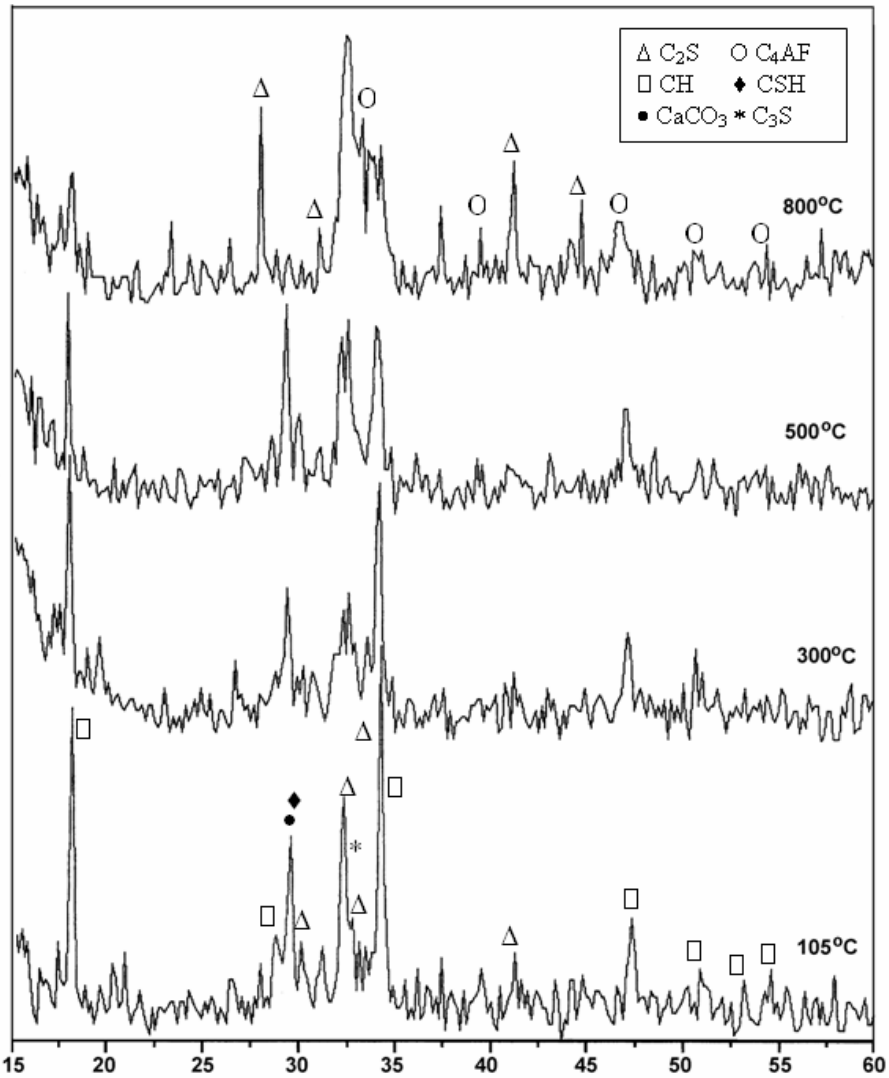

Fig. 4: XRD Patterns of OPC Specimen at 105, 300, 500 and 800°C.

Figure 5 illustrates the XRD diffraction patterns of blended cement pastes containing 30% WCS (S1), thermally treated at 105, 300, 500 and 800oC. The diffraction patterns contain, CH, CSH and tobermorite. The intensity of characteristic lines for Ca(OH)2 decreases with the treatment temperature. At 500oC the lines of CH nearly decomposed or disappeared and the lines of CSH and tobermorite still present. There are new lines of anhydrous calcium silicate phases such as -C2S at 800oC. The decrease of CH lines from 105oC up to 300oC due to the self autoclaving condition, which transformed the anhydrous grains to hydrated phases in presence of water vapour and temperature up to 300oC. As a result of formation of additional calcium silicate hydrate and tobermorite phase, from the hydrothermal reaction of slag grains with Ca(OH)2 liberated from the hydration of OPC phases.

The lines of CSH hydrated phases show a maximum at 300oC. At 800oC the most hydrated phases were completely disappeared, this mainly replaced by crystalline phase with structure similar to C2S at diffraction limes. The formation of C2S as shown in Figure 6 started at 500oC, this due to the decomposition of CSH and tobermorite phases.

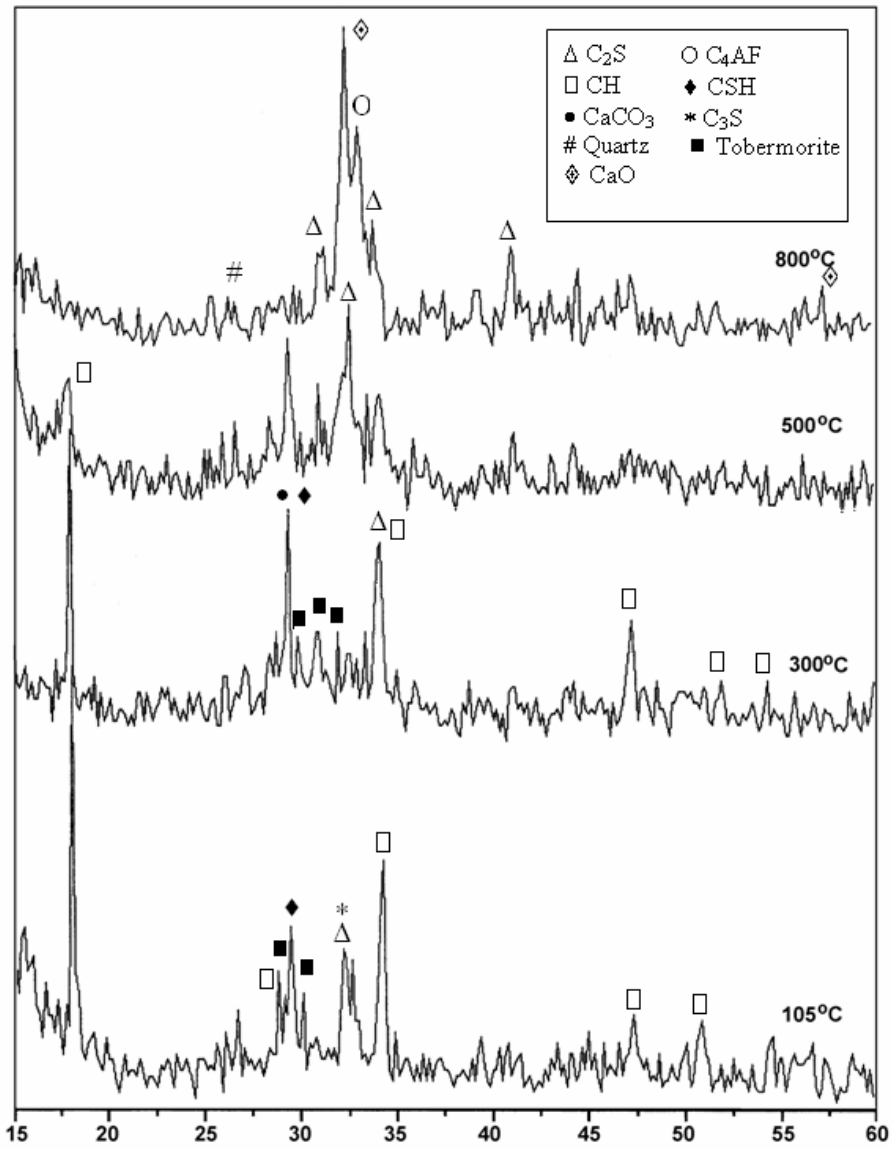

Figure 5: XRD Patterns of S1 Specimen at 105, 300, 500 and 800°C.

Microstructure

High-resolution SEM provides a useful information on the morphology of hydration products of OPC thermally treated at 105, 300, 500 and 800oC as shown in the micrograph in Figures 6-9, and blended cement containing 30% WCS (S1) in Figure 10.

Figure 6 shows the micrograph of hardened OPC at 105oC which reveals well developed hydrated phases such as Ca(OH)2 crystals intermixed with C-S-H and calcium aluminate crystals. While at 300oC, the morphology of effective OPC pastes showed deformed Ca(OH)2 crystals, CSH gel, voids as shown in Figure 7. The Ca(OH)2 appears as a sheets are stacked as parallel layers.

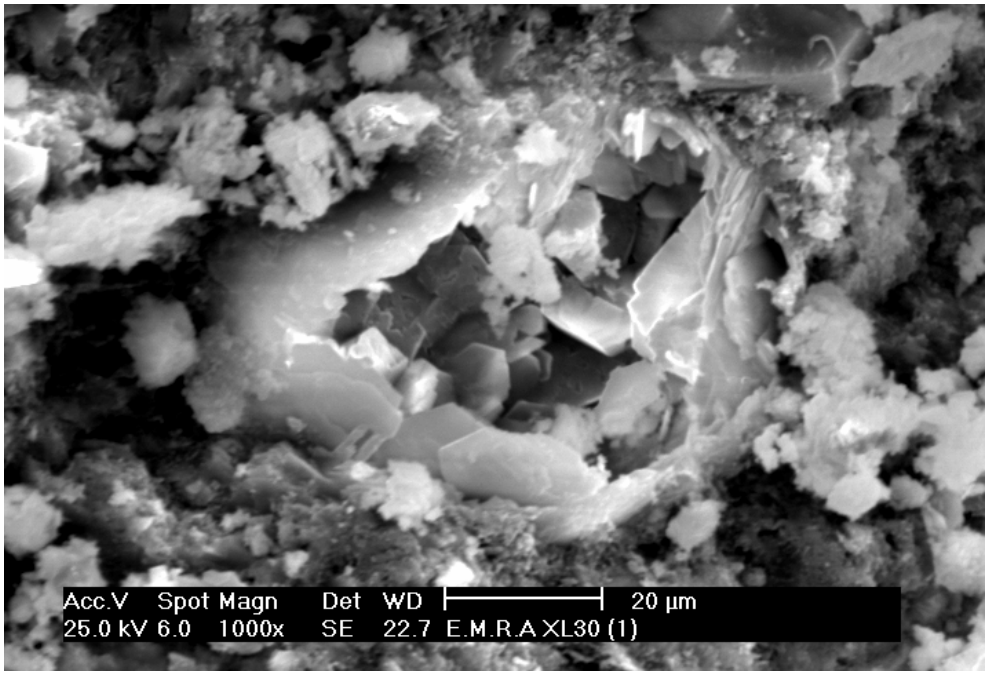

Fig. 6: SEM of OPC cement Pastes Cured at 28 days and Dried at 105oC for 24 Hours.

Further increase in treatment temperature to 500oC, leads to the predominance of micro-crakes intermingled with voids due to increase of porosity. The diminished of the void 166 m × 168 m as shown in micrograph Figure 8, as well as distorted Ca(OH)2 and CSH gel. Further SEM investigation on OPC specimens exposed to 800oC Figure 9, revealed massive change in the microstructure, due to the predominance of microcraks, varied between 2.96-5.92 m, voids increasing the porosity, deformed of Ca(OH)2 and CaCO3 and completely decomposed into CaO as well as disrupted CSH phase boundaries. Therefore, the the strength of OPC paste is completely destroyed at the thermally treated temperature (800oC). This is attributed to the loss of bound water, increased porosity and consequently, increased permeability, which lead to further destruction or failure.

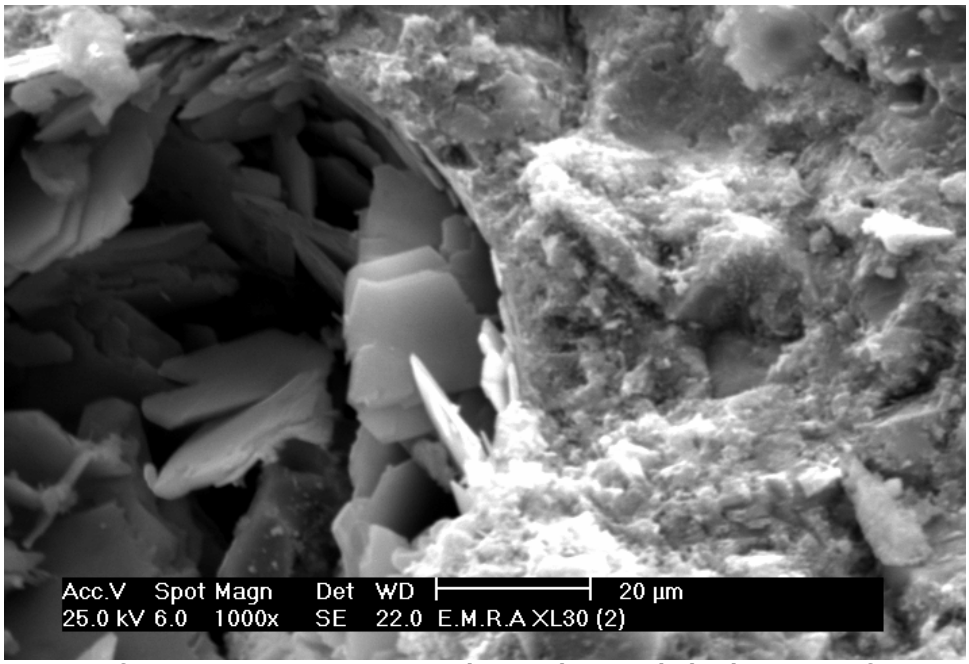

Fig. 7: SEM of OPC Cement Pastes Cured at 28 days and Fired at 300oC for 3 Hours.

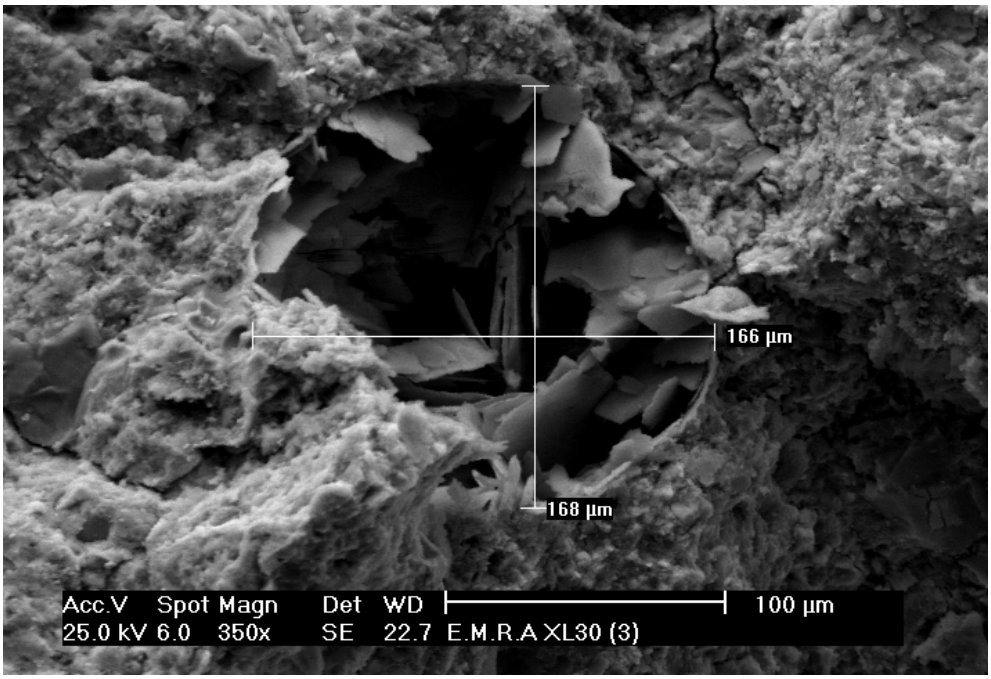

Fig. 8: SEM of OPC Cement Pastes Cured at 28 Days and Fired at 500oC for 3 Hours.

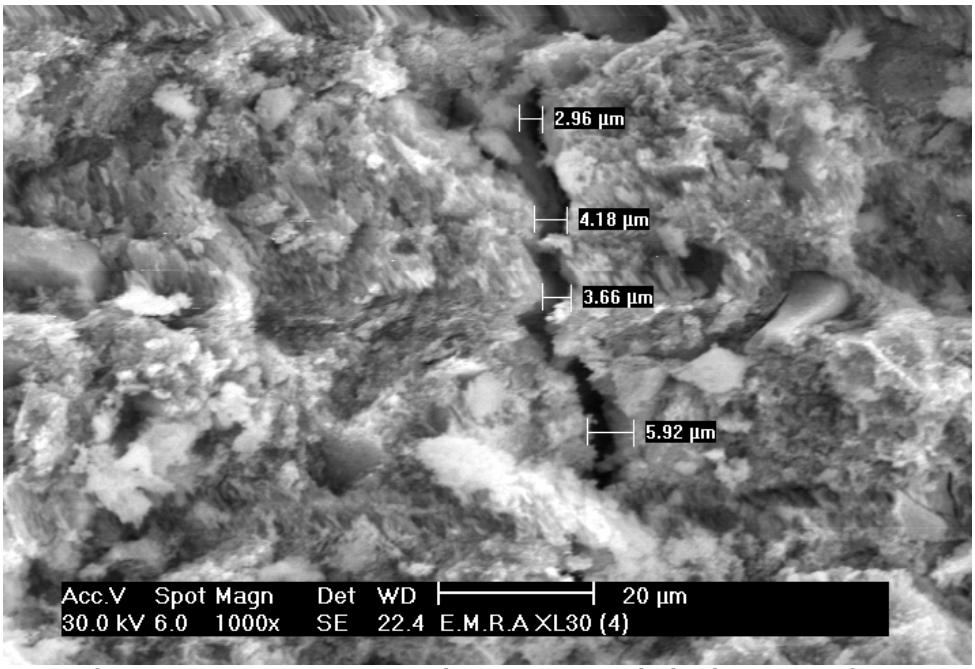

Fig. 9: SEM of OPC Cement Pastes Cured at 28 Days and Fired at 800oC for 3 Hours.

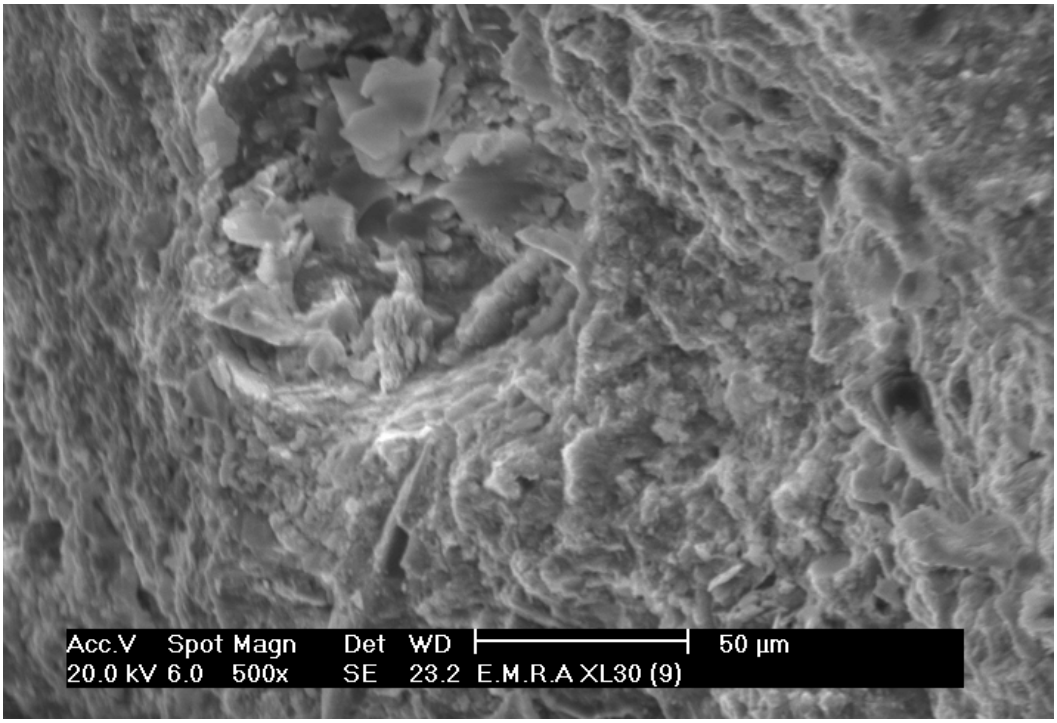

Fig. 10: SEM of Blended Cement Pastes Containing 70% 30% WCS Cured at 28 Days and Fired at 500oC for 3 Hours.

Figure 10 shows the micrograph of blended cement pastes containing 30% WCS (S1) thermally treated at 500oC. The micrograph shows dense closed microstructure, displayed the absence of microcracks as shown in the micrograph. Evidently, the pore space is available for the deposition of hydration products. This attributed from the formation of C-S-H, which is produced as a result of the consumption of hydrated lime by silica fume and alumina containing WCS. These hydrates were deposited within the pore system and around the cement grains, which can accommodate larger amount of hydration products especially C-S-H leading to relatively compressive strength values as compared with those of OPC pastes. The micrograph also shows the presence of thin flaky plate like morphology of gehlenite hydrates (C2ASH8) together with fibrous particles of CSH, with the absence of the Ca(OH)2 crystal in the micrograph as shown also in the XRD patterns of thermally treated at 500oC.

CONCLUSIONS

- Blended cement pastes show lower porosity at all heat temperature than OPC pastes. The blended cement composed of 20% granulated slag and 10 % Homra gives the lowest porosity.
- The compressive strength of blended cement pastes increases up to 400oC, then decreases at 800°C, the blended cement pastes are durable to heat than OPC.
- OPC specimens exposed to 500oC, leads to the predominance of micro-crakes intermingled with voids due to increase of porosity as well as distorted Ca(OH)2 and CSH gel. Where the specimens exposed to 800oC revealed massive change in the microstructure, due to the predominance of microcraks, deformed of Ca(OH)2 and CaCO3 and completely decomposed into CaO as well as disrupted CSH phase boundaries.
- The micrograph of thermally treated blended cement pastes at 500oC shows dense closed microstructure, displayed the absence of microcracks. The micrograph shows the presence of thin flaky plate like morphology of gehlenite hydrates (C2ASH8) together with fibrous particles of CSH, with the absence of the Ca(OH)2 crystal in the micrograph.

REFERENCES

1. Kropp J., Seeberger J. and Hilsdorf H.K. "Chemical and physical properties of cement paste and concrete containing fly ash after hydrothermal exposure", ACI SP vol. 91, pp 201-218 (1986).

2. Rostasy F.S., Weiss R. and Wiedemann G. "Change of pore structural of cement mortars due to temperature" Cement and Concrete Research, 10, p. 157-164 (1980).
3. Galle C. and Sercombe J. "Permeability and pore structure evolution of silico-calcareous and hematite high strength concrete submitted to high temperature" Materials structural, 33, p. 619-628 (2001).
4. Gustafero A.H., Experiences from evaluating fire-damaged concrete structure – fire safety of concrete structures" ACI SP-80 (1983).
5. Poon C.S., Kou S.C. and Lam L.: "Compressive strength development, chloride-ions resistance and pore size distribution of metakaolin concrete". The Hong Kong Polytechnic University, Hong Kong, (2000).
6. Poon C.S., Kou S.C. and Lam L.: "Compressive strength development, chloride-ions resistance and pore size distribution of metakaolin concrete". The Hong Kong Polytechnic University, Hong Kong, (2000).
7. Morsy M.S., Galal A.F. and Abo El-Enein S.A. "Effect of temperature on phase composition and microstructure of artificial pozzolan – cement pastes containing burnt kaolinitic clay" Cement and Concrete Research, 28, p. 1157-1163 (1998).
8. Heikal M.: "Effect of Temperature on the Physico-Mechanical and Mineralogical Properties of Homra Pozzolanic Cement Pastes" Cement and Concrete Research, Vol. 30, p. 1835-1839 (2000).
9. Heikal M., "Effect of temperature on the structure and strength properties of cement pastes containing fly ash alone or in combination with limestone, ceramics-silicaty 50(3), p. 167-177 (2006).
10. ASTM Designation: C109-80 [ASTM Designation: C109-80, “Standard Test Methods for Compressive Strength of Hydraulic Cements”, ASTM Standards (1983).
11. Alonso C. and Fernandez L., Journal Materials Science 39, p. 3015 (2004).

PROPERTIES OF NEW CEMENTS PRODUCED IN EGYPT AS PER ES 4756/2005:

Dr. Khalid M. Yousri
Associate Professor, Housing and Building National Research Center, Cairo, Egypt
Email: kyousri@hbrc.edu.eg

ABSTRACT

Cement -being a vital constituent in the construction industry -must meet international standards to verify quality and maintain product uniformity. On June 2005, the Egyptian Organization for Standardization & Quality (EOS) issued new standard for cement ES 4756/2005 based on European Standard EN 197/2000 and as a result, a number of former Egyptian Standards were withdrawn.

This paper aims to provide information on the types and properties of cements specified in the new standard and already produced in the market to assist the designers and users to choose the same cement performance as before and to make the transition to the new standard ES 4756/2005 as easily as possible.

To accomplish this task, a total number of 380 samples - collected during the last six months from 6 companies - comprising 7 types of cement (CEM I 32,5 N, CEM I 32,5 R, SRC 32,5 R, CEM II B-S 32,5 N, CEM I 42,5 N, CEM I 42,5 R, SRC 42,5 N) mostly used in the construction industry has been tested for compressive strength. In addition, a comparative study was carried out using CEM I 32,5 R, CEM I 32,5 N, sulfate resisting cement (SRC) 32,5 R, CEM II B-S 32,5 N, CEM I 42,5 N, CEM I 42,5 R and CEM I 52,5 N cements to evaluate the difference between the old withdrawn standard ES 373 and its relevant standards and the new standard ES4756 and its relevance upon mechanical properties of the resulting mortar specimens. Strength development of cement mortar was determined at 2, 3,7, 28, 56 and 90 days respectively. Conformity of CEM I 42,5 N is also included.

Test results revealed that all the cement types tested comply with the requirements for the Egyptian standards 4756 for compressive strength at 2 or 7 and 28 days. The results of the comparative study clearly indicated that the cement produced according to the new standard ES 4756 are meeting the strength requirements stated in the old withdrawn standard ES 373 and it's relevant. More research is still needed to explore the durability performance of the new cements.

Keywords: Common cements, EN 197, ES 4756 standard, properties, types, Strength class,

INTRODUCTION

Standards are the basis to verify quality and maintain product uniformity. In Egypt, the Egyptian Organization for Standardization & Quality (EOS) is considered the only official and competent national authority in all matters, related to standards. During the last few years, the (EOS) has started harmonizing the Egyptian Standards under the harmonization of the Egyptian standards with the European ones under the project signed with Industrial Modernisation Programme (IMP) to meet international criteria. With regard to the construction materials, the EOS technical

committee on cement (committee 2/11), composed of representatives from cement industry representatives, academic, professional associations and other government agencies, started revising all the issued cement Egyptian Standards to keep them updated on the latest developments in the international construction guidelines. Cement -being a vital constituent in the construction industry -must meet international standards to verify quality and maintain product uniformity. Up to the last two years, Portland cement was produced in the market in accordance with ES 373/1991 [1] which totally complied with the requirements of British Standard BS 12/89 [2]. On the other hand, British Standard Institute (BSI) withdrew the latest version of BS 12/96 from April 2001 under the umbrella of the harmonisation of European standards. From this date, member companies of the British Cement Association (BCA) were enabled to manufacture their cements in conformity to the new BS EN 197–1 specification [3]. Accordingly, it was found that Egyptian standards were lagging behind International Standards. On June 2005, the EOS issued - through its national technical committee 2/11- new standard for cement ES 4756/2005 Part 1: "Composition, specification and conformity criteria for common cements" [4] and Part 2: "Conformity Evaluation [5]. These standards are harmonised with the European standards EN 197 Part 1 [3] and Part 2 under the umbrella of harmonizing the Egyptian standards with the European ones to upgrade the quality of local cement to meet international criteria which will lead to the CE Marking of cement throughout Europe. Part one of this Egyptian Standard (ES 4756-1) defines and gives the specifications of 27 distinct common cement products and their constituents ranging from simple Portland cement to composite cements containing up to three major constituents. As a result of issuing the new standard, a number of former Egyptian Standards were withdrawn on 18 November, 2005 after 6-month transition zone. This includes the following standards (sulfate-resisting Portland cement ES 583/2005 [6] is outside the scope of EN 197-1):

- ES 373 /91 : Ordinary Portland Cement and Fast Setting cement,
- ES 2796/95 : High Slag Cement,
- ES 974/92 : Portland Blast Furnace Cement,
- ES 1031/92 : White Ordinary Portland Cement,
- ES 1450/79 : Super fine Ordinary Portland Cement 4100,
- ES 3374 : Portland Cement Clinker,
- ES 541/1992 : Low-Heat Portland Cement

Currently, many significant differences exist between the withdrawn ES 373/91 and the new ES 4756/2005 standard. Table 1 illustrates main differences between the two standards and their relevant standards with regard to materials used, preparing, mixing, and testing.

Table 1 – Main Differences between ES 373 and ES 4756

Items	ES 373 and its relevant	ES 4756 and its relevant
Moulds	70.7-mm cubes	40x40x160 mm prisms
Sand	1-Pass Sieve 850 micron and retained on sieve 600 micron 2- Silica content ≥ 90% 3- Moisture content ≤ 0.1%	1- ISO reference sand 2- Silica content ≥ 96% 3- Moisture content ≤ 0.1%
Mixing constituent by weight (gm)	Cement : sand : water 185± 1 : 555±1: 74±1 (w/c =0.4)	Cement : sand : water 450±2 :1350±5 :225±1 (w/c = 0.5)
Mixing	Manual	Automatic
Mixing time (seconds)	300	240
Vibration	Vibrating machine	Standard jolting apparatus
Setting time	Initial and final	Initial
Tests at	3,7 and 28 (optional)	2 or 7 and 28 days
Rate of loading	35 N/mm^2.min	2400±200 N/sec
SO_3	2.5 – 3.5 %	≤ 3.5 %
Insoluble residue	≤ 1.5 %	≤ 5 %

Chloride limit	Not stated	0.1% max.
Fineness	Stated	Not stated
Loss on ignition	≤ 4%	≤ 5 %
Conformity criteria	Not included	Included

With regard to the composition of cement, there is one main difference. Until the end of the eighties, Portland cements were in general expected to be 'pure'; that is, with no minor additions other than gypsum or grinding aids. Then, appropriate inorganic materials, termed 'cementitious materials', were introduced to Portland cement mainly in order to develop various desirable properties of concrete in which the cement was a constituent. The resulting product is termed 'Blended Portland Cement' or 'Portland Composite Cement'. This method has already become popular because it has a number of potential advantages [7]:

- Increased plant capacity without the installation of a new kiln.
- Reduced fuel consumption per ton of cement.
- Reduced Carbon Dioxide (CO_2) emissions (greenhouse gas) per ton of cement.
- Control of alkali-reactivity even with high-alkali clinker.
- Reduced production of cement kiln dust if the alkali content of the clinker is increased.

Thus, the new standard opens up the option of producing cements containing higher levels of latent-hydraulic, pozzolanic and inert main constituents which because of their particle size can improve the physical properties of the cement, e.g. workability or water retention. From now on cements with up to 35 % limestone, up to 95 % blastfurnace slag, up to 55 % pozzolana and up to 80 % of a combination of blastfurnace slag and pozzolana are also covered by the standard. The ES 4756-1 categorizes cements into five types based on their composition, these are:

- **CEM I** Portland cement; comprising Portland cement and up to 5% of minor additional constituents
- **CEM II** Portland composite cement; comprising Portland cement and up to 35% of certain other single constituents
- **CEM III** Blastfurnace cement; comprising Portland cement and higher proportions of blastfurnace slag than in a CEM II cement.
- **CEM IV** Pozzolanic cement; comprising Portland cement and higher proportions of pozzolana than in a CEM II cement.
- **CEM V** Composite cement; comprising Portland cement and combinations of blastfurnace slag and pozzolana or fly ash.

The ES583 covered the sulfate resisting cement.

Cement Production in Egypt:

The construction sector in Egypt has grown rapidly since the 1990s due to the booming construction industry and increased government expenditure on infrastructure and major national projects (The Grand Egyptian Museum, The Nagga Hammadi Barrage and hydropower plant..etc). In 2000, the Egyptian construction market ranked 36th in the global construction markets, constituting 0.4% of this market, for a value of $12.711 billion [8]. At the same time, the Egyptian cement industry has undergone drastic change. Large extensions and upgrades to existing plants to raise production efficiency have been carried out accompanied by the privatization of government-owned companies and the sale of majority stakes to international and local investors; new private companies entering the market to establish their own plants; and multi-nationals acquiring a number of local companies. The result of upgrades and new capacities, in addition to the downturn of local consumption due to the general economic slump and the slowdown in construction activities, has been the emergence of a large surplus that has turned Egypt from a net importer to a net exporter to cement. Egypt's total cement production hits around 35 million tons annually while the local market's needs do not exceed 25 million tons [9]. In 2003, Egypt became a major exporter of cement. Egyptian producers succeeded in exporting more than 10m tons of cement and clinker over 2002 and 2003, with the same quantity through 2004, putting Egypt among the world's top exporters of cement [10]. Namely Egypt, Iran and Saudi Arabia constituted about 77% of total cement produced in the Middle East [11]. The global cement industry has been growing at an estimated 3% pa over the past

decade. Current global production is estimated at 1,900m mtpa. Of this, China produces 43%, while the whole Middle East produces less than 6%. In 2002, Egypt ranked 13th among the major cement producing countries. HC Brokerage has forecast that within the next few years Egypt will become one of the top five global exporters of cement. Egypt's production capacity has increased by almost 21% since 2001, reaching 36.2 million tons in 2004. Industry analysts estimate capacity will climb to 37.6 million tons in next few years. The historical production and consumption of cement in Egypt is plotted on Fig.1.

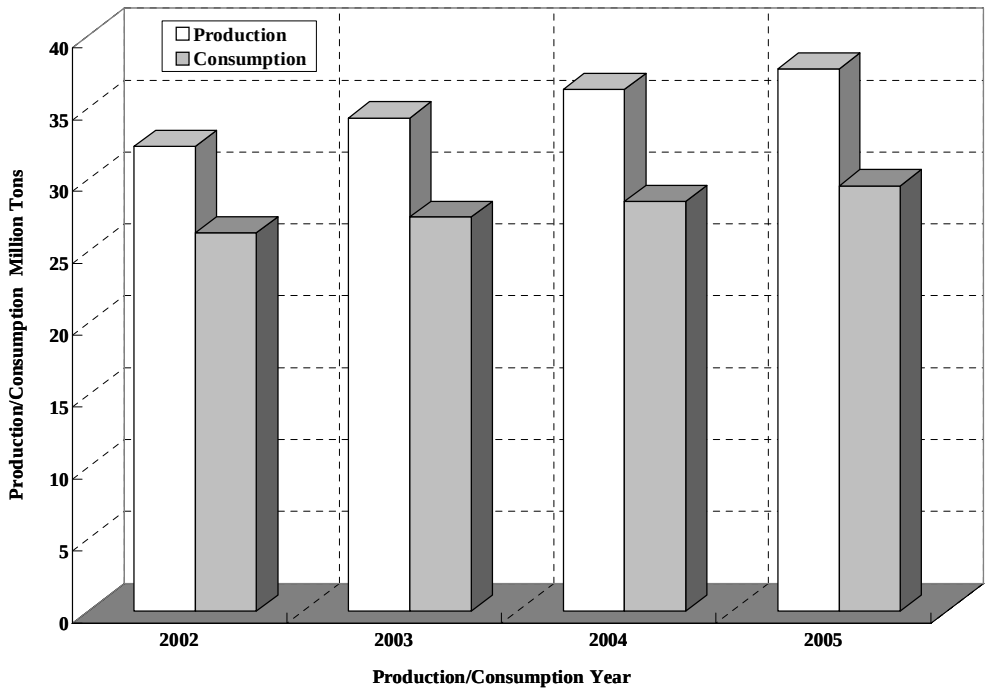

Fig. 1: Cement Production Vs Consumption in Egypt [12]

As it can be seen, the cement production is increasing gradually and recent trend analysis showed that it is likely to continue increasing in the few coming years. Egypt's cement sector was established in the 1927s following inauguration of the first cement plant (Tourah Cement Co). Currently, the Egyptian cement industry comprises twelve players with a production capacity of 35 million tons per annum, ranking 11th among the largest cement producing countries in the world. National, Quena and Misr Beni Suef are three main wholly-Egyptian key players in the Egyptian cement market. The government is controlling only one of the twelve cement companies operating in the country (National Cement Co.). Lafarge/Titan group, Holcim of Swizzerlamd, Italcementi of Italy and Cemex of Mexico are among the giant foreign companies that entered the local market. Italcementi Group has five production facilities (Suez, Kattameya, Tourah, ASEC and El-Minya), for a total capacity of approximately 12 million metric tons of clinker. Lafarge -Titan group has two production facilities (Alexandria Portland Cement and Beni Suef Cement Co.). Cemex has one production facilities Assiut Cement Co. Cimpore of Portugal has one production facilities Amreyah Cement Co. Holder Bank of Swizerland has Egyptian Cement Company. ASEC and Sinai Cement are the only two local producers in the white cement industry. ASEC Cement Company now has two white cement plants in Helwan and El Minya. Fig. 2 illustrates the nominal as well as actual production of cement players in Egypt during 2004 [18]. As it can be seen Suez Cement (as a group) is the largest producer with a production capacity of 7.85 million metric tons per annum, followed by the Egyptian Cement Company and Assuit Cement with production capacities 6.95 and 4.60 million tons respectively.

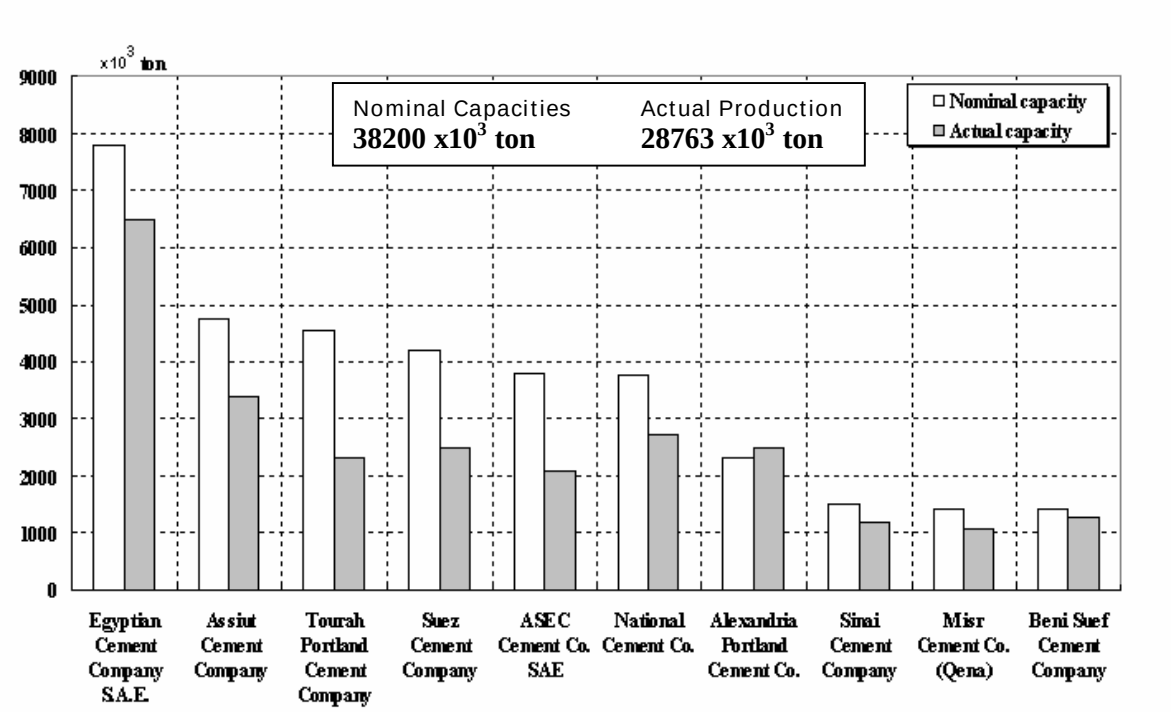

Fig. 2: Nominal and Actual Capacity of Cement Produced in Egypt During 2004 [12]

Egyptian Cement Types, Properties and Conformity:

After the six-moth transition zone of standard adaptation, cement companies has started producing several types of Portland cement in the market as per ES 4756/2005 (EN 197). Currently there are about 10 types of cements produced according to the ES 4756-1. Among the cements produced, Portland cement CEM I 42.5 N is by far the most common type used. In order to evaluate the properties of the cement available in the market, a survey work including total number of 380 random samples comprising 7 types of cement sampled from nine cement companies collected during the last eight months has been carried out. The statistical analysis is made which relies on the assumption that the cement properties are normally distributed about their mean value. For the purpose of analysis of test results, the statistical parameters Mean (X), range, standard deviation (S.D) and coefficient of variation (C.V.) are calculated. Only the strength property is included in the statistical study. The compressive strength of cement samples was carried out in accordance with ES 2421-7. On the basis of test results, the control charts for compressive strength at 2 and 7 and 28 days is presented through Figs. 3 to 9. Comparing the test results with the requirements of the ES 4756/2005, it is observed that all the samples complied with the requirements stated in the Egyptian standards for compressive strength at 2 or 7 and 28 days. For example, the lowest values of CEM I 32,5 N is higher than the minimum standard limit of 16 MPa at 7 days and the highest values at 28 days are lower than 52.5 MPa. Fig. 7 shows the compressive strengths for CEM I 42.5 N produced from 3 manufactures, referred to as F1, F2 and F3 in Table 2. As it can be seen, typical mortar prism strengths at the age of 2 and 28 days are in the average of 20, 21.5 and 21 and 55.8, 48.3 and 50.7 MPa respectively. This means that approximately 45% of the 28-days strength being achieved at 2 days while the typical mortar prism strength for CEM II B-S 32.5 N at the age of 7 and 28 days are in the average of 26.5 and 40.MPa respectively which means approximately 65% of the 28-days strength being achieved at 7 days. Table 2 lists the average, range, standard deviation and coefficient of variation for the types of cement produced. The low standard deviation and as a result the coefficient of variation denote the high quality control applied by the manufactures.

Table 2: Strength Properties of Cement used in the Study

Cement Type & Strength Class		CEM I						SRC	CEM II B-S
		32,5N	32,5 R	42,5 N			42,5 R	32,5 R	32,5 N
				F1	F2	F3			
Number of samples		30	30	30	30	30	60	30	40
2-days-MPa	Minimum value		19.6	19.8	20.2	20.8	21.2	18.9	
	Maximum value		21	20.4	22.8	22.9	25.4	20.3	
	Average, x		20.1	20	21.5	22.4	22.2	19.9	
	Range		1.4	0.60	2.6	2.1	4.2	1.4	
	Standard deviation,		0.26	0.17	0.42	0.53	0.77	0.32	
	Coefficient of variation,%		1.3	0.8	1.9	2.4	3.5	1.6	
7-days- MPa	Minimum value	28.3							21.5
	Maximum value	30.6							33
	Average, x	29.6							26.5
	Range	2.3							11.5
	Standard deviation	1.43							2.99
	Coefficient of variation, %	4.8							11.3
28-days- MPa	Minimum value	39	41.4	53.9	44.2	48.3	46.6	38.7	37.3
	Maximum value	44.1	43.7	58.5	49.4	52.7	50.3	46.2	42.1
	Average, x	42.2	42.7	55.8	48.3	50.7	48.9	43.9	40.1
	Range	5.1	2.3	4.6	5.2	4.4	3.7	7.5	4.8
	Standard deviation	1.25	0.56	0.90	0.91	0.93	0.68	1.5	1.00
	Coefficient of variation,%	2.9	1.3	1.6	8	1.8	1.4	3.4	2.5

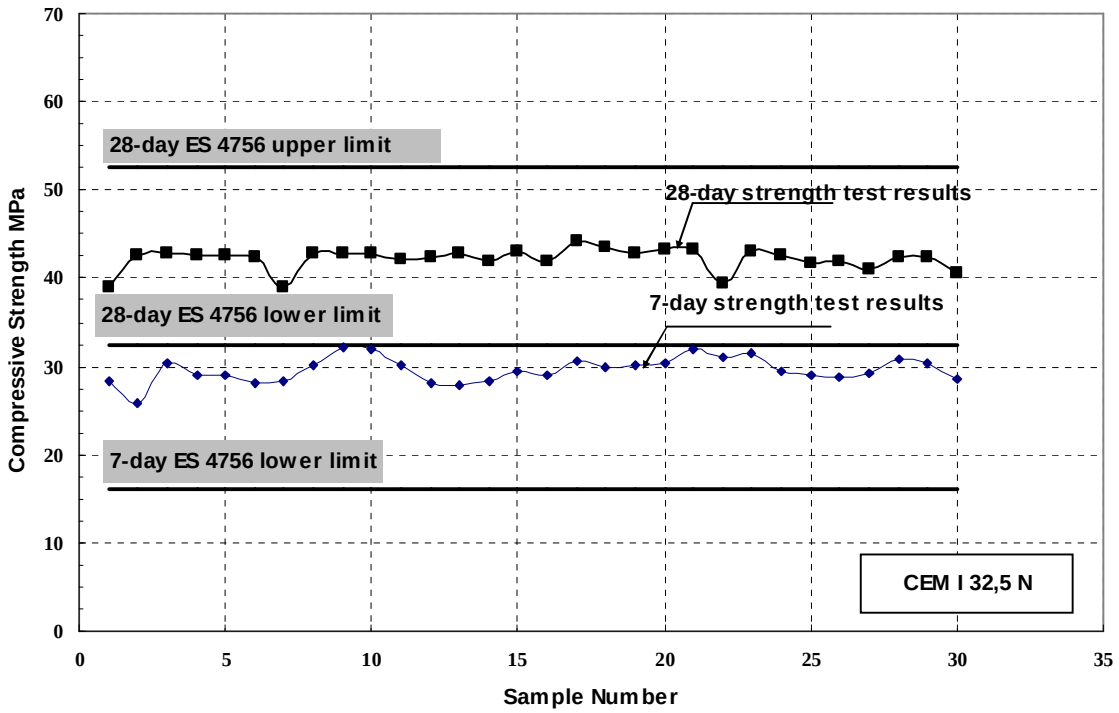

Fig. 3: 7 and 28 day Compressive Strength for CEM I 32,5 N

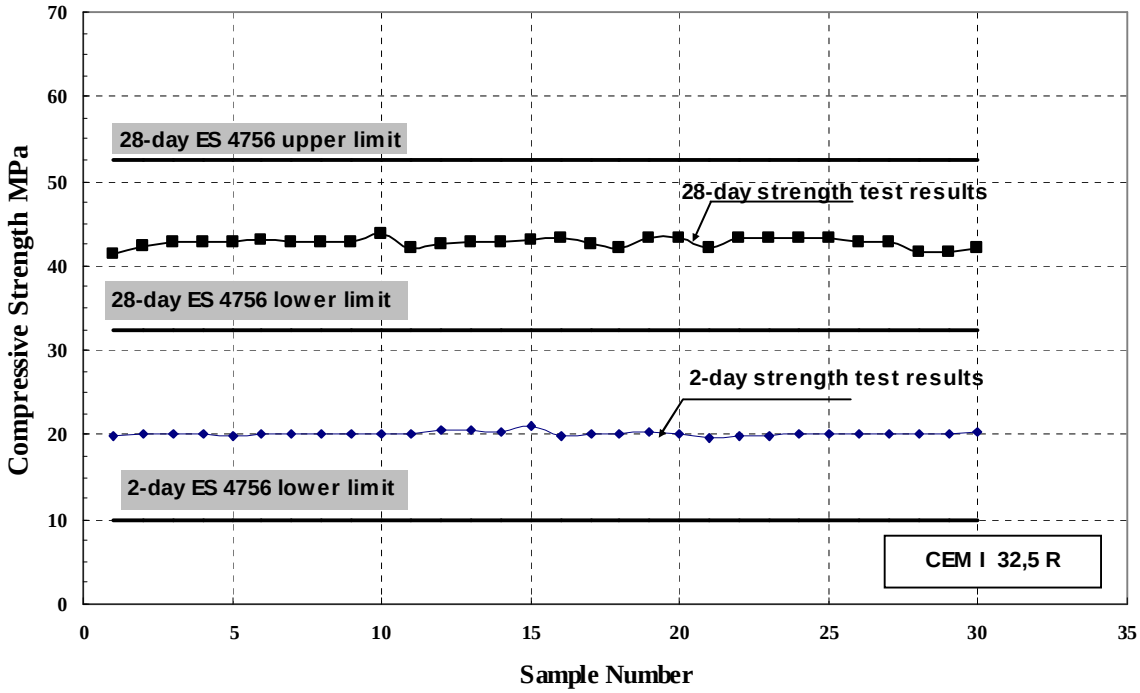

Fig. 4: 2 and 28 day Compressive Strength for CEM I 32,5 R

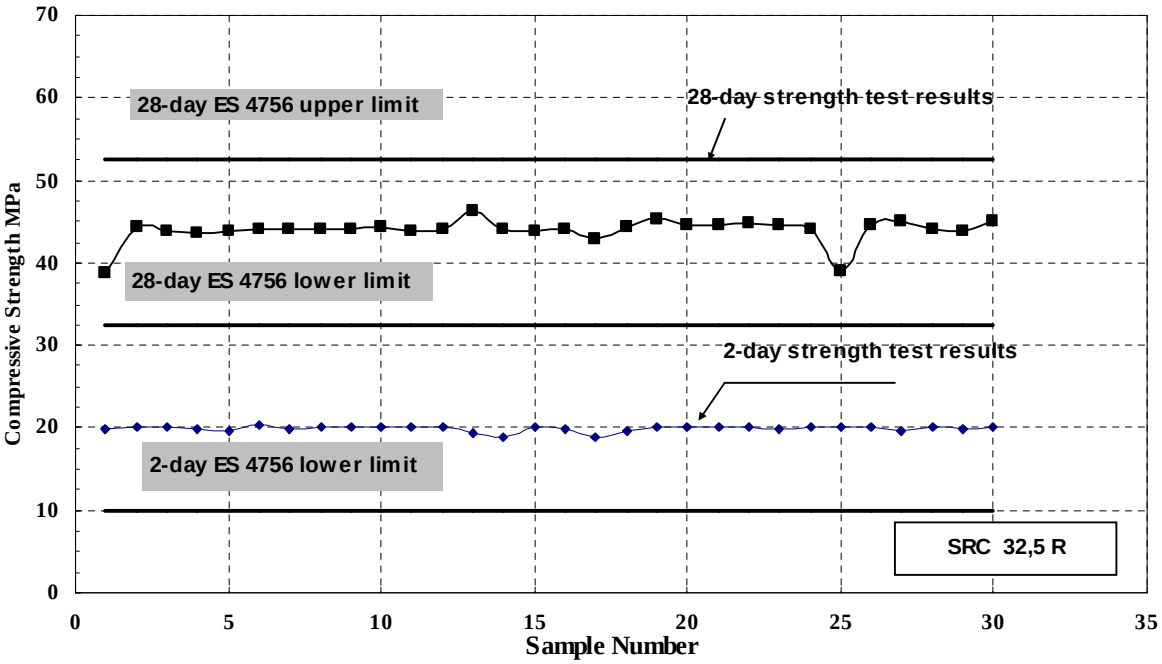

Fig. 5: 2 and 28 day Compressive Strength for SRC I 32,5 R

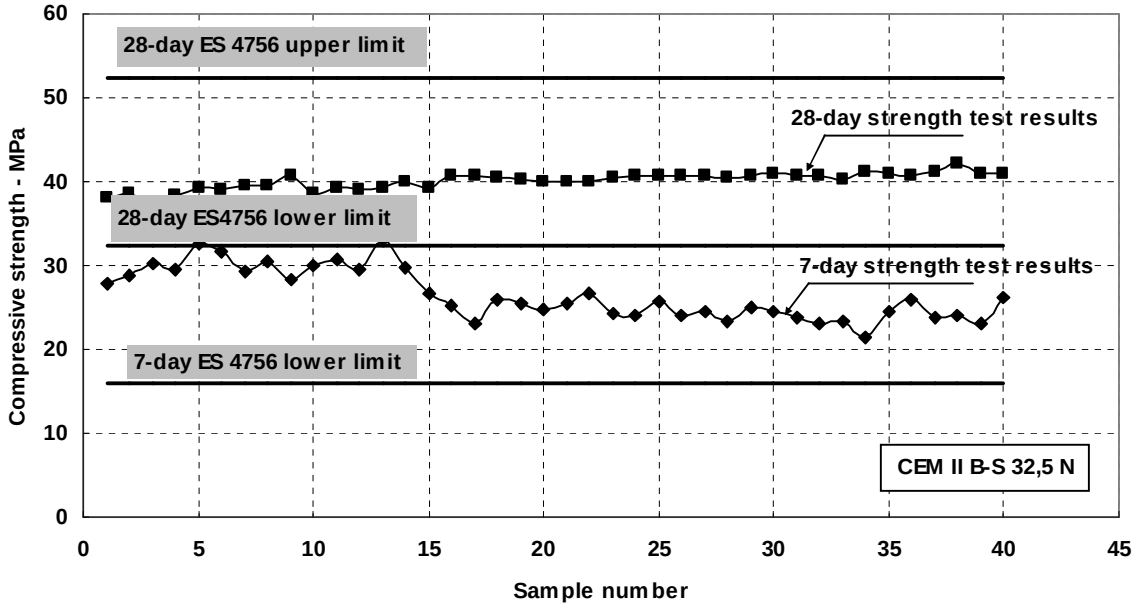

Fig. 6: 7 and 28 Day Compressive Strength for CEM II B-S 32,5 N

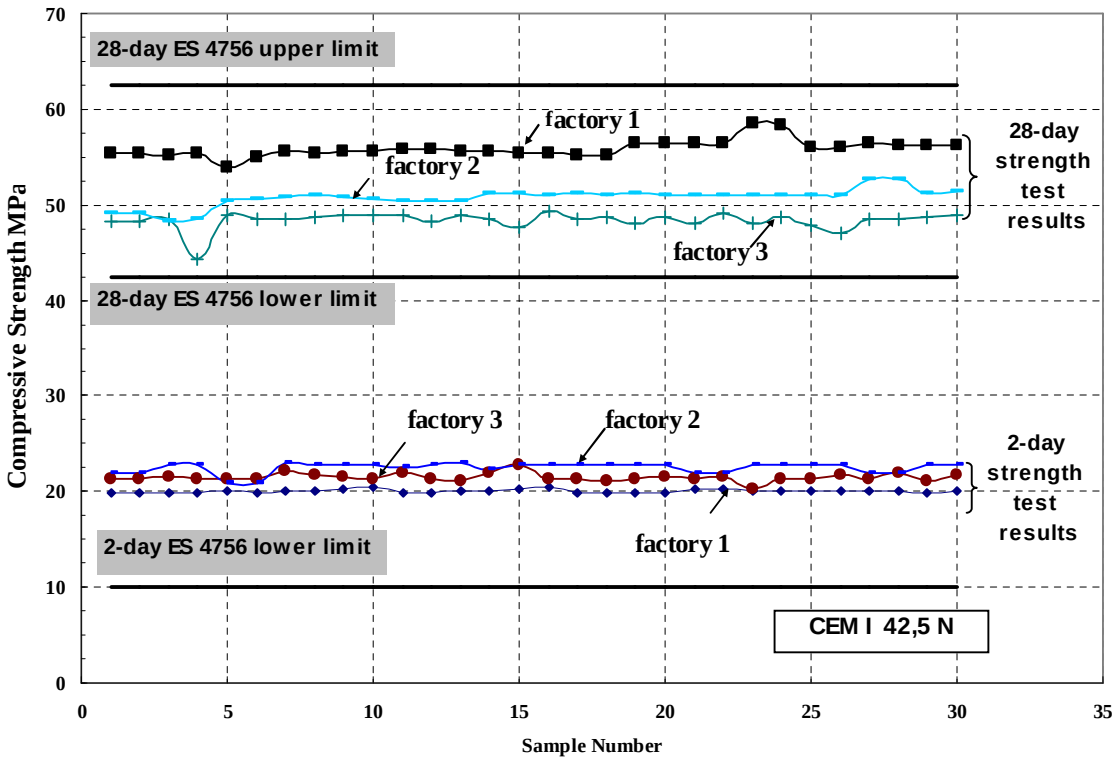

Fig. 7: 2 and 28 Day Compressive Strength for CEM I 42,5 N

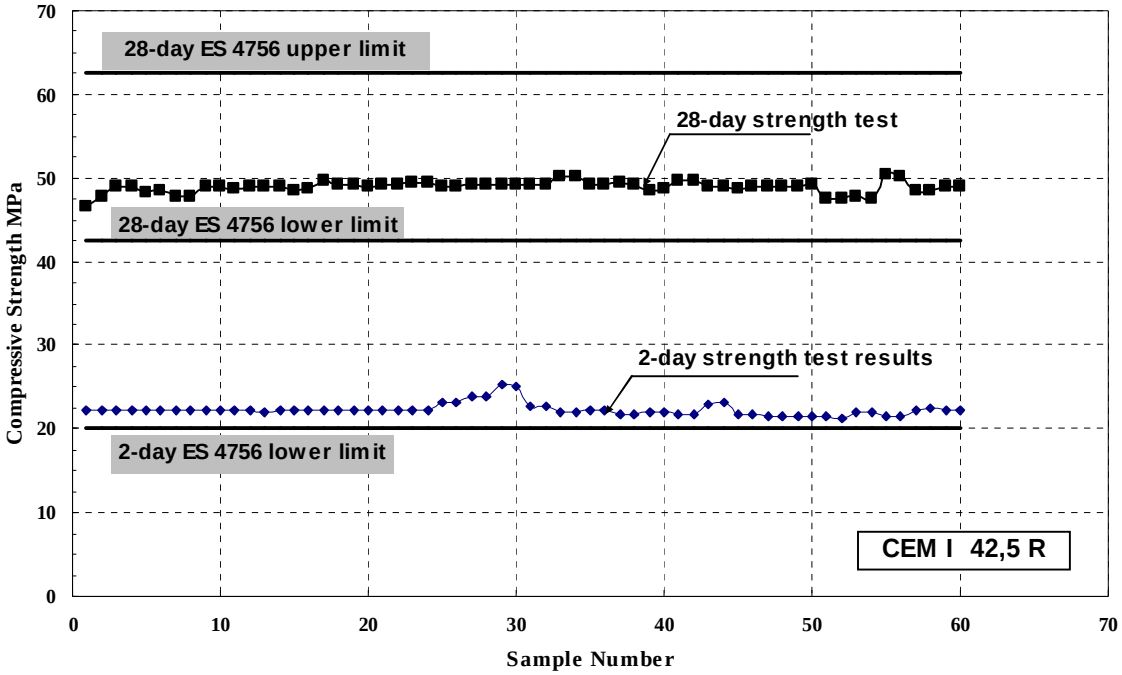

Fig. 8: 2 and 28 Day Compressive Strength for CEM I 42,5 R

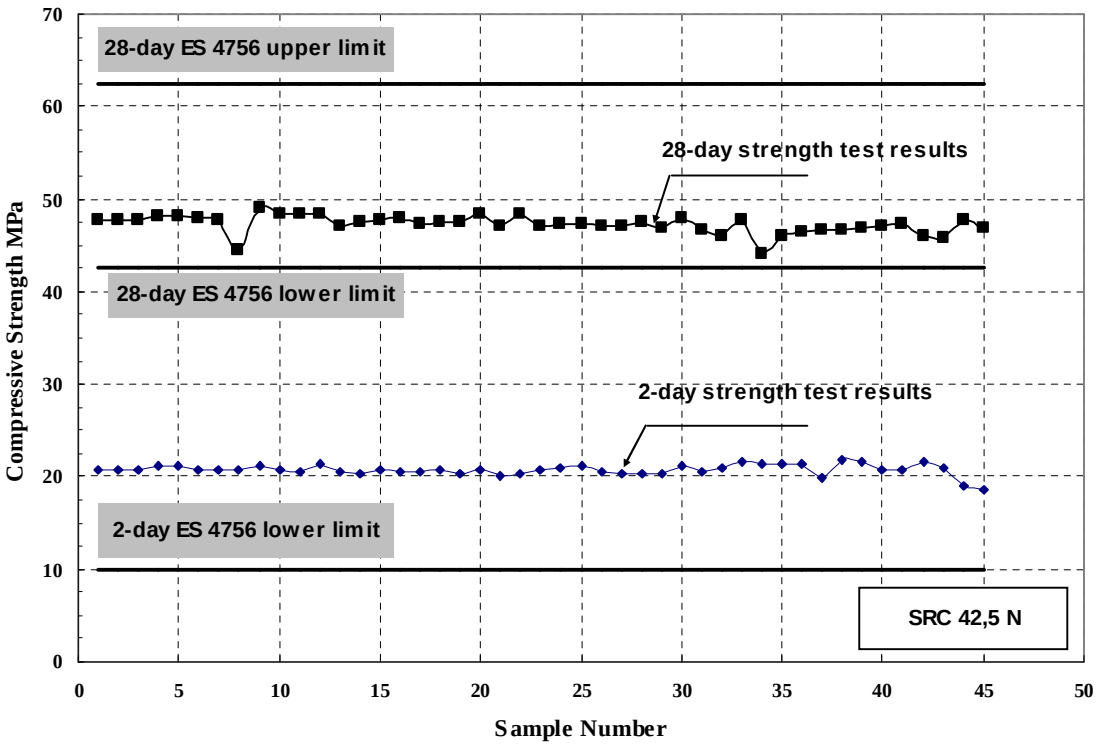

Fig. 9: 2 and 28 Day Compressive Strength for SRC 42,5 N

Withdrawn ES 2421/1993 Vs New ES 2421/2005:

A comparative study of mortar compressive strength was carried out in order to evaluate the difference between the old withdrawn ES 2421/1993 [13] and its relevant standards and the new standard ES 2421/2005 [14] upon measured mechanical properties of the resulting mortar specimens. In the withdrawn ES 2421/1993, the compressive strength is evaluated by directly subjecting the cube specimens (70.7 mm) to compressive load, where as in ES 2421/2005, the standard mortar prism (40x40x160 mm) is first broken to two halves by flexural test, and then each half prism is subjected to compressive stress by distributing the axial compressive stress on the specified area on the two plane faces (40x40 mm). The testing program included a total of 7 different cement types CEM I 32,5 N, CEM I 32,5 R, SRC 32,5 R, CEM II B-S 32,5 N, CEM I 42,5 N, CEM I 42,5 R, CEM I 52,5 N chosen from five different manufacturers. The strength classes investigated represent the strength classes mostly used in the construction industry. The study covered the influence of different factors, such as the grading of the sand and the size of the mould. Four sets of mortars from each cement type were prepared: C (for cubes), and P (for prisms). In C and P mortars 2 different sands were used, both conforming to ES 2421/2005 (N) and ES 2421/1993 (O) requirements. Mixing and compaction of mortars of set CN and set CO samples were carried out as per the method described in ES 2421/1993 while mixing and compaction of mortars of set PN and PO samples were carried out as per ES 2421/2005 requirements. After the compaction procedure, the moulds were placed in the humidity cabinet for 24 hours at the relative humidity of 95% and the temperature of 20^{o}C. Following this period, the specimens were removed from the moulds and kept in water until the testing date. Strength development was measured at 2, 3, 7, 28, 56 and 90 days curing. Table 3 shows the composition of some cements examined in the present work.

Table 3: Chemical Analysis of some of the Tested Cements

Oxide	CEM I 32,5 N	CEM I 32,5 R	CEM I 42,5 N	ES limits	CEM I 42,5 R	ES limits
SiO_2	19.75	19.75	20.12		20.31	
Al_2O_3	4.12	5.25	5.61		5.62	
Fe_2O_3	3.82	3.41	3.37		2.68	
CaO	64.11	62.85	63.35		61.62	
MgO	1.67	2.44	1.18		1.76	
SO_3	2.39	2.49	2.36	≤ 3.5 %	2.54	≤ 4 %
L.O.I.	3.02	2.35	2.65	≤ 5 %	3.82	≤ 5 %
I.R.	0.71	0.93	0.81	≤ 5 %	0.81	≤ 5 %
Na_2O	0.37	0.42	0.39		0.41	
K_2O	0.08	0.06	0.07		0.17	
Total	99.94	99.95	99.91		99.74	
Cl^-	0.04	0.05	0.05	≤ 0.10 %	0.04	≤ 0.10 %
Na_2O Eq.	0.42	0.46	0.44	≤ 0.60 %	0.53	≤ 0.60 %
LSF	1.00	0.96	0.95		0.92	
C_3A	4.46	8.15	9.17		10.36	

L.O.I.= loss on ignition, I.R. = insoluble residue,

Figures 10 to 16 show the compressive strength development of cement mortar specimens of CEM I 32,5 N, SRC 32,5 R, CEM II B-S 32,5 N, CEM I 32,5 R, CEM I 42,5 N, CEM I 42,5 R, CEM I 52,5 N, respectively, prepared and tested as per ES 2421/1993 and ES 2421/2005. As it can be seen from the figure, the 7-days and 28-days strength of cube mortar specimens (70.7 mm) were found to be higher than the strength of prism mortar specimens (40x40x160mm). For cement CEM I 32.5 N, typical mortar cube strengths for specimens CO at the age of 7 and 28 days are in the average of 45 and 54 N/mm^2 respectively while the typical mortar prism strengths (PN specimens) at the age of 7 and 28 days are in the average of 30 and 42 MPa which means that cement mortar prism compressive strength is equal approximately to 70% of the cement mortar cube compressive strength. With regard to the other types, the ratio of 7 and

28 days strength of PN mortar specimens to 7 and 28 days strength of CO mortar specimens were found to be 55 % and 70 % for SRC 32 R, 75% and 85%. For CEM II B-S 32,5 N, 90% and 70 for CEM I 32,5 R, 85% and 95% for CEM I 42.5 N, 85% and 95% for CEM 42,5 R, 90% and 95% CEM 52,5 N. Fig 17 shows the regression line for the best fitting of the test results. The linear regression equation obtained by computer software is:

Cement mortar prism compressive strength = 1.0317(x) – 8.22 ……..MPa
Where x = cube mortar compressive strength

The test results clearly indicated that the cements produced according to the new standard ES 4756 are meeting the strength requirements stated in the old withdrawn standard ES 373 and it's relevant.

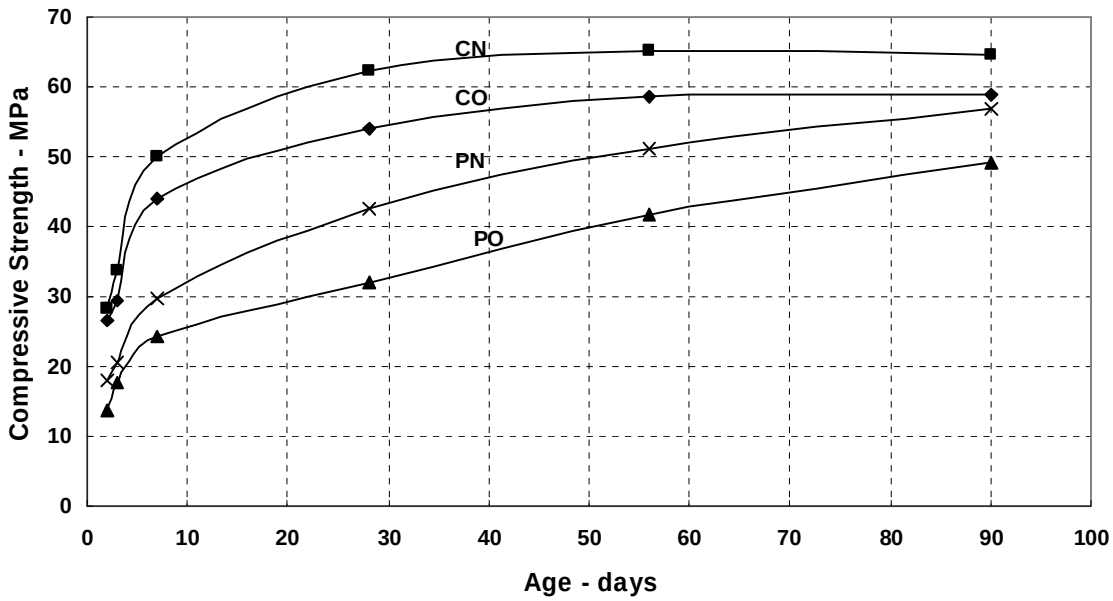

Fig. 10: Effect of Mould Size and Sand on CEM I 32,5 N Strength Development

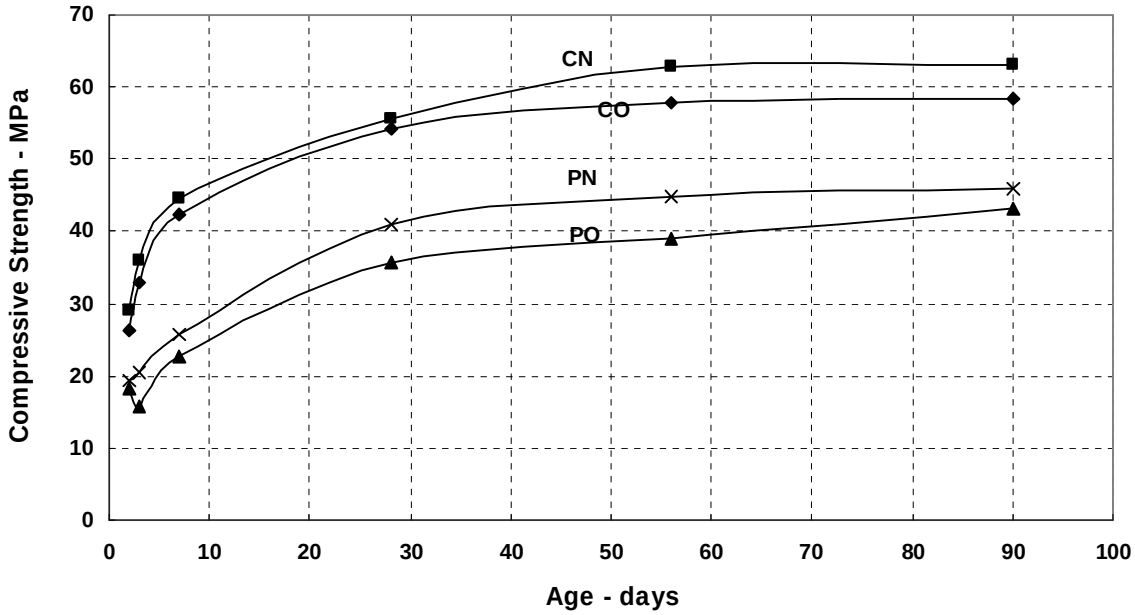

Fig. 11: Effect of Mould Size and Sand on SRC 32,5 R Strength Development

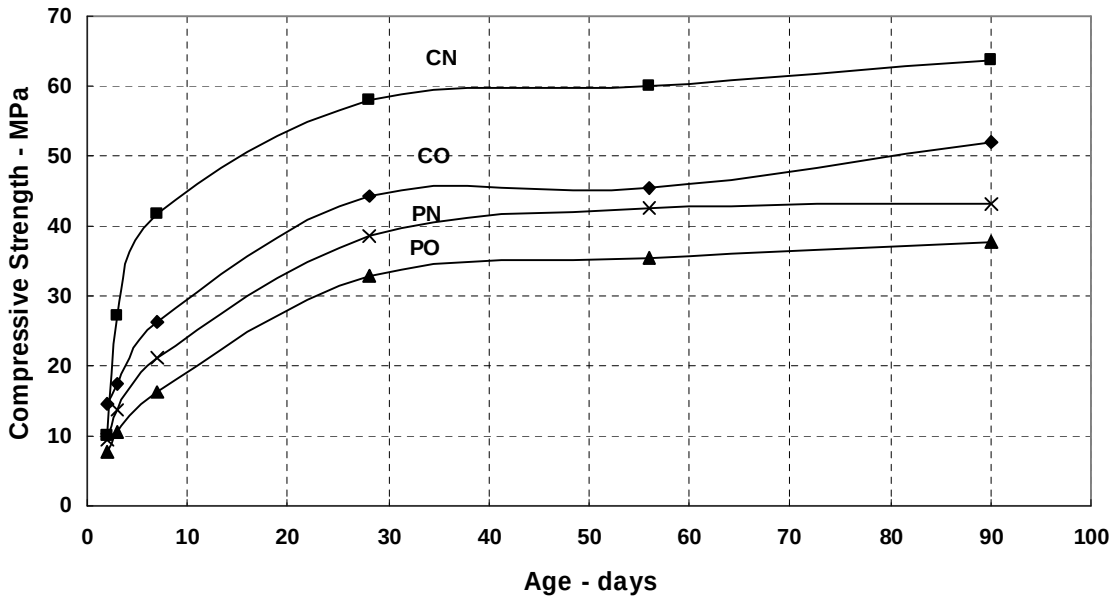

Fig. 12: Effect of Mould Size and Sand on CEM II B-S 32,5 N Strength Development

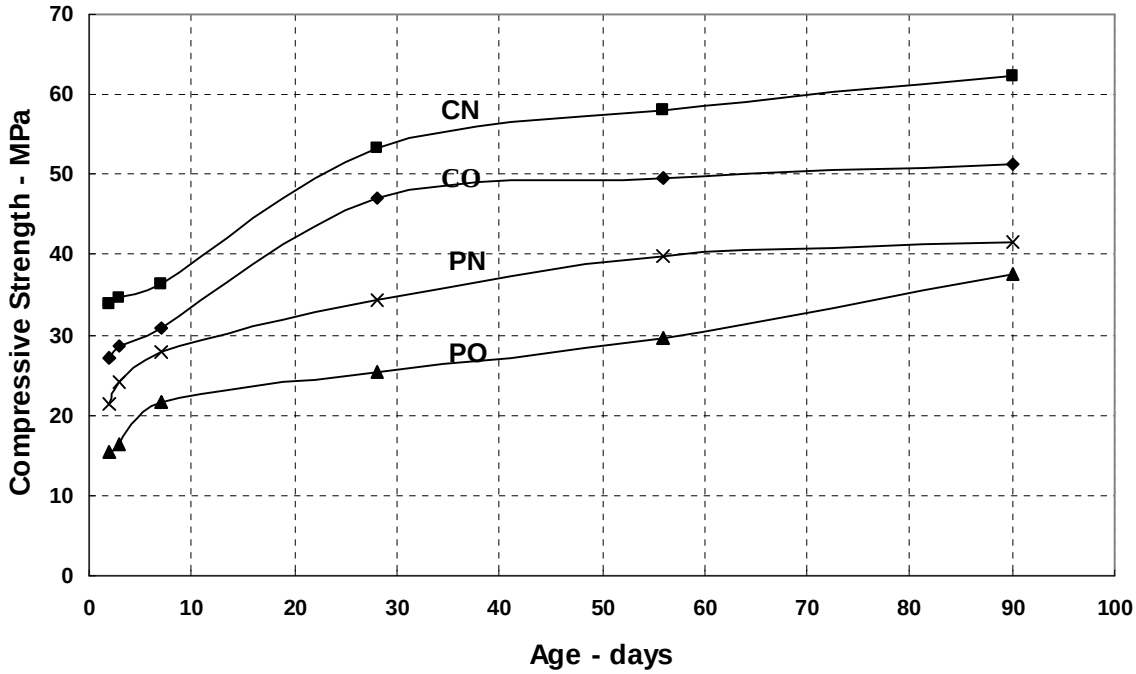

Fig. 13: Effect of Mould Size and Sand on CEM I 32,5 R Strength Development

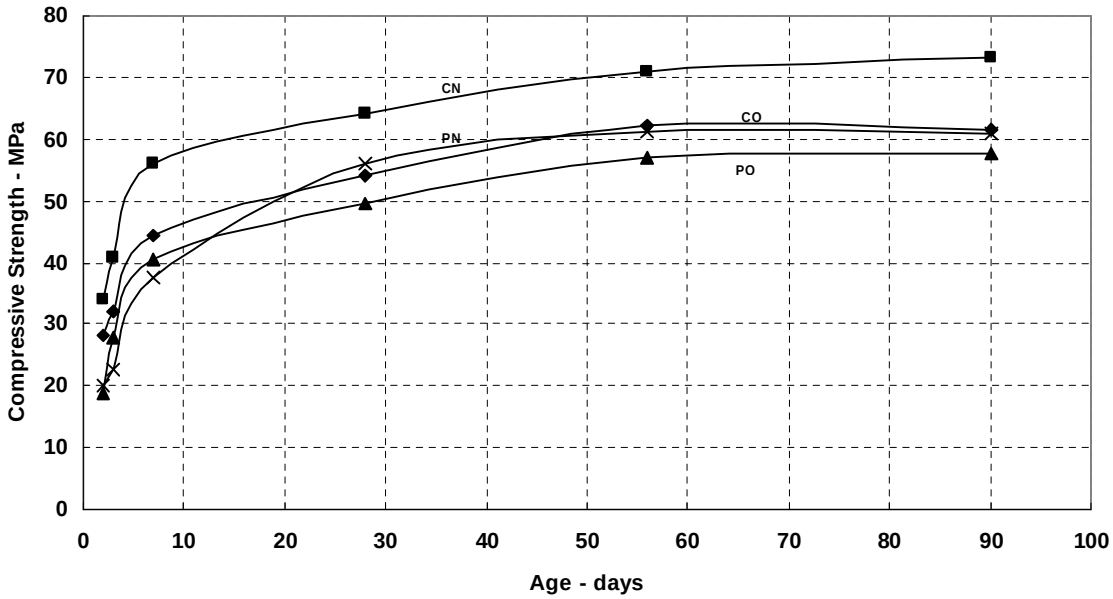

Fig. 14: Effect of Mould Size and Sand on CEM I 42,5 N Strength Development

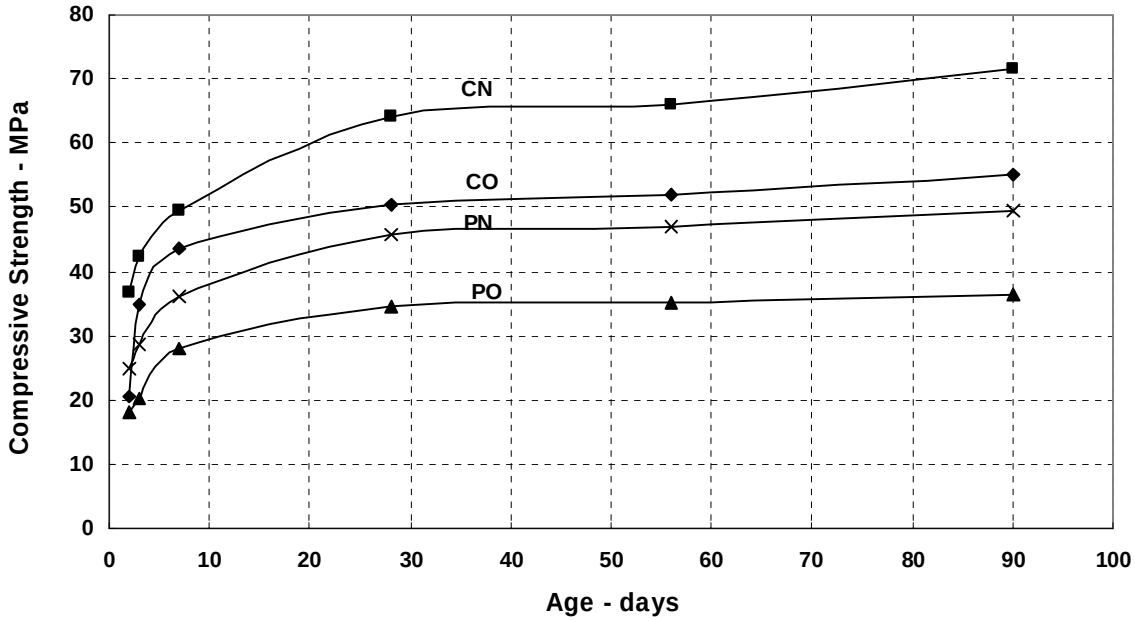

Fig. 15: Effect of Mould Size and Sand on CEM I 42,5 R Strength Development

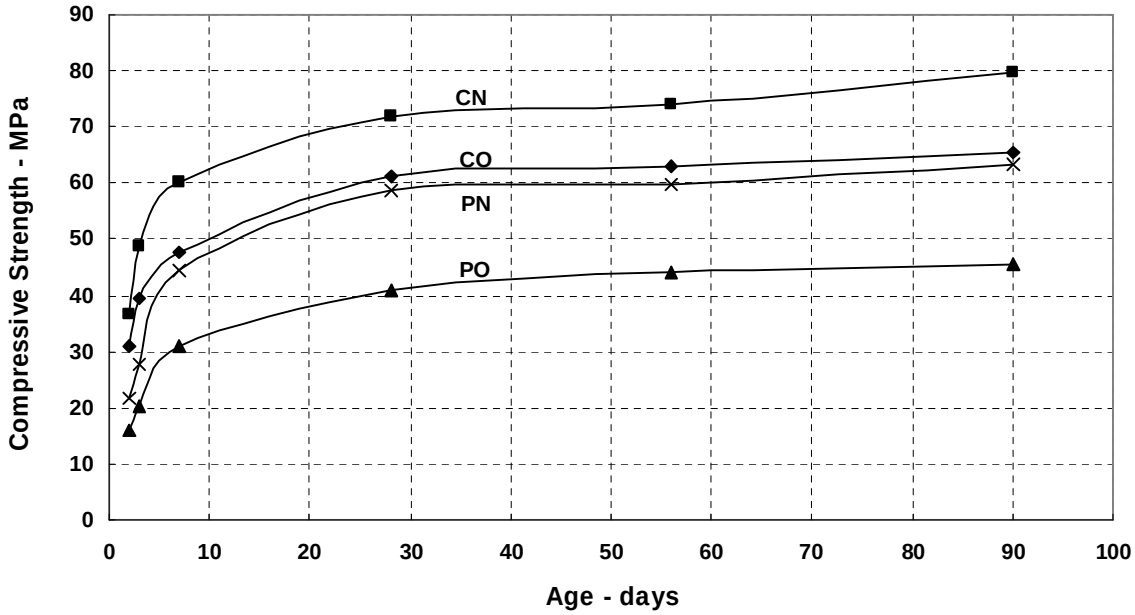

Fig. 16: Effect of Mould Size and Sand on CEM I 52,5 N Strength Development

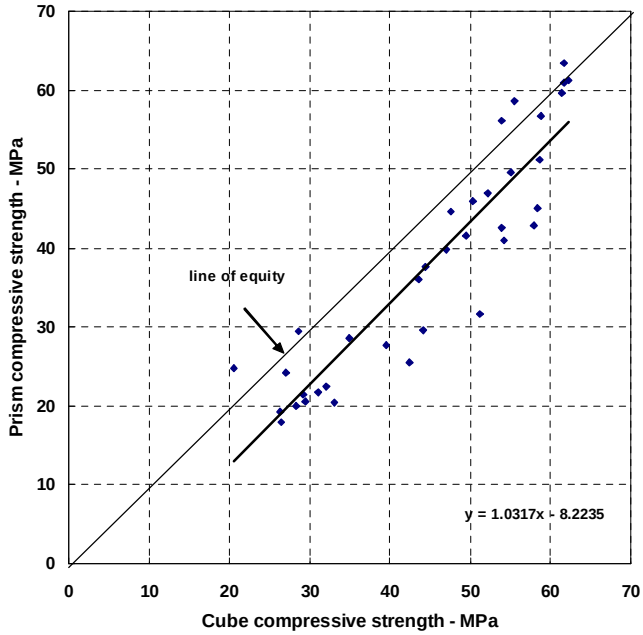

Fig. 17: Test Results and Regression Line for the Tested Cements

Conformity Evaluation:

To evaluate the conformity of the cement produced to the requirement of ES 4756/1 (EN 197-1), a total number of 32 random samples of CEM I 42.5 N from one cement company were selected. The conformity was conducted since the adaptation of the new standard. The conformity is based upon inspection by variables. Conformity is verified when equations (1) and (2), as relevant, are satisfied:

$\overline{x} - k_A * s \geq L$ .....(1) and
$\overline{x} + k_A * s \leq U$ .....(2) where

$\overline{x}$ is the arithmetic mean of the totality of the autocontrol test results in the control period;
s is the standard deviation of the totality of the autocontrol test results in the control period;
k_A is the acceptability constant;
L is the specified lower limit and
U is the specified upper limit

Comparing the test results with the requirements stated in the Egyptian Standards ES 4756/2005, it can be seen from Fig.18 that the test results lie within the acceptable limit of ($\overline{X} \pm k_A * s$) i.e. 10 N/mm^2 , 42.5 MPa and 62.5 10 MPa.

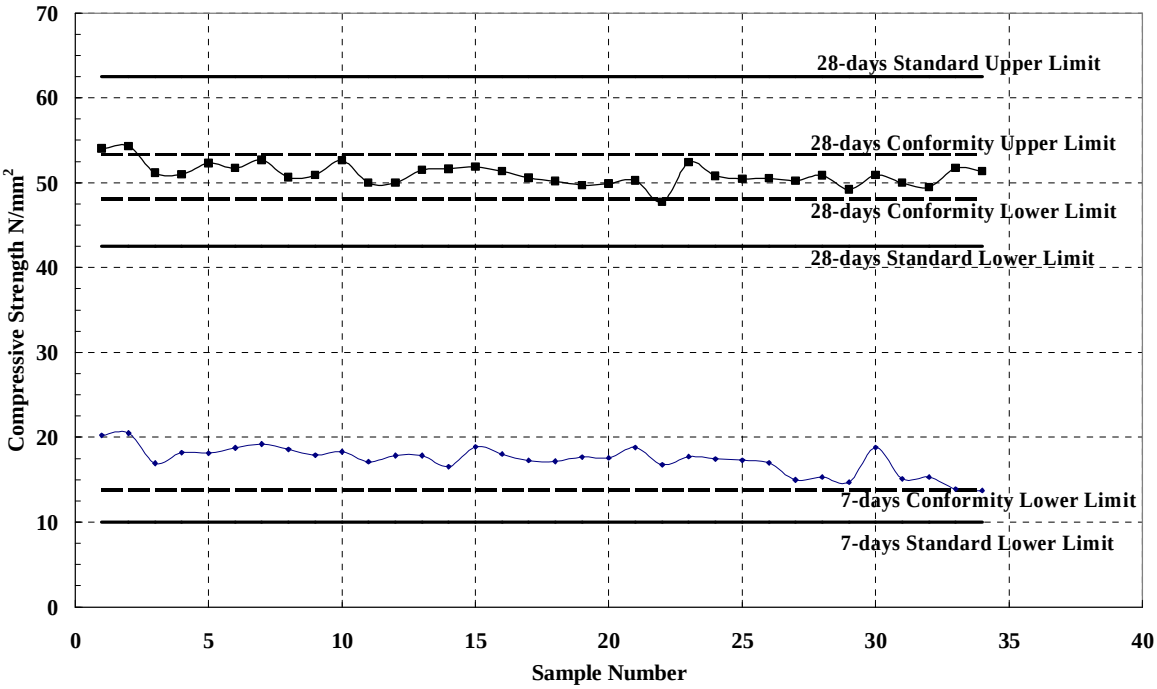

Fig. 18: Conformity of CEM I 42.5 N

CONCLUSIONS:

The following conclusions can be drawn from the current study:

- Test results of 380 samples - collected during the last six months from 6 companies - comprising 7 types of cement (CEM I 32,5 N, CEM I 32,5 R, SRC 32,5 R, CEM II B-S 32,5 N, CEM I 42,5 N, CEM I 42,5 R, SRC 42,5 N) mostly used in the construction industry complied with the requirements stated in the Egyptian standards for compressive strength at 2 or 7 and 28 days.
- Within the range of the tested specimens in the comparison study, the cement types produced according to the new standard ES 4756 and prepared and tested according to the withdrawn standard ES 2421/1993 were found to meet the strength requirements of the withdrawn ES 373.
- More research is still needed with regard the investigation of the durability performance of the new cements in sever environment to adopt the applications to be used in the construction industry.

REFERENCES

1. Egyptian Standards ES 373/1991 (1991) "Ordinary Portland Cement and Rapid Hardening Cement " Egyptian Organization for Standards & Quality, Arab Republic of Egypt.
2. British Standard Institution BS 12/ 1989 " Specifications for Ordinary Portland cement and Rapid Hardening Portland Cement" BSI , London, UK
3. European Committee for Standardization CEN/TC 51, EUROPEAN STANDARD EN 197-1 (2000) "Cement - Part 1: Composition, specifications and conformity criteria for common cements
4. Egyptian Standards ES 4756-1/2005 (2005) "Cement Part 1: Composition, Specifications and Conformity Criteria for common cements" Egyptian Organization for Standards & Quality, Arab Republic of Egypt.

5. Egyptian Standards ES 4756-2/2005 (2005) "Cement Part 2: Conformity Evaluation" Egyptian Organization for Standards & Quality, Arab Republic of Egypt.
6. Egyptian Standards ES 583/2005 (2005) "Sulfate Resisting Cement" Egyptian Organization for Standards & Quality, Arab Republic of Egypt.
7. The Environmental Technology Evaluation Center (2001) “Guidelines for the Evaluation of Innovative Cement Technologies” Pennsylvania Department of Environmental Protection, Harrisburg, PA 17105-2063
8. American Chamber Of Commerce in Egypt Am. Cham. BSAC (2003) " The Construction Sector in Egypt: Development and Competitiveness" Business Studies & Analysis Center
9. Construction sector , http://www.presidency.gov.eg/html/construction_sector_1.html.
10. Omayra Bermúdez-Lugo (2003) "The Mineral Industry of Egypt" U.S. Geological Survey Minerals Yearbook.
11. HSBC Bank Middle East Limited (2005) “Cement industry in the GCC” www. research.hsbc.com
12. Arab Union for Cement and Building Materials (2005) " Arab Republic of Egypt -cement figures:2005
13. Egyptian Standards ES 2421-3/1993 (1993) "Cement – Physical and Mechanical Tests Part 3 – Test of Compressive strength" Egyptian Organization for Standards & Quality, Arab Republic of Egypt.
14. Egyptian Standards ES 2421-7/2006 (2006) "Cement – Physical and Mechanical Tests Part 7 – Determination of Strength Prism Method" Egyptian Organization for Standards & Quality, Arab Republic of Egypt.

LOAD SHARING OF MASONRY PANELS WITHIN REINFORCED HIGH STRENGTH CONCRETE SYSTEMS

Ahmad M. R. Moubarak
Expert Engineer in the Ministry of Justice

Salah El-Din Fahmy Taher
Director, Higher Education Enhancement Project Fund, HEEPF, Ministry of Higher Education and state for Scientific Research. Professor of Concrete Structures, Faculty of Engineering, Tanta University, Egypt.

ABSTRACT

Existence of infill has a direct effect on the system behavior and the transmission of internal forces. However, data about load sharing characteristics in frames made of high strength concrete is still limited. In this study, an experimental and numerical program has been performed using high strength concrete taking in our consideration the effect of infilled frames, inclusion of side columns, the method of construction of upper beam of the system and the masonry strength, in order to establish the salient features of the behavior of the system, modes of failure, deformational characteristics and strain development. To conduct an extensive parametric study, nonlinear three-dimensional finite element analysis has been carried out. The computational model has been verified against several experimental testing. The numerical work aimed at providing more insight about the behavior and load path of the composite systems.

KEYWORDS: Reinforced concrete, Masonry, High strength concrete, Experimental, Nonlinear finite element.

INTRODUCTION

Although, many researches have focused on the composite behavior of RC frames made of ordinary strength concrete with masonry infill, the studies related to systems made of high strength concrete are still scarce and need further consideration. Composite masonry walls supported on reinforced concrete beam are commonly used in traditional buildings either as load-bearing walls stiffened by beams, or space divider in-fill loaded on the beam. With the increasing use of masonry as a load-bearing material because of many advantages and the great possibility of major wall-beam structures, it is essential to know more accurately the behavior of the system [1]. A masonry wall loading a beam changes the distribution of the external load on the beam and concentrates the load over the support, thus relieving the middle portion. A general theoretical investigation of the composite beam-wall action and its application to the particular case of the foundation beam have shown that the wall behaves like a tall girder, with tension concentrating in the beam (which acts as a tension tie) and compression being distributed along the height of the wall [2].

There are many similarities in the behavior of the masonry and concrete. Like concrete, masonry is good at resisting compression, not so good at resisting pure shear, and not very good at all at resisting tension [3]. The compressive strength of units is determined from 'single unit' tests wherein individual units are compressed between the platens of a testing machine. The strengths determined in single unit tests do not reflect directly in masonry strength. This is not because of the platen effect in single unit tests alone, but also because of the effect of the mortar in the masonry [3].

Rosenhaupt [4] presented experimental study of masonry walls on beam. The effect of wall height, reinforcement ratio in foundation beam, masonry material and inclusion or non-inclusion of ties at the vertical wall edges was investigated. The wall height determined the moment of inertia, and, therefore, the magnitude of the deflection. Also, the masonry had a major effect on the characteristics of the structure behavior and the inclusion of ties reduced the deflections in the elastic stage and increased the failure resistance of the wall.

In this paper, an experimental investigation on composite masonry panels and reinforced concrete girders were carried out in order to study their behavior and the transmission of internal forces. The forces are transmitted through the masonry panels where the existence of masonry, side columns at the wall edges and the method of construction affect on the ultimate capacity, failure mode and the crack pattern of the system. Furthermore, an elaborate finite element analysis is made to investigate other parameters including the stiffness characteristics of wall panel relative to the RC skeleton.

RESEARCH FRAMEWORK

Six experimental and eighteen numerical specimens were studied in this research divided into five groups to study the load sharing of masonry panel with different cases of concrete grade, masonry strength, inclusion of side columns of the system and the method of construction of upper beam under vertical loading as shown in Table (1).

Table 1: Summary of Research Specimens

Group	Objective	Specimen	Methodology		fcu, Concrete Grade (MPa)	fcm, Masonry Strength (MPa)
			Exp.	F.E.		
G0	Beam behavior	G0-1	P	P	70	6
		G0-2	P	P	70	6
GI	Effect of infill load sharing	GI-1	P	P	72	6
		GI-2	P	P	70	6
GII	Effect of inclusion of side columns	GII-1	P	P	74	6
		GII-2 *	P	P	70	6
GIII	Effect of the method of construction of upper beam	GIII-1*	P	P	70	6
		GIII-2	P	P	75	6
GIV	Effect of concrete grade	GIV-1	—	P	25	6
		GIV-2	—	P	45	6
		GIV-3	—	P	80	6
		GIV-4	—	P	125	6
GV	Effect of masonry strength	GV-1	—	P	70	2
		GV-2	—	P	70	6
		GV-3	—	P	70	10
		GV-4	—	P	70	15

* Exactly similar to GI-2. Exp. = Experimental. F.E. = Finite element.

EXPERIMENTAL PROGRAM

Six full-scale test specimens were made of high strength concrete. One of these specimens were built as a bare reinforced concrete frame. Another was built without side columns. The others were built with side columns including two methods of construction of the upper beam of the system as shown in Fig.(1). Conventional reinforcement detailing as commonly used in residential buildings was fabricated for all case studies. This means no special detailing for framing action was made and rebars similar to G0-1 were adopted. Nominal yield stress of reinforced was 360 and 240 MPa for main steel and stirrups, respectively. The mix proportions for 1m of concrete consisted of 500 kg ordinary Portland cement , 1100 kg granite as coarse aggregate, 600 kg sand as fine aggregate and 5 liters of Glenium C315 as superplastizer admixture with water cement ratio 0.26. The admixture was used in order to attain acceptable level of workability of the fresh concrete.

Six masonry prism panels were cast according to ASTM [5] provisions and were tested under axial compression to determine the compressive strength of the masonry assemblage as shown in Fig. (2). Standard cylinders, were cast from the concrete used and were tested under compression to determine their compressive strength. Fig. (3) shows the mode of failure of concrete cylinders.

The variables studied have been the effect of side columns at the edges of the wall and the method of the construction of the upper beam of the system.

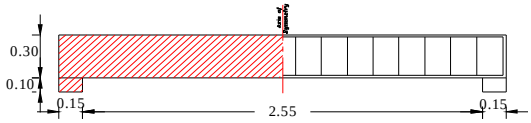

Fig. (1-a) Details of specimen G0-1.

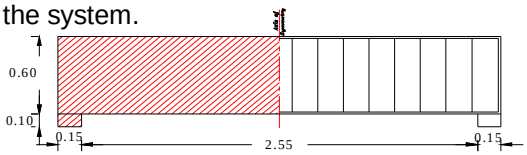

Fig. (1-b) Details of specimen G0-2.

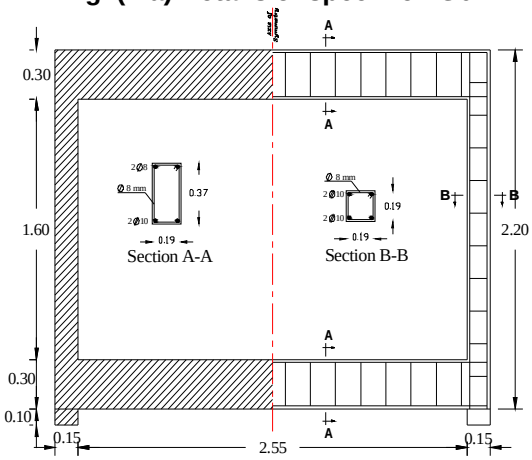

Fig. (1-c) Details of specimen GI-1.

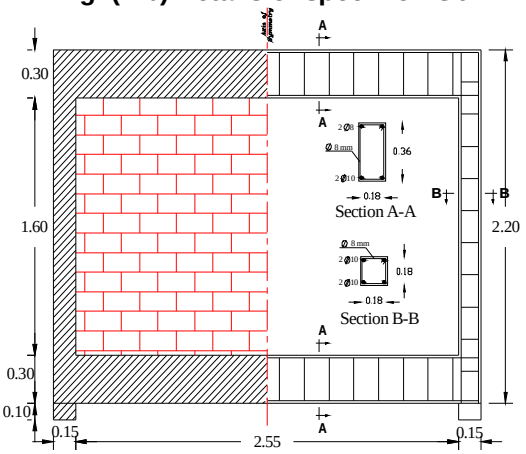

Fig. (1-d) Details of specimen GI-2.

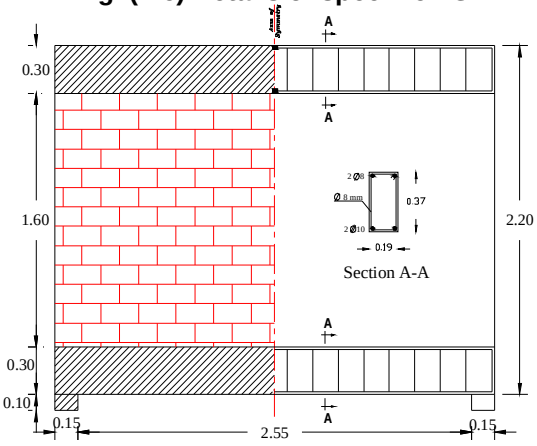

Fig. (1-e) Details of specimen GII-1.

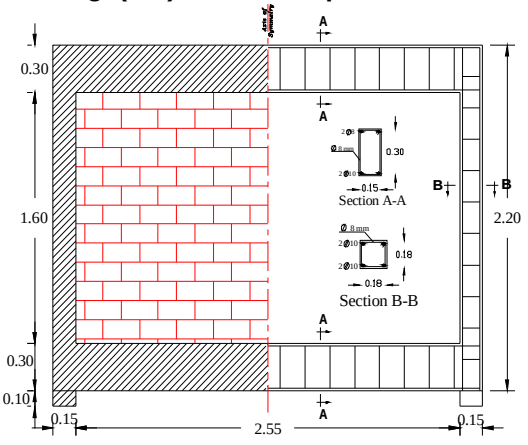

Fig. (1-f) Details of specimen GIII-2.

Fig. 1: Details of Test Specimens.

All concrete specimens were cast in steel mold and electrical strain gages were mounted on the reinforcement at several positions and demecs were glue on the concrete and wall panels at several positions. Fig.(4) shows the method of the construction for the upper beam of the system.
The test program was performed in the testing frame as shown in Fig. (5). Two concentrated loads were applied to the specimen incrementally by using a testing machine up to failure and measured by the load cell attached to the jack. Reading of strain gauges and load cells were monitored by strain-meter. A dial gauge was placed vertically at middle of the beam to measure the vertical deflection.

Fig. 2: Testing of Masonry Prism.

Fig. 3: Failure Mode of High Strength Concrete Cylinder.

Fig. 4-a: The Method of the Construction of Specimen GI-2.

Fig. 4-b: The Method of the Construction of Specimen GIII-2.

Fig. 4: Shows the Method of the Construction of Specimen.

Fig. 5: Test Setup.

NUMERICAL SIMULATION

Using only experimental approach for investigation is usually limited and the data required for a comprehensive parametric study is normally inadmissible in an experimental program as the cost and time of conducting an extensive number of experiential tests would be prohibitive. ANSYS 5.4 [6] modeling as a three-dimensional finite element tool was used for computation. Eight – nodded brick element with unilateral behavior due to cracking and crushing was used to model concrete and masonry. Link element with 2 nodes was used to simulate the steel elements. Perfect bond was postulated between reinforcement and the confounding media as its effect was proved to be minor in previous studies. The finite element mesh for the study cases of specimens is shown in Fig. (6).

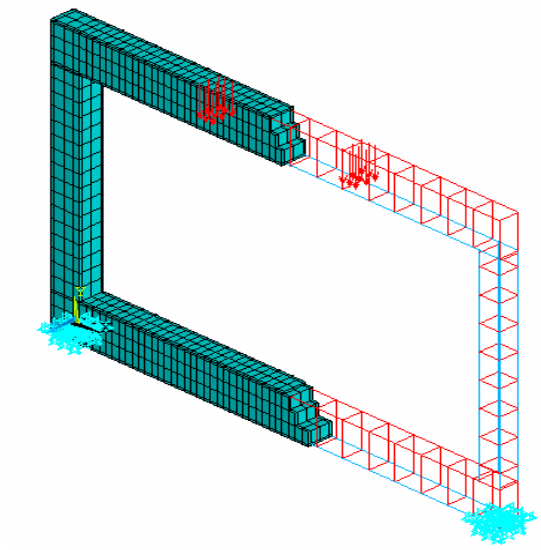

Fig. 6-a: Finite Element Mesh for Bare Frame.

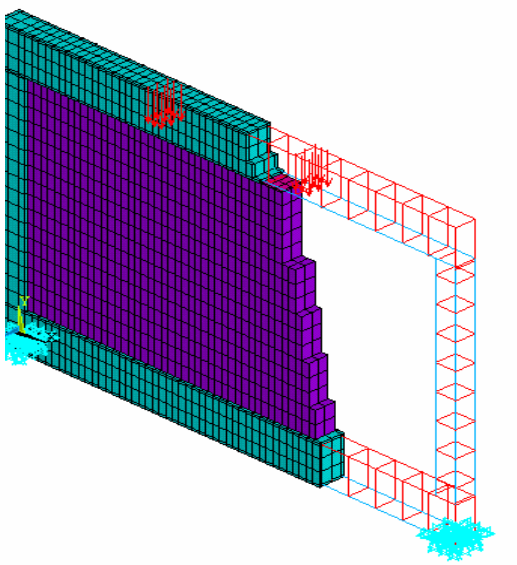

Fig. 6-b: Finite Element Mesh for Infilled Frame.

Fig. 6: Finite Element Mesh for the Various Case Studies.

VERIFICATION OF FINITE ELEMENT PREDICTIONS

To verify the accuracy of the numerical model, results of the system for reinforced concrete-masonry, were compared against the data obtained from the experimental testing. Load-deflection of the system and strain distribution in steel bars are illustrated in Fig. (7). The results obtained numerically were noted to be in very close agreement with the experimental data.
The maximum difference in ultimate load capacity was 15% for the case of bare frame with maximum variation in ultimate strain prediction. A part from these comparisons, the agreement in deflections, horizontal strain and their distribution measurements were also checked.

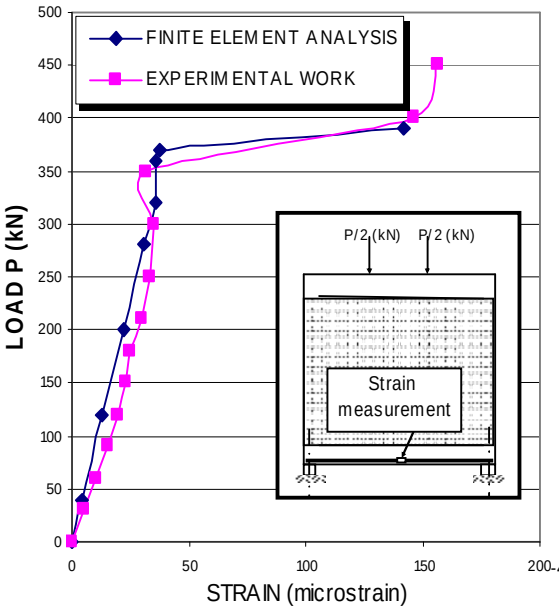

Fig. 7-a: Strain in Bottom Rebar of Lower Beam vs Load, Specimen (GII-1).

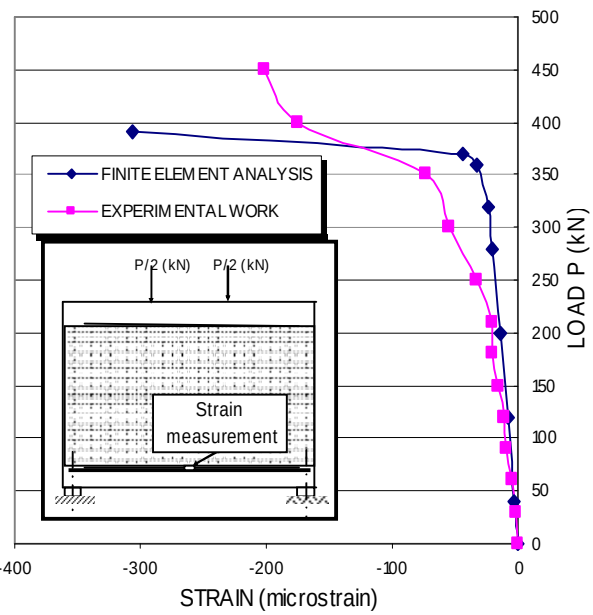

Fig. 7-b: Strain in Top Rebar of Lower beam vs load, Specimen (GII-1).

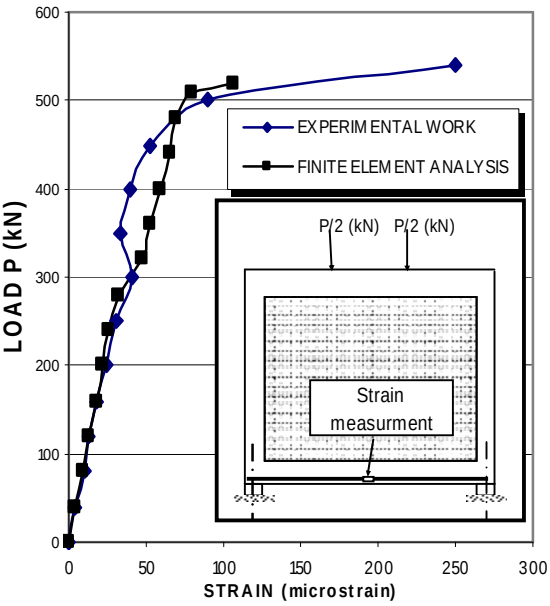

Fig.7-c: Strain in Bottom Rebar of Lower Beam vs load, Specimen (GI-2).

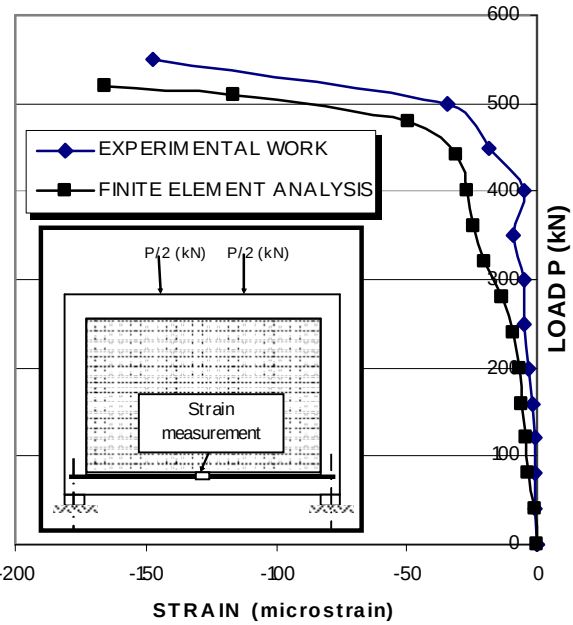

Fig.7-d: Strain in Top Rebar of Lower Beam vs Load, Specimen (GI-2).

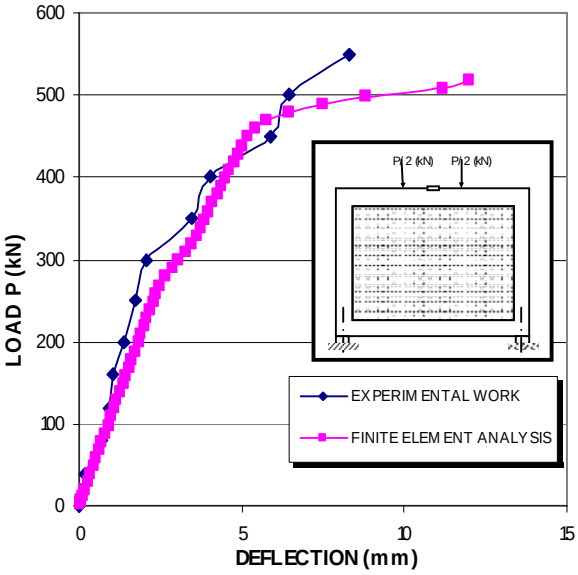

Fig.7-e: Load Deflection Curve at Mid Span of the Upper Beam, Specimen (GI-2).

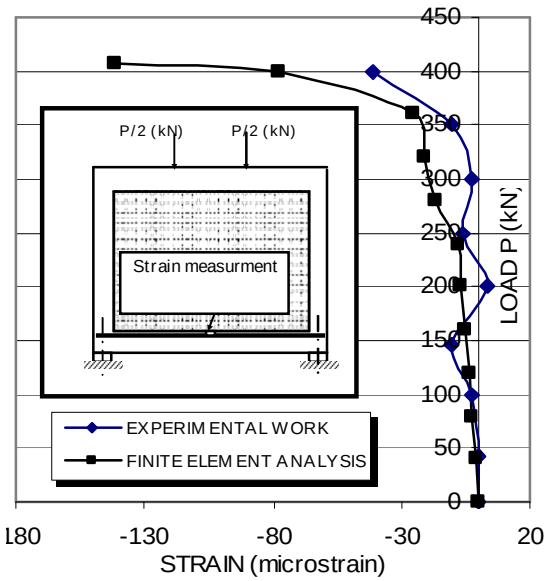

Fig.7-f: Strain in Top Rebar of Lower Beam vs Load, Specimen (GI-2).

Fig.7: Verification of Finite Element Prediction.

LOAD PATH TO SUPPORTING ELEMENTS

The manner in which the applied forces transmitted to supporting element differed considerably due to the existence of masonry wall and inclusion of side columns. Table (2) illustrates the difference in the load path for different specimens.

Table 2: Summary of the Load Path for Different Specimens

Specimen	Description	Load Path
G0-1, G0-2	Beam specimens.	Shallow beam action.
GI-1	Bare frame.	Through RC frames within side columns, Fig. (8-a).
GI-2	Infilled frame with side columns and the upper beam was cast above the masonry panel directly without gap.	Simultaneous transfer through two components RC frame and masonry wall by framing action and strut - and - tie mechanism, Fig. (8-b).
GII-1	Wall masonry panel with upper and lower beam without side columns.	Through masonry wall by strut – and – tie mechanism, Fig. (8-c).
GIII-2	Infilled frame with side columns and the upper beam was cast first then the masonry panel was later constructed.	Framing action until contact overcame the interfacial gap between wall panel and upper RC beam. This was followed by transfer through RC frame and masonry wall similar to GI-2,Fig. (8-d).

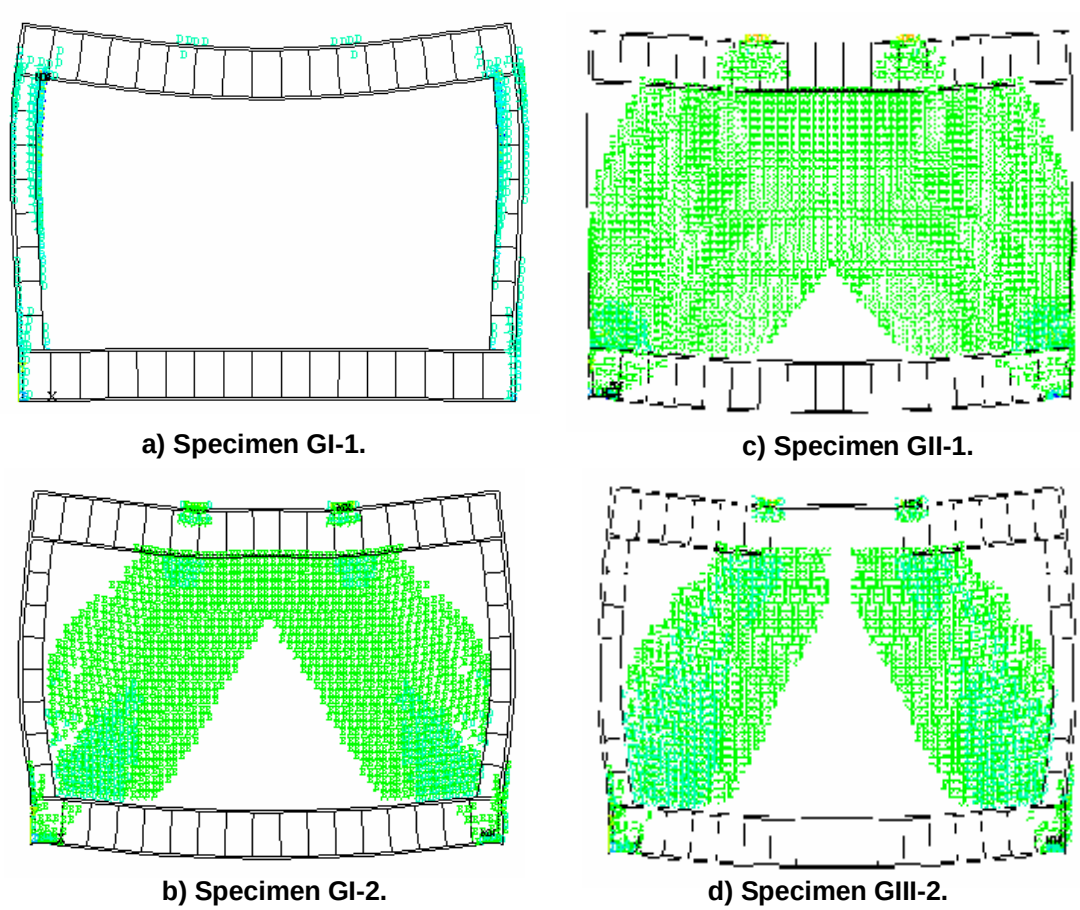

a) Specimen GI-1. c) Specimen GII-1.

b) Specimen GI-2. d) Specimen GIII-2.

Fig. 8: Nodal Force Data for Different Case Studies.

From the previous Table and Fig. 8, many observations have to be pointed out. In specimen GI-2, the applied load transmitted to the support through the upper beam and the masonry panel which act together as one unit due to the execution procedure as we explained before. Otherwise, in specimen GIII-2, the load path transmitted first through the upper beam to the masonry wall at top by two concentrated points with existence of a small gap between the upper beam and the masonry panel. Then, the forces transmitted in the masonry through two diagonal struts which had smaller width compared with that in the specimen GI-2. On the other hand, the transmission of forces through both frames and masonry wall, explained possession of the specimen GI-2 higher ultimate capacity more than specimen GII-1.

Failure Pattern

The progress of cracking provided useful information regarding the failure mechanism of the specimens. In the bare frame, specimen GI-1, the first crack appeared at the bottom of the upper beam at mid-span at about 0.3 of the failure load. As the load increased, cracks extended along the full height of the upper beam and cracks appeared at the lower beam at mid-span as well. In addition, cracks appeared at the upper beam column joint due to the rotation of the upper beam as a result of the deflected beam. In sequence, the column rotated due to the framing action of the bare frame and a plastic hinge occurred at the connecting joint as depicted in Fig. (9). In specimen GI-2, the first cracks appeared at about 0.8 of the failure load and no cracks were noticed before that. These cracks were small cracks at the upper beam under the points load. As the load increased, the cracks took place suddenly in the masonry in inclined

orientation between each point load and the support. Cracks appeared along the lower beam at failure and crushing occurred for masonry at the bottom of masonry wall near the supports due to the compression failure. Tendency of side columns to buckle outwards was noticed and cracks took place at the top third of the columns. At failure loads, the width of cracks of the masonry increased and also the width of the cracks at the lower joints between beam and column as shown in Fig. (10).
In specimen GII-1, the first crack appeared near the failure load without any visible cracks. Abrupt formation of cracks in masonry inclined between the point load and the support were observed. As the load increased, flexural cracks took place at the third of the lower beam and crushing happened at the bottom of the masonry wall near end supports due to compression failure as shown in Fig. (11).
In specimen GIII-2, the first crack appeared at about 0.8 of the failure load with small width at the upper beam under the applied load. Similar crack propagation to other specimens was observed as shown in Fig. (12). However, it has to be pointed out that existence of side columns or execution procedure eventually showed the difference in the mode of failure as listed in Table (3).

Table 3: Collapse Mechanism for Different Specimens

Specimen	Description	Collapse mechanism
G0-1, G0-2	Beam specimens.	Flexural failure by yielding of tensile reinforcement.
GI-1	Bare frame	Plastic hinge at beam column joint due to the framing action with absence of special reinforcement for frame connection.
GI-2	Infilled frame with side columns and the upper beam was cast above the masonry panel directly without gap.	Crushing at the bottom of masonry wall above the supports due to the diagonal compression strut.
GII-1	Wall masonry panel with upper and lower beam without side columns.	Crushing of extreme masonry wall above the supports due to the diagonal strut with concentration of the compression strain in this region.
GIII-2	Infilled frame with side columns and the upper beam was cast first then the masonry panel was later constructed.	Diagonal crack between the point loads and the support due to the diagonal compression strut.

a. Global View **b. Plastic Hinge Formation.**

Fig. 9: Cracks Pattern and Mode of Failure for Bare Frame, Specimen GI-1.

Fig. 10: Cracks Pattern and Mode of Failure for Specimen GI-2.

a. Global View **b. Magnified View.**

Fig. 11: Cracks Pattern and Mode of Failure for Specimen GII-1.

a. Global View b. Magnified View for Strut Information.

Fig. 12: Cracks Pattern and Mode of Failure for Specimen GIII-2.

Infill Contribution

Figures (13) and (14) present the effect of infill of masonry to the reinforced concrete frame. From these Figs. the following observation were noted:-

1- The use of masonry to infill the reinforced concrete frame increased the capacity of system by about five times.

2- Large sagging deflection of lower beam in specimen GI-2 compared with hagging camber in specimen GI-1.

3- Large tension and compression strain in main reinforcement of upper beam in specimen GI-1 compared with specimen GI-2 in which the masonry panel acts as an additional support for the upper beam. otherwise, large strain in main reinforcement of lower beam in specimen GI-2 compared with GI-1 because of the nonexistence of the media to transmit the forces between the upper and the lower beam.

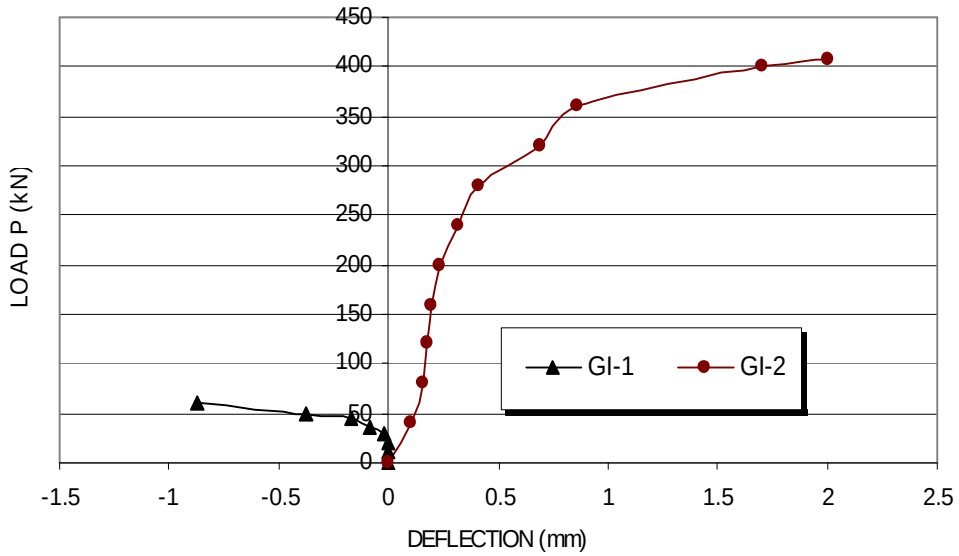

Fig. 13: Load Deflection Curve at Mid-Span of Lower Beam.

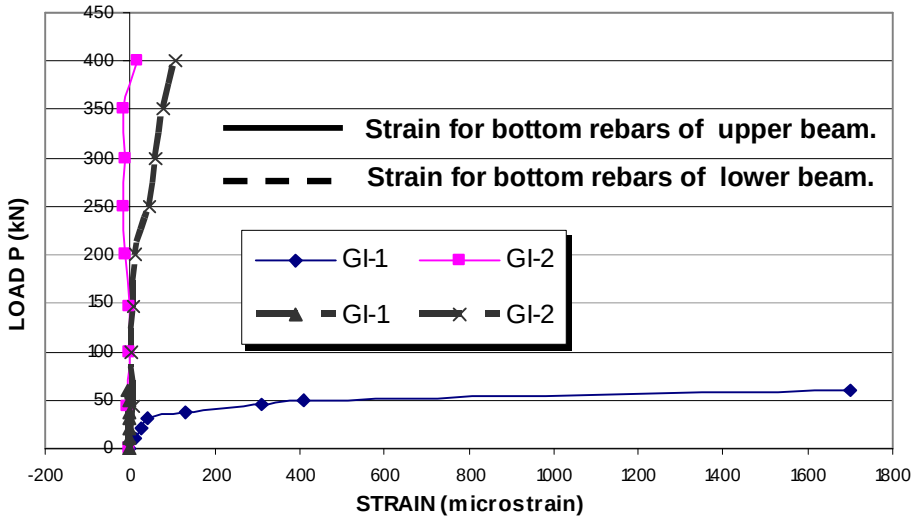

Fig. 14:Strain development at bottom rebars of upper and lower beams.

RC Framing Action

The framing action was investigated through the following sub-groups as illustrated in Fig.(15).

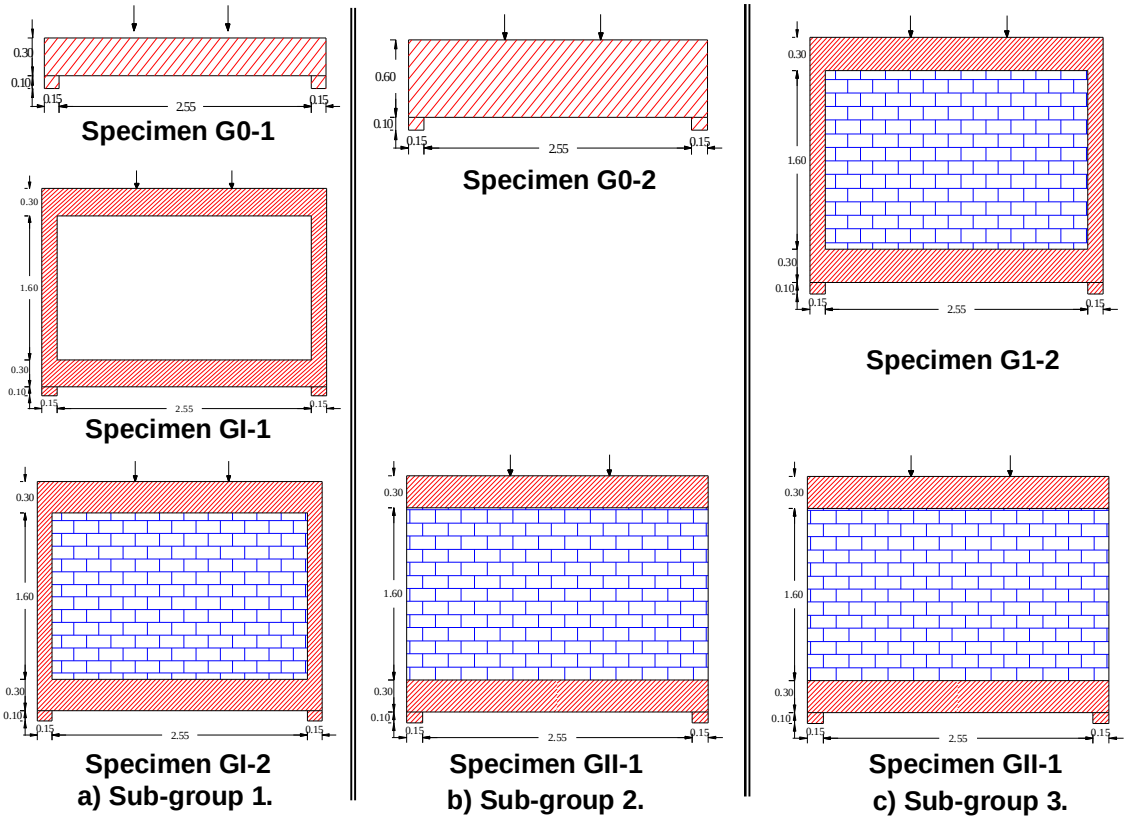

Fig. 15: Study Cases used to Address the Framing Action.

Sub-group 1: Beam versus frame behavior: The results of specimens G0-1 and GI-1 depicted in Fig.(16) indicates that the framing action of specimen GI-1 was not fully developed because of the used reinforcement detailing which simulated real-life practice. On the other hand, the infill contribution was highly significant.

Sub-group 2: RC only versus composite behavior: The results illustrated in Fig.(16) show that the contribution of infill for specimen GII-1 cannot be ignored even in the absence of side columns.
Sub-group 3: Effect of side columns: Figures (17-a) and (17-b) present the effect of inclusion or non inclusion the specimen of side columns at the vertical wall edges for GI-2 and GII-1. From these Figs. the following observation were noted:-
1- The use of side columns at the wall edges increased the capacity of system by about 15 % compared with the specimen constructed without side columns. This is due to the confinement of masonry panel by side columns. This increased may have been more with better detailing of reinforcement in the RC connections of specimen GII-2.
2- Existence of side columns provided higher stiffness of the entire system and therefore specimen GII-1 showed softer behavior.
3- The tensile strains in bottom rebars of lower beams in specimens GII-1 and GI-2 nearly equal up to the onset of cracking.

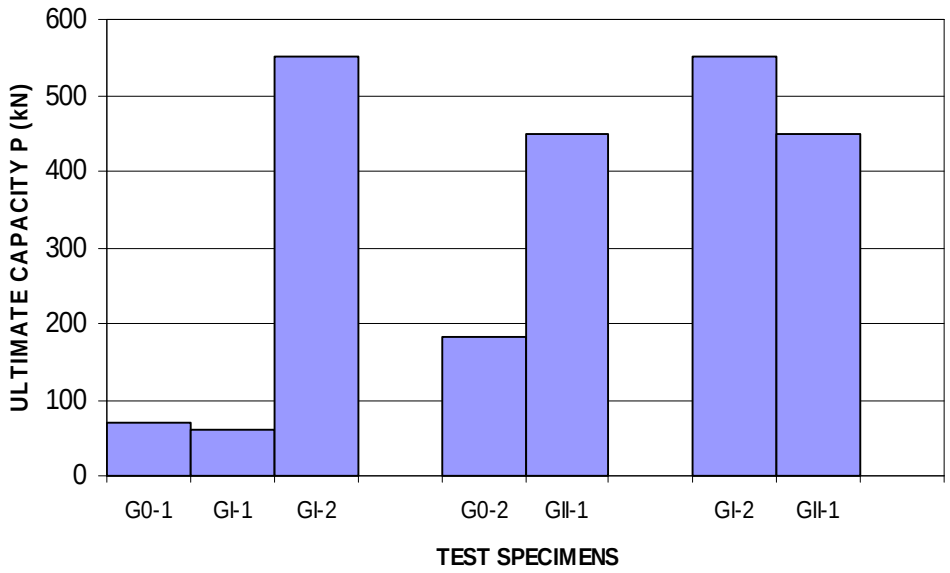

Fig. 16: Ultimate Capacity for the Different Sub-Groups.

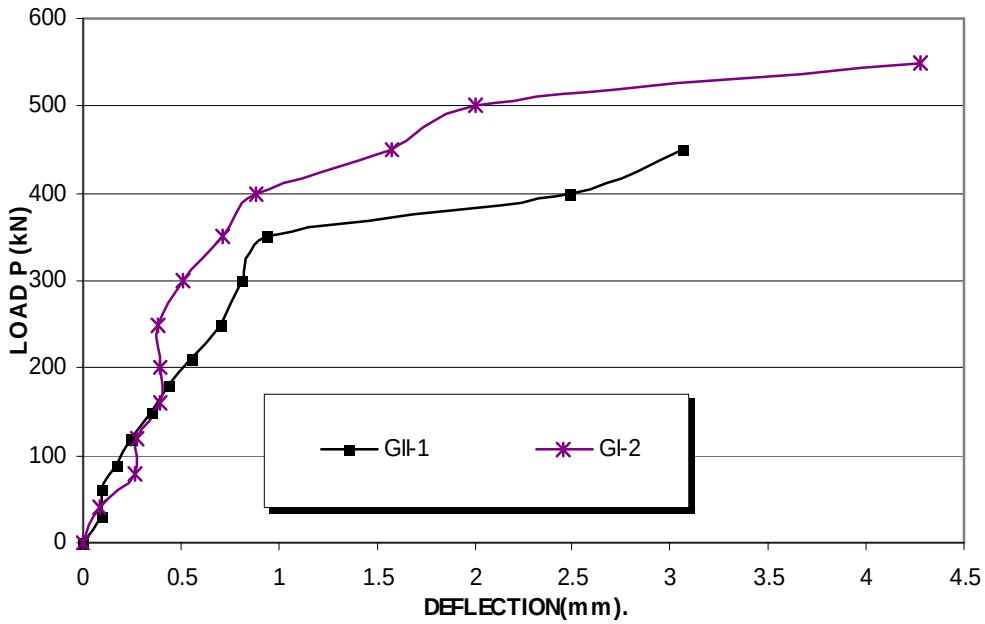

Fig. 17-a: Load Deflection Curve at Middle Point of Lower Beam.

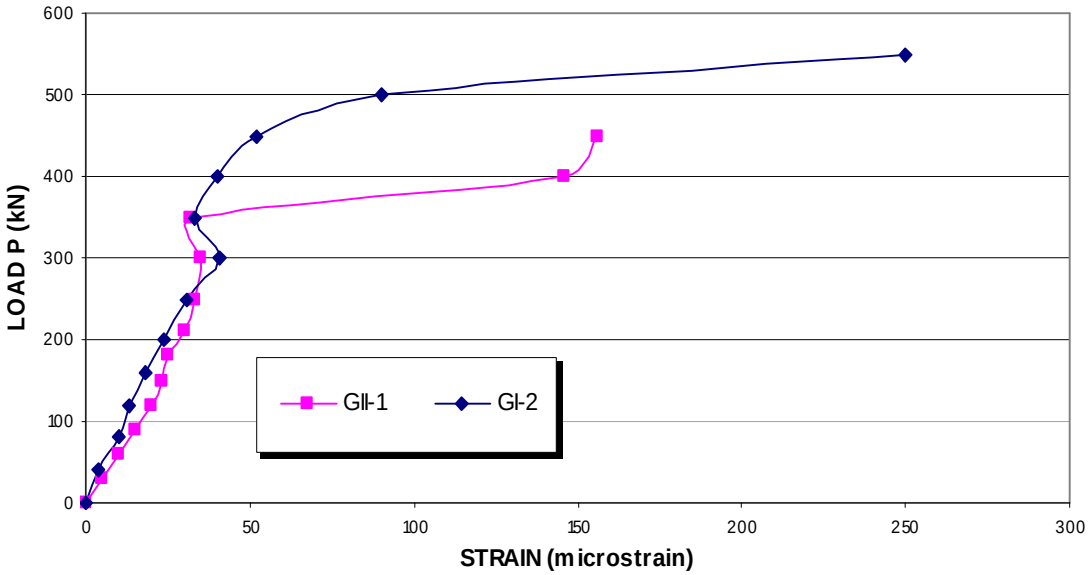

Fig. 17-b: Strain Development at Bottom Rebar of Lower Beam.

EXECUTION METHODOLOGY

The method of the construction of the upper beam of the system affected on the ultimate capacity of the system. In this article, we made a comparison between specimens GIII-1 which the upper beam constructed above the masonry brick panel directly as shown in Fig. (4-a) and specimen GIII-2 which the upper beam was constructed first and then the masonry brick panel as shown in Fig. (4-b). Figure (18) illustrates the effect of the method of construction for GIII-1 and GIII-2. From this Fig., the following observation was noted:-

1- The use of construction for GIII-1 in which the upper beam was constructed above the masonry brick panel directly increased the capacity of system by about 38% over the specimen GIII-2 in which the upper beam was constructed first and then the masonry brick panel was constructed.

2- Large deflection in specimen GIII-1 compared with GIII-2 due to the increasing of failure load.

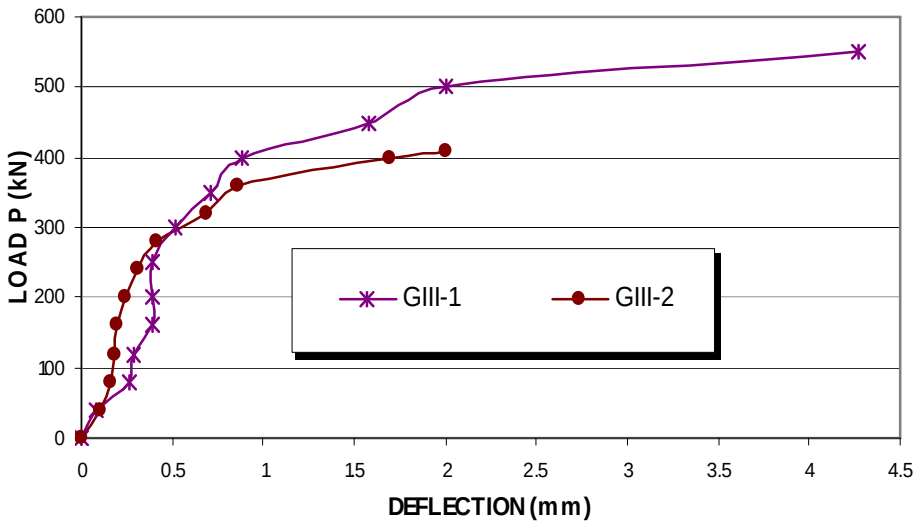

Fig. 18: Load Deflection Curve at Middle Point of Lower Beam.

Load Sharing Parameters

Apart from the previous factors in items (8) to (10), the relative stiffness was expected to represent the major load sharing parameter. Of course, employment of high strength concrete affects the strength parameters. This investigation is carried out in three folds:
i. Studying the effect of concrete grade.
ii. Studying the effect of masonry strength.
iii. Studying the effect of relative concrete to masonry strength.

i. Effect of Concrete Grade

The ultimate capacity of the system increases with improving the concrete grade as shown in Fig. (19). As the concrete grade was increased from 25 MPa to 125 MPa which was almost 250% of the limiting grade of high strength concrete (40 MPa), the ultimate carrying capacity of the system increased by 190%, 130 % for the bare frame and infilled frames, respectively. For the same concrete grade, the nonexistence of masonry which fill the panel was very significant that the ultimate capacity of the system was decreased by about 75-80 %.

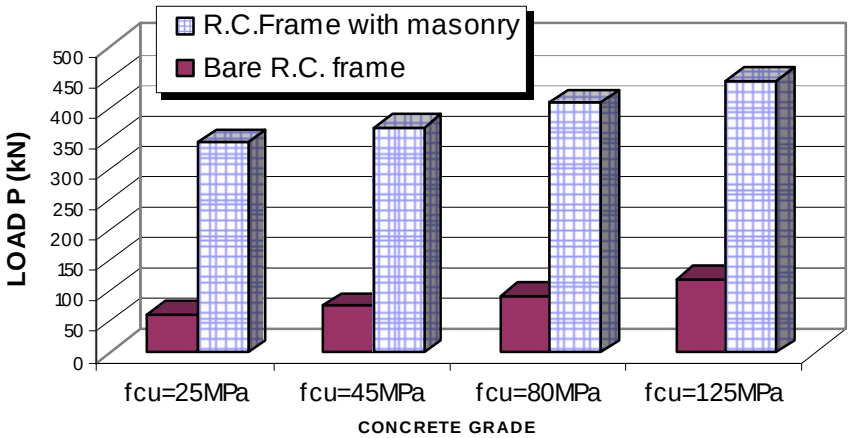

Fig. 19: Effect of Concrete Grade on the System Ultimate Load.

ii. Effect of Masonry Strength

The ultimate system capacity increased with improving the masonry strength as shown in Fig. (20). As the masonry strength was increased from 2 MPa to 15 MPa, the ultimate carrying capacity of the system increased by about 300 % with the same mode of failure which was compression in the masonry brick panel. The big difference in the overall ultimate capacity of the system happened because of the masonry height constituted the major portion of the system which was about 75% of the total height. This reflected the great effect of masonry strength on the relative load sharing.

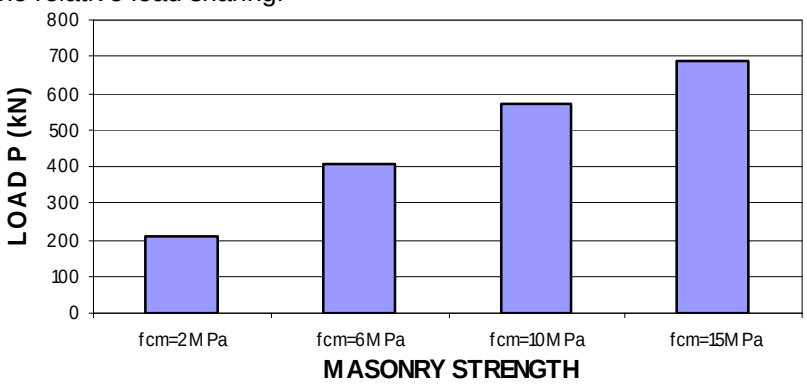

Fig. 20: Effect of Masonry Strength on the System Ultimate Load.

iii. Effect of Relative Masonry to Concrete Strength

To visualize the combined effect of the strength of the constituent materials, the relative strength is investigated using the results of the previous case studies. Fig. (21) illustrates the division of ultimate capacity between the RC frame and the wall panel. As the relative masonry to concrete strength was increased, the load share of RC frame decreased as such. Indeed, the relative strength seemed to be the governing strength parameter that controlled the load share rather than that of the individual components.

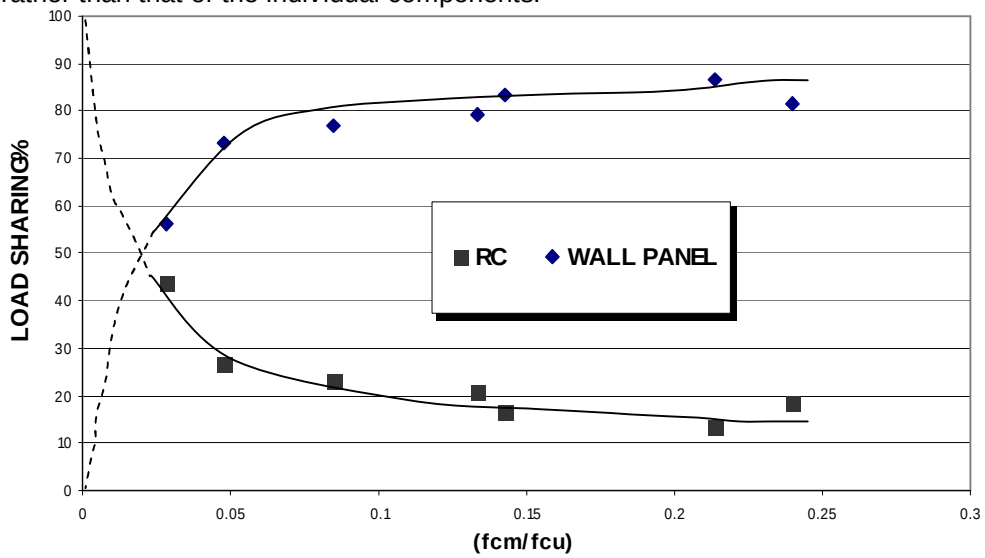

Fig. 21: Effect of Relative Masonry to Concrete Strength on the Load Sharing.

CONCLUSIONS

- The use of side columns at the wall edges increased the capacity of the system by about 15 % compared with the system without side columns.
- The use of masonry; which fill the panel, increased the overall capacity of the system approximately 5 times compared with the system without masonry.
- Large strains in lower reinforcement of upper beam in the case of bare frame compared with the case of infilled frame in which the masonry panel acts as an additional support for the upper beam.
- The method of construction in which the upper beam was constructed directly above the masonry brick panel increased the capacity of system by about 38% over the system in which the upper beam was cast first and then the masonry brick panel constructed.
- The relative masonry to concrete strength was addressed as the main load sharing parameter.

REFERENCES

1. Emam, A.A, Nassef, M.E., Youssef, A.A., (1985) " Composite Action Between Masonry Walls And Their Supporting Beams", Master of science in structural Engineering, Cairo University.
2. Rosenhaupt , S., Bulletin, (1961) " Elastic Analysis of Composite Walls, A General Theory," Research of Israel, Jerusalem, Vol. 10 c, No., 1-2.
3. Arnold W. Hendry, "Reinforced and Prestressed Masonry." University of Edinburgh, 1997.
4. Rosenhaupt, S., (1991) "Experimental Study Of Masonry Walls On Beams", ASCE Structural Journal, Vol. 88, No. ST 3.
5. ASTM Standards, (2002), Annual Book Of ASTM Standards, Volume 04.05, Masonry, Philadelphia, Pa.
6. ANSYS User's Manual, Theory, Commands, Analysis and Element, Release 5.4 ANSYS Inc. Houston, Pa., 1997.

SIMULATION ANALYSIS AND ASSESSMENT OF 40M SPANS PRE-STRESSED BOX-GIRDER BRIDGES

Dr. Hesham A. Mahdi
Assis. Professor Sixth of October University, Consultant Engineer of Bridges, Cairo, Egypt
Email: heshamnecb@menanet.net

ABSTRACT

Most of the Bridges constructed in Egypt over the river Nile possessed 40 m spans for the approaches bridges (east and west of the main navigable spans), this is attributed to the available resources needed for the superstructure construction in the Egyptian market and the associated cost optimization as well.
This paper presents a summary of the major methods utilized in the design of box-girder bridges and proposes a numerical finite element approach for a precise structural analysis taking into account crucial structural actions as warping, distortional warping, shear lag effects, transversal cracking of the top slab and concrete long term loading effect using creep functions. The monitoring results of the superstructure via in-situ loading tests on the 40 m span box girder bridges having a top slab width of 10.50 m are summarized for three prodigious bridges crossing the Nile and Mubarak El-Salam bridge crossing the Suez canal. Deflections and strains are recorded at the critical sections of the superstructure under symmetrical and unsymmetrical loading. Finally yet importantly, the comparison between the analytical and different recorded results are presented as well as the general assessment of the whole process to assure the reliability of the proposed structural analysis together with discussions regarding recommendations for future enhancement of the proposed analytical model

Keywords: warping, shear lag, performance index, finite element, creep, smeared cracking

INTRODUCTION

Until 2012, the process of planning new highway networks is evident for the next decade in response to the needs of international trade. The Government of the Arab Republic of Egypt has embarked on economic linearization by opening up various sectors of the economy to private investments, through measures of decontrol and the abolition of restrictive rules and regulations. To handle the forecast substantial growth in traffic, to allow for rapid modernization and to meet the demands of the anticipated growth, our government trend is to increase the interconnection between the East and the West road highway networks of the river Nile via the construction of bridges at an investment = one billion pounds, examples are :

1- El-Wasta Nile Bridge
2- Malawi Nile Bridge
3-Bani-Mazar Nile Bridge
4- Talkha Nile Bridge
5- Tema Nile Bridge
6- Gerga Nile Bridge

With the rapid development of intricate formwork, the connection of plate-like elements to obtain monolithic cellular or box-like structure and the extensive development work have led the concrete box girder bridges to be the most economically competitive and aesthetically attractive, Schlaich [1].
This paper proposes a new analytical method for analyzing the box girder of the Nile bridges approaches to cater for structural effects as shear lag, torsional and distorsional warping. In addition, the analytical method is compared with the in-situ loading test results carried out in the field and the validation degree of the model is examined.

Selection of Approach Bridge Span

As emphasized by the author [2], the critical success factors of bridges design and construction technology presides in what so-called five-E series:
Engineering, Experience, Economy, Equipment, and Environment
Serving the economical aspect, Labib [3] demonstrated the cost analysis and breakdown of the substructures of prestressed approach bridges constructed in Egypt. It represents an average of 41.60% of the total cost distributed as follows: (22.80% piles, 11.80% pile caps, 7% piers) while the superstructure represents in average 47.80% distributed as follows: (18.40% concrete, 10.60% reinforcing steel and 18.8% for prestressing steel)., bridge accessories (bearings, expansion joints, hand rails, and other finishing works) represents 10.60% of the total bridge cost.
Moreover, the author of this paper as a technical consultant to General Authority for Roads and Bridges GARBLT scanned the cost of 10 bridges over river Nile since the last 15 years (Minya, Dessouk, Banha, Farskur, Mansoura, Luxor, Assiut, Mit-Ghamr, Sherbeen, and Aswan Bridges). The approach bridges had been constructed with spans ranging between 30m to 48.0m with a preferable typical span of 40.0ms. It is evident from fig. 1 that increasing the bridge's span increases the super-structure's cost and decreases the foundations cost.
A critical or optimum span originates from fig 1 where the total cost of the approach bridges is minimum where a value about the 40 m span proved to provide such most advantageous cost. It has to be borne in mind that the cost of piles and the total weight of the foundations cost is sensitive to soil conditions as in Farskur bridge where long piles had been procured due to the impotence of the surface soil layers until a depth of 38.00 m below ground surface.

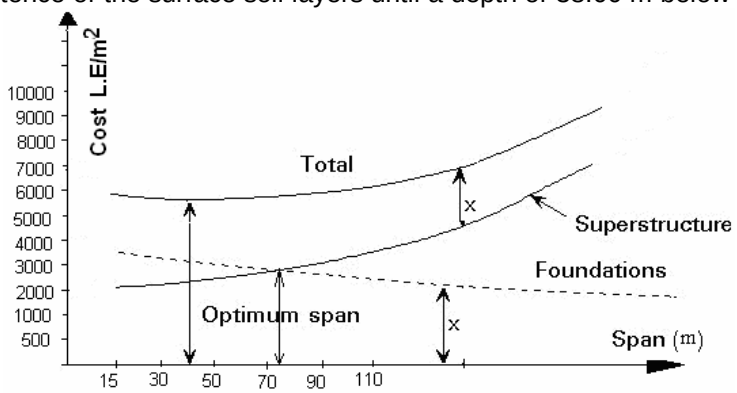

Fig 1: Cost versus Span for Approach Bridges

Moreover, most of the construction companies working in bridge industry in Egypt possess the relevant equipment/resources required for constructing the 40 m spans from conventional cast in-situ scaffolding system, to tailor made scaffolding. In addition advanced shoring techniques as mobile scaffolding system in Suez Canal Bridge and deck pushing system as in Dessouk and Assiut bridges participated in the success of using 40 m span in the approach bridges.

Summary of Structural Actions of Box-Girders

The thin-walled box beam possesses two main types of structural action in addition to simple beam action.

- Deformation or distortion of cross-section; this behavior is raised when eccentric loading acts leading to alteration in the shape of cross-section due to transverse bending. This is obvious especially when no intermediate diaphragms exist… Fig. (2.a-1, 2-a-2)
- Warping of the cross-section which is an out-of-plane displacement of points due to torsional or eccentric loading; these points were on the plane of cross-section …fig (2.b). These out of plane displacement are torsional warping displacements and are associated with shear deformations in the flanges and webs plans. Additional warping displacements are generated when cross diaphragms are widely spaced leading to distortion of the section…fig (2.c) associated with in plane bending of flanges and webs.

- Box-girder of wide single cell or box-girder of large side cantilever when subjected to symmetrical loading undergoes a differential longitudinal movement in both flanges. This effect is known as shear lag effect as flange shear deformation reduces the effective width of flange. Moreover, the normal longitudinal stresses for wide flanges vary across the flange with obvious concentration at web-flange connection…fig (2.d).

Analysis Methods of Box-Girders

- For thick webs capable of hindering the pre-mentioned warping displacements simple beam theory is applicable and St. Venant's torsion theory is considered more than convenient for economical structural design purposes.

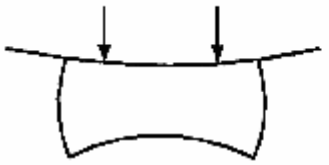

Fig 2.a.1
Distortion of Cross-Section
Due to Symmetric (Bending) Loading

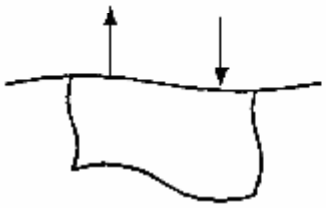

Fig 2.a.2
Distortion of Cross-Section
Due to Anti Symmetric (Torsional) Loading

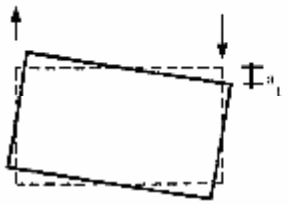

Fig 2.b
Twisting of Mid Span Cross- Section without Distortion

At Vertical Deflection of Web due to Torsion without Distortion (Case of Close Spaced Rigid Cross-Section)

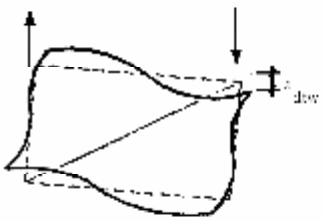

Fig 2.c
Additional Twisting of Mid Span Cross- Section when Distortion is Permitted.
Add Vertical Deflection of each Web due to Distortion (Case of Widely Spaced Cross Diaphrams)

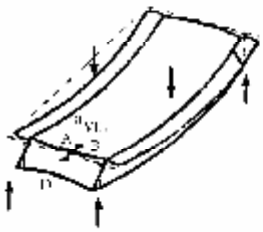

Fig 2.d.1
Shear Lag in Bending

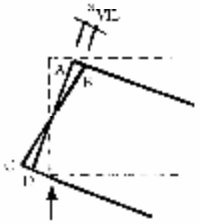

Fig 2.d.2
Enlarged Elevation of the Support Region of Box Beam showing Out-Off-Plane Displacements of End Cross-Sections due to Shear Lag in Bending

Fig 2: Structural Actions of Box-Girder

- A more sophisticated analysis rises to the surface as the web thickness decreases for economical reasons and the trend to attain the minimum dimensions for reducing self-weight and consequently reducing amount of reinforcement and prestressing percentage, in such a case distorsional and warping actions have to be carefully assessed.

Former rigorous investigations were conducted neglecting warping and shear lag effect, Kollbrunner [4] accounting for torsional warping and assuming no cross-sectional distortion, Kupfer [5] accounting only for distortion, Reissner [6] accounting for shear lag only for single box girders without side cantilevers. Shear flexible grillage analysis, folded plate theory and finite element theory. The degree of precision for adopting any method of analysis for a particular structure is difficult to predict or even check as it depends on the ability of the model to represent three very complex phenomena:

1. Behavior of material
2. Structural geometry
3. Actual loading

Using DIANA 9 [7] software package and the outline basis attached in Computer-Unterstuetzte Berechnung des Uberbaus (Internationale Vereinigung Fur Brueckenbau and Hochbau) "IVBH" [8]] the bridge is idealized by an assemblage of curved shell element formulation which has a combination of membrane and plate bending behavior.

The in-plane lamina strains ε_{xx}, ε_{yy} and γ_{xy} vary linearly in the thickness direction. The transverse shear strains γ_{xz} and γ_{yz} are forced to be constant in the thickness direction. Since the actual transverse shearing stresses and strains vary parabolically over the thickness, the shearing strains are equivalent to constant strain on a corresponding area.

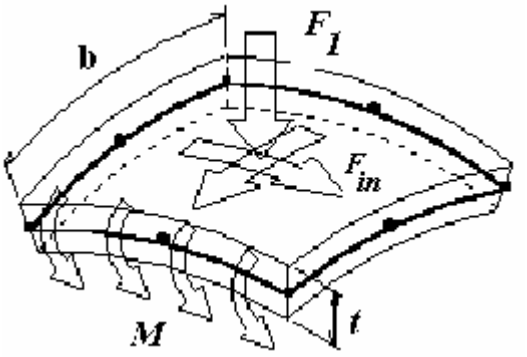

Fig. 3 Curved Shell Element

Five degrees of freedom have been defined in every element node, three translations (μ_x, μ_y and μ_z) and two rotations (φ_x and φ_y). It is considered to obtain thin elements, *i.e.*, the thickness *t* must be small in relation to the dimension *b* in the plane of the element. Force loads *F* act in any direction between perpendicular to the surface and in the surface. The total idealized bridge length equal *160m* and breadth *10.50 m*.

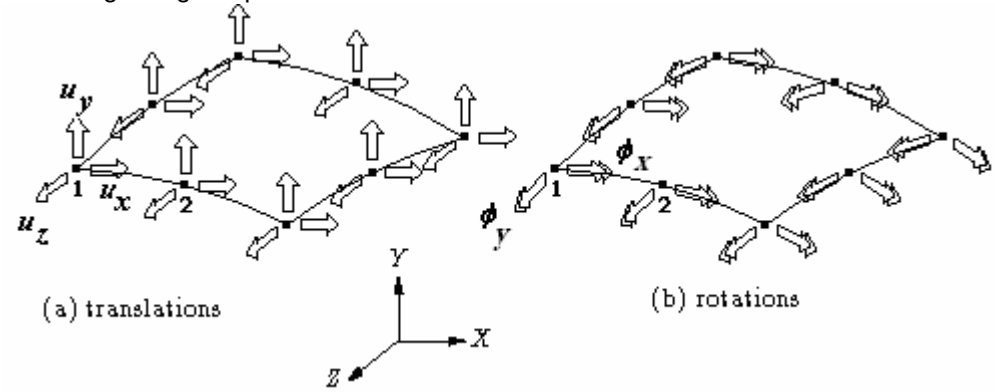

Fig. 4 Translations and Rotations of the Curved Shell Element

In addition to the modeling of concrete structural elements, the pre-stressing bars are modeled by an embedded bar reinforcement element which adds stiffness to the finite element model implying perfect bond between the reinforcement and the surrounding material. Pre-stressing was implemented in the longitudinal direction only of the bridge using 2 pair of cables (*1200.6"*) in each web arranged in four rows parallels to each other (total no. of cables/web=*4*2=8*cables). Each tendon has a total area = *12* strands**140= 1680mm*^{2}. The tendons were tensioned at *0.70 uts* (ultimate tensile strength = *1860 N/mm*^{2}). The cables profile took the shape of sinusoidal curve with a relative straight portion over the support and at mid span). The pre-stressing is modeled by one bar each web having the characteristics of the cables and taking into account the center of gravity of the modeled bar. Mahdi, and El-Kadi [9] proposed an analytical method for analyzing box-girder bridges by the finite element analysis**.** The concrete is modeled according to a smeared crack approach for tensile states of stress, combined with a Drucker-Prager model to cater for the effect of biaxial state of stress in both the longitudinal and transversal direction of the bridge after Mahdi, H.A [10].

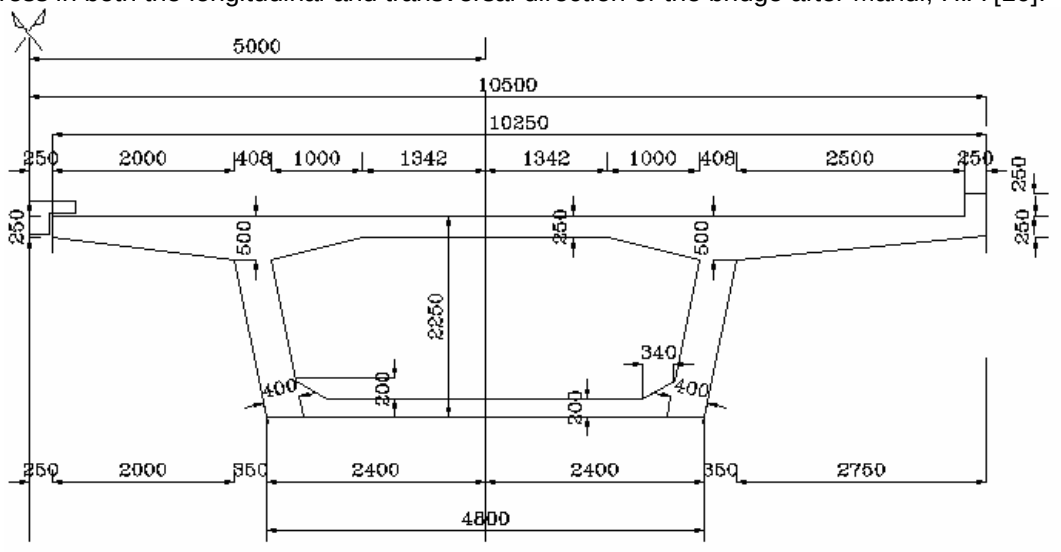

Fig. 5: Box-Girder Bridge Typical Cross Section

The smeared cracking provides for the cracking of the top slab in the transversal direction when the tensile stress in the concrete section reaches a cut-off value (corresponding to the concrete class *45N/mm*^{2}). Its direct influence is reducing the shear modulus of the concrete that sequentially increase the deflection of the box-girder. Two types of structural systems were adopted; the first is a continuous box-girder resting on pot bearings and the other is a continuous box-girder monolithically connected with the pier columns.

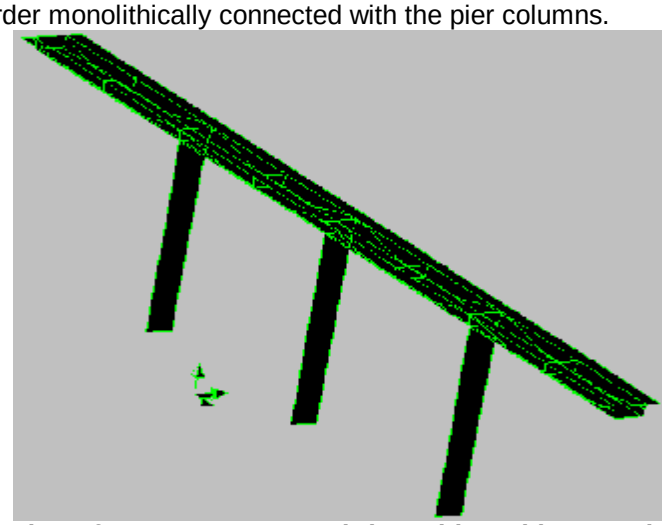

Fig. 6: Idealization of Four Spans Box-Girder Bridge with Curved Pre-Stressing Tendons

Background of the Proposed Concrete Creep Model

In this paper, a creep model is presented, owing to the fact that construction time of the Nile Bridge's superstructure exceeds two years, with the construction of the approaches always ahead of the construction of navigable span that is attributed to the long time the offshore substructures take. Accordingly, it is vital in the current analysis to take into account the development of strength and elasticity modulus with time for comprehensive corroboration of the analytical results with the in-situ loading tests. For pre-stressed bridges, the strain history affects the current stresses, accordingly, for this type of behavior, creep experiments are implemented where a stress is applied at time zero and the strains are recorded as a function of time, the *creep function*. Based on the principle of superposition, the creep function can be employed to calculate the strain as function of the stress history. This principle reduces the applicability of the formulation to linear visco-elasticity.
A vital part of the Finite Element implementation of the visco-elastic models is to find an algorithm in which it is not necessary to `remember' the complete strain or stress history, because this would require too much computer memory for box-girder structures.

According to CEB-FIP [11] a creep function *E (t, t)* in which the relation between stresses and strains follows from:

$$e(t) = \int_{-\infty}^{t} E(t,t)\,\bar{D}s\,(t)\,dt \qquad \text{.....(1)}$$

Where

$\bar{D}$: is a dimensionless matrix that relates the three-dimensional deformation states to the one-dimensional relaxation function by using Poisson's ratio u of the concrete.

$$\bar{D} = \frac{1}{(1+u)(1-2u)} \begin{bmatrix} 1-u & u & u & 0 & 0 & 0 \\ u & 1-u & u & 0 & 0 & 0 \\ u & u & 1-u & 0 & 0 & 0 \\ 0 & 0 & 0 & \frac{1-2u}{u} & 0 & 0 \\ 0 & 0 & 0 & 0 & \frac{1-2u}{2} & 0 \\ 0 & 0 & 0 & 0 & 0 & \frac{1-2u}{2} \end{bmatrix} \text{.....(2)}$$

Consistent with Maxwell model, the relaxation function is expanded in a truncated Dirichlet series, resulting in the following exponential series.

$$E(\Gamma,t) = \sum_{a=0}^{n} E_a\,(t)\,e^{-\frac{\Gamma-t}{l_a}} \text{.....(3)}$$

For a one-dimensional situation, this relaxation function can be physically interpreted as a parallel chain of springs and dampers as in Figure (7).

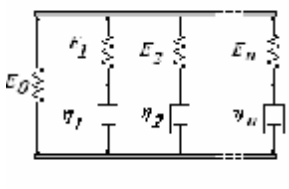

Fig. 7 Maxwell Chain

In equation (3), $E_a\,(t)$ indicates that the stiffness of the model can be time dependent, for instance due to temperature or maturity influences. The stiffness of the spring E_a and the viscosity of the damper h_a in the model both determine the relaxation time l_a.

$$\lambda_\alpha = \frac{\eta_\alpha}{E_\alpha} \tag{4}$$

First element in the Maxwell Chain is represented by single spring or with $h_0 = \infty$.

By substituting (1) in (3) for time *t* and time $t + \Delta t$, interchange the order of summation and integration, and assume that nothing has happened from time $t = -\infty$ until *t*=0, we get

$$\boldsymbol{\sigma}(t) = \bar{\mathbf{D}} \sum_{\alpha=0}^{n} \int_0^t E_\alpha(\tau) e^{-\frac{t-\tau}{\lambda_\alpha}} \dot{\boldsymbol{\varepsilon}}\, d\tau \tag{5}$$

$$\boldsymbol{\sigma}(t + \Delta t) = \bar{\mathbf{D}} \sum_{\alpha=0}^{n} \int_0^{t+\Delta t} E_\alpha(\tau) e^{-\frac{t+\Delta t-\tau}{\lambda_\alpha}} \dot{\boldsymbol{\varepsilon}}\, d\tau \tag{6}$$

We can calculate the stress increment by subtracting (5) from (6) where the integral from 0 to $t + \Delta t$ is split into a part from 0 to *t* and a part from *t* to $t + \Delta t$. The partial stress in every element of the Maxwell Chain is called s_a.

$$\boldsymbol{\sigma}_\alpha(t) = \bar{\mathbf{D}} \int_0^t E_\alpha(\tau) e^{-\frac{t-\tau}{\lambda_\alpha}} \dot{\boldsymbol{\varepsilon}}\, d\tau \tag{7}$$

If we assume a constant strain rate from *t* to $t + \Delta t$ the stress increment follows from

$$\Delta\boldsymbol{\sigma} = \sum_{\alpha=0}^{n} \left(1 - e^{-\frac{\Delta t}{\lambda_\alpha}}\right) \left(\frac{E(t^*)\lambda_\alpha}{\Delta t} \bar{\mathbf{D}} \Delta\boldsymbol{\varepsilon} - \boldsymbol{\sigma}_\alpha(t)\right) \tag{8}$$

Here t^* is a sampling point, usually halfway the time increment. This is only relevant if Young's modulus *E* changes during the analysis. All above equations are incorporated in the analytical model to cater for the creep effect.

Development of strength and modulus of elasticity with time according to CEB-FIP Model Code (11)

The compressive strength of concrete f_{cm} at an age of *t* days depends on the type of cement, temperature, and curing conditions according to the following:

$$f_{cm}(t) = b_{cc}(t)\, f_{cm28} \tag{9}$$

In which f_{cm28} is the mean compressive strength at the age of 28 days and b_{cc} is a time dependent coefficient whose expression is

$$b_{cc}(t) = \exp\left(s\left(1 - \sqrt{\frac{28}{t_{eq}}}\right)\right) \tag{10}$$

Where coefficient *s* depends on the type of cement (s=0.20 for rapid hardening high strength and 0.25 for normal and rapid hardening cement). Parameter t_{eq} is the equivalent age of concrete, defined as :

$$teq = \int_0^t c_A \left(\frac{1}{T_{ref}} - \frac{1}{T(t)}\right) dt$$

in which $T(t)$ is the temperature of concrete at an age of (t) days,

Creep Assumptions and Related Basic Equations

Within the range of service stresses $|s_c| < 0.4 f_{cm}(t_o)$, creep is assumed to be linearly related to stress. The creep function $J(t,t_o)$, also called the creep compliance, defined in equation (1) may be formulated as:

$$J(t,t_o)=\frac{1}{E_c(t_o)}+\frac{j(t,t_o)}{E_{c28}} \quad (11)$$

Where $E(t_o)$ is the modulus of elasticity at the concrete age of loading t_o and $f(t,t_o)$ is the creep coefficient. The model takes into account the effects of the cement type and the curing temperature by modifying the age at loading according to

$$t_{o,\mathrm{mod}}=\max(0.5,t_{o,T}(\frac{9}{2+t_{o,T}^{1.2}}+1)^{a}) \quad (12)$$

Where α coefficient which depends on the cement type and $t_{o,T}$ is defined as

$$t_{o,T}=\int_0^{t_o}c_A\left(\frac{1}{T_{ref}}-\frac{1}{T_{(t)}}\right)dt \quad (13)$$

Implemented Creep Coefficient

The creep coefficient may be calculated from

$$j_{(t,t_o)}=j_o b_{c(t-t_o)} \quad (14)$$

Where f_o is the notational creep coefficient and $b_{c(t\text{-}to)}$ is the coefficient which describes the development of creep with time after loading. These two coefficients are respectively defined by (15) and (20). The notational creep coefficient may be calculated from

$$j_o=j_{R,H}b_{(f_{cm28})}b_{(t_o)} \quad (15)$$

$$j_{R,H}=1+\frac{1-\frac{RH}{RH_O}}{0.46\left(\frac{h}{h_o}\right)^{\frac{1}{3}}} \quad (16)$$

$$b_{(f_{cm28})}=\frac{5.3}{(\frac{f_{cm28}}{f_{cm0}})^{\frac{1}{2}}} \quad (17)$$

$$b_{(t_o)}=\frac{1}{0.1+t_0^{\frac{1}{5}}} \quad (18)$$

$$h=\frac{2A_c}{u} \quad (19)$$

Where R_H is the relative humidity of the ambient environment [%], RH_0= 100%, h is the notational size of the concrete member [mm], (with A_c the cross-section and u the perimeter in contact with the atmosphere) and h_0 = 100mm.

The development of creep with time is given by

$$b_{c(t-t_0)}=\left(\frac{t-t_0}{b_H+(t-t_0)}\right)^{0.3} \quad (20)$$

With

$$b_H=\min\left(1500,150\left(1+\left(1.2\frac{RH}{RH_0}\right)^{18}\right)\frac{h}{h_0}+250\right) \quad (21)$$

In the analysis conducted by the model, the following parameters are considered:

Effective thickness (notational size)	= 220 mm
Poisson's ratio	= 0.20
Relative humidity "R_h"	= 60%
Modulus of elasticity at 28 days	= 31.0 KN/m^2
S "depending on cement type"	= 0.25

ANALYSIS RESULTS

Live loading was applied to the analytical model for both continuous box-girder on bearings and the monolithic system in consistent with the vehicle loads scheme shown in the Fig. (8). Eight trucks 35 tons each were used. The output results (deflection and longitudinal stresses) of the linear analysis and the smeared crack analysis combined with the consideration of concrete creep model are compared taking into account that time elapsed from casting concrete – prestressing is 28 days, and the time till applying the live loading = 365 days. The following figures exhibit the deflection of the bridge due to edge span maximum-maximum live loading according to the influence line of the statical system.

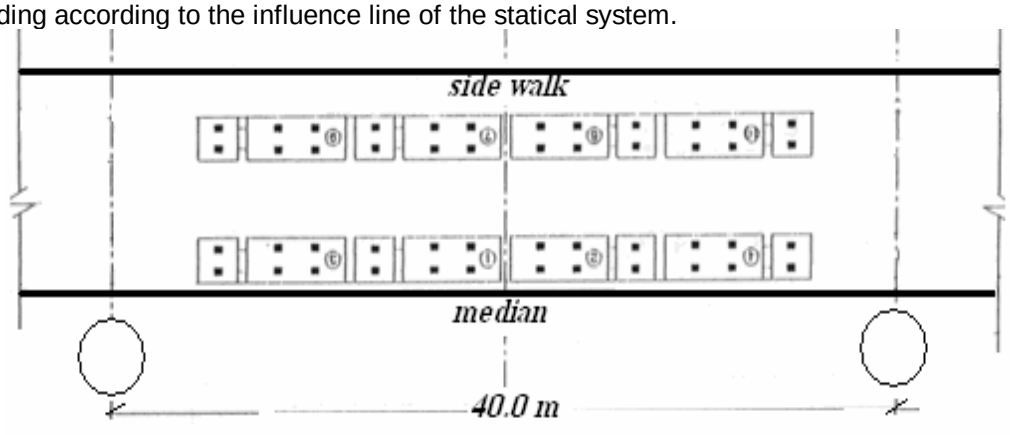

Fig. 8: Live Loading Scheme "Max- + ve"

Table 1: Edge span loading on 40m span Box-Girder resting on Bearings

Straining Actions	Linear Analysis	Crack -Creep Analysis
Maximum deflection in edge span	*7.95 mm*	*10.3 mm*
Maximum Long tensile stresses in bottom slab	*3.43 MPa*	*3.88 MPa*
Max. Longitudinal compressive stresses in top slab	*-1.36 MPa*	*-1.56 MPa*

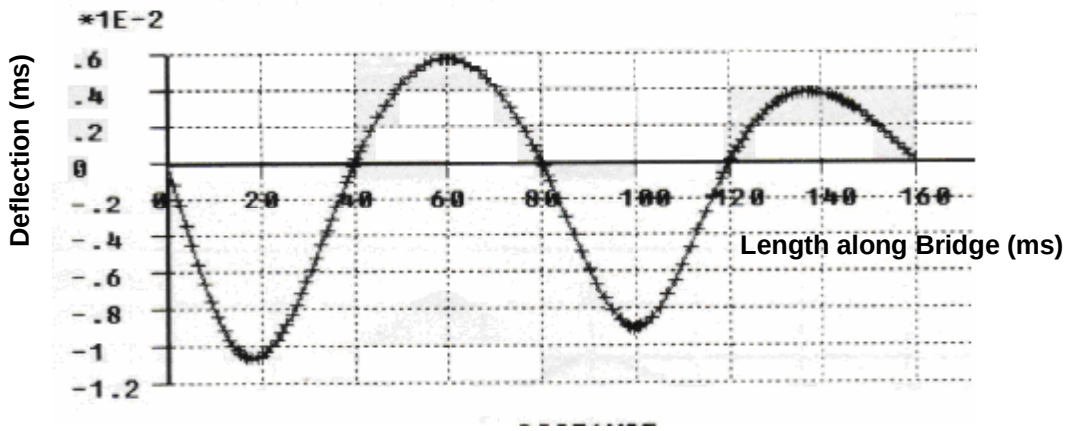

Fig. 9: Deflection "m" along Bridge Resting on Bearings "Crack-creep Model" due to Edge Span Maximum Loading

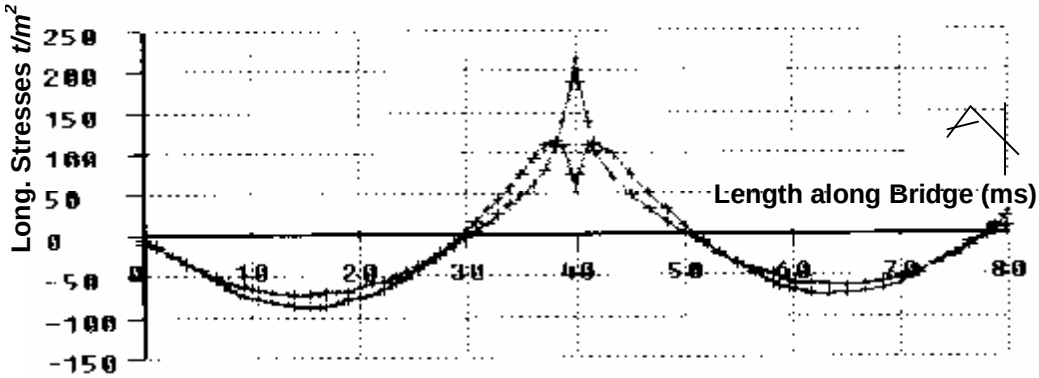

Fig. 10: Longitudinal Stresses "t/m^2" in the top slab" due to Edge Span Max. Loading

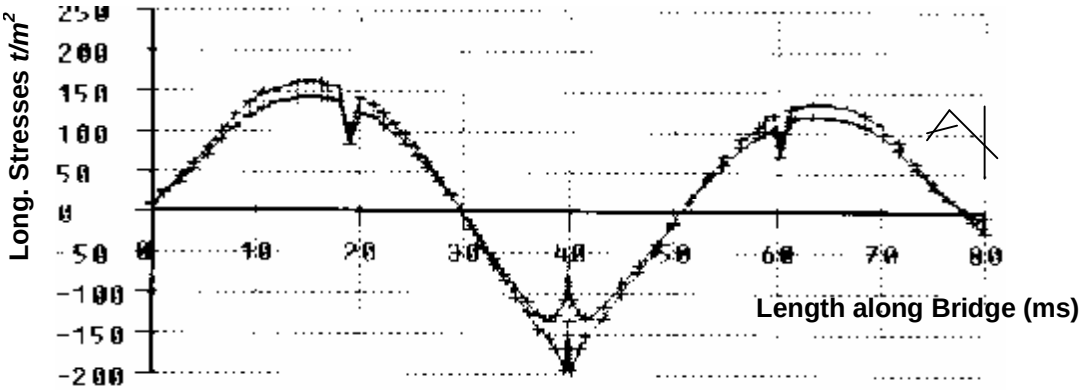

Fig. 11: Longitudinal Stresses t/m^2 in the Bottom Slab" due to Edge Span Max. Loading

Table 2: Edge Span Loading on 40m Span Box-Girder Cast Monolithically with Piers

Straining Actions	Linear Analysis	Crack -Creep Analysis
Maximum deflection in edge span	*5.32 mm*	*6.80 mm*
Maximum Long tensile stresses in bottom slab	*2.52 MPa*	*2.88 MPa*
Max. Longitudinal compressive stresses in top slab	*-2.08 MPa*	*-2.31 MPa*

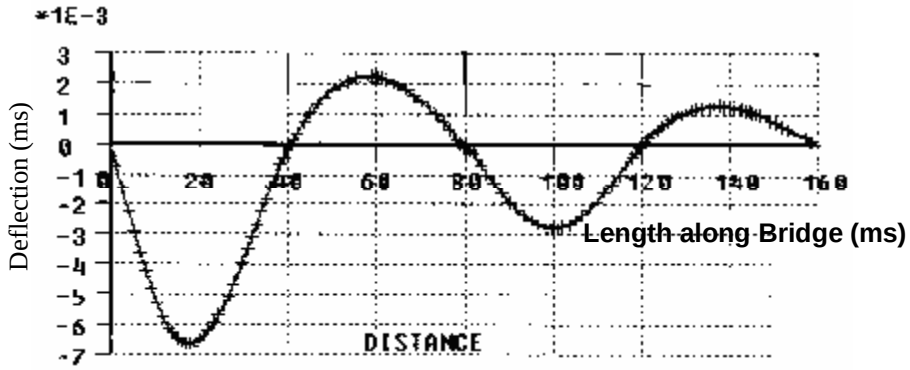

Fig. 12: Deflection "m" along Bridge "Monolithic System "Crack-Creep Model"

From the above table it is deduced that the maximum tensile stresses generated do not exceed the limited tensile stress of the concrete rank (*45.0MPa*) which is 3*.0 MPa*, in view of that, the reduction in Young's modulus due to cracking is not that amount that might cause a substantial increase in the bridge deflection. To expound the substantial effect of smeared cracking model a parametric crack analysis had been adopted taking into account inferior

tensile strength for concrete (*1.6 N/mm²*) which corresponds to lower concrete class (*25.0 N/mm²*), Fig. 13.

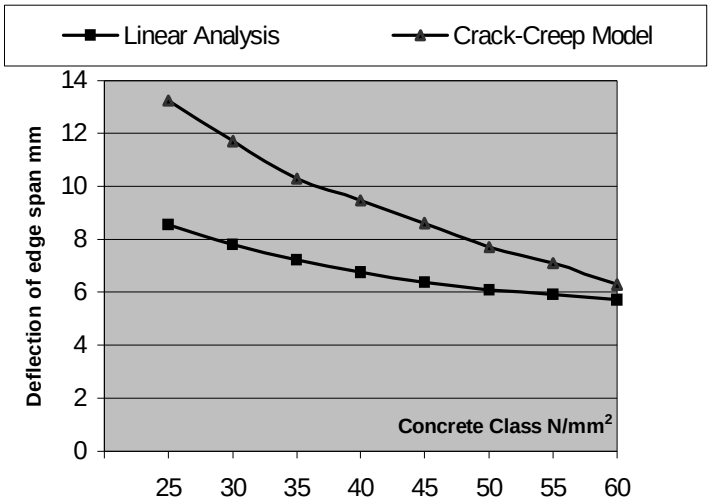

Fig. 13: Deflection of Edge Span "mm" v_s Different Concrete Class

Prominent variation between linear and crack analyses can be identified as the generated transversal tensile stresses in top slabs exceeds the limiting tensile stress of the corresponding concrete class. In such case, reduction in Young's and shear modulii results in excessive displacement as can be deduced from figure 13. It is obvious that the gap between linear analysis results and creep-crack model gets narrower with enhancing the concrete quality.

Long Term Behavior

The long term behavior of the bridge is considered taking into account the creep effect of the concrete material under dead loading (own weight "*O.W*" and superimposed load "*SIL*") and prestressing. Fig. (14) and (15) explicitly delineate the evolution of vertical displacement and bending moments with the elapsed time for the edge span up to 5000 days for box-girder connected monolithically with the piers. From the figures it is construed that long term deflection is as double the value of the displacement after 30 days, this effect increases substantially with the increase of the pier height for the same column inertia. The long-term deflection value due to *OW+ SIL+* prestressing is about 2.50 times the short-term deflection for long pier columns due to loss of prestressing force with time and concrete creep strains.

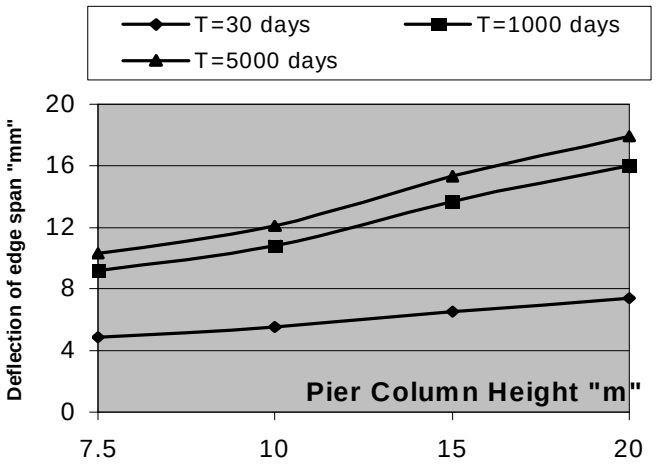

Fig. 14: Deflection of Edge Span "mm" v_s different Pier Heights

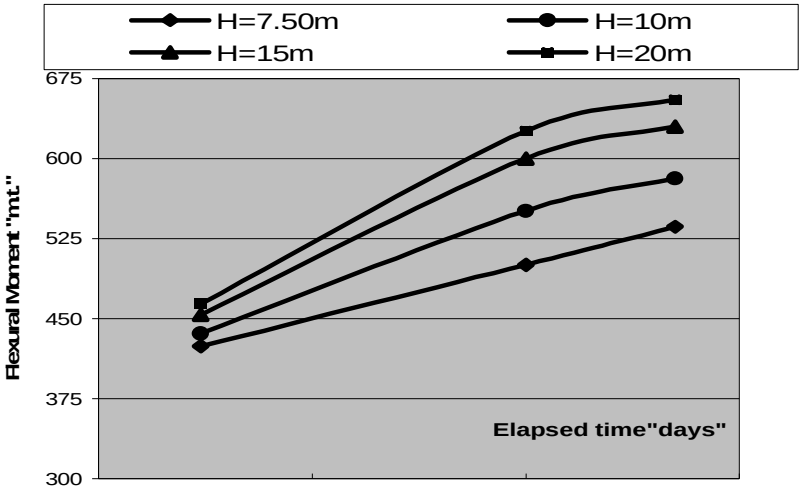

Fig. 15: Flexural Moment of Edge Span "*m.t*" $v_{s.}$ elapsed Time for Different pier Heights

The longitudinal stresses induced in the curved shell element of the top slab, bottom slab and the webs are converted to flexural moment; the results are presented in Fig. (15) for different pier heights having the same inertia. It can be deduced that for lower columns positive bending moment of edge spans increases by 26%, while for long columns the longitudinal moment increases by 40% at 5000 days compared with the positive moment of the edge span at 30 days.

In-situ Loading Test

Loading tests were carried out after the completion of the bridge construction works. The objectives of the test are as follows:

- Confirm the bridge structural rigidity as a whole and clarify the bridge construction work as designed.
- Obtain the initial condition of the bridge structural rigidity for future maintenance works.

To realize the objectives, static loading tests were conducted on the 40 m span box-girder by loading trucks 35 tons capacity as configured in fig. 8 and fig 16. Deflect meters were mounted at the mid span, quarter span and three-quarter span; longitudinal strain gauges were installed on the concrete at the top and bottom slabs of the box-girder just under and above the webs. The total bridge rigidity was examined through the comparison of testing results (12) with the theoretical estimates based on the above analytical model. Comparison had been held for Assiut and lower approaches of Suez Canal representing continuous box-girder supported on pot bearings. Besides, assessment has been held for Sohag bridge and higher approaches of Suez Canal where the box girder is monolithically connected to the pier columns.

Fig. 16: Loading test of the Suez Canal Approach Bridge 40m span

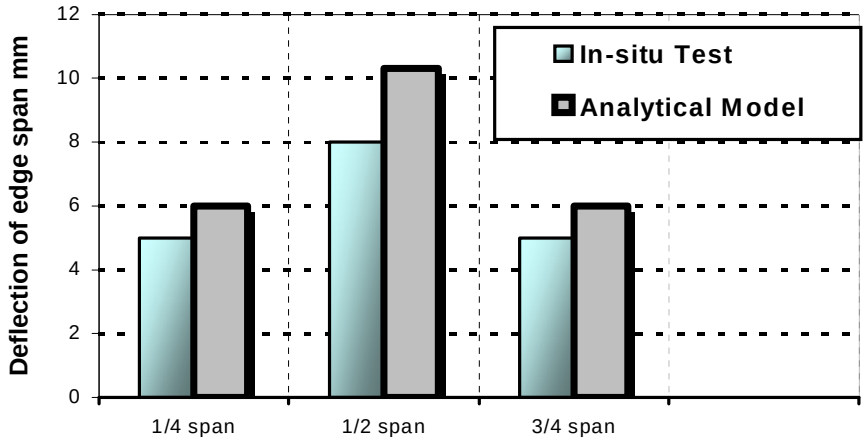

Fig. 17: In-situ Deflection of Edge Span v_s Theoretical Records for Box-girder Bridge Resting on Pot Bearings

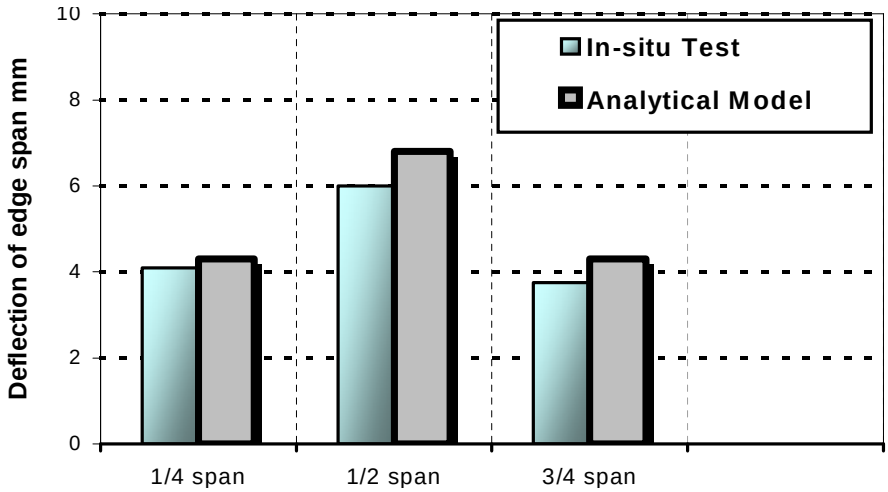

Fig. 18: In-situ Deflection of Edge Span v_s Theoretical Approach for Box-girder Bridge Monolithically Connected to Piers

It is concluded out of Fig. 17 and 18 that the analytical approach provides deflection values slightly higher than the measured records, this may be attributed to the better quality concrete attained at the site, difference in the elapsed time from prestressing to live loading application, slight difference in cement type, ambient temperature and relative humidity.

Research Findings:

a- The application of finite element method makes the combined design criteria possible as it depends on assessing strength and displacements, a feature that has become a crucial part of modern design practice. It releases the doubtful feeling of the designer to the requirements of his structures taking into account the required precision of the constitutive modeling and its interpreted parameters.

b- Finite element process has to be validated against in-situ testing. Moreover, in-situ loading tests upon completion of remarkable Nile bridges are crucial for the sake of future maintenance as they evaluate the initial condition data of the bridge and assess the structural rigidity of the bridge at the time of taking over the project.

c- Use of concrete crack model furnishes productive results in particular the effect of cracking of top slab –due to its transversal behavior- on concrete Young's modulus and the subsequent redistribution of longitudinal stresses. It was found that increasing the quality of concrete superstructure to 45N/mm^2 results in insignificant distinction

between crack and conventional linear models for bridges prestressed in the longitudinal direction only of top slab width 10.50m.

d- Long-term effect of prestressed concrete bridges such as creep is vital for a comprehensive and full understanding of stresses, deflections, and for precise consideration of the mandatory camber during construction.

e- It is vigorously recommended to conduct live loading tests on bridges after 5000 days to convey the results of analytical model authenticating the bridge rigidity after mobilization of creep.

Acknowledgement

The author would like to express his deep appreciation to Ministry of Transportation in Egypt and General Authority of Roads and Bridges. Special appreciation to Expertise house Nile Engineering Consulting Bureau for providing productive thoughts for preparing this paper.

REFERENCES

1. Schlaich, J. and Scheef, H. (1982), "Concrete box-girder bridges, ", IABSE,
2. Mahdi, H.A, (2006), "Bridges construction technology", key note lecture, sixth of October University.
3. Labib, G., Taha, M., Bakhoum, M. and El-Said, M. (1996), "Construction cost breakdown of prestressed concrete bridges in Egypt", 7th international colloquium on structural and geotechnical engineering, Ain-Shams University, vol1, pp-57-68.
4. Kollbrunner, C.F. and Hajdin N, (1966), "Warping torsion of thin-walled beams of closed section", auf Deutsch, Mitteilungen der Technischen Kommission Heft 32, Zurich, Shweizer Stahlbau-Vereinigung.
5. Kupfer, H "1969)," Box beam with elastically stiffened cross-section under line and point loads", Stahlbeton bau, berichte ans forschung und praxis.
6. Reissner, E, (1946), "Analysis of shear lag in box beams", Quart, App. Math, P.268.
7. DIANA, (2005), Software package Release (9.0), TNO Institute, Netherlands
8. Computer-Unterstuetzte Berechnung des Ueberbaus (Internationale Vereinigung fuer Brueckenbau und Hochbau (IVBH), “Computer aided design for Superstructures, International Association for Bridges and Structural Engineering, in German Language).
9. Mahdi, H.A and El-Kadi, F. (2001), "Precise structural analysis of Suez Canal Bridge", (2001), fourth international conference on structural and geotechnical engineering, Alexandria University, pp. 561-572.
10. Mahdi, H.A, (2003) "New Approach combining soil Mohr-Coulomb constitutive law with concrete smeared cracking model for precise evaluation of aged water structures foundations", fifth international conference on structural and geotechnical engineering, Alexandria University, GT-139-151.
11. CEB-FIP Model Code, MC90, Committee Euro-International du Beton, (1993). Model Code for Concrete Structures, 1990 (MC90), Thomas Telford, London.
12. Concrete research laboratory, "Loading test report of Assiut Bridge (1999), Suez Canal Bridge (2001) and Sohag Bridge (2005)", Cairo University.

INFLUENCE OF HORIZONTAL CONSTRUCTION JOINT ON THE FLEXURAL BEHAVIOUR OF REINFORCED CONCRETE SLABS

Ibrahim M. Metwally
Ass. Prof., Reinforced Concrete Dept., Building Research Centre, 87, El-Tahrir St., Dokki, Giza, Egypt, E-Mail: im2aa@yahoo.com
Mohamed S. Issa
Ass. Prof., Reinforced Concrete Dept., Building Research Centre, 87, El-Tahrir St., Dokki, Giza, Egypt,

ABSTRACT

Some concrete casting contractors fall in certain mistake during casting of reinforced concrete slabs in field by casting them in two layers. The first layer is usually casted up to cover the reinforcement steel mesh to allow the concrete trolley (which carries the fresh concrete) to move easily above the rough surface of the slab (after hardening) for casting the second layer without any destruction of the arrangement of steel mesh. This technique of casting creates a horizontal joint which is considered as a plane of weakness which may be subjected to leakage, deterioration, and possible failure due to tensile or shear stresses. This paper concentrates on the effect of the horizontal joint and the type of the different bonding materials (which are used to bond the two layers) on the flexural response of reinforced concrete slab. Test results show many surprises as being of horizontal joint in reinforced concrete slabs do not affect the performance of slabs in flexure. Moreover, jointed slabs with and without bonding materials recorded higher values of ultimate load carrying capacities, stiffness, ductility, flexural toughness, and less deflection compared with the reference slab (solid slab without joint).

Keywords: Horizontal Joint; Slab; Adhesive; Flexural Behavior; Stiffness

INTRODUCTION

Horizontal lift joints in roller-compacted concrete structures as shown in Fig. 1 are planes of weakness subject to leakage, deterioration, and possible failure from tensile or shear stresses[1].

Fig. 1: Construction of Horizontal Joint [1]

Codes Requirements for Joint Treatment:-

1- American Concrete Institute: ACI 318-89R [2]
The requirements of the 1977 code for the use of neat cement on construction joint have been removed, since it is rarely practical and can be detrimental where deep forms and steel congestion prevent proper access. Often wet blasting and other procedures are more appropriate. Since the code set only minimum requirements, the engineer may have to specify special procedures if condition warrant. The degree to which mortar batches are needed at the start of concrete placement depended on concrete properties, congestion of steel, vibrator access, and other factors. ACI Code recommended that the concrete surface of construction joint shall be cleaned and laitance removed. Immediately before new concrete is placed, all construction joints shall be wetted and standing water removed.

2- British Standard: BS 8110 [3]
It is necessary for a joint to transfer tensile or shear stresses, the surface of the first pour should be roughened to increase the bond strength and to provide aggregate interlock. With horizontal joints, the joint surface should, if possible, be roughened, without disturbing the coarse aggregate particles, by spraying the joint surface, approximately 2-4 hours after the concrete is placed, with a fine spray of water and / or brushing with stiff brush.

3- Australian Standard: AS 1480-1982 [4]
Before fresh concrete is placed against hardened concrete at a construction joint, the joint surface of hardened concrete shall be thoroughly roughened and cleaned, so that all loose or soft material, free water, foreign matter and laitance are removed. At the time of placement of the fresh concrete, the joint surface of the hardened concrete shall be damp but there shall be no free water.

4- Indian Standard: IS 456:1978 [5]
For horizontal joints, the surface shall be covered with a layer of mortar about 10 to 15 mm thick composed of cement and sand in the same ratio as the cement and sand in concrete mix. This layer of cement slurry or mortar shall be freshly mixed and applied immediately before placing the concrete.

5- Egyptian Code 1990 [6]
When the work has to be resumed on the horizontal construction joint (after more than one day), the surface of the hardened concrete shall be carefully scrabbled to expose the coarse aggregate. The surface shall be cleaned and loose or soft material removed. The surface shall be then thoroughly wetted. A layer of water-cement grout or bonding new to old concrete paint shall be sprayed.

The aims of this research is to investigate the different techniques of bonding the horizontal joint in reinforced concrete slab by using several bonding materials, and to explain their effects on the flexural performance of slabs. Materials used for this purpose are**:-**

1- Combination of water glass, and Portland cement
Water glass is consisted of several compounds containing sodium oxide (Na_2O), and silica (SiO_2). The solution is strongly alkaline and viscid.
Thompson et al. [7] concluded that sealing concrete surface with soluble sodium silicate may improve surface properties such as hardness, permeability, chemical durability, and abrasion resistance.
Sodium silicate (water glass) is unique in that it can undergo four very distinct chemical reactions. These reactions have been defined as: hydration / dehydration, gelatin, precipitation, and surface charge modification. These reactions allow silicate to act as a: film binder, matrix binder, and chemical binder [8].

It is the very quick reaction with Ca^{+2} that allows silicate to be used as a cement accelerator. A problem commonly encountered with using Portland cement as a matrix binder is the

achievement of sufficient green bond strength. The incorporation of silicate into a cement-based formulation will accelerate the set of the cement [8].

2- Combination of water glass, silica fume, and Portland cement

Silica fume is a by-product material resulting from the production of ferrosilicon alloys.
Silica fume reacts chemically and pozzolanically with liberated lime during cement hydration at ordinary temperature and in the presence of moisture to form a strong compound material (calcium silicate hydrates, gel), which has an adhesive characteristic [7].
The benefits of using silica fume as a matrix binder are that it tends to be more absorbent of liquids and produce a highly durable product [8].
In order to achieve the necessary green strength, silica fume must be activated either by heat or chemically by alkali. Silicates (water glass) are widely accepted as the best material to activate pozzolans (as silica fume) in general. The alkali serves to activate the siliceous material present in pozzolans, and the silica portion contributes to the formation of calcium silicate hydrate; a cementitious phase that is the matrix binder [7].

3- Epoxy Resin

Polymer adhesives provide a better bond of plastic concrete to hardened concrete than can be obtained by relying on the cement itself or on a cement slurry, because polymer adhesives shrink less than cement paste upon curing, and because they tolerated a wider range of moisture conditions in the plastic concrete and the hardened substrate. The primary use of all types of water-borne adhesives with concrete is to bond plastic concrete to hardened concrete. The only solvent-free adhesives used for bonding plastic concrete to hardened concrete are epoxy adhesives because, unlike other solvent-free adhesives, they can be readily formulated to cure and bond in the presence of water [9].
To ensure adequate bonding using epoxy adhesives, the following requirements should be met: [10]
A- Prepared surface should be strong, dense, and sound.
B- Prepared surface should be clean and free from such contaminants.

Epoxy adhesives are supplied as a two-part system, one containing the epoxy resin and the other containing the hardened or curing agent. Prior to combining the two components, it is recommended that each component is thoroughly mixed to ensure uniformity [10].

Although the epoxy adhesives provides satisfactory adhesion if the freshly mixed concrete is placed immediately after applying the adhesive, the contractor should wait for five to ten minutes so that the adhesive can wet the existing surface prior to contact with the freshly mixed concrete. The freshly mixed concrete must be placed while the adhesive is tacky [10].

Six reinforced concrete slabs were tested to investigate the effect of the two-step casting procedure and the bonding materials on strength, deflection, stiffness, toughness, and failure mode. As well as, making a comparison between the effects one-step and two-step casting procedures of reinforced concrete slabs.

EXPERIMENTAL PROGRAM

Concrete Materials

The concrete mix was designed to produce a 28-day cube compressive strength of 30 MPa. The mix proportion of 1.0 m^3 was 1224 kg of gravel, 612 kg of sand, 350 kg of ordinary Portland cement, and 154 liters of water (w/c=0.44). The slabs were reinforced with one bottom smooth steel mesh 6ø8/m (yield strength = 330MPa) in two directions.

Specimens

The test slab specimens were square with 1100 mm side length and 60 mm thickness. The test specimens were simply supported along two edges. Fig. 2 shows reinforcement details and dimensions of the slabs.

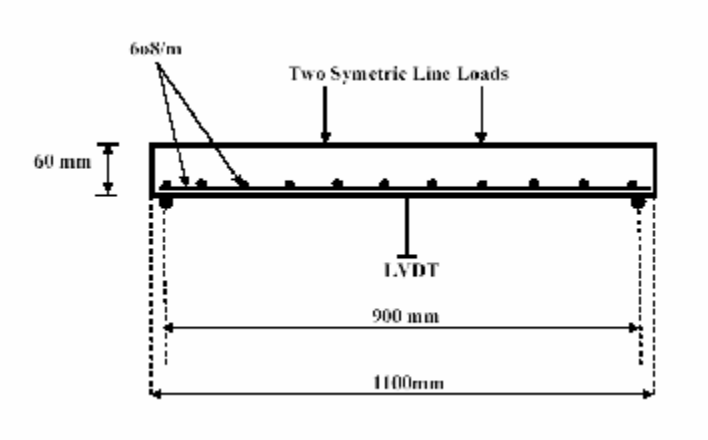

Fig. 2: Details of a Typical Test Specimen

Casting and Joint Treatment

All the specimens were cast horizontal. Control was cast by the traditional method to the full depth of 60 mm. In contrast, the other slabs were cast by the two-step procedure; the bottom portion of 30 mm was cast first and the top portion of 30 mm was cast in the following day. The bottom layer was casted under the direct sun and exposed to the direct sun till casting the top layer in the second day as a field simulation. The surface of the first fresh concrete layer was kept rough without any leveling to create the bond stresses between the two layers. During the first seven days after hardening, all concrete slabs were cured by water spraying twice every day. Then the slabs were left under the sun for six months till testing.
This paper discusses also the effect of different bonding materials for the two layers on the slab performance as follow:
SS: "Control Slab": Slab was cast to the full depth (without horizontal joint)
S0: Slab was cast in two layers without binder

In the following slabs, different binders were used between two layers as follow:-

S1: Cement slurry (water: cement; 1:1 by weight) as a binder;
S2: Epoxy resin;
S3: A mixture of water glass, cement and water (0.1:1:1 by weight); and
S4: A mixture of water glass, cement, water, and silica fume (0.1:0.9:1:0.1 by weight).

Test Setup

All the specimens were tested under two line loads using hydraulic jack until failure. The slabs were instrumented with LVDT under midspan (the slab center) to monitor deflection. During testing, cracks were marked. Midspan deflection and load were recorded for each slab. Fig. 3 shows the test setup.

Fig. 3: Test Setup

TEST RESULTS & DISCUSSION

Load-Deflection Response

The load-deflection curves were obtained using LVDT and X-Y plotter connected to the testing machine. The applied two line loads versus the deflection at the center of the slab for all test specimens are shown in Figures 4, 5, 6, 7, 8, and 9.

Ultimate Load

The ultimate loads (Pu) of the studied slabs are shown in Table 1
The maximum ultimate load was obtained by slab S0 (jointed slab without adhesive). It attained a noticeable increase in Pu equal 17.5% over the reference slab SS (without joint).
The most useful adhesive bonding material for the jointed slabs were developed by using a mixture of water glass , cement, and water as in slab S3 and a mixture of water glass , cement, water , and silica fume as in slab S4. They recorded an increase in the ultimate load carrying capacity of 13.3% and 12.6% respectively compared with the reference slab SS.
In general, from the above results, it can be noticed that horizontal joint in R. C. slabs (whether with or without adhesive) improve the ultimate load clearly. This is due to that the slab horizontal shear resistance at the joint was enhanced (by the friction forces between the two layers) compared to the slab without joint.

Deflection

Deflection of R. C. slab is considered as a measure of its rigidity; with decrease of deflection, the rigidity increases.
Table 1 show that all the jointed slabs deflected less than the reference slab (SS). The drops of deflection of the jointed slabs were very clear. For example, at ultimate load, S3 slab recorded the least deflection. It deflected 0.33 times the deflection of the reference slab.

Stiffness

From the load-deflection curves (Fig. 4 to 9), two values of the stiffness of the tested slabs were obtained. The uncracked stiffness K_i is indicated by the slope of the line at a value less than the initial crack load (1 mm deflection), and the ultimate stiffness K_u is measured by the slope of the line at about 90% of the ultimate load[11].
Stiffness degradation is defined as the ratio between the ultimate stiffness and the uncracked stiffness [11]. Values of K_i, K_u and stiffness degradation are given in Table 1.

From the deflection curves, it can be seen that the slope of S3 slab is very steep. It recorded the maximum value of K_i and K_u with increments of 175 % and 29 % compared with the reference slab SS.
Stiffness degradation is considered as a measure of the ductility. As the stiffness degradation increases, the slab specimen indicates lower ductility [11].
From the results in Table 1, all jointed slabs have shown small values of stiffness degradation than the reference slab. This lead to more ductile behavior than the reference slab SS, which agrees with the experimental results of Mo and Lai [12].
The lowest stiffness degradations were obtained for slabs S1 and S3. Therefore, it can be concluded that S1 and S3 slabs have the higher ductility. For example, S3 slab has an increase in ductile response by about 53 % than the reference slab SS. This phenomenon may be explained as the horizontal construction joints create the springy effect between the two layers of the R. C. slabs resulted in improvement of ductility.

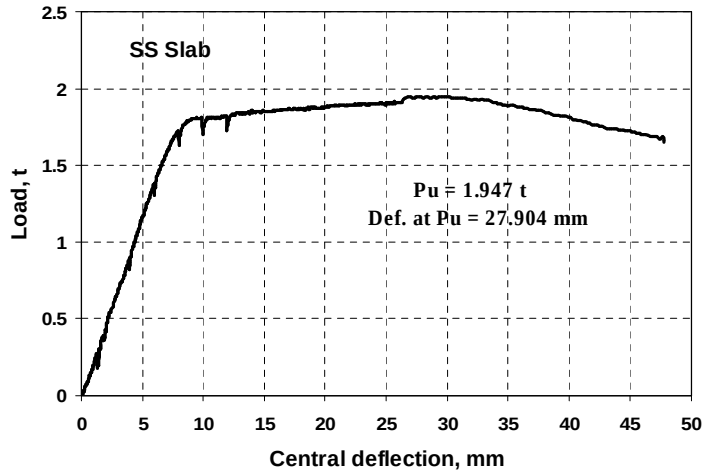

Fig. 4: Load-Deflection Curve of Slab SS

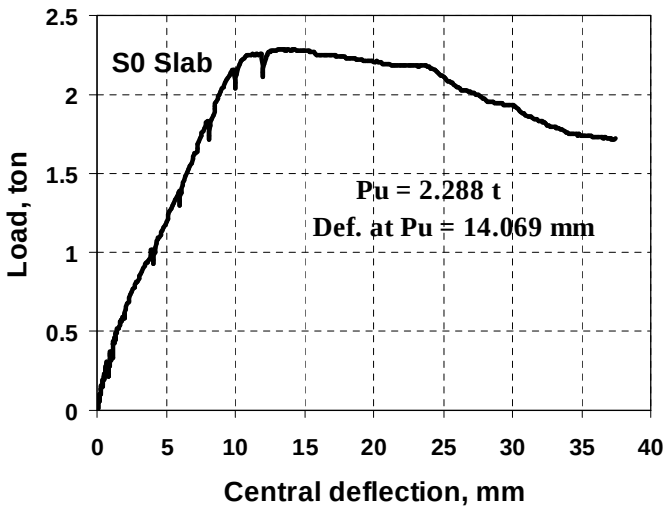

Fig. 5: Load-Deflection Curve of Slab S0

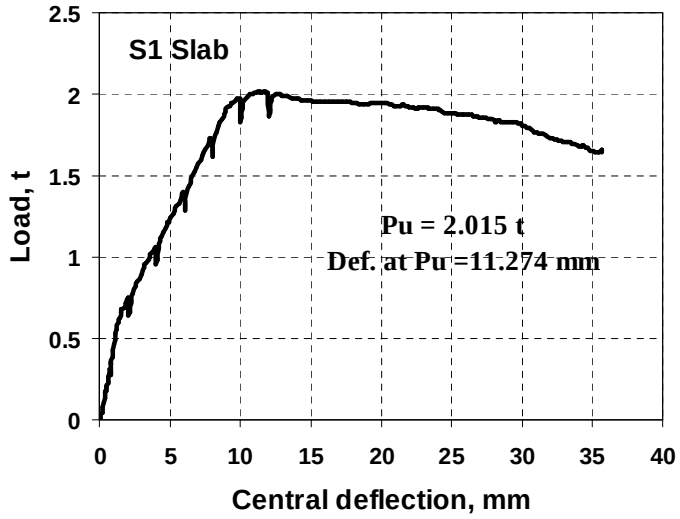

Fig. 6: Load-Deflection Curve of Slab S1

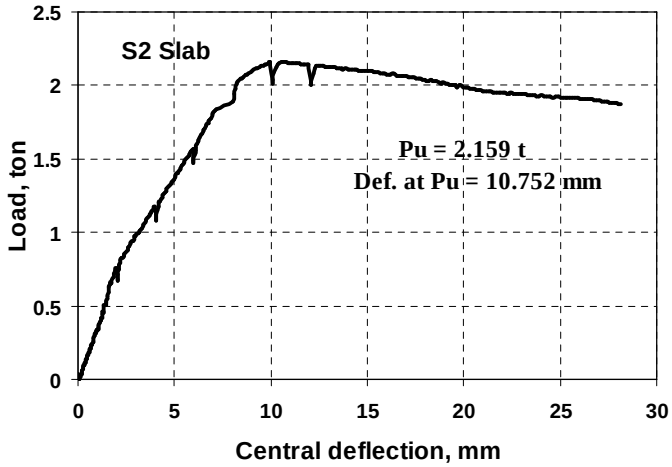

Fig. 7: Load-Deflection Curve of Slab S2

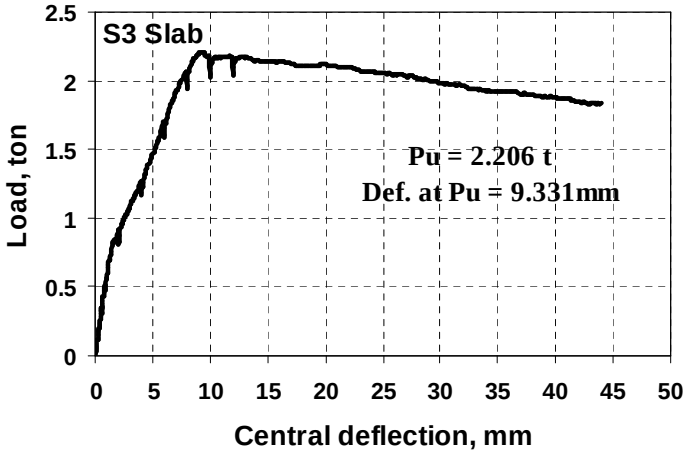

Fig. 8: Load-Deflection Curve of Slab S3

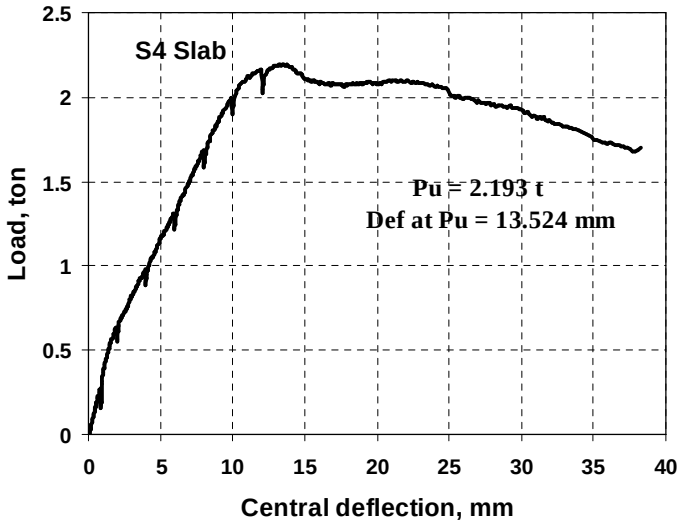

Fig. 9: Load-Deflection Curve of Slab S4

Toughness

Flexural toughness or energy absorption is defined as the area under the load-deflection curve up to a deflection equal to the span length divided by 150[13]. The flexural toughness values for various slabs calculated at the designated deflection of 7 mm are shown in Table 1 and Fig.10 respectively. It can be concluded that the jointed slabs have the biggest toughness values. The maximum value of 8.1 t.mm was obtained for slab S3. It attained 54 % increase in toughness compared with the reference slab.

Table 1: Results of the Tested R. C. Slabs

Slab Code	Ultimate Load, P_u (ton)	Ultimate Central Deflection, Δ_u (mm)	Initial Stiffness, K_i (t / mm)	Ultimate Stiffness, K_u (t / mm)	Stiffness Degradation, K_u / K_i	Flexural Toughness, ψ (t. mm)
SS	1.947	27.904	0.20	0.21	1.05	5.25
S0	2.288	14.069	0.29	0.22	0.76	6.35
S1	2.015	11.274	0.45	0.21	0.47	6.27
S2	2.159	10.752	0.33	0.24	0.73	7.64
S3	2.206	9.331	0.55	0.27	0.49	8.1
S4	2.193	13.524	0.37	0.20	0.54	6.25

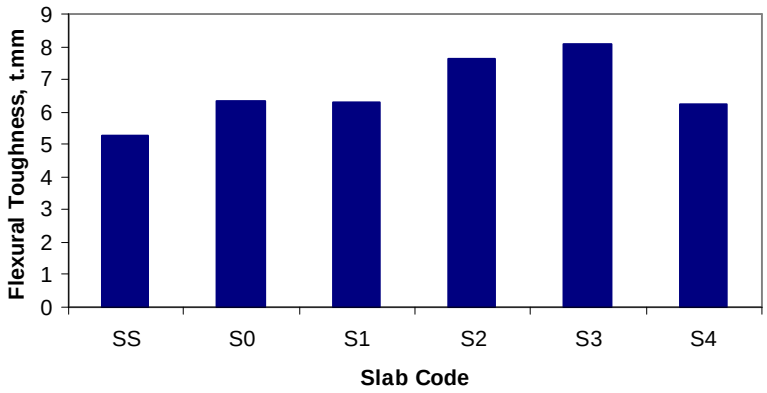

Fig. 10: Flexural Toughness of the Tested Slabs

Cracking and Mode of Failure

At low level of load, the slab behavior was linear elastic with no crack occurrence. As load level increases, the extreme fiber concrete stress reaches its limiting concrete tensile stress and hair fine flexure cracks occur. The first crack was nearly under the position of the loaded area. As the load increases exceeding the first cracking load, the cracks seem to widen and start to propagate, and generally extend (to be initiated) and deviate towards the slab boundaries in all directions up to failure.

As the load increases, all the flexural cracks propagate upwards with extensive cracking parallel to the longitudinal tensile reinforcing bars which develop and extend diagonally toward slab corners. The cracking pattern and mode of failure for all tested slabs are shown in Fig.11. From the above analysis, it can be concluded that, the mode of failure of solid slab (without joint) and jointed slabs are nearly the same and almost all slabs failed due to flexural type mode.

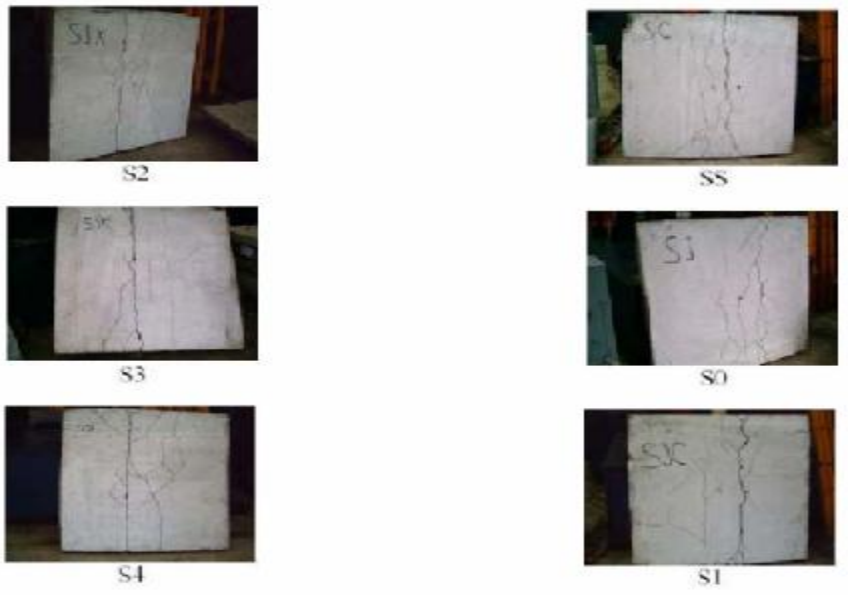

Fig.11: Crack Pattern at Failure of the Tested Slabs

CONCLUSIONS

Conclusions related to the influence of horizontal construction joint on flexural behavior of reinforced concrete slab:-

1- Horizontal construction joint inside the reinforced concrete slab improves its ultimate load carrying capacity compared with reference slab without joint.

2- R. C. slabs with horizontal joints attained a clear reduction in deflection.
3- R. C. slabs with horizontal joints exhibited more stiffness than the slab without joint.
4- Jointed slabs have more ductile behavior than the reference one.
5- Horizontal joint in R. C. slab is very effective in improving the toughness.
6- Mode of failure of all slabs with and without horizontal joints is nearly the same.

Conclusions related to the influence of bonding materials type upon the flexural behavior of jointed slabs:-

1- A mixture of water glass, cement, and water (0.1:1:1 by weight) as in slab S3 is the best adhesive for bonding the two horizontal layers of the jointed slab. This adhesive technique attained the superior flexural response of R. C. jointed slab regarding minimum deflection and maximum ultimate load, stiffness, ductility and toughness.

RECOMMENDATIONS

If the R. C. slabs can not be directly cast to the full depth in the field due to construction requirements or problems. It can be cast by the two-step procedure; the half bottom portion can cast first and the top portion will cast in the following day with using a mixture of water glass, cement, and water (0.1:1:1 by weight) as an adhesive coating compound between the two layers.

FUTURE RESEARCH TOPICS

It is recommended that, some studies must be carried out regarding:-
1- Effect of horizontal construction joint using the recommended adhesive compound on the behavior of R. C. slab exposed to: high temperatures, chemical attack, and drying and wetting cycles.
2- Effect of horizontal construction joint using the recommended adhesive compound on the flexural and shear behavior of R. C. beams.

REFERENCES

1- Hess, J. R., Jan., "RCC Lift-Joint Strength", Concrete International, 2002, pp. 50-56.
2- ACI Committee 318R-89, "Commentary on Building Code Requirements for Reinforced Concrete", 1989.
3- British Standard: BS 8110:, "Structural Use of Concrete", Part 1, Code of Practice for Design and Construction of Construction Joint, 1985.
4- Australian Standard: AS: 1480-1982.
5-Indian Standard: IS: 456-1978.
6-Egyptia Code of Practice for Reinforced Concrete Structures: Construction and Design, 1990.
7-Thompson, L. R.; Silsbee, M. R.; Gill, P. M.; and Scheetz, B. E., "Characterization of Silicate Sealers on Concrete", *Cement and Concrete Research*, Vol. 27, No. 10, 1997, pp. 1561-1567.
8-McDonald, M.; and Thompson, L. R., "Sodium Silicate as a Binder for the 21st Century", Report of *The PQ Corporation: Industrial Chemicals Division*, 2005, 6pp.
9-ACI Committee 503.5R,"Giude for the Selection of Polymer Adhesives with Concrete", 1989 15pp.
10- ACI Committee 503.6R, "Guide for the Application of Epoxy and Latex Adhesives for Bonding Freshly Mixed and Hardened Concretes", 1997, 4pp.
11- Osman, M.; Marzouk, H.; and Helmy, S., "Behavior of High-Strength Lightweight Concrete Slabs under Punching Loads", *ACI Structural Journal*, V. 97, No. 3, May-June 2000, pp. 492-498.
12- Mo, Y. L.; and Lai, H. C., " Effect of Casting and Slump on Ductilities of Reinforced Concrete Beams", *ACI Structural Journal*, V. 92, No. 4, July-August 1995, pp. 419-424.
13- Japanese Concrete Institute, "JCI Standard for Test Methods of Fiber Reinforced Concrete," Report No. JCI-SF-1984, 68pp.

SUBSTITUTION OF CUTTING BOTTOM REINFORCEMENT OF THE RECTANGULAR REINFORCED CONCRETE BEAMS WITH DIFFERENT TECHNIQUES

T. K. Mohamed, S. M. Elzeiny, and O. E. El-Salam
Assistance Professor, Housing and Building National Research Center, Cairo, Egypt
Email: shmelzny@gmail.com

ABSTRACT

This study deals with the restoring of the flexural strength of reinforced concrete beams with opening at tension side. It presents experimental and theoretical studies using different external techniques to restore the flexural strength after cutting the reinforcing steel at the original section. Seven reinforced concrete beams were tested, and retrofitted to study the effect of bonding or bolting steel plates, using side bars over opening, and using side CFRP strips on the behavior of beams. The ultimate strength, stiffness, ductility and mode of failure of theses beams were recorded. It was reported from the output data that, retrofitting using bolted steel plates is structurally efficient and restores the flexural strength, value superior to those of the original section without opening at tension steel. Further retrofitting using other techniques restores the above parameters with different percentages of the original one. The reported output data showed high confidence and reliability in applying these techniques considering some restrictions.

Keywords: opening, flexural, retrofitting, external steel plates, CFRP, reinforced concrete beams.

INTRODUCTION

Creation of openings in reinforced concrete beams at tension steel to facilitate the installation of electromechanical equipment or for architectural modifications is a common practice. If there was no special reinforcement placed around the opening, which is a typical case, strengthening of the opening zone is required to: (a) restore the flexural strength after cutting the reinforcing steel at the original section, (b) minimize cracking and deflections and (c) avoid stress concentration. Steel plates can be used for strengthening RC beams; they are relatively cheap and have good tensile and stiffness properties. They are most effective when used in bending to reduce or limit deflections and deformations. References [1, 2, 3, 4 and 5] reported that, strengthening beams for increasing flexural capacity with external bonded steel plate or by external bolted steel plate of length not covering tension face, improves ductility and has no significant effect in improving ultimate load capacity. The ultimate load capacity increases for plate bolted at tension face of beam using four bolts than for that using two bolts. Hussain et al.[6] evaluated the effectiveness of the plate bonding repair technique for severely damaged RC beams on their tension faces. Reinforced concrete beams were preloaded to 85 percent of their ultimate capacity and subsequently repaired by bonding steel plates of different thicknesses with and without anchorages. Anchor bolts were used for end anchorages. The repaired beams showed higher strength than the original beams, while, the used plates thickness did not exceed a certain limit. End anchorages to the bonded plates could not prevent the premature failure of the beams but improved ductility with decreasing significance as the plate thickness increased; and yielded a marginal improvement in ultimate strength.

EXPERIMENTAL WORK

The current research program was carried out to evaluate the suggested techniques for restoring the flexural strength of reinforced concrete beams having no tension reinforcement due to creating openings at the bottom of the beams at mid span.

Details of Test Specimens

Seven reinforced concrete beams were cast, retrofitted and tested to study the effect of bonded and bolted steel plates, using of side bars over opening and using side CFRP strips on the behavior of beams. The ultimate strength, stiffness, ductility and mode of failure were recorded for all tested beams. All the seven beams had cross-sectional dimensions of 200x400 mm and 2400 mm length. Reference beam BR had no opening at mid span. Other six beams from B1 to B6 had an opening at the bottom of the mid span of length 400 mm, depth 100 mm and width 200 mm as shown in Fig. 1 (A to D). All the beams were reinforced with two 12 mm diameter steel bars in tension side and two 10 mm diameter steel bars in compression side. Bars of 8 mm diameters were used for stirrups. Beam B1 had two 12 mm diameter steel bars over the opening (which is ideal for pre-opening case). Fig. 1 (A to D) shows the reinforcement details of all tested beams.

Beams B2 and B3 were retrofitted using steel plates with dimensions and shape as indicated in Fig. 1-B. For beam B2, the concrete surface where the steel plate was bonded, was prepared using a mechanical metal brush, consequently, a vacuum cleaner was used to remove any dust or loose particles then, the steel plate was bonded using epoxy adhesive. While for beam B3 the steel plate was fixed to the beam by using eleven steel bolts drilled through the beam width.

Beam B4 was retrofitted using two reinforcing steel bars of 12 mm diameter and 1600 mm length. The concrete cover at both beam sides over the opening were removed with length equal to 1600 mm, then; the two steel bars mentioned before were welded to the beam stirrups. A layer of epoxy mortar was applied to cover the bars up to the beam surface. Beam B5 was retrofitted similarly to beam B4, but, the bars were just attached to the beam stirrups without welding. A layer of epoxy mortar was applied to cover the bars to the surface of the beam.

Beam B6 was retrofitted using CFRP strips of width 50 mm, length 1600 mm and 1.2 mm thickness. A grove was made over the opening on both sides with the same dimensions of length and width of the CFRP strips and 20 mm depth of concrete cover. Then the surface was prepared using a mechanical metal brush, consequently, a vacuum cleaner was used to remove any dust or loose particles. A base layer was made using a proper epoxy mortar. Then, preparation of CFRP adhesive has been carried out according to the manufacture instruction to bond the CFRP over the epoxy base layer. Finally the carbon fiber strips was coated by another epoxy layer.

Properties of Material Used in the Study

The average concrete compressive strength used in the tested beams was 35 MPa. The steel reinforcement used for stirrups was mild steel with 8 mm diameter, and for main reinforcement was high grade steel of 10 mm and 12 mm diameter. Table 1 shows the mechanical properties of the steel reinforcement. Carbon fiber strips used in beam B6 was 50 mm wide and 1.2 mm thick. The strip tensile strength was >2800 MPa, E-modulus was 165000 MPa and elongation at failure was 1.7%. The used adhesive was epoxy-based two-component mortar and working time of 30 minutes. The steel plates used in retrofitting beams B2, and B3 had yield strength (f_y) of 240 MPa.

Table 1: Mechanical Properties of Steel Reinforcement.

Diameter (mm)	f_y (MPa)	f_u (MPa)	Elongation %
8	340	520	22.50
	380	520	15.00
	350	530	21.25
10	480	780	13.00
	480	780	13.00
	490	780	13.00
12	470	770	18.33
	450	710	20.00
	450	690	14.17

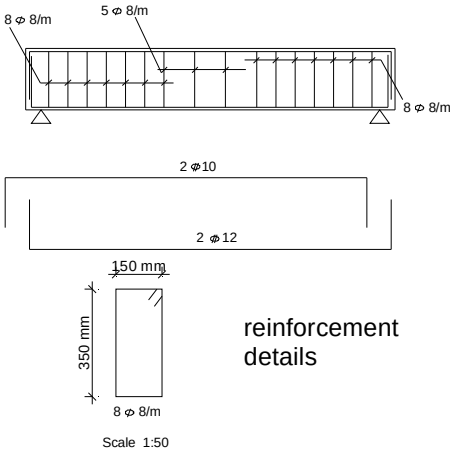

reinforcement details

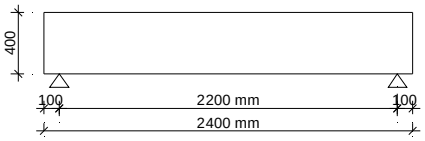

concrete dimensions

Details of Beam BR

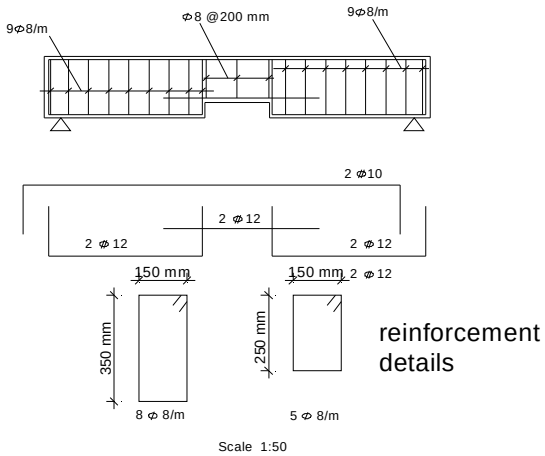

reinforcement details

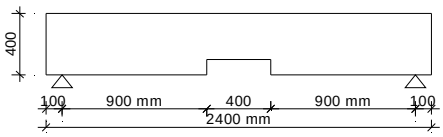

concrete dimensions

Details of Beam B1

Fig. 1-A: Details of Tested Beams BR and B1.

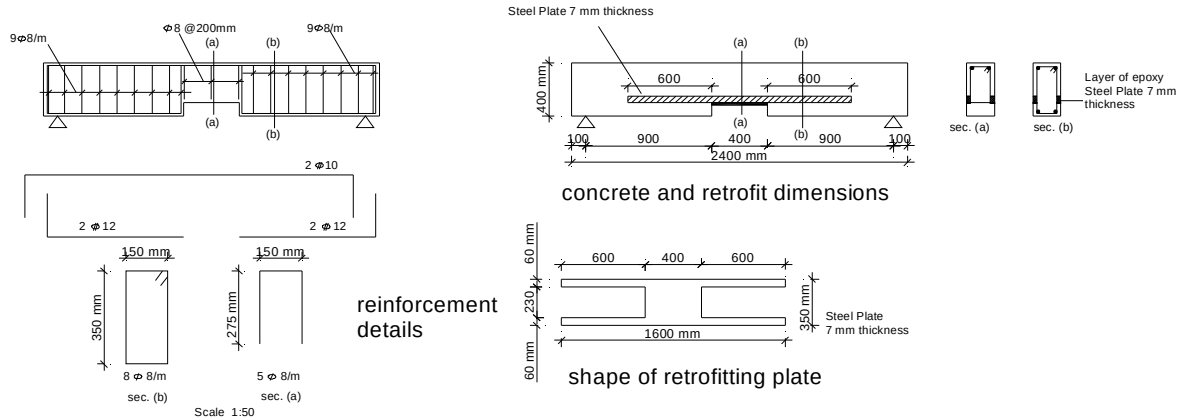

Details of Beam B2

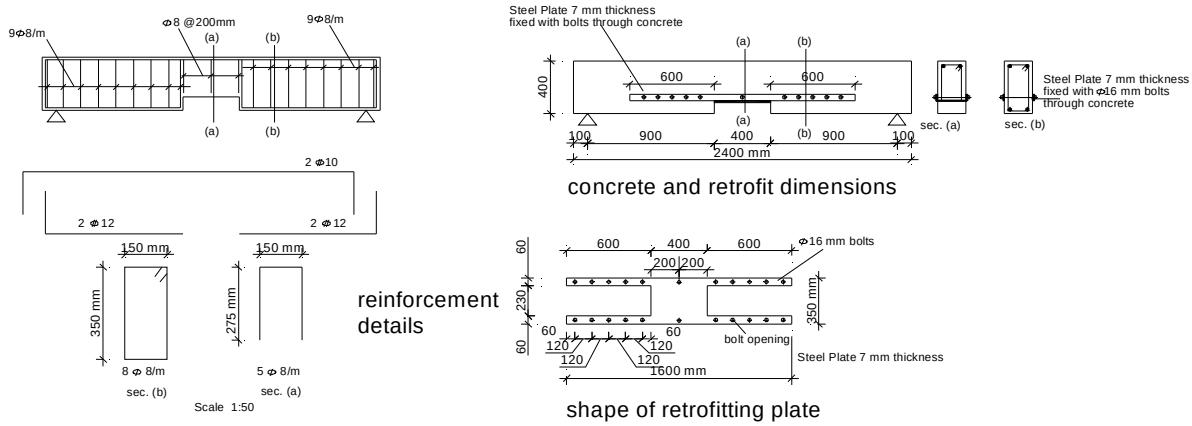

Details of Beam B3

Fig. 1-B: Details of Tested Beams B2 and B3.

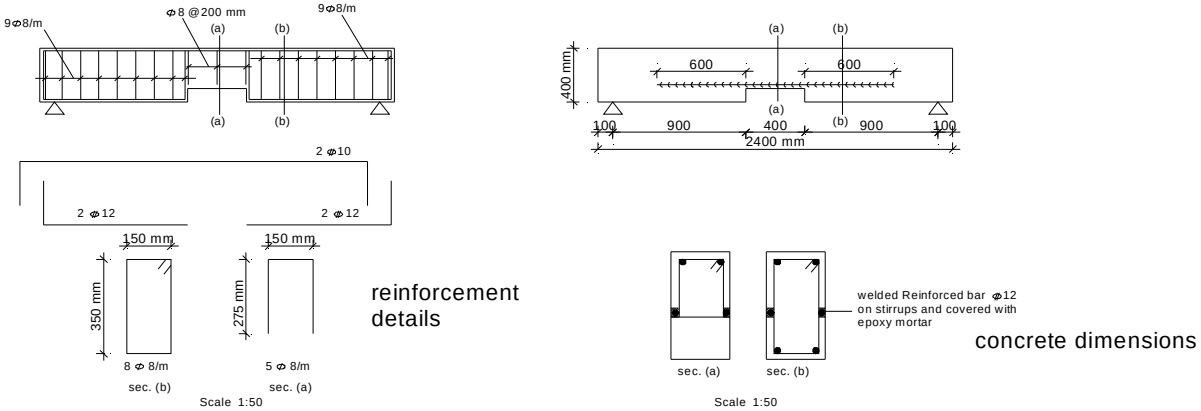

Details of Beam B4

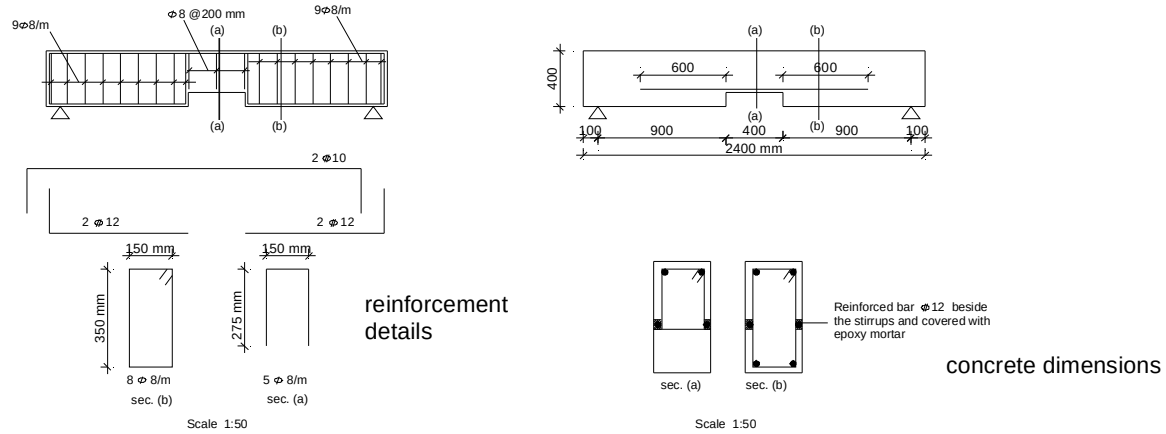

Details of Beam B5

Fig. 1-C: Details of Tested Beams B4 and B5.

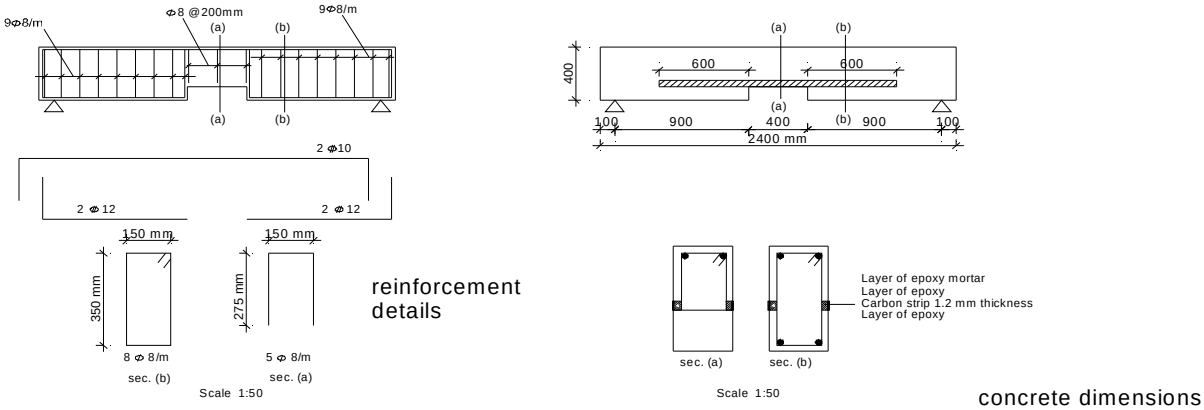

Details of Beam B6

Fig. 1-D: Details of Tested Beams B5 and B6.

Test Setup, Procedure and Measurements

The tested beams were simply supported over two rigid girders as shown in Fig. 2. A two-point-bending load applied to all beams was monotonically increased. The load was applied vertically at the center of a rigid steel beam which, distributed equally on two bearings placed directly on the beam. All tested beams were loaded gradually up to failure. The deflection was measured at the mid span and at a distance 300 mm from the center, by using $\pm$100 mm linear variable differential transducer (LVDT). The strain of steel bars, stirrups, CFRP strips, and steel plates were recorded using electrical strain gages (S.G.). The beams were applied to a displacement central test, performed by using data acquisition online computer system programmed using Lab View software, as shown in Fig. 3.

Fig. 2: General View of the Test Setup.

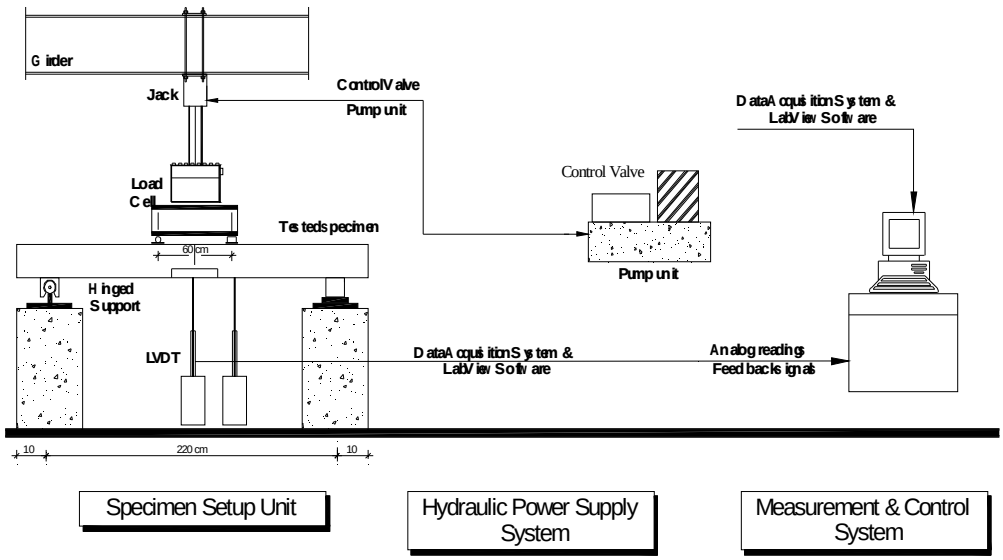

Fig. 3: Schematic of Test Setup and Control System.

TEST RESULTS

Cracking Patterns

Figs. 4-A and 4-B show the crack patterns at failure for the tested beams, and Table 2 shows the deflection at cracking, yielding and at ultimate stage and its corresponding load at mid span. The mode of failure of the tested beams can be divided into three categories. First is flexural failure for beam BR and B1. Second is sudden failure due to cut in the added steel bars or steel plates (side bars for beam B4 and side steel plates for beam B3). Third is sudden failure due to debonding of the Epoxy bonding layer for beam B2, B5, and B6.

Table 2: Deflection and Corresponding Load.

Beam	Deflection (mm)			Corresponding Load (KN)		
No.	cracking	yielding	ultimate	cracking	yielding	ultimate
BR	1	2.2	38	54	73.3	135
B1	3.2	4.0	20	55	97.5	121
B2	2.5	10.7	32	30	72.0	125
B3	2	4.9	40	62	113.0	194
B4	2	5.0	85	52	77.0	107
B5	3	6.0	108	47	68.0	103
B6	3	5.7	18	25	64.0	116

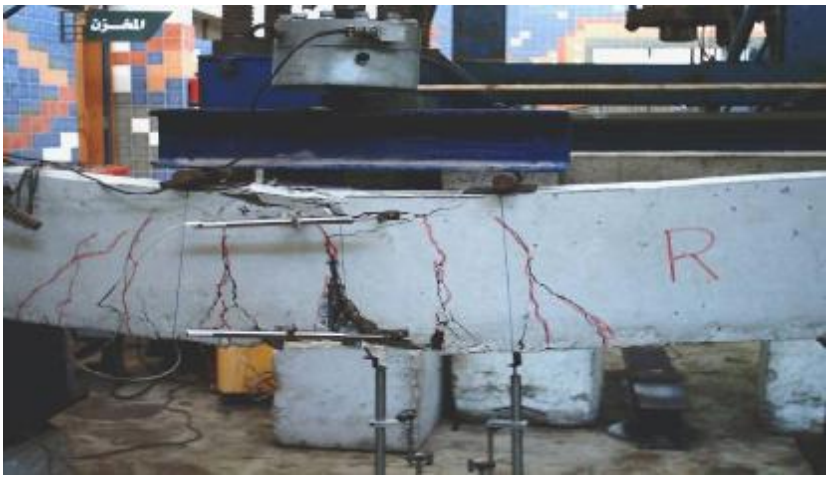

Beam BR

Beam B1

Beam B2

Beam B3

Fig. 4-A: Crack Patterns at Failure for the Tested Beams.

Beam B4

Beam B5 **Beam B6**

Fig. 4-B: Crack Patterns at Failure for the Tested Beams.

Cracking Strength

Table 3 shows the actual cracking moment for the tested beams. The presence of the bolts in beam B3 improved the flexural cracking resistance to be 115% of the beam BR. Also using welded bars at beam side in beam B4 gives a premature flexural cracking to be 96% of beam BR. Further, using epoxy adhesive for bonding side bars in beam B5, steel plates in beam B2 and CFRP in beam B6 reduced the flexure cracking to be 87%, 55% and 46% (respectively) of beam BR.

Table 3: Cracking Moments for the Tested Beams.

Beam No.	$M_{cr.}$ (KN.m)	$M_{ult.}$ (KN.m)
BR	21.6	54.0
B1	38.2	48.4
B2	12.0	50.0
B3	24.8	77.6
B4	20.8	42.8
B5	18.8	41.2
B6	10.0	46.4

Load deflection behavior

Fig. 5 shows the load deflection curves of the tested beams in the study. Table (2) shows the deflection of the tested beams at the mid span at different load stages.

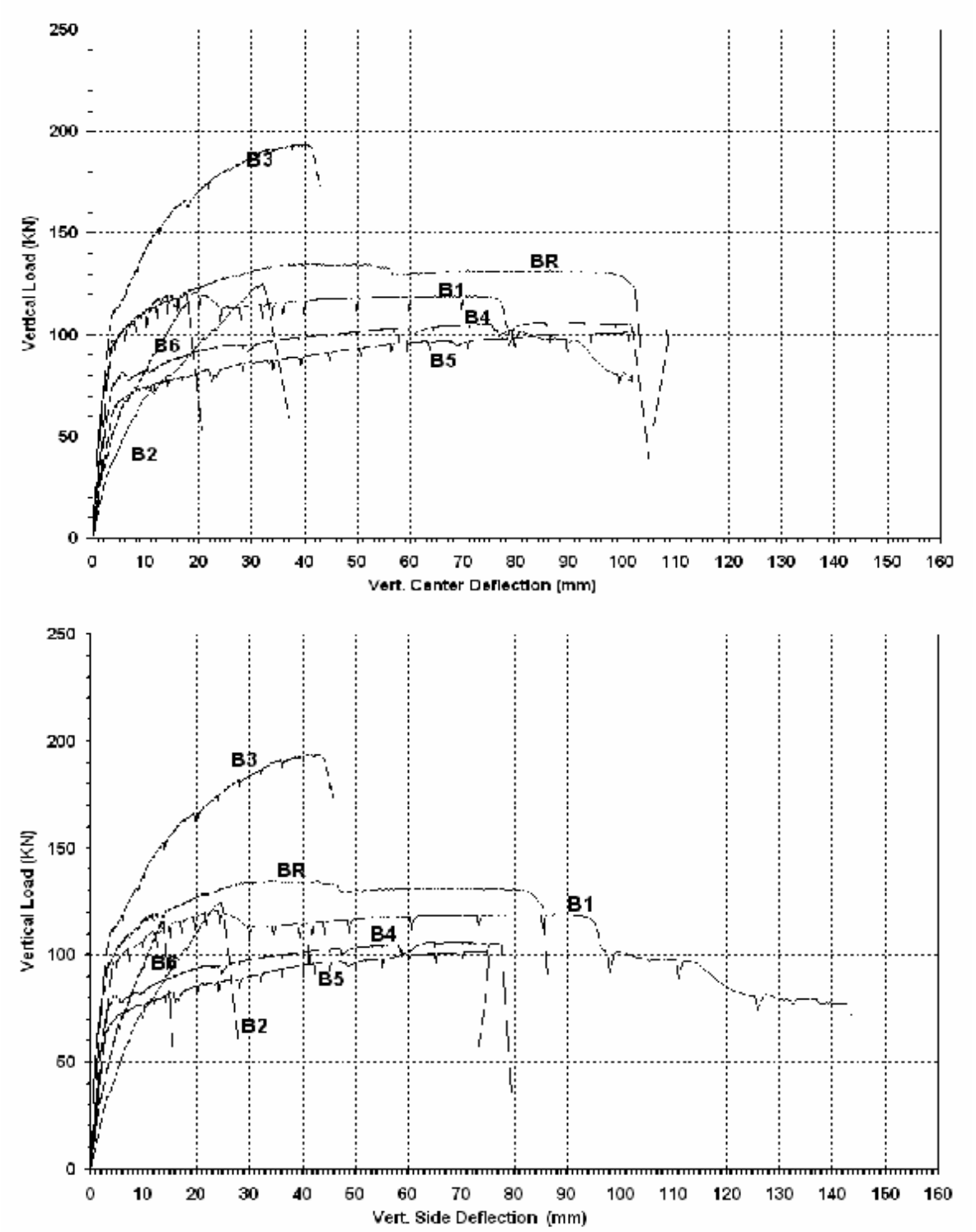

Fig. 5: Load Deflection Curves of Tested Beams (Center, Side).

Table 4 shows the slope of the relation between load and deflection in the uncracked, working and ultimate stages. Slope of load-deflection was used to indicate the flexural rigidity

(stiffness degradation) of the tested beams during loading stages. For beam BR, the rigidity after cracking dropped to about 30% relative of that before cracking. For Beam B1 which had a reinforcement arrangement for opening before casting, the rigidity decreased to be about 8.5% of the stiffness before cracking. For beams B2, B5 and beam B6 which used Epoxy adhesive for bonding steel plate, steel bars, and CFRP to beam sides, the rigidity after cracking dropped to approximately 43%, 45% and 46% respectively, relative of that before cracking due to the rapid progress of cracks through the section height. For beam B3 where bolts were used to fix the side steel plate with the beam surface, the slope of load deflection relationship in the cracking stage was 56% relative to that before cracking showing the effect of using bolts for fixing steel plate. For Beam B4 which was retrofitted by welded bars to beam stirrups, its rigidity was 32% of the stiffness before cracking.

Table 4: Slope of P-Δ Curve.

Beam No.	slope of P-Δ curve (kN/mm)		
	$0 \rightarrow P_{cr}$	$P_{cr} \rightarrow P_y$	$P_y \rightarrow P_{ult.}$
BR	54.0	16.08	1.72
B1	29.8	2.50	1.46
B2	12.0	5.12	2.48
B3	31.0	17.58	2.30
B4	26.0	8.33	0.37
B5	15.6	7.00	0.34
B6	19.2	8.86	4.22

Ultimate Flexural Strength

In the present study, all beams failed in flexural. In case of using side steel plates bonded with Epoxy, beam B2, the ultimate flexural strength reached about 92% of the original section. Using bolts for fixing the side steel plate through the beam width, B3, increased the ultimate flexural strength to reach 143% of the original section. In beams B5 and B6 where the Epoxy adhesive was used to bond the side steel bars and CFRP, the flexural strength reached 76.3% and 86% respectively from the original section of the reference beam BR. For beam B4 where its side bars were welded with the stirrups, the flexural strength reached 79.2% of the strength of beam BR. Comparing beam B1 with the reference beam BR its flexural strength reached 89.6% of beam BR.

Stiffness

The stiffness factor was defined as the inclination of the initial tangent of the load-deflection curve as shown in Fig. 6 and the following equation.

Table 5: Stiffness Factor of the Tested Beams.

Beam No.	$K = \frac{P_u}{\Delta_y}$
BR	6.14
B1	3.03
B2	1.17
B3	3.96
B4	2.14
B5	1.72
B6	2.04

$$K = \frac{P_u}{\Delta_y} \qquad \text{.....(1)}$$

Where

- K is defined as a Stiffness factor.

- P_u is defined as the ultimate load.
- P_y is defined as the yield load.

It's clear from table 5 that, from the techniques used in this study, using bolted steel plate in beam B3, improved beam stiffness than other techniques to be about 53% of beam BR. This is due to the force between the bolts and the side steel plate resisting and sustaining bottom tension forces. This force works till it reaches its ultimate strength which improves the global behavior.

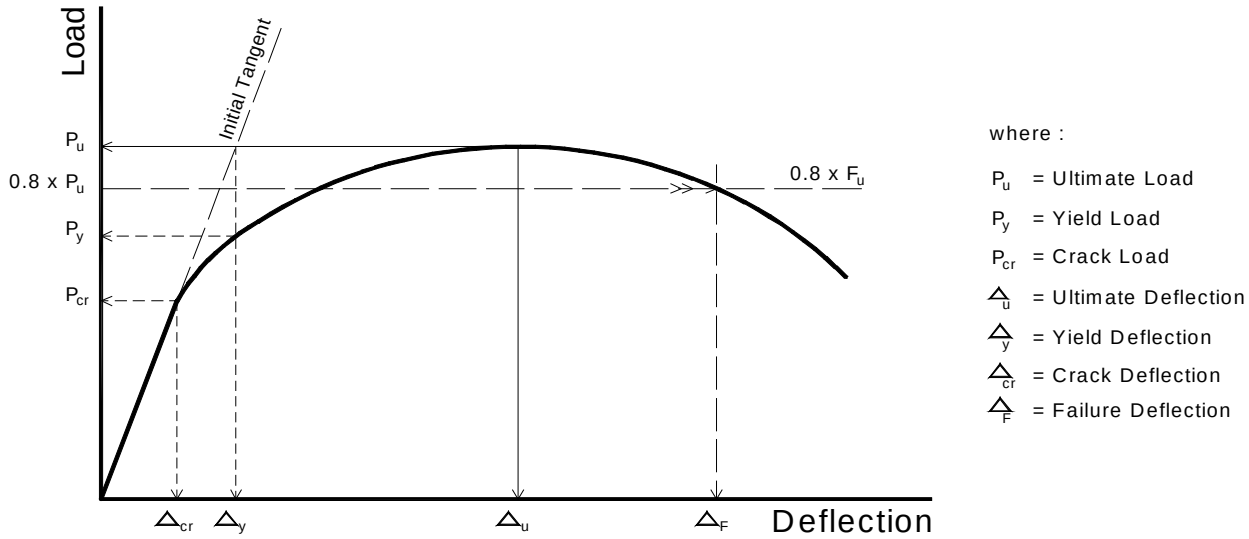

Fig. 6: Details of Ductility, Stiffness and Failure.

Ductility

The ductility factor was defined as the enclosed area of the load displacement curve till failure. Table 6 shows the ductility factors of the tested beams. Techniques used in beam B4 and beam B5 gives 80 % and 78 % of the ductility of beam BR representing highest ductility compared to the other used techniques. Technique used in beam B6 (CFRP bonded at beam sides) gives 10% of the ductility of beam BR. Thus using welded side bars with stirrups in beam B4 as a technique for substituting the bottom reinforcement, improved ductility than other techniques used in the study.

Table 6: Ductility Factor of the Tested Beams.

Beam No.	μ (kN x mm)
BR	12372
B1	8672
B2	2599
B3	6597
B4	9832
B5	9659
B6	1335

THEORTICAL ANALYSIS

The ultimate flexural strength of the tested beams was theoretically calculated, as shown in Fig. 7, based on the first principles, and experimental observations of the tested beams and according to the Egyptian code of practice [7] and the following assumptions.

- Full bond between side steel bars, steel plates, and CFRP with concrete surface.
- All ultimate theory principles for design of reinforced concrete sections were applied.
- All safety factors were considered to be unity.

Table 7 shows comparison between the theoretical and experimental results. The theoretical calculation of the ultimate flexural strength of tested beams based on the ultimate theory was conservative.

Table 7: Comparison between the Theoretical and Experimental Analysis.

Beam No.	$M_{ult.TH}$ (KN.m)	$M_{ult.EXP}$ (KN.m)
BR	53.55	54.0
B1	44.90	48.4
B2	48.07	50.0
B3	72.00	77.6
B4	42.60	42.8
B5	40.90	41.2
B6	42.58	46.4

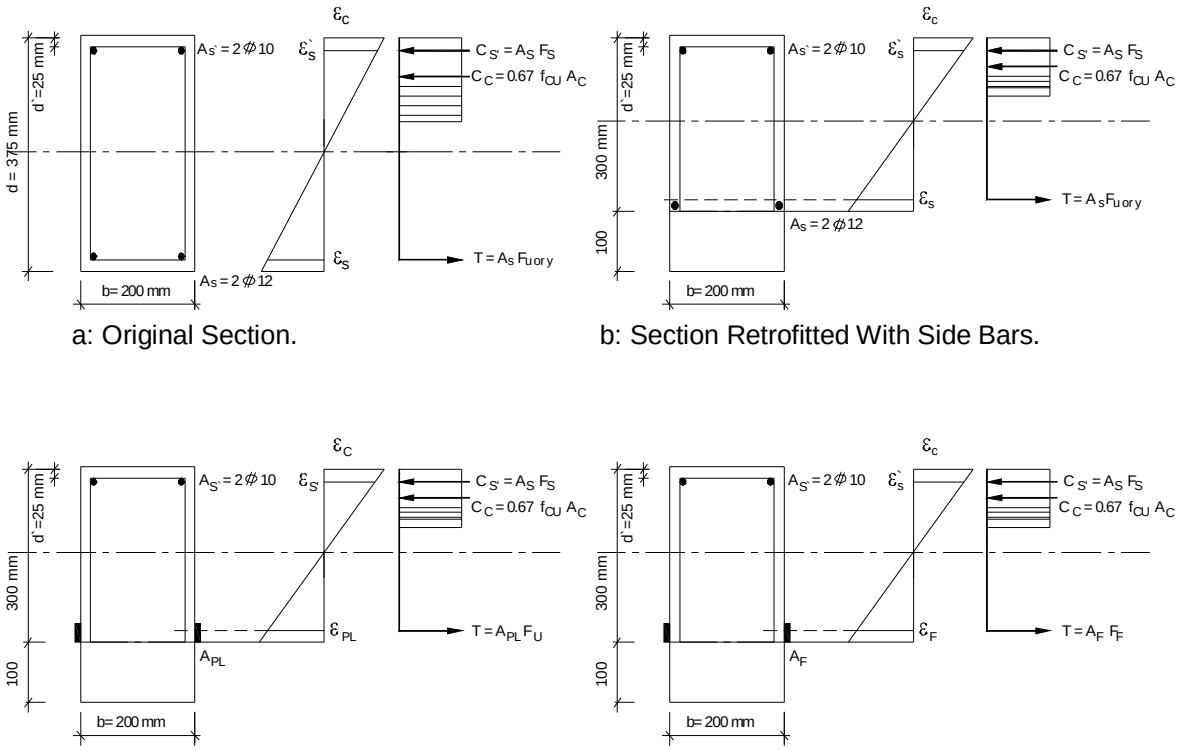

a: Original Section.

b: Section Retrofitted With Side Bars.

c: Section Retrofitted With Steel Plate.

d: Section Retrofitted With CFRP.

Fig. 7: Sectional Analysis of the Tested Beams.

CONCLUSIONS

Based on the experimental and theoretical analysis of the current study, it can be concluded that :

- All the techniques used in this study were able to restore the required flexural capacity with different percentages.
- Using side bars over opening as a technique to restore the flexural capacity, gives a good ductility than other used techniques.
- Using welded side bars with beam stirrups is better than using side bars without welding for restoring the required flexural capacity.

- Using bolts to fix side steel plate, attained more than the original required flexural capacity for beam without opening.
- Using bolts for fixing steel plate at beam sides is better than using epoxy adhesive to bond steel plate at beam sides.
- To prevent deboning of steel plate bonded at beam sides at earlier stages of loading, essential further modifications should be made for development length and end zone condition.
- Using CFRP bonded at beam sides required additional modifications for anchorage length and end zone condition to prevent deboning at earlier stages of loading.
- The ultimate design theory can be applied to predict the flexural strength of the tested beams.

REFERENCES

1. ZAKI Y.L., and IBRAHIM W.W., "Strengthening of RC Beam in Flexural by Externally Bonded and/or Bolted Steel Plates". International Conference (Future Vision and Challenges for Urban Development), Cairo, EGYPT; 20 – 23 December, 2004.
2. Taljsten B., "Strengthening of Beams by Plate Bonding". Journal of Structural engineering, ASCE, 1997, Vol. 9, N 4, pp. 206-212.
3. Oehlers D. J., "Reinforced Concrete Beams With Plates Glued To Their Soffits". Journal of Structural engineering, ASCE, 1992, Vol. 118, N 8, pp. 2022-2038.
4. Oehlers D. J., and Moran J. P., "Premature Failure of Externally Plated Reinforced Concrete Beams". Journal of Structural engineering, ASCE, 1990, Vol. 116, N 4, pp. 979-995.
5. Zirab Y.N., Baluch M. H., Basundul I. A., Sharif A. M., Azad A. K. and A.-Sulaimani G. J., "Guidelines Toward the design of reinforced concrete beams with external plates," ACI Structural journal, Nov-Dec 1994, V91, N6, pp. 639-646.
6. Hussain M., Al Farabi Sharif, Basuntl, I. A. Baluch, M. H., and Al-Sulaimani G.J., "Flexural Behavior of Precracked Reinforced Concrete Beams Strengthened Externally by Steel Plates". ACI, Structural Journal, V.92, No. 1, January-February 1995.
7. ECCS 203-2004, Egyptian Code of Practice for Design and Construction of Reinforced Concrete Structures, Second Edition, 2004.

HOUSING FOR THE URBAN POOR; A CASE STUDY OF LAHORE METROPOLITAN AREA, PAKISTAN

Dr. Ihsan Ullah Bajwa
Professor, Department of City and Regional Planning,University of Engineering and Technology, Lahore, Pakistan
Ijaz Ahmad
Assistant Professor, Department of City and Regional Planning,University of Engineering and Technology, Lahore, Pakistan,E-mail: ijaz47@wol.net.pk

ABSTRACT

Provision of low cost housing to human beings is the foremost goal of every government. The governments of various countries adopted varied nature of approaches to provide cheap houses to homeless people. In this modern age, provision of low cost housing has become a complex task involving physical, political, administrative and organizational dimensions. The important debate is about the role of government in low cost housing provision. Most of the welfare states considered that it is their duty to provide subsidized housing to the poor sections of the society. But the fact is that no government has ever been able to claim that it has provided cheap housing completely.
This paper highlights the role of government agencies in the provision of low cost housing to the urban poor. The study focused on the second biggest city of Pakistan, i.e. Lahore, which has a population of more than 06 millions and it is constantly increasing at a much faster rate. The paper firstly explored the major problems aroused due to urbanization and then at end certain recommendations are made so as to solve this problem of housing shortage.

Keywords: Urbanization, Housing Shortage, Government Agencies

INTRODUCTION

One of the main problems causing poor delivery of low cost housing is the rapid increase of size of cities. This is the major cause of fast growing population in cities of developing countries. The developing countries have experienced a tremendous rate of urbanization in this century, specifically after the Second World War. According to UN (1980), Between 1950 and 1975, the urban population of all developing countries grew at a very high annual average rate of nearly 4.2 per cent, and is projected by the United Nations studies to continue growing at more than 4 per cent a year until the 1990s [1]. This urbanization phenomenon is either due to migration of people from rural to urban areas or rapid natural increase. Due to urbanization, the sizes of cities are increasing at a much faster rate and in most of the countries the physical development is appearing in form of slums and squatters. The cities are growing haphazardly without any planning converting the raw land into slums where human habitation is difficult to survive. According to UN (1980) and Todaro (1980), An enormous number of urban dwellers will be added to the populations of Third World cities by the end of this century. The United Nations projects that more than 66 per cent – nearly 2.2 billion – of the world's population will be living in developing countries by the year 2000. This will be an increase of more than 265 million urban dwellers in African cities, and 93 million in Asian urban centers [2]. Barat (1982) showed a comparison of this growing population after taking cities of various countries. According to him, Over the next two decades, more than 40 cities in developing nations are expected to reach a population of 5 million or more. Indeed, most of the world's largest cities will be found in poor countries by the end of this century. If United Nations projections hold true, 21 of the world's 30

largest metropolitan areas will be in countries that are currently considered to be underdeveloped. Some of these cities will reach unpresecendented size. Mexico city's population is expected to reach 31 million; Sao Paulo will grow to 26 million, Shahangai and Peking to 21 million each, and Rio de Janeiro to more than 19 million. Bombay, Calcutta, and Jakarta are expected to have populations of more than 16 million each; Cairo, Seoul, Madras, Manila, Bangkok, Karachi and Bogotá are likely to grow to more than 10 million each. In Brazil, the basis for these projections is already well established. The population of nine largest metropolitan areas grew from about 19 million in 1950 to about 78 million in 1980. Sao Paulo's population has already increased from 2.3 million to almost 13 million, and Rio de Janerio's from 3 million to more than 9 million over the past 30 years. This population growth trend has created severe demand of shelter. Pakistan is also facing acute shortage of housing due to rapid population growth and relatively diminishing housing stock [3].

In Pakistan, the increasing rate of urbanization has caused a tremendous population growth in urban areas. This population adds more problems to the shelter provision. The government agencies working in the big cities are trying to combat the fast growing population but desired results so far could not be achieved.

LAHORE METROPOLITAN AREA

The Case Study

After independence in 1947, Lahore has expanded along north-south areas from the original fort with succeeding zones increasing in area but reducing in density in the shape of rectangular built up areas. The city has expanded along with three major highways, viz-a-viz; Grand Trunk (G.T.), Ferozepur and Multan roads. This growth trend is mainly due to the availability of suitable land and adequate infrastructure present in the south of the city.

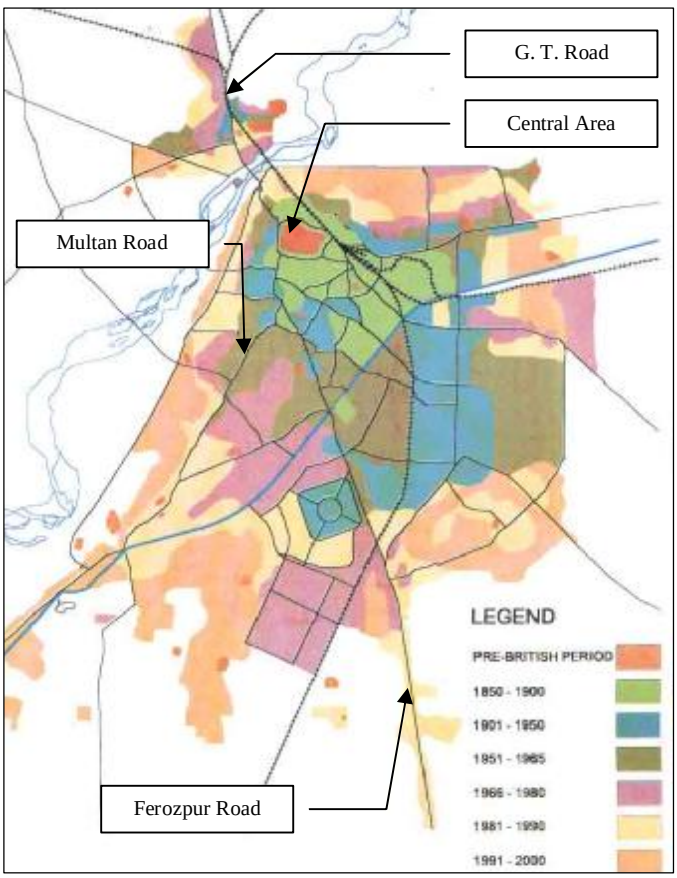

Fig.1: Growth patterns of Lahore Metropolitan

Presently, Lahore has attained the status of being second biggest city of Pakistan and the provincial capital of Punjab. Lahore Metropolitan Area (LMA) comprises of District Lahore, *Tehsil* (sub district) *Ferozewala* (District *Sheikhupura*) in the north and part of *Tehsil Kasur* in the south. Growth of Lahore during 1961-1970 is remarkable (see Fig. – 1) and especially when in 1966 a master plan was prepared to control the unplanned growth of Lahore. Major development started after the formation of Lahore Development Authority (LDA) in 1975. After 1978, number of housing schemes both in the public and private sectors are developed. There was a boom of housing schemes in Lahore during the period 1981-1990.

Population Growth Trends

According to the Population Census 1998 [6], the population of Lahore Metropolitan Area (LMA) was 6.94 million which is estimated to have grown to 7.71 million in 2001. More than 91% of

this population (7.04 million) lives in Lahore City District, 7.0% (0.54 million) in Tehsil Ferozewala of District Seikhupura and 1.7% in parts of Tehsil Kasur of District Kasur (see table 1). Out of 7.04 million populations living in Lahore District, 82% (5.77 million) lives in the urban areas comprising of Ex-Municipal Corporation Lahore (Ex-MCL)) Area, Lahore Cantonment, Walton Cantonment and two small urban settlements (Ex-Town Committee) of Kahna Nau and Raiwind.

Table 1: Population Distribution in LMA (1998-2001)

District	Population			
	1998	2001	% age Growth	% age of total population
Lahore	6,318,745	7,041,839	3.39	91.28
Seikhupura (Share of LMA)	499,012	541,682	2.56	07.02
Kasur (Share of LMA)	120,838	131,097	2.54	01.70
LMA	6,938,591	7,714,618	3.32	100.00

Source: Master Plan for Lahore, 2004 [4]

Since 1972, the population growth rate of District Lahore (urban) has been constantly declining. It was 4.48% during 1961-72, reduced to 3.75% in 1971-81 and further declined to 3.32% during 1981-98. Likewise, district population is reducing which has also affected the pace of growth of LMA (see table 2).

Table 2: Population Increase in Lahore District (1951-1998)

Census year	Intercenneial Period (year)	Lahore District		Lahore District Urban	
		Population	ACGR*	Population	ACGR
1951	-	1,134,757	-	861,279	-
1961	10.00	1,625,810	3.66	1,312,495	4.30
1972	11.67	2,587,621	4.06	2,189,530	4.48
1981	8.46	3,544,942	3.79	2,988,486	3.75
1998	17.00	6,18,745	3.46	5,209,088	3.32

Source: Integrated Master Plan for Lahore, 2004 ** Annual Compound Growth Rate*

While the urban population grew from 2.19 million to 5.21 million from 1972 to 1998 (see table 3). The proportion of urban population in Ex-MCL area reduced from 75.52% (in 1961) to 72.44% (in 1998), whereas the proportion of urban population in Lahore Cantonment rose from 4.21% in 1961 to 8.92% in 1998.

Table 3: Urbanization (1951-1998) In Lahore District

Census Year	Population		Proportion of Urban Population (%)
	Lahore District Urban	Lahore District	
1951	861,279	1,134,757	75.90
1961	1,312,495	1,625,810	80.73
1972	2,189,530	2,587,621	84.62
1981	2,988,486	3,544,942	84.30
1998	5,209,088	6,18,745	82.44

Source: Integrated Master Plan for Lahore, 2004

Housing Situation

According to 1998 census [6], the housing stock in LMA was 967,202 of which 77.62% was in urban areas of LMA. More than 91% of the total stock was in District Lahore, around 7% in District Seikhupura and around 2% in District Kasur areas. Whereas the 1980 Housing Census gave the total figure of housing units as 536,724 in the whole District that included 83.4% of housing units in urban areas. It is interested to note that between 1981 and 1998 population increased at the rate of 3.46% per annum whereas the housing stock during this period increased at the rate of 2.79% only. This shows that the increase in housing stock has not kept pace with the growth in population.

Various estimates have been made to indicate housing backlog in Lahore. The Master Plan for Greater Lahore (1966) estimated housing shortage to be between 39,086 and 80,399 dwelling units, whereas the Lahore Urban Development and Traffic Studies (1980) estimated this backlog as high as 300,000 dwelling units. But the estimates worked out by National Engineering Services Pakistan (NESPAK) in 2001 indicate the backlog in Lahore District (Urban) was around 154,000 dwelling units as detailed below:

	1998	2001 (Projected)
Urban population in Lahore District	5,209,088	5,774,886
Houses required (assuming optimum HH* size of 6)	868,181	962,481
Existing housing stock	731,348	808,484
Housing backlog	136,833	153,997

* *Household*

According to Integrated Master Plan for Lahore-2021 (IMPL-2021), the supply in the formal housing market does not exceed 2500 plots per annum [6]. According to an estimate of NESPAK (2001), 37% of the dwelling units in the urban areas of Lahore District were constructed in the last 10 years while another 29% were built during 1970 – 1990. Of the total housing stock one-fifth has already attained a life of more than 30 years and an additional 14% was built more than 50 years ago.

It is stated in Integrated Master Plan for Lahore (IMPL), the proportion of house construction to the total plots in some LDA's (Lahore Development Authority) schemes is 16% to 20%. The comparable figures for private cooperative housing schemes are 10.2%. Thus a very large number of developed plots are lying vacant due to varied reasons. The reasons explored appeared in form of speculation, high construction cost, lack of facilities in the proposed scheme, deficient transport services between these schemes & the place of work and alike. The supply side is also distorted due to the fact that the demand is for lower income groups whereas the supply of land is not targeting to poor people. Likewise, the private sector in Lahore is also contributing its share in this sector of housing. These private developers are developing land in form of planned housing schemes and few developers are involved in the illegal sub-divisions of undeveloped land along the peripheral areas of LMA boundary.

CONCLUSIONS

Following conclusions are derived:

i. Housing demand is increasing with urbanization rate. Due to urbanization the population is increasing and has created more demand for housing.
ii. The supply of land for housing is mostly targeting the upper middle income group people and is far beyond the poor. Whereas in case study area majority of people are poor. Resultantly, homeless people are increasing due to housing shortage.
iii. There are present lot of plots so far could not be developed. These plots are in hands of investors who are not ready to sell at low price. As a result land could not be developed.
iv. Very few housing schemes are developed by government agencies. Although the main target of these agencies is poor but supply of plots is not proportional to number of poor people.
v. There is no tax on the vacant plots whereas a specific amount is imposed on a house in form of property tax. Resultantly, the land owners are hesitant to develop the land which leads to shortage of housing.

RECOMMENDATIONS

Based on conclusions following recommendations are made:

i. Government agencies should keep an eye on the fast growing population and their demand of housing. Based on previous trends realistic forecasts can be made. This will surely enable the government to formulate specific policies those will be helpful to solve this problem of housing shortage.
ii. Taxes can be imposed on vacant plots and this act will compel the land owners to develop the land. As a result, more houses will be available in the market which may reduce the intensity of housing shortage problem.
iii. Although Government agencies are trying to provide cheap plots to poor but supply is very less. If supply of small plots is increased then housing problem can be solved.
iv. There exists a need on the creation of cost effective and efficient public-private partnership that includes mechanisms for attracting private capital for urban infrastructure provision. Investment of the private sector would be developed as a process that institutionalizes the enabling role of government.

REFERENCES

1. United Nations (UN, 1980), Department of International Economic and Social Affairs, Patterns of Urban and Rural Population Growth, Population Studies No. 68 (New York: United Nations, 1980)
2. Todaro, Micheal P. (1980), Urbanizations in Developing Nations: Trends, Prospects and Policies, Journal of Geography, Vol. 79 (1980)
3. Barat, Josef (1982), The Financing of Urban Development in Brazil: The Case of Sao Paulo Metropolitan Area, Third World Planning Review, Vol. 4 (1982)
4. Integrated Master Plan for Lahore (IMPL) 2021; Lahore Development Authority, Final Report Volume-I Existing Scenario.
5. LUDTS, (1980), “Lahore Urban Development and Traffic Studies”, Lahore Development Authority / Metropolitan Planning Wing; World Bank.
6. Population Census Organization, Statistical Division, Government of Pakistan, Population and Housing Census of Pakistan, July 1998, p-23

CONTRACTOR SELECTION MODEL FOR DEVELOPMENT INTERNATIONAL NON-GOVERNMENTAL ORGANIZATION

Dr. Mohamed I. Amer
Lecturer, Department of Construction Engineering and Utilities, Zagazig University, Egypt
*Email: **m1ismail@yahoo.com**; **Mohamed.ismail@plan-international.org***

ABSTRACT

Contractor selection is the process of selecting the most appropriate contractor to implement the project as specified so that the achievement of the best value for time, quality and money is ensured. International non-governmental organizations (INGOs) are working in most of poor developing countries for purpose of helping these countries to achieve the millennium development goals (MDGs) defined by United Nation. Huge budget of these organizations is spent in infrastructure projects using contractors. Construction clients as well as INGOs are becoming more aware of the fact that selection of a contractor based on tender price alone is quite risky and may lead to the failure of the project in terms of time delay and poor quality standards. So, to reduce those risks a short list of contractors based on evaluation criteria is suggested. Evaluation of contractors based on multiple criteria is, therefore, becoming essential. This paper presents a trial model for evaluating contractors in a systematic procedure based on criteria to evaluate the capability of a contractor to deliver the project as per the INGO requirements. The criteria are drafted based on previous researches as well as author's background. The criteria defined with its relative importance based on analysis of questionnaire filled by consultant engineers, contractors as well as big construction companies. The proposed model is not intended to supplant the work of technical evaluation of each tender, but rather to help them make quality evaluations of the available candidate contractors from predefined evaluated short list. The proposed system for dealing with contractors to improve the quality of projects implementation presented in this paper.

Keywords: Contractor, Selection, Model, Evaluation, Development.

INTRODUCTION

The International Non-Governmental Organizations works aims to help the poor developing countries through implementing development programs. The programs goals are different from one organization to the other, however most of the programs oriented to achieve the united nation millennium development goals. The implementation of these programs covers the hardware component of the projects to secure the services and software component to ensure the sustainability of the services. Most of the hardware components are the construction projects to establish the services. These constructions projects like access the poor families with potable water, this mean establishment of water treatment unit and distribution system, or like reduce the dropout rate from school and increase the enrolment through establishing or rehabilitating school building. All these type of construction projects mainly implemented by contractors that selected through tender process.

Investing fund resources requires any INGOs to establish a process, which identifies the most productive uses for limited funds, and monitors their subsequent expenditure to assure that the greatest net benefit to society is produced. Planning, programming, financing and management control systems are the tools used by INGOs administrators to allocate the resources to high priority objectives. INGOs in implementing construction projects (program hardware part) always try to choices and assure that the selected contractors are potentially the most worthy among

competition one to ensure achieving the project goals in timing, quality and with pre-defined budget.

This paper presented a proposed system for developing contractors' shot list. The proposed system coded into a computer program. Contractor selection has long been an area of attention of construction practitioners and researchers, because engaging an inept contractor could lead to project failure and adversarial relationships. Previous research efforts have been diverted to methods of reducing the subjectivity when assessing potential contractors' capability and suitability. While these methods provide valuable solutions to the improvement of contractor selection practices, many clients are still using their own idiosyncratic contractor selection systems [1]. The evaluation of tenders still relies heavily on the use of value judgments by the decision-makers, although the experience of such decision-makers varies widely from organization to organization [2]. Excessive subjectivity in contractor assessment may also give rise to corruption and other abuses of privileges. What is needed is a more rational, informed, systematic approach to contractor selection [3]. A recent survey found contractors to be in favor of clear process in which the selection criteria, together with any associated scoring mechanism, are made available to contractors [4].

BACKGROUND

The construction industry is characterized by cost and duration overruns serious problems in quality standards, an increased number of claims, counterclaims, and litigation. To minimize or optimize all these risks, selection of an appropriate contractor to deliver the project under consideration as per requirements is the most crucial challenge faced by any construction client. The construction industry is also one of the most dynamic, challenging, rewarding, full of uncertainty and associated risks, and these arise from the nature of the industry itself. Low entry barriers to the industry has also encouraged in many countries mushrooming of construction firms ranging from small-scale firms to large firms. The proliferation of these construction firms, along with the shrinking construction markets in developed and developing countries, has led to a fierce competition for the limited number of construction projects and they usually compete in a high volatile construction environment, full of uncertainties and associated risks. Furthermore, the peculiarity of construction is that no two projects are identical in terms of site conditions, design, use of construction materials, labors requirements, and plants and equipment requirements, construction methods, technical complexity, and level of management skill required. In such a situation, the crucial dilemma faced by all construction clients is which contractor to be selected for the job. Owners as well as INGOs in different private construction sectors practice different procedures for evaluating tender proposals. They mostly develop their own procedure for selecting the most appropriate contractor for the job. In public sectors, however, the tender price is the main criterion for selecting the contractor, because clients are publicly accountable and must demonstrate that the best value for their money has been achieved [5].

Hatush [6] opined that the selection of the contractor based on the lowest tender price is one of the major reasons for project delivery problems, as contractors desperately quote low prices by reducing their quality of work and hope to be compensated by submitting claims. Fong [7] after review of attitudes cited by researchers since 1967 concerning the influence of the tender price on the final selection of a contractor, summarized: (1) Apart from the acceptance of the lowest tender price, there should be a tradeoff between cost, time and quality in the final selection of contractor. (2) However, in public projects, tender price still dominates over other criteria in tender evaluation exercise. Contractor selection is, in practice, a complex multi-criteria decision making problem in which multiple decision makers evaluate the contractors' attributes to deliver the project at hand against a large number of the decision criteria [5].

Construction researchers and practitioners have proposed different methods or procedures for contractor selection. D. Singh [5] name a few of them: a multi-attribute utility model by Diekmann (1981); a fuzzy bid evaluation model by Nguyen (1985); a statistic model by Jaselskis (1988); a dimensional weighing method by Jaselskis and Russell (1991); a performance

assessment scoring system by Hong Kong Housing Authority (1994); and analytical hierarchy process (AHP) for contractor selection by Fong [5] also mention that most of these researchers have incorporated multi-criteria decision analysis methods in their models. However, their models or methodologies are generally based on single principal decision criterion such as time, quality to evaluate the capabilities of the contractor in addition to the price criterion, and on the assumption that the decision is made by a single person rather than multiple decision makers or heavy reliance on historical data in the case of neural network models. D. Singh [5] also showed that Mahdi (2002) proposed a model based on AHP that considers the multi-criteria approach to contractor selection. But his model also has some shortcomings that are associated with AHP method: (1) it does not take into account the uncertainty associated with the mapping of one's judgment to a number; (2) the subjective judgment and preferences of decision makers (DMs) have great influence on the final decision based on the AHP method; and (3) it is mainly used in nearly crisp decision applications and hence contractor selection is not a perfect case for its application. Pongpeng (2003) using utility theory also proposed a multi-criteria model for tender evaluation. Their model also has some disadvantages: (1) it requires the DMs to give a crisp utility value of a particular criterion to be used in a utility function; and (2) it also does not take into account the uncertainty and risk associated with mapping of one's judgment to a crisp value.

The current proposed paper tried to ensure that the only capable suitable contractors will be invited to the tender project through developing evaluated contractors' short list. This will led that the selection of the contractors at tender process will be within qualified ones. Also, this paper aimed to design a computer-based decision model for contractors' selection to be in the short list for the INGOs tender projects.

PROPOSED SYSTEM FOR DEALING WITH CONTRACTORS

The proposed system for dealing with contractors to improve the quality of projects implementation covered three stages:

- System for establishing a record for the contractors and developing a qualified contractors' short list to be invited for tender process.
- System for evaluating the contractors nominated for the tenders and selecting the most appropriate contractor for implementing the tender project.
- System for evaluating the contractors during and after implementing the project and updating the record of the contractors

This paper presented the whole system with more detailed of developing the first system "establishing a record for the contractors and developing a qualified contractors' short list to be invited for tender process".

First: Establishing a record for the contractors and developing qualified contractors' short list to be invited for tender process:

Establishing an updated record for the contractors and evaluating them according to their qualifications based on pre-defined criteria. Develop contractors' short list appropriate to be invited for the tenders' process.

System Layout: The frame of the system consists of the following steps:

An advertisement should be made in the newspaper before that start of the fiscal year by two months to invite the contractors to register their names and submit their profile to INGO record for the contractors.

An application registration form designed to enable the contractors to register and select the types of projects that they prefer to work with as well as the project financial budget limit.

A computer program designed to enter the contractors' data then evaluate and select the most appropriate contractors according to agreed selection criteria.

The system input: The contractors' registration application forms

The system output:

List with the names of the contractors classified by their technical qualifications with the type and the budget of the project. This list will be used in inviting the contractors to join the tenders.

Provide any information required about any contractor.

Second: Evaluating the contractors nominated for the tenders and selecting the most appropriate contractor for implementing the tender project:

Helping the consultant engineer in developing tender technical report through unifying the main points used in evaluating the contractors submitted their offers for the tender project.

System Layout: The frame of the system consists of the following steps:

A technical report was designed to evaluate the contractors offers submitted for the tender project.

The technical report is designed to measure the qualifications of each contractor to implement the project type of the tender. It is not to measure contractors technical abilities as all those submitted for the tenders are technically accepted, as they should have been selected from qualified contractors' short list.

The design of the technical report of the project will ensure that contractors who submitted unbalanced offer or asking for conditions that may affect negatively on the project cost will not be selected.

At tender process, Technical criteria in evaluation the invited contractors will depend on the type of the projects and includes: proven construction and completion of projects with similar construction type and value; current workload with INGO; and ensure that the contractor has submitted detailed technical sound work methodologies

The system input: The contractors' offers for the project (technical and financial)

The system output:

A technical report evaluates the contractors' offers according to project condition and defined the best ones for implementing the project (N.B.: This report is very technical and it should be a guidance for the tender committee and they should consider also the cost of the offer while making the decision)

It is not a must that the tender committee selects the cheapest price (The cheapest offer may be an unbalanced one and it would lead to increasing the cost during the implementation or the contractor who submitted the cheapest offer didn't implement a similar project before. So, it will be the first experience for him and that will affect the quality of the implementation)

Third: Evaluating the contractor during and after implementing the project and updating the record of the contractors:

Update the data of the contractors during and after implementing the project in order to improve their performance if it is good or stop dealing with them and put their names in the record of bad contractors whom we are prohibited to deal with.

System Layout: The frame of the system consists of the following steps:

An evaluation form for the contractor was designed to be filled by the consultant engineer supervised the contractor during implementing the project.

Another evaluation form for the contractor was designed to be filled by the program unit manager of the unit where the project is implemented.

An evaluation form for the contractor was designed to be filled by the tender secretary who is responsible for the tenders showing how much the contractors are responding to joining the tender.

The result of the evaluation should be entered to the computer for updating contractors' status.

At renewal existing contractors

These criteria for evaluation existing contractor in last year contractors' short list for renewal registration based upon parameters. The contractor performance evaluation report will be filled by consultant engineer supervised contractor work in cooperation with program unit

manager at which the project implemented. The contractor performance evaluation reports includes but are not limited to:

- A work history that indicates specialization and quality of workmanship in a particular construction skill, including the extent to which the Contractor follows project specifications and drawings provided by INGO.
- Degree of participation in the INGO bid process, i.e., demonstrating a high degree of attendance at bid meetings and submitting viable, competitive bids when invited to bid. Contractors not actively participating in the bid process may be removed from the list.
- Contractor's degree of quality control.
- Cooperation with other contractors on the project and in the vicinity. Ease of daily coordination. Courteous and cooperative nature.
- Degree of INGO supervision and coordination necessary before, during, and after construction. Preferred contractors require minimal supervision or progress inspection.
- Safety consciousness on the job site. Demonstrated safety measures to protect workers and people. Maintaining a secured, safe site on a daily basis.
- Job site cleanliness during projects and upon leaving job sites.
- Submission of change orders in timely fashion with adequate cost breakdowns. Flexibility and cooperation when resolving delays

The system input: contractors' evaluation forms
The system output: contractors' renewal yes or no.

PROPOSED SYSTEM COMPONENTS AND DETAILS

The proposed system consists of three components that are linked with each other to reflect the integration of the system:

Input: The data of the contractors will be collected using a system data input sheet (contractor registration application forms).

Processing: This involves the selection of the most appropriate contractors (based on the weighted evaluation technique of the contractor data that agreed with the proposed selection criteria)

Output: The output of the proposed system includes the contractors' short list and the most appropriate contractors from short list based on pre-defined project criteria.

The proposed system coded to be computerized by using the Visual Basic Language. The user interface designed by using Microsoft Access for Windows.

System Data Input Sheet (The contractors' registration application forms)

The system data input sheet will depend on the data submitted by the contractors in the registration application form. The system data input sheet can be considered as an identification card for the contractor. It was designed to be general and contain all the detailed data that can be translated to valuable information useful for the evaluation the contractor. It consists of six blocks, which contain a group of questions. The questions are designed to be simple and clear and its answer quantified by either Yes, No, writes a number, or select from predefined answers. This prevents a written answer that may be vague and have different meanings.

The designed system data input sheet proceed by different consultation process through asking people (at different levels from consultants, contractors, construction owners and governmental bodies) about the minimum data required to describe and identify contractor. The designed system data input sheet checked many times. After the final design of the system data input sheet, it passed again to relevant people to take their opinion and make any changes. The system data input sheet designed in a way to be general and contain all the detailed data that can provide valuable information useful for the evaluation process.

The proposed system data input sheet (registration contractor form) contains the following:
1- Block A: Basic Data

This block is designed to collect information about the basic data of the contractor:

- Company or contractor name and the commercial name.
- Company or contractor legal address for mailing
- Company or contractor telephones numbers
- Contact person name and his telephone numbers
- Select work location at which he/she prefers to work. (selection from location at which the INGO program area work)

2- Block B: Project Type selection

This block is designed to allow the contractor to select the type of project preferred to be invited on.

3- Block C: Project Budget Selection

This block is designed to allow the contractor to select the project budget he/she prefers to be invited on.

4- Block D: Qualifications with INGO

This block is designed to collect information about the finished projects the contractor implemented with INGO:

- Project name.
- Tender number
- Project type
- Total project value in the final project payment
- Program unit name at which the project implemented
- Project delivered date to the program unit.

5- Block E: Other qualifications

This block is designed to collect information about the finished projects the contractor implemented with other projects' owners:

- Owner name
- Project name
- Project type
- Total project value in the final project payment
- Project delivered date to the owners.
- These questions are repeated based on the number of owners the contractor work with.

6- Block F: company Documents

This block is designed to ensure that the company documents required for registration are submitted and data of expire are valid. It contains the following documents:

- Letter form contractor express his willingness to be in the contractors' short list of the INGO.
- Photocopy of ID/Family card for the contractor or the company's official
- Photocopy of tax card
- Photocopy of commercial register
- Photocopy of membership of the Egyptian Federation for Construction and Building Contractors.
- Photocopy of sales tax registration
- A brief of the contractor showing the most important dealers
- Bank name you deal with and its address
- An original document of the contractor should be submitted for revision only.

Selection of contractor to be in the short list

The selection of contractors is made using Desired Selection Technique. It uses the weighted evaluation technique to rank the contractors according to desired criteria based on the questionnaire results.

The methodology of Desired Selection Technique involves the following steps:

- Study the existing procedures for contractor evaluation criteria
- Investigate the desires and preferences regarding the development of the selection technique (based on questionnaire and interviews).
- Systemize the desired selection technique.
- Formulate the desired technique.
- Implement the desired technique.
- Outline the basic concept of the desired technique.

Contractor Selection Criteria

Based on previous research as well as authors' opinion, the contractor selection criteria can, in general, be summarized as tender cost, experience, past performance, financial, technical, managerial, quality, and health and safety aspects.

The lowest price alone may not necessarily offer the “best value”. Discretion in determining the lowest responsible bidder, and identifies specific criteria to consider in making this determination:

- The ability, capacity, skill and sufficiency of the financial resources and financial ability of the bidder to perform the contract within the time specified, without delay or interference
- The character, integrity, reputation, judgments, experience, and efficiency of the bidder
- The quality of performance of previous contracts.
- If future maintenance and service is part of the contract requirements, the ability of the bidder to provide future maintenance and service on the improvement being constructed, including guarantees.
- Must be accredited with Egyptian Federation for Construction and Building Contractors for Administrative and Information Services Contractor Pre-Qualification for Construction Contracts
- Contractor information (managerial capability, Staffing Levels, Key Personnel and Experience, In-house resources)
- scale and type of the projects executed

Questionnaires Form and Results

The questionnaire form is designed in a way to be simple and have all the data required in the system data input sheet. It contains questions and sub-questions about the blocks of the system data input sheet. The first questionnaire version send to sample of people their work are closing to contractor works. Their feedback helped in developing the final version of the questionnaire. The final questionnaire had been filled by a sample of the different opinions of people whose jobs are related to the contractors and tenders process.

The data analysis aims to analyze the entered data and develop the evaluation process and finally produce contractors' short list. The weighted evaluation technique is used to rank the entered contractors profile according to predefined criteria. This technique will be used to produce contractors' shot list according to the desired criteria based on the questionnaire results. The average is calculated as the sum of the questionnaire weights, divided by the number of questionnaires. The average is rounded and entered into the weight column. By applying statistic rules to the sample, the degrees that reflect the relative weights of the various blocks are calculated.

Desired Selection Technique

The selection of contractors is based on ranking them according to their priorities, which are calculated using the weighted evaluation technique. Weighted evaluation is a formally organized process for the selection of optimum solutions in areas involving several criteria [8]. In this

process, criteria are assigned different values according to their potential impact on a contractor selection. The contractors are then evaluated against these criteria. The contractors whom gain the highest score will appear on the top of the entered contractors' list.

Degrees for various blocks of the system data entry sheet are calculated from a questionnaire including a sample of people who have direct relation with contractors' works at different levels. By applying statistic rules to the sample, the degrees that reflect the relative weights of the various blocks are calculated. These calculations are based on the following equations:

$$C_{degree} = DPN_{1,2 \text{ or } 3} + DPV_{1,2 \text{ or } 3} + EON_{1,2,3 \text{ or } 4} + EPN_{1,2,3 \text{ or } 4} + EPV_{1,2,3 \text{ or } 4}$$

Where:

C_{degree} = Contractor degree

DPN = number of project implemented with INGO, if N=1 degree is 2; N=2 degree is 3; N=3 degree is 5.

DPV = total project implemented value, if V=1 degree is 2; V=2 degree is 3; V=3 degree is 5.

EON = number of owner with whom projects implemented, if N=1 degree is 15; N=2 degree is 20; N=3 degree is 25; N=4 degree is 30.

EPN = number of projects implemented, if N=1 degree is 15; N=2 degree is 20; N=3 degree is 25; N=4 degree is 30.

EPV = total project implemented value, if V=1 degree is 15; V=2 degree is 20; V=3 degree is 25; V=4 degree is 30.

System Coding

Coding the proposed system into a computer program was carried out using the Visual Basic Language. The inputs, processing, and outputs of the proposed system are carried out by designing computer modules and libraries. The computer modules consist of tables for saving the basic data, forms for entering data, and queries for calculations. A lot of programming work and computer time has been devoted to designing and testing the program.

System Verification

The computer program was designed to work under normal conditions, when any error is found the program stops working until the error is corrected. Any value entered to the system is tested against correctness as of being the required type or not. For example, testing an integer value, not to include a decimal point, alphabetic letters; or testing a real value as of accepting to include only the letter E or e between the numbers of the value; etc. Errors caused by the user will lead to raise a proper message to correct the error.

The program structure is revised. The logic adopted in designing the program is revised as:
The screen pull-down menus is used to controls the work.
Logic of performing facilities: as add, edits, save, process, print, and others program support facilities.
Integrate between the program elements.

Computer System Description and Operation

Working with the proposed computer system is carried out through a number of menu screens, which guide the user in his operation to the system. The screens are organized to be of the same structure of the system, input screens, processing screens, and outputs screens as shown in Fig. 1.

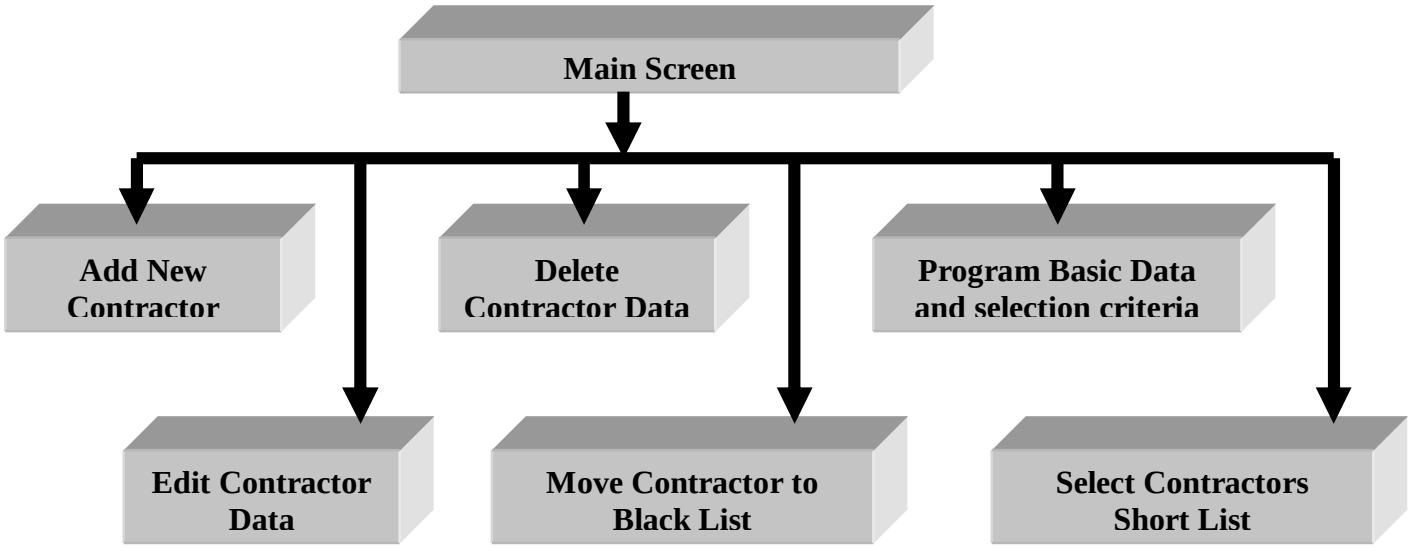

Fig. 1: computer system main screens

The computer main opening screen showed in Fig. 2. Fig. 3 and 4 showed how to enter company basic data and company documents. Company entered qualification with INGOs presented in Fig. 5; Fig. 6 showed company qualification with all projects owners.

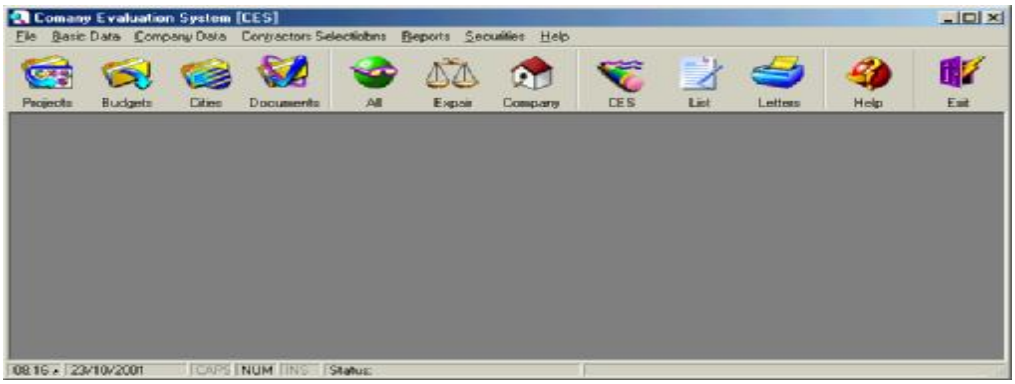

Fig. 2: Computer system main opening screen

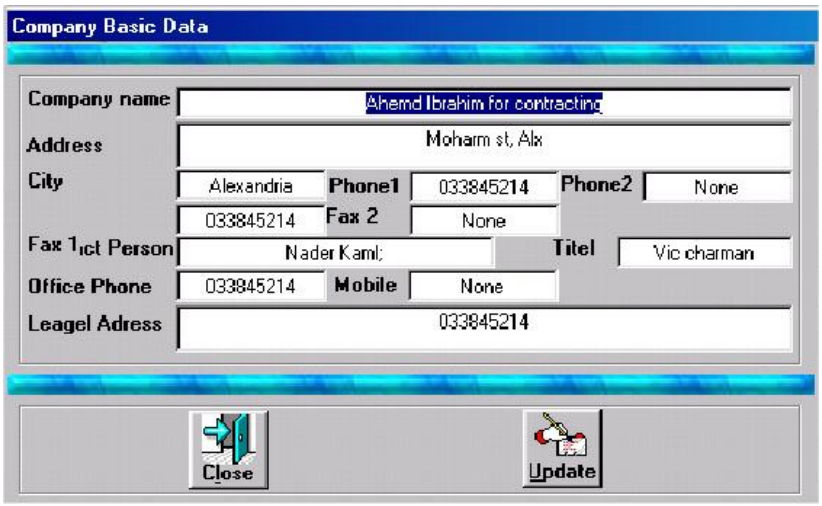

Fig. 3: company basic data

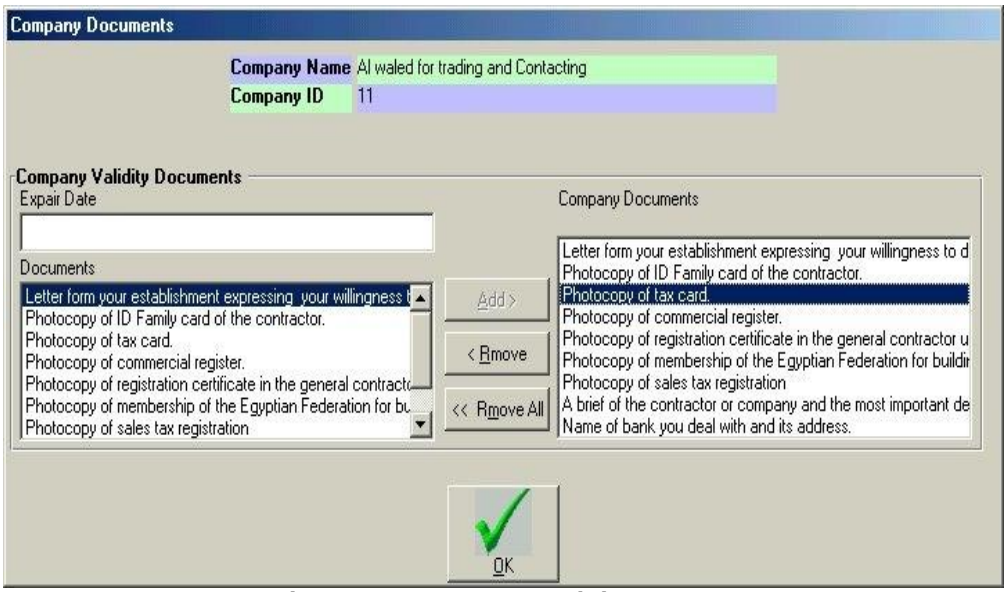

Fig. 4: Company entered documents

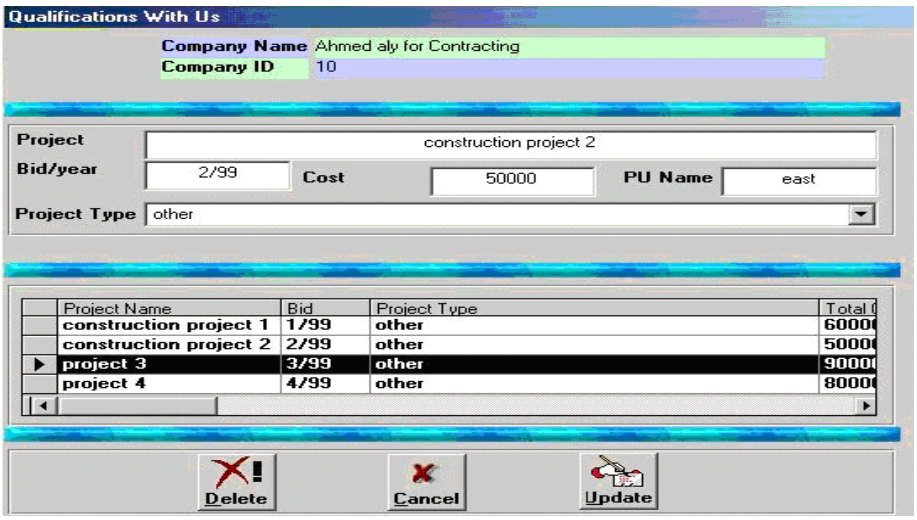

Fig. 5: Company qualification with INGOs

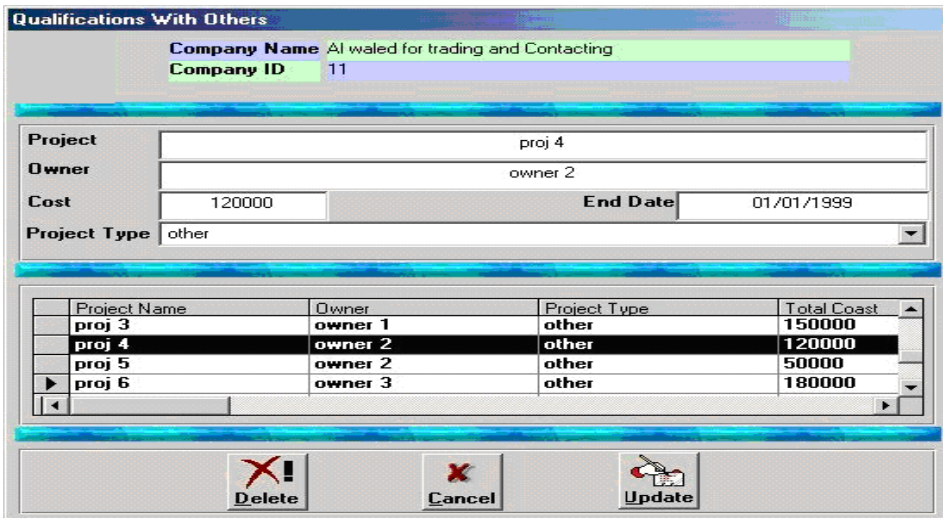

Fig. 6: Company qualification with all projects owners

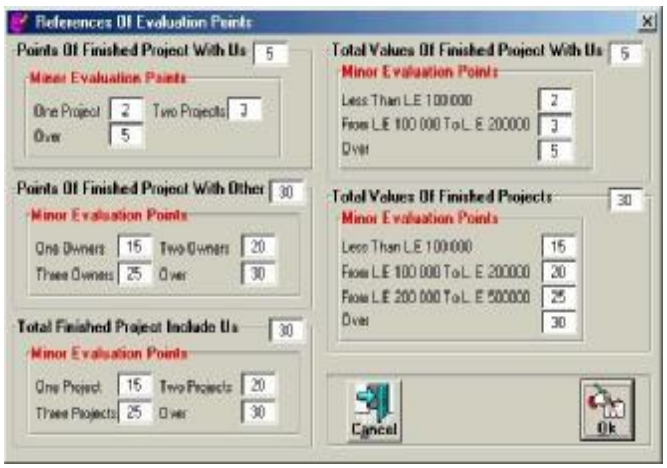

Fig. 7: Evaluation points

Evaluation points divided into five major parts namely; Point of finished project with INGO, Point of finished project with others; Total value of finished projects with all; Total value of finished of finished projects; and Total finished project includes INGO presented in Fig. 7. The degree showed in Fig. 7 based on the result of the questionnaire.

CONCLUSIONS

This study presents a proposed computerized system for developing contractors' short list that can be invited for tenders' process.
The desired selection technique uses the weighted evaluation technique to rank the contractors according to the desired criteria.
Date collection is considered the most important aspect in implementing the proposed system. The contractors' data entered into the developed program should be as accurate and complete as possible to obtain appropriates results. Using the system data input sheet, which eliminates the problem of insufficient data.
Contractor Performance Management System is a crucial instrument.

REFERENCES

1- Ng, S. T., and Skitmore, R. M. ~1995!. ''CP-DSS: Decision support sys- tem for contractor prequalification.'' Civ. Eng. Sys., 12, 133 – 159.
2- Holt, G. D., Olomolaiye, P. O., and Harris, F. C. ~1995!. ''A review of contractor selection practice in the U.K. construction industry.'' Build. Environ., 30~4!, 553 – 561.
3- Hatush, Z. A., and Skitmore, R. M. ~1997a!. ''Common criteria for con- tractor prequalification.'' Constr. Manage. Econom., 15~1!, 19 – 38.
4- S. Thomas Ng; Ekambaram Palaneeswaran, M.ASCE; and Mohan M. Kumaraswamy, M.ASCE "2003" "Web-based Centralized Multiclient Cooperative Contractor Registration System" JOURNAL OF COMPUTING IN CIVIL ENGINEERING.
5- D. Singh and Robert L. K. Tiong "2005" "A Fuzzy Decision Framework for Contractor Selection" JOURNAL OF CONSTRUCTION ENGINEERING AND MANAGEMENT ASCE.
6- Hatush, Z., and Skitmore, M. (1998). "Contractor selection using multi- criteria utility theory: An additive model." Build. Environ., 33(2), 148–164
7- Fong, P. S.-W., and Choi, S. K.-Y. (2000). "Final contractor selection using analytical hierarchy process." Constr. Manage. Econom., 18, 547–557.
8- Feighan, K.J.; Mohamed, Y.S. and Sinha, K.C. (1987). "A Dynamic Programming Approach to Optimization for Pavement Management Systems." Proceedings of North American Pavement Management Conference, Toronto, Ontario, Canada, Vol. 2, November, pp. 2195-2206.

A RELIABLE TECHNIQUE FOR ESTIMATING CONSTRUCTION PROJECTS TOTAL DURATIONS IN ORDER TO REDUCE CRASHING RISKS AND AVOID SLOW PROGRESS

DR. MOHAMED IHAB SHERIF ELMASRY
Assistant Professor, Construction and Building Eng. Dept., AASTMT[⊗], Alex.
Email: elmasryi@aast.edu
ENG. ABEER E. A. E. YOUSSEF
M.Sc. Graduate Student, Construction and Building Dept., AASTMT, Alex.
Email: eng_abeer_youssef@yahoo.com

ABSTRACT

One of the major measures of success of construction projects is the validity of finishing such projects within the anticipated total duration. However, a 1992 worldwide survey reported that the majority of construction projects fail to achieve the objectives of the schedule due to unforeseen events that even experienced construction managers couldn't anticipate [8]. On many of these projects a schedule overrun did not seem probable at the beginning of the projects. Moreover, a survey by Laufer and Stukhart (1992) [10] of 40 U.S. construction managers and owners indicated that for scope and design objectives, only 35% of projects, with average cost of $5,000,000, had low uncertainty and the remaining 65% had medium to very high uncertainty at the beginning of construction. Another report by Laufer and Howell (1993) [9] went even further by indicating that 80% of projects at the beginning of construction possessed a high level of uncertainty. Accordingly, the amount of uncertainty in the internal and external environments of a project is an important factor in determining whether there will be a schedule overrun or not. This paper introduces a method that adopts reliability principles in the evaluation of the total duration of construction projects. The method is tested through simulation. The case study here is a construction project involving ten major activities, with uncertain durations, planned in the form of four paths till the end of construction. The constructed building is assumed composed of a ground floor for parking and four floors for commercial centers. The analysis assumes that the activities durations are independent random variables. In addition, the distributions of the different activities are assumed normal distributions. A Monte Carlo simulation is applied on the studied project chart to obtain the project critical path in a probabilistic sense. The risk associated with different total project durations is evaluated. Finally, based on a separate criterion to assume a suitable amount of risk in the solved problem, an estimate of what can be defined as reliable contract total project duration is obtained.

Keywords: Reliability, Construction Project Durations, Crashing Risks, Uncertainty.

INTRODUCTION

A main challenge that exists in construction projects is the fact that the different activities encounter high uncertainty and risks as a result of unforeseen conditions or uncontrolled delays. This is even more complicated by having each construction project as a unique experience of its

[⊗] AASTMT: Arab Academy for Science and Technology and Maritime Transport

own. Accordingly, scheduling construction projects by fixed and known activity durations is unfortunately not correct [2]. Alternatively, the different activities durations can be treated as estimates of the actual time anticipated. This is consistent with Hendrickson and Au (2000) [5] who stated that there is a good potential to have a significant amount of uncertainty associated with the actual durations of the different activities within a construction project.
A 1992 worldwide survey reported that the majority of construction projects fail to achieve the objectives of the schedule due to unforeseen events that even experienced construction managers cannot anticipate [8]. On many of these projects a schedule overrun did not seem probable at the beginning of the projects. Moreover, a survey by Laufer and Stukhart (1992) [10] of 40 U.S. construction managers and owners indicated that for scope and design objectives, only 35% of projects, with average cost of $5,000,000, had low uncertainty and the remaining 65% had medium to very high uncertainty at the beginning of construction. Another report by Laufer and Howell (1993) [9] went even further by indicating that 80% of projects at the beginning of construction possessed a high level of uncertainty. Accordingly, the amount of uncertainty in the internal and external environments of a project is an important factor in determining whether there will be a schedule overrun or not.
Generally, during the preliminary planning stages for a project, the uncertainty in activity durations is particularly large since the scope and obstacles to the project are still undefined. Moreover, activities that are outside of the control of the owner are likely to be more uncertain. For example, the time required to gain regulatory approval for projects may vary tremendously. Other external events such as adverse weather, trench collapses, or labor strikes make duration estimates particularly uncertain [5]. This paper introduces a method that adopts reliability principles in the evaluation of the total duration of construction projects. The method is tested through simulation. The case study here is a construction project involving ten major activities with uncertain durations and planned in the form of four paths till the end of construction. The constructed building is assumed composed of a ground floor for parking and four floors for commercial centers. The analysis assumes that the activities durations are independent random variables. In addition, the distributions of the different activities are assumed normal distributions. A Monte Carlo simulation is applied on the studied project chart to obtain the project critical path in a probabilistic sense. The risk associated with different total project durations is evaluated. Finally, based on a separate criterion to assume a suitable amount of risk, an estimate of what can be defined as reliable contract total project duration is obtained.

PROBLEM DEFINITION

Problems with Schedules Estimates

Studying the problems of scheduling of construction projects, one could figure out that there are three main problems associated with deterministic scheduling estimating [2]. First of all, no point estimate of full schedule duration of a project that pushes state of the art in one or more areas can be a final correct answer. This may be attributed to the fact that the point estimates of activities durations are not exact, thus leading to calculating the total Project duration estimate as a sum of incorrect activities durations' estimates. In contrast, actual total project durations usually fall within some range surrounding what schedulers interpret as point estimates with some degree of confidence. The second problem faced is the absence of a standard definition of the term "best estimate" total project duration since there are three assumptions of what can be anticipated and substituted for that term. The best duration estimate for each activity may be the most likely duration (mode), the 50^{th} percentile duration (median) or the expected duration (mean). Adding any of these three assumed durations for all activities consecutively would lead to a sum (total project duration) that is almost always different from adding the other two. On the other hand the best estimate of complete project duration is almost never one of these [2]. The third problem as well can be defined by the fact that rolling up of most likely activities' durations is not the same as the most likely total duration. This is shown in Fig.1 where the probability

distributions of the different activities' durations are assumed triangular whereas the total project duration probability distribution is always taken as normal.

Scheduling Uncertainty

Based on the problems mentioned above, it is evident that there is a certain percentage of uncertainty in calculating the durations of every construction project. These percentages depend on the accuracy of calculating the time of each activity. Consequently, there are three ways to deal with such uncertainty. Firstly, the uncertainty maybe ignored and that would affect the project success and will raise the risk especially if this project is exposed to high uncertainty. Secondly, the uncertainty is considered as a contingency allowance, which can be estimated by using the experience of different staff members. This could be done either through formal meetings or through the distribution of a questionnaire, whichever relevant. Thirdly, the uncertainty could be estimated by preparing a simulation model or any other computer program that helps estimating the uncertainty accurately [7,11].

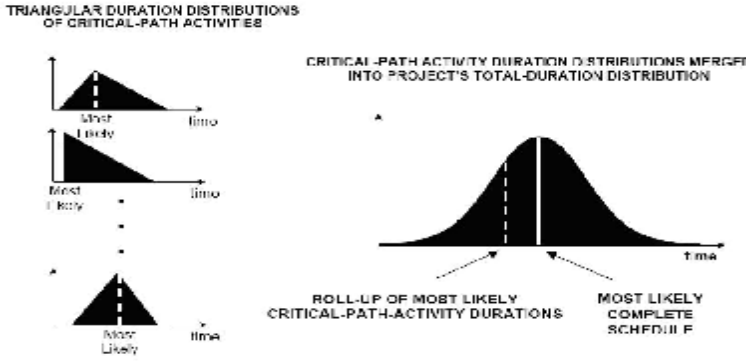

Fig. 1: Sum of Most Likely Activities' Durations with Triangular Distributions versus the Most Likely Complete Project Duration Estimate Distribution

PROPOSED TECHNIQUE SUMMARY

Problem Idealization and Modeling

In this paper, the scheduling uncertainty is studied through a case study simulation of a construction project model. The case study is a general construction project of a building, which consists of a ground floor and four floors for a commercial center involving ten activities with uncertain durations [4]. The activities are nominally A, B, C, D, E, F, G, H, I, and J. The precedence relationships for these activities are shown in the project plan network in Fig. 2.

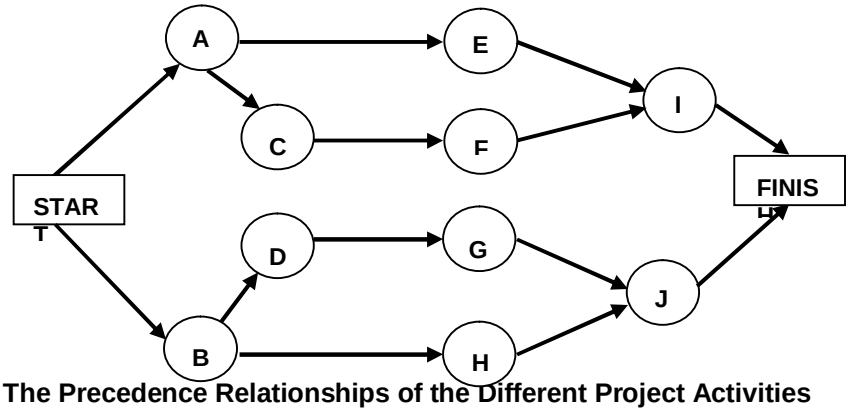

Fig. 2: The Precedence Relationships of the Different Project Activities

Each of the above project activities is assumed to be composed of several sub-activities with uncertain durations and different probability distributions of such durations. Accordingly, the probability distribution of the duration of each activity is assumed to be normal as per the central limit theorem [6,12]. Moreover, it is assumed that a most likely estimate, an optimistic estimate, and a pessimistic estimate of the duration of each activity are available. Table 1 shows the most likely, optimistic, and pessimistic estimates of the durations of the different project activities (A-J). Note how the great uncertainty in the duration of the project activities causes each pessimistic estimate to be several times larger than either the optimistic estimate or the most likely estimate.

Table 1: The Optimistic, Most Likely and Pessimistic Durations for the Different Project Activities

Activity	Optimistic Estimate (months)	Most Likely Estimate (months)	Pessimistic Estimate (months)
A	1.5	2	15
B	2	3.5	21
C	1	1.5	18
D	0.5	1	15
E	3	5	24
F	1	2	16
G	0.5	1	14
H	2.5	3.5	25
I	1	3	18
J	2	3	18

Using PERT (Program Evaluation and Review Technique) [1,3] formulas, estimates of the mean and variance of the probability distribution, of each activity's duration, are evaluated. The mean value of the duration of each activity is calculated according to the equation

$$m_{ij} = \frac{(o_{ij} + 4m_{ij} + p_{ij})}{6} \tag{1}$$

where the term "o_{ij}" refers to the optimistic estimate of the duration of the i^{th} activity in the j^{th} path, the term "m_{ij}" refers to the most likely estimate of the duration of the i^{th} activity in the j^{th} path, and the term "p_{ij}" refers to the pessimistic estimate of the i^{th} activity in the j^{th} path. Moreover, the standard deviation, s_{ij}, of the duration of each activity is calculated from

$$s_{ij} = \frac{(p_{ij} - o_{ij})}{6} \tag{2}$$

and thus the variance is

$$s_{ij}^2 = \frac{(p_{ij} - o_{ij})^2}{36} \tag{3}$$

Since the main goal of doing the whole simulation is to obtain a reliable overall total project duration. Thus, based on the calculated means for the different activities, the mean value of the total project duration (T_P) is calculated for the expected critical path as per

$$(m_{T_P})_j = \sum_{i=1}^{n} m_i \quad (4)$$

where n is the total number of activities in the j^{th} path. Consequently, the variance of the total project duration (T_P) is calculated for the critical path from

$$(s^2_{T_P})_j = \sum_{i}^{n} s_i^2 \quad (5)$$

By obtaining the mean and the variance of the total project duration (T_P) then the corresponding probability distribution can be obtained. It is evident that the resulting probability distribution of the total project duration (T_P) is normal which is compatible with the central limit theorem [6,12]. Accordingly, the probability that the construction project is completed within a specific duration can be easily evaluated from the resulting probability distribution. However, from a probabilistic perspective, the critical path can be any one of the project progress paths. Thus, the risk of not finishing within the specified deadline, that is associated with any value of T_P, can be obtained using the theorem of total probability using probabilities of having each path as the critical one [6,12]. By evaluating the risk associated with different values of T_P then the relation between the total project duration and the associated risk is obtained. Finally, by defining a suitable amount of risk that can be encountered in the estimation of the total project duration (T_P) then a reliable estimate of the total project duration can be assumed and be included in the contract. The resulting total project duration estimate should make account for the cost and quality benefits of both the owner and the contractor responsible of the fulfillment of works. A summary of the simulation process of the proposed technique that is undergone to obtain a final estimate of the total project duration is shown in Fig. 3.

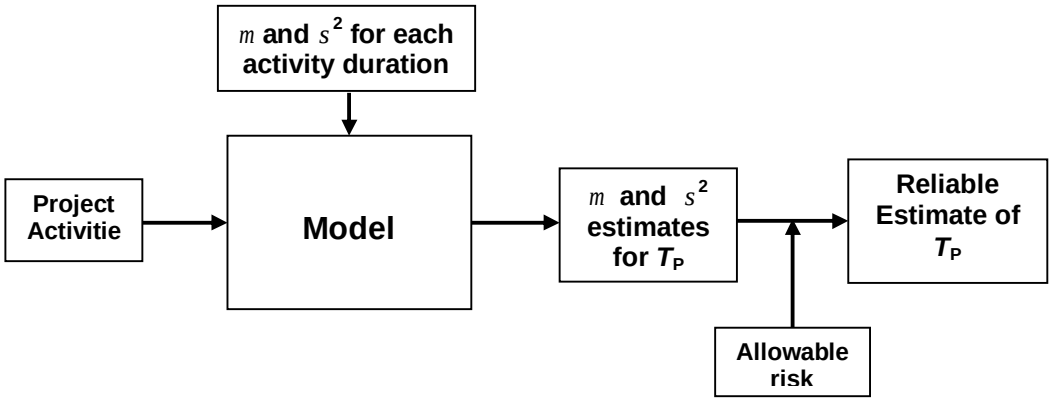

Fig. 3: Simulation Process Diagram for Obtaining a Final Reliable Estimate of T_P

ANALYSIS OF RESULTS

On applying the introduced technique, the Microsoft Excel® software template was used in the simulation process and in calculating the mean and variance of the probability distribution of the duration of each activity as well. The latter application is done for each activity by using the optimistic, most likely, and pessimistic estimates. In addition, a Monte-Carlo simulation was performed by running the simulation of the project for a number of 10000 iterations. This was done to define the critical path of the project in a probabilistic sense. Accordingly, there is a probability that any of the four progress paths of the project would be the critical path. Moreover,

in order to show the credibility of the introduced technique in evaluating a reliable total project duration, the results are compared to those obtained using the traditional PERT technique as well as the deterministic method. The following results summarize the different cases of either using a deterministic method of summing all given durations or using the PERT technique in each activity or finally using the introduced reliable technique in calculating the total project duration.

Case (*i*): A deterministic method to calculate the total project duration

In summary, we have three choices to pick the duration of completing the full project. As a first option, the optimistic durations of the different activities are added for each path to get an optimistic estimate of the total project duration. Thus, the total project duration in this case study is 6.5 months. The second option however is to add the most likely durations of the different activities for each path. Therefore, the most likely total project duration is 10 months. Finally, the third option is adding the pessimistic estimates of the different activities for each path to get pessimistic total project duration of 68 months. The decision of choosing which of the three total project durations estimates chosen as specified contract duration is governed by the owners' preferences, and the time flexibility that is based on contemporary circumstances of the project.

Case (*ii*): Using PERT technique to calculate the total project duration

In this case, each activity is considered to have a fixed optimistic, most likely, and pessimistic durations as shown in Table 1. The total duration of each path in the project is calculated using the PERT technique by evaluating the means and standard deviations of each activity as shown before in Equations 1 and 2. Afterwards, the means and variances of the activities on the same path are added to obtain the mean total duration for each path and the corresponding standard deviation as shown in equations 4 and 5. Finally, a single critical path, corresponding to the maximum path duration, is defined. The total duration of the project is thus taken as the total duration of the critical path. Table 2 shows results for the traditional PERT technique.

Table 2: The Theoretical Mean and Standard Deviation for the Activities

		Estimates				
	Activity	*O*	*m*	*P*	Theoretical m	Theoretical s
Path I	A	1.5	2	15	4.1	2.3
	E	3	5	24	7.8	3.5
	I	1	3	18	5.2	2.8
Path II	A	1.5	2	15	4.1	2.3
	C	1	1.5	18	4.2	2.8
	F	1	2	16	4.2	2.5
	I	1	3	18	5.2	2.8
Path III	B	2	3.5	21	6.2	3.2
	D	0.5	1	15	3.3	2.4
	G	0.5	1	14	3.1	2.3
	J	2	3	18	5.3	2.7
Path IV	B	2	3.5	21	6.2	3.2

	H	2.5	3.5	25	6.9	3.8
	J	2	3	18	5.3	2.7

Based on the above results in Table 2 and considering the plan flowchart of the case study project in Fig. 3 then the critical path based on mean values would be path IV (activities B-H-J) with a mean total project time of 18.4 months and with a standard deviation of 5.65 months.

Case (*iii*): Proposed technique considering uncertainty distributions in each activity

As mentioned earlier in the paper, the probability distributions of the different activities are considered normal. This is attributed to the fact that each activity in the case study of this paper is assumed composed of many sub-activities. Thus, as per the central limit theorem [6,12], one would expect that the probability distribution of each activity should tend to normal. The means and standard deviations of the normal distributions for the different activities are assumed to be equivalent to the values obtained from the PERT equations 1, 2 and tabulated in Table 2.
A Monte-Carlo simulation is applied to the project model in this paper. The simulation is applied for 10000 iterations to have a good sense of the progress flow from a random activity duration point of view. During simulation, the duration of each activity is assumed randomly but consistent with the probability distribution of the duration of this activity. For each iteration, the total durations of the different project paths are calculated. Thus, by taking the maximum duration out of the four paths (all possible paths in the project) for every iteration, the critical path is defined. Table 3 shows the resulting total durations of the different paths and consequently the corresponding critical path duration for some of the simulation iterations.

Table 3: Total Duration of the Project Progress Paths and the Corresponding Critical Path

Iteration	Path I (A-E-I)	Path II (A-C-F-I)	Path III (B-D-G-J)	Path IV (B-H-J)	Duration (Months)
1	18.17	19.03	9.64	3.44	19.03
2	19.75	21.25	21.52	31.36	31.36
9987	15.48	11.68	8.06	9.6	15.48
9990	19.01	14.81	6.62	17.6	19.01
9992	20.07	13.07	15.48	29.65	29.65
9996	4.17	7.77	24.76	24.69	24.76
9997	16.08	19.73	6.51	6.02	19.73
9998	14.09	15.16	21.97	18.54	21.97
			Mean total duration=$T_{P(mean)}$=22.06		

By studying the results of the simulation iterations as shown in Table 4, one can conclude that any of the project progress paths can be the critical path for the project total duration. This is expected since a delay may occur in any of the activities thereby leading to a delay in the progress path associated with this delayed activity. Moreover, by studying the total durations of the different paths, the resulting probability distribution is normal as shown for example in the histogram graph of path (I) in Fig. 5 and the corresponding cumulative distribution curve in Fig. 6.
In addition, the mean of the project total duration ($T_{P(mean)}$) is observed to be equivalent to 22.06 months which is bigger than the PERT mean estimate and also bigger than the optimistic and most likely estimates of the total project duration obtained as per the deterministic approach. However, the result in this probabilistic approach seems more reasonable since it considers the fact that activity durations are random. Furthermore, the resulting mean value of the total project

duration is only slightly bigger than that of the PERT technique and closer to the most likely and optimistic estimates than the pessimistic estimate of the deterministic technique. Moreover, the standard deviation of the total project duration (T_P) is observed to be 4.1 months, which is smaller than the standard deviation obtained from the PERT technique. Consequently, that gives more confidence in the results from the proposed technique considering uncertainty.

The probability for each path to be the critical path is calculated by the number of iterations out of the 10000 iterations that it had the maximum duration over other paths. Thus, the probability of having the critical path as path I, path II, path III, or path IV is given in Table 4. Moreover, the results from Table 4 indicate that Path IV is the most probable to be the critical path. This is consistent with the results from the PERT technique. In spite of that, probability results indicate that there is a good probability that any of the other three paths would be the critical path as well.

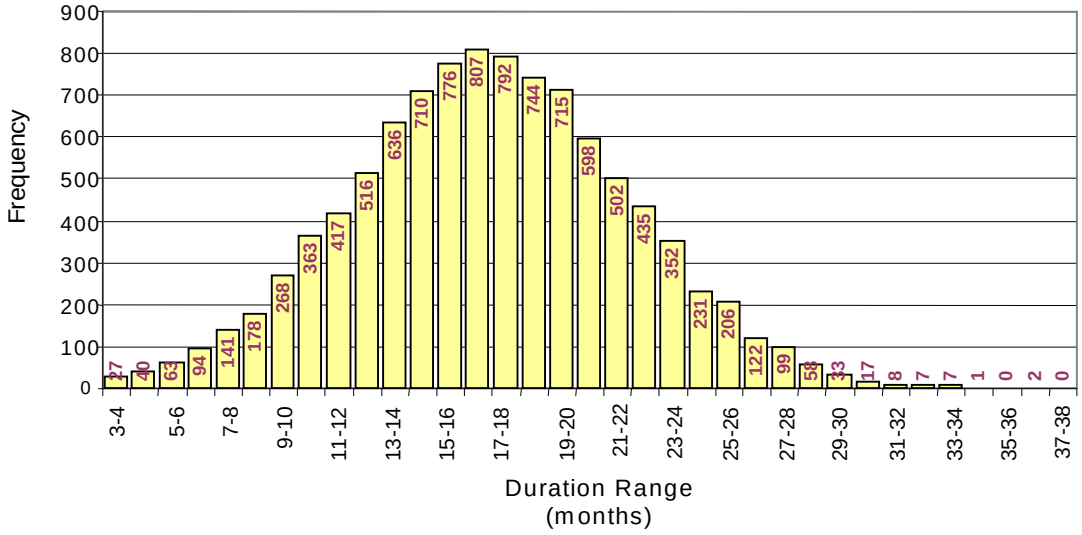

Fig. 5: Histogram of Path I total duration in 10000 simulation iteration

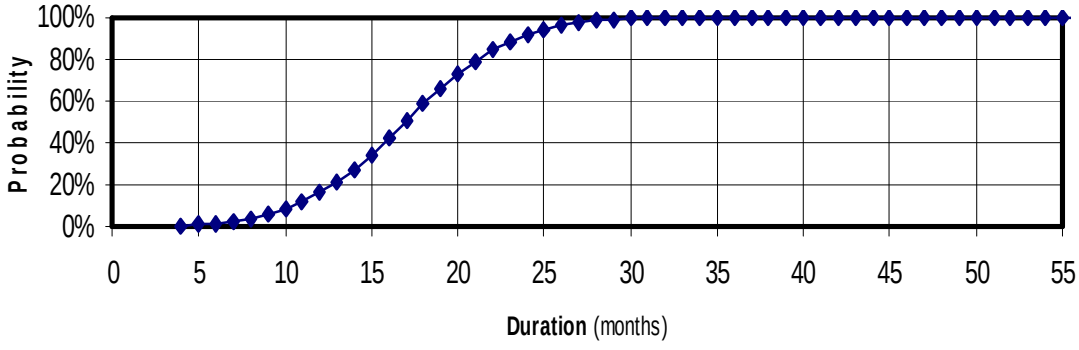

Fig. 6: Cumulative distribution for Path I total duration

Table 4: Probability for Each Path Being the Critical Path within 10000 simulation iteration

	Path I	Path II	Path III	Path IV
No. of occurrences	2255	2469	2112	3164
Probability of being the critical path	22.55%	24.69%	21.12%	31.64%

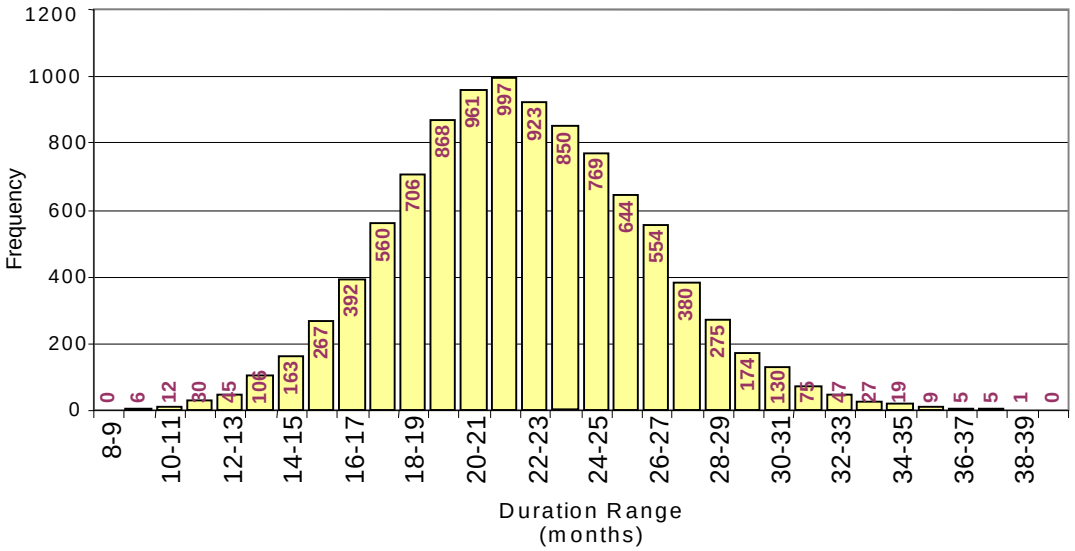

Fig. 7: Histogram for Total Project Duration (T_P) over 10000 Simulation Iterations

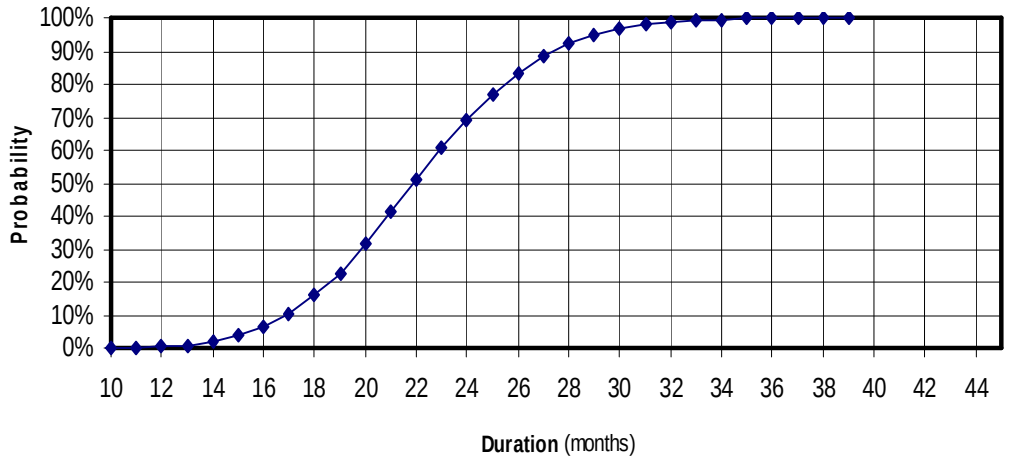

Fig. 8: Cumulative Distribution for the Total Project Duration (T_P)

Estimation of risk associated with different total project durations (T_P) assumptions

Once the total project duration (T_P) is evaluated then it is appropriate to substitute its value for the actual contract duration. However, the risk associated with such a choice remains a question. If the risk of not finishing the project can be defined then by assigning what is assumed to be the allowable risk of finishing the project, then the corresponding T_P can be reliably chosen as the contract total project duration. Knowing that any of the progress paths, as shown earlier in the paper, can be the critical path then the risk of finishing within the contract duration depends on the probability of each path being the critical path. Thus, the risk associated with any T_P can be assumed by using the theorem of total probability [6,12] such that

$$R = 1 - [P(T_P \le T_C \mid I)P(I) + P(T_P \le T_C \mid II)P(II) + P(T_P \le T_C \mid III)P(III) + P(T_P \le T_C \mid IV)P(IV)] \quad (6)$$

where R is the risk probability of not finishing within the specified contract project duration, T_C, $P(T_P \le T_C \mid I)$ is the probability that the project is finished within the specified contract project duration given that path I is the critical path and $P(I)$ is the probability that path I is the critical path. The same definition applies to the other four terms but for the other paths II, III, and IV respectively. Clearly, these terms can be obtained from the probability distributions of paths I, II, III, IV respectively. Therefore, by evaluating the risk associated with different values of total project durations (T_P) as shown in Table 5, one would obtain the relation between the different total project durations and their associated risks as shown in Fig. 9. Consequently, by assuming the amount of allowable risk, one would obtain a reliable estimate of the total project duration that can be eventually set to total contract duration.

Table 5: Risk Associated with Different Total Project Durations (T_P)

T contract (months)	Risk %
6.5	98.17
10	92.11
18	44.99
22	18.92
30	1.09
32	0.32
40	0
68	0

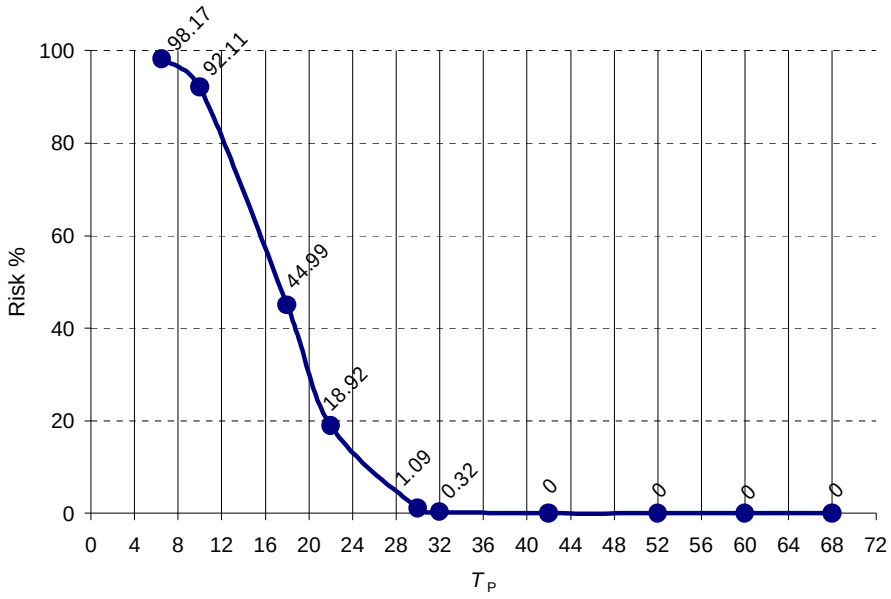

Fig. 9: Risk Distribution for Different Total Project Durations (T_P)

Studying Fig. 9, it can be easily observed that the deterministic optimistic and most likely estimates are associated with very big risks of not finishing in due time, 98.17% and 92.11% respectively. Thus, using such estimates in the project planning (scheduling) process would probably lead to schedule crashing. Moreover, using the total project duration mean estimate as per the PERT technique is also associated with a 45% risk of not finishing within the contract project due time. Despite the risk is lower in the PERT technique than the deterministic technique yet the risk value is still high. In contrast, by looking at the risk associated with the mean estimate of the total project duration, T_P, from the introduced technique, one would observe an associated 18.92% risk. This value is definitely more reasonable and does not press on the contractor as much as estimates from the deterministic and PERT techniques do. Moreover, in the application here, the allowable amount of risk that can be encountered in the estimation of the total project duration is assumed to be 20%. Thus, the contract total project duration can be set to 21.5 months. However, the amount of allowable risk is a matter of tradeoff between the urgency of finishing the project quickly as per the owners' preferences and the necessity of not pressing much on the contractor, which eventually may affect the required quality of the project. It is thus left to the consultant engineer in responsibility to decide the amount of risk that would be encountered in the total project duration estimation. This can be related to the delay costs laid on the contractor as well as the necessity of finishing within a due date.

CONCLUSIONS

A probabilistic method that adopts reliability principles in the evaluation of the total duration of construction projects is introduced. The method is tested through simulation using Microsoft EXCEL® software. The case study in the paper is a construction project involving ten major activities, with uncertain durations, planned in the form of four paths till the end of construction. The constructed building is assumed composed of a ground floor for parking and four floors for commercial centers. The analysis assumes that the activities durations are independent random variables. In addition, the distributions of the different activities are assumed normal distributions. Moreover, the introduced technique respects the rationale that any of the progress

paths in a project chart can be the critical path. Accordingly, a Monte Carlo simulation is applied on the studied project chart to obtain the project critical path in a probabilistic sense. The risk associated with different total project durations is evaluated. Finally, based on a separate criterion to assume a suitable amount of risk in the solved problem, an estimate of what can be defined as reliable contract total project duration is obtained. Moreover, the results obtained from the reliable technique in the paper showed smaller risks of failure to cope with the expected contract deadlines. This is shown in contrast to estimates obtained from the deterministic methods or even the PERT method. In addition, the total project duration estimates obtained form the introduced reliable technique also showed less variation than those obtained from the PERT method.

RECOMMENDATIONS

It is essentially recommended to consider uncertainty in the scheduling and planning of construction projects. The reliable technique introduced in this paper is a good tool for consultant engineers responsible for assigning total project durations in contracts and thus is recommended especially for sensitive deadline projects. Moreover, the method introduced in the paper can be a good reference for judging whether assigned total project durations obtained through other techniques include sufficient accuracy or not. More emphasis in future research should be considered in the estimation of the allowable risk that is encountered in the estimation of the total project durations and the aspects behind its choice need to be studied.

REFERENCES

1. Marold, K. A., and W. A. Haga (2004), “A Simulation Approach to the PERT/CPM Time Cost Trade off Problem.” *Project Management Journal*, Vol. 35(1).
2. Stephen A. (2002), “Schedule Risk Analysis: Why it is Important and How to Do it?" paper presented to session on Business Cases and Acquisition Strategies Ground System Architectures Work Shop (GSAW), The Aerospace Corporation, El Segundo, CA 13-15 MARCH, 2002.
3. Haga, W. A., and T. O’Keefe (2001), “Crashing PERT Networks: A Simulation Approach paper presented on the 4th International Conference of the Academy of Business and Administrative Sciences Conference Quebec City, Canada.
4. Frederick S. H., and G. J. Lieberman (2001), *Introduction to Operations Research*, 7th Edition, Irwin McGraw-Hill, New York, USA.
5. Hendrickson, C., and T. Au (2000), *Project Management for Construction Fundamental Concepts for Owners, Engineers, Architects and Builders*, 2nd Edition, Prentice Hall Upper Saddle River, New Jersey, USA.
6. Andrews J. D., and T. R. Moss (2000), *Reliability and Risk Assessment*, 2nd Edition, Professional Engineering Publishing, London.
7. Mulholland, B., and J. Christian (1999), “Risk Assessment in Construction Schedules”, *Journal of Construction Engineering and Management*, Vol. 125(1).
8. Cooper, K. G. (1994), “The $2,000 hour: How Managers Influence Project Performance Through the Rework Cycle.” *Probabilistic Mechanics Journal*, XXV(1), 11–24.
9. Laufer, A., and G. A. Howell (1993), “Construction planning: Revising the paradigm.” *Probabilistic Mechanics Journal*, XXIV(3), 23–33.
10. Laufer, A., and G. Stukhart (1992), “Incentive Programs in Construction Projects: The Contingency Approach.” *Probabilistic Mechanics Journal*, XXII(2), 23–30.
11. Halligan, D. W. (1987), “Managing Unforeseen Site Conditions.” *Journal of Construction Engineering and Management*, ASCE, 113, 273–287.
12. Ang, A.H-S., and W.H. Tang (1975), *Probability Concepts in Engineering Planning and Design, Basic Principles*, Vol. I, Wiley, NY.

DESIGN CONSIDERATION AND SOCIO-CULTURAL AND ENVIRONMENTAL ASPECTS OF STABILIZED SOIL TECHNOLOGY

Dr. Tahar. Bellal
Associate Professor, Department of architecture, Setif University, Algeria.
Email: bellal56@yahoo.fr

ABSTRACT

This paper examines the level of technical achievement in design and the level of social acceptance of cement-stabilized building blocks. The purpose here is to show the possibilities offered by stabilized soil with cement as applied to various stages of design and construction work. The methods described are those normally used for simple buildings in their fundamental aspects producing a built environment that characterizes such technology. It is a common experience that the choice of any technology is not only affected by technical and economical features but also by many closely related factors of social, cultural and institutional nature. Accordingly the second part of the paper is to concentrate on these aspects with particular emphasis on the problems associated with attempting to introduce stabilized soil technology.

Keywords: Stabilized Soil, Design aspects, Construction, Socio-Cultural Factors.

INTRODUCTION

Earth building as an architectural technique has a very long history. Since towns were first built up, ten thousands years ago, men have used earth to build entire cities; palaces and temples; churches and mosques. The earliest surviving remains having been found in the Middle East. By the end of the pre Christian era, earth building has spread throughout all the world's ancient civilizations, from China through to North Africa and the eastern Mediterranean and including central and part of South America [1], this humble material has been used in every continent and has responded to the different climates [2]. In Algeria, the utilization of earth in house construction dates from centuries ago. Even today and despite the supremacy of modern building materials, many areas still make much use of it. However, despite all the good qualities earth offers in building construction, the building material has many weaknesses. In order to overcome the disadvantages of earth as a building material, attempts have been made to improve the empirical earth building techniques used in the past to make it eco-friendly, inexpensive, and that rely largely on labor rather than expensive and often environmentally-damaging outsourced materials [3]

The quality as a building material of nearly any inorganic soil can be improved remarkably with the addition of the correct stabilizer in a suitable amount. The aim of soil stabilization is to increase the soil's resistance to destructive weather conditions by cementing the particles of the soil together, leading to increased strength and cohesion, and reducing the movements (shrinkage and swelling) of the soil when its moisture content varies due to weather conditions and also by making the soil waterproof or at least less permeable to moisture. A great number of substances may be used for soil stabilization. Because of the many different kinds of soils and the many types of stabilizers, there is not one answer for all cases. It is up to the builder to make trial blocks with various amounts and kinds of stabilizers.

Portland cement greatly improves the compressive strength and imperviousness and may also reduce moisture movement, especially when used with sandy soils. As a rough guide, sandy soils need 5 to 10% cement for stabilization, silty soils 10 to 12.5% and clayey soils 12.5 to 15%.[4] Compaction when ramming or pressing blocks will greatly influence the result. The cement must be thoroughly mixed with dry soil. This can be rather difficult especially if the soil is clayey. As soon as water is added the cement starts reacting and the mix must therefore be used immediately (I to 2 hours). If the soil - cement hardens before moulding, it must be discarded. Soil-cement blocks should be cured for at least seven days under moist or damp conditions.
The purpose of this paper is to deal with the use of stabilized soil, to look at the ways in which it is used, its performance as a building material.

Definition of Stabilized Soil with Cement

A block of stabilized soil with cement is defined here as one formed from a loose mixture of soil, sand, cement and water (a damp mix), which is compacted to form a dense block before the cement hydrates. After hydration the stabilized block should demonstrate higher compressive strength, dimensional stability on wetting and improved durability compared to a block produced in the same manner but without the addition of cement. This definition includes a range from hand-tamped soil blocks containing only enough cement to enhance their dry strength a little to close-tolerance high-density concrete blocks, mechanically mass produced and suitable for multi-storey construction without a render. For the purpose of this paper stabilized soil with cement is defined as a permanent durable material which is produced from a natural or modified soil containing sufficient fines to provide cohesion on densification, sufficient to allow unsupported handling of the freshly molded block. Good soil-cement blocks may thus be stacked for curing. Quasi-static compaction is usually employed and block depth is typically restricted to 120mm. Using depths greater than this leads to excessive variation in density within the block as a result of high internal friction. Ideally block depth should be 100mm or less [5] the paper deals only with ordinary Portland cement. At present this is the most widely available and quality-consistent stabilizer.

APPROPRIATE DESIGN CONCEPT

The use of stabilized soil with cement in construction work may influence or modify the form of the building since the structural capacity of the material itself will determine the spaces, spans and volumes. Amos Rapoport wrote [6]: The availability and choice of materials and construction techniques in an architectural situation will greatly influence and modify the form of the building.
When building with stabilized soil, appropriate design and structural details should be applied to counter the material's weaknesses; that is to say the low compressive strength. Hence this section of the paper deals with design potentials of stabilized soil buildings. These will include among others, spatial requirements, building volumes and height, etc…

Space's Potential

As stabilized soil is of lower compressive strength, the compressive forces should be optimally exploited through appropriate structural elements which in turn determine the spans, and volumes of the buildings. The main structural elements to be considered are arches, vaults and domes in any design concept of space. One should consider the structural capacity of stabilized soil material is the major determinant of spans; however the length of the structural element [i.e. vault] can be of any desired dimension. As an illustration vault spans were standardized to 384 cm in the project of Maadher village, Algeria by Elminiawy brothers' disciples of the great and late Egyptian architect Hassan Fathy. The vaults length can cover as many as two rooms [See figs1-2]. When the programme needs call for wider spans as in the project of Nianing in Senegal, arched opening were made in the bearing wall to extend the space. As many as three vaulted spaces are combined into

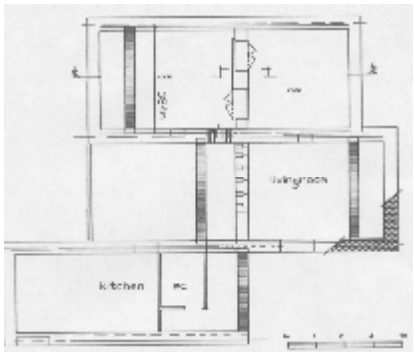

Fig 1: Plan of a Dwelling. The Vault Span Covers the width of the Room Thus Creating Usable Spaces

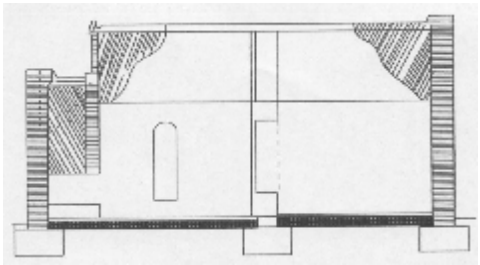

Fig 2: Section Showing the Vault Length Covering Two Rooms

a single room through arching. The vault spans were standarised to 301 cm. By varying the vault's length, connecting parallel spaces with arched openings, it become possible to create spatial hierarchy.

Volumes

As mentioned earlier, stabilized soil is of lower compressive strength. Under these conditions, the three dimensional form of structure should be considered in construction since neither the one nor the two dimensional form of structure will work for creating usable spaces [7], this implies the use of some form of arches and vaults or domes which can be to characterize stabilized soil buildings. We should mention the advantage of such structural elements [vaults and domes] which tend to be very suitable for resisting the sun and reducing the heat and glare of their surface mainly in hot dry climates. In this context Norton puts it as follows [8]: The air temperature under the dome which is in the shade and the temperature difference between the shaded area and the top of the dome is at least 5°C.

Building Height Considerations

Although earthen buildings may be up to six stories in height [examples from the Yemen] most stabilized soil buildings are of single story or two stories in height as are the entire experimental projects using this material in Algeria. The main reason for the limitation of buildings height is due to the low compressive strength of the material [9]. This characteristic [low rise] should be regarded as
a main disadvantage of the building material [buildings tend to occupy more space]. However, one should mention the advantages of such a concept and these include among others: Individuals can build their own houses, buildings can be extended horizontally, may be suitable for areas with traditions of low rise buildings.

Architectural Details

It is essential to understand the characteristics and limitations of stabilized soil, if there is a need for a durable and comfortable building particularly with respect to architectural details. There is no universal and standard solution for the architectural details; local climatic conditions, specific earth techniques require rigorous attention to details. The designer must adapt appropriate solutions to areas where defects can occur: wall bases, doors and windows.

Earthquake Considerations

In region subject to very intense seismic disturbances [i.e. parts Algeria are seismic regions] buildings made with stabilized are capable of withstanding certain shocks and stresses caused by seismic disturbances, provide that care is taken in the sitting, structure, building configuration, reinforcing and opening components [10].

ENVIRONMENTAL ASPECTS

The thermal characteristics as well as the life span of stabilized soil buildings are described in this section. These are the most important features together with the technical characteristics of any building material.

Thermal Characteristics

Generally speaking, traditional earth buildings tend to require less heating and cooling, for the earth walls provide good thermal capacity, Dethier.J wrote [11]: Earth walls ensure a substantial reduction in heat loss and a general feeling of what is called thermal comfort.
The above quotation mainly applies to hot dry climates. Earth material has a time lag that ranges from 8 to 12 hours to delay the inside heat emission to the time of lower temperature that is after midnight and pre dawn hours when the extra heat may be welcome in the otherwise chilly conditions. As far as stabilized is concerned tests have revealed that the material presents good thermal characteristics. The following example gives a clear idea of the thermal characteristics of stabilized soil.

Tamanrasset Experimental Project Test

Following the construction of an experimental prototype house in Tamanrasset, Algeria. tests have revealed that stabilized soil with cement has a high thermal capacity and a good insulating value. The tests have been carried out by the CNERIB [Centre National des Etudes et Recherches Intégrées du Bâtiments]. The measurements have revealed that the type of stabilized soil used in the construction of the prototype has a high thermal capacity and a good insulating value [12] [See figs 3-4]. The Inter- Ministerial instruction n° 8 feb/85 noted [13]: The stabilized soil material presents good thermal features that are twice better than those of conventional materials such as cement concrete [time lag twice as good as that of cement concrete]. It is clear that stabilized soil material tends to suit hot dry climate. Since the whole part of southern Algeria is characterized by a hot dry climate, it would be wise to stress the use of such material in housing in this area.

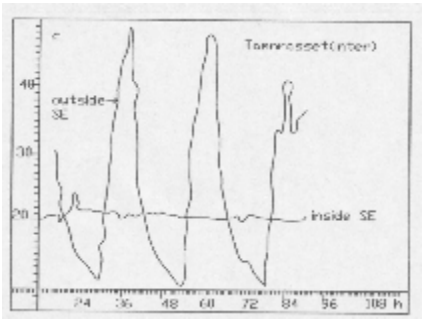

Fig 3: The Diagram Shows Good Thermal Performance of Stabilized Soil [source CNERIB]

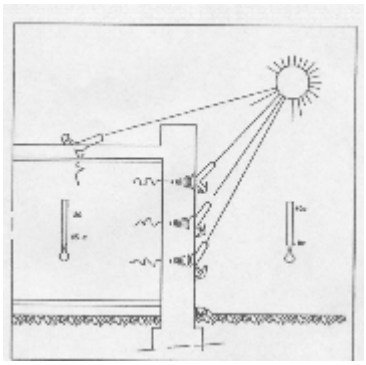

Fig 4: Stabilized Soil Buildings Tend to Suit Hot Dry Climate

Durability

One of the most important problems of earth buildings is the lack of durability, resulting in permanent maintenance. Life span can be increased and maintenance reduced to a minimum provided that care is taken in design and construction work. The durability of stabilized soil block is no great if compared to concrete, but performance of already implemented projects and experimental building are sufficiently good to lead to the expectation of longer periods of useful services. As an illustration, an experimental building constructed of stabilized soil at the UK British Research Establishment in Garston in the middle of last century prove nearly eighty years after its erection the good qualities and performance of the material [See fig 5].
The finding suggested that stabilized soil could find many uses in reasonable sheltered surroundings provided that care is taken to ensure the exclusion of excessive quantities of water. The bricks are unlikely to be durable in areas which receive large amount of driving rain [8]. In brief, the life span of stabilized soil buildings can be increased in comparison to earth building. The maintenance could be reduced to a minimum by rendering the walls protecting the wall bases and providing good drainage. This can be achieved if care is taken in design and construction to prevent the devastating effects of erosion.

Fig 5: Experimental Building Constructed of Stabilized Soil at Garston [UK].

SOCIO-CULTURAL ASPECTS

The preceding parts of this paper have dealt with the many technical questions associated with stabilized soil technology. It is a common experience world-wide; that the choice of any technology is not only affected by technical and economical features but also by many closely related factors of social, cultural, cultural and institutional nature. Accordingly the purpose here

is to concentrate on these aspects with particular emphasis on the problems associated with attempting to introduce stabilized soil in housing.

Factors Affecting Stabilized Soil Technology

The factors that should be considered are of socio-cultural and institutional nature. It is important to accept that people's values and opinions about the building material will exert a powerful influence over the choice of such technology. With regards to the institutional aspects, the standards, by-laws and frequently the political decisions may either dictate or prohibit construction work with any building material. All these contributory factors have to be understood and taken account of, if relatively untried materials such as stabilized-earth are to be used.

Socio-cultural factors

Earth building material has been widely used in housing throughout Algeria. Yet nowadays there are questions raised about its use in both urban and rural areas. This is mainly due to the changing mode of life and higher aspirations induced among people, thus leading to the use of more –permanent and durable- building materials. These are considered sometimes as symbols of modern life style [14]**.** Over the years earth building material has acquired the notion of being of low status, less durable and generally associated with housing the poor in the community.

Approach to the problem

In an attempt to understand the socio-cultural implications of the use of stabilized soil in housing visits were made to two projects where stabilized soil has been used as a main building material. The aim was to get opinions and prejudices of people about the building material and how it was regarded socially and culturally

Selection of case studies

The projects selected for the study were those of the experimental agro-pastoral village of Maadher near M'sila and Feliache, Biskra in Algeria [See figs 6-7]. Both projects have been constructed with stabilized soil. In the case of Feliache, where the project was abandoned in its early stages; the interviews were carried out with people living close to the site.

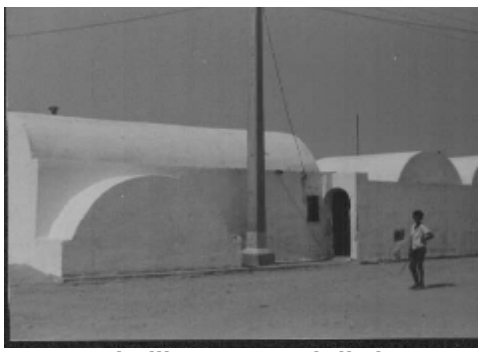

Fig 6: Maadher Agro Pastoral Village Near M'Sila is a Successful Project both Architecturally and Technically

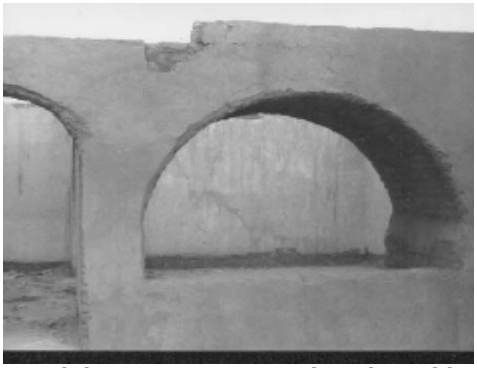

Fig 7: Feliache Project Near Biskra: It Has Been Abandoned in its Early Stages Because of Technical Failures.

Interview techniques

The interviews were carried out in an informal way in both places. We talked in two occasions to people in Maadher village and only once in the other case. With regards to the first mentioned project, the first talk took place in the village square, where more than fifteen people were present, the second one was held over a meal the next day. In the case of Feliache-Biskra, the interviewed people were previously shanty town dwellers living in the suburb of the capital Algiers and were evicted and transported to live in a site close to the project.

Questions

The questions put forward in the interviews were all related to housing in general and stabilized soil building material in particular. They range from the status of the building material, its performance, to how it is perceived in comparison to other building materials such as concrete. As follows are the major points drawn from the interviews.

Material status

From the talks we had with people, it soon became clear that stabilized soil was regarded as being of low status and was generally associated with poor housing. To demonstrate this fact, the following question was put forward in both sites [Do you want to live in earth houses?]. The answer was no in most of the cases. Almost, unanimously the reply was: We have high expectation in this life, and we do not want to live our whole life in earth houses.
To understand this judgment, we should mention that all the people living in Maadher were previously landless peasants and the implementation of the village was entirely financed by the government. Over the years [between the implementation of the project and the visit] people increased their expectations, consequently wanted houses built with modern materials. They generated increased agricultural incomes; they have moved several ranks on the socio-economic ladder and looked for better housing.
Another factor which affects the use of stabilized soil is the importance attached to social status and symbols. Most of the interviewed people prefer hollow concrete blocks for walling and concrete slab for roofing. They regard this building material as being of high status. In this regard Spence quotes [9]: The poorer the society is, the greater the symbolic significance of materials and techniques appears to be, perhaps because of the lack of alternative means of displaying status and positions.
On the whole, there is a clear indication that the effects of socio-cultural factors on the acceptability of improved earth are very strong. Earth in general is considered as a building material for the poor [10]. And it is possible to affirm that the connection [technical performance/low income population] has made even worse the acceptability of the building material earth.

Stabilized soil/Concrete

People are more familiar with concrete than any other building material. They make much use of it. In fact this use can be seen in operations all across the country in both rural and urban areas. Compared to concrete, stabilized soil with cement is relatively a new experimental material and regarded with suspicion. People feel imprudent to take a risk on an untested building material. In his respect Kamel Noui Mehidi, an Algerian architect who spent some months in the rural areas of Algeria as part of the government's plan to build 1000 villages in the seventies of last century wrote [15]: Compared to the stone and Diss [mud and straw] buildings with which they had unfortunate experiences all their lives, the solidity of concrete gives them the feeling of security.

Institutional factors

Stabilized construction is greatly influenced by the building laws, standards and regulations enforced by the institutional framework. The building regulations in most of the cases bore no relation to local building material [traditional] in general and earth building material in particular and this encourages the rejection of even improved earth material, in this context Bouadi. S wrote [16]: Generally speaking and as far as housing and urbanism are concerned, the decision makers prefer to adopt regulations and techniques generated and tested in the west.

Media factor

Since independence, the media, which is partially government controlled, has become an increasingly important channel for communication. The country has seen the growth of newspapers, magazines and most of all a rapid spread of radio and television. What is equally important, if no more important, than this communication boom is the effect of the media on society. For instance, and as far as the construction sector is concerned, over the years TV programmes, newspapers, etc. show and highlight pictures and images of modern building materials such a concrete, fibre glass, steel, and aluminum. There is no doubt that the media have a great influence on people's attitude concerning the issue of building materials [17].

CONCLUSION

Experimental projects all over the world including Algeria have proved the potential of stabilized soil with cement as an important structural building material which appears most promising when used in the making of durable building with a satisfactory thermal comfort. The poor reputation of the material [in this case Algeria] is less often the fault of the material itself, than the way it is used. The use of inappropriate technology of production, the poor selection of the raw material and many other factors have led to beliefs which are not reflected in the actual performance of the material.

Accordingly, people in general and the users in particular were reluctant to accept it as a credible building material. It is vital that tests should be performed in order to determine the suitability of the raw material, the best stabilizers to use, the likely quantities of stabilizers and the appropriate means of production technology, before stabilized soil is specified for construction. Given these considerations, the building material can perform as well as other conventional materials such as concrete and burnt clay brick. The limitations of the building material mean that its use is somewhat restricted, and cannot be applied in all conditions. In regions subject to seismic disturbances buildings with stabilized soil cannot withstand the stress unless reinforced with concrete and steel, consequently the construction cost will increase. Buildings also with stabilized soil are only one to two stories in height. Despite these restrictions however, the material can be successfully in many parts of the country here low rise is the traditional form of housing and where seismic disturbances do not present a problem.

The negative attitude toward the use of stabilized soil in housing may affect the promotion of the building material. The belief that earth materials are not credible and of lower quality are due mainly to the social and physical changes that took place in the Algerian society since independence and to both the impact of technical deficiencies that occurred in the experimental

projects, and the negative role played by the professionals towards the promotion of traditional building materials.

These problems could however be overcome if there is a concerted effort made by the authorities, housing institutions, and professionals to promote the material in housing. A complete change in the social attitude towards earth is very difficult to achieve. Happily, the present position adopted by the authorities towards the building material is encouraging, leading to the belief that once the political and economic actions are taken, social attitude could begin to change. The evaluation of stabilized soil as a building material can serve to demonstrate the inter-dependence between technical, economic, and institutional factors; all are related within a broad socio-cultural framework. It must be acknowledged however that building materials are only part of the whole problems of housing. Despite the advantages it offers, this material cannot however be realistically regarded as providing a miraculous solution to the housing problem in Algeria.

REFERENCES

1. Keefe, L [2005], “Earth building- Methods and materials, repair and conservation”, Technology & Industrial Art, Taylor & Francis, London, p, 7.
2. Givoni, B. [1998], “Climate Consideration in Building and Urban Design”, John Wiley& sons, p, 207.
3. Hunter, K. & Kiffmeyer, D. [2004], “Earth building- The tools, Tricks, and techniques”, New society Publishers, p, 3.
4."Earth as building material", http://in_fao.org/docrep/S1250E/1250E06.htm#content, (1998), accessed March. 25, 2005.
5. Gooding, DE & Thomas, TH. [1995], “The Potential of Cement-Stabilized Building Blocks as an Urban Building Material in Developing Countries**”,** in Working paper n° 44, Development Technology Unit Publications pp, 1-22. [7].
6. Rapoport, A. [1969], “House form and culture”, Prentice hall Inc, Englewood Cliffs, New Jersey, p, 140.
7. Rapoport, A. [1969], “House form and culture”, Prentice hall Inc, Englewood Cliffs, New Jersey, 122.
8. Norton, J. [1984], “Appropriate technology, training responding to the need of the poor”, in Appropriate Technology II, N° 1, London, p, 14.
9. Varghese, PC. [2005], “Building materials”, Prentice Hall of India, New Delhi, p 3.
10. Odul, P [1984], “The technical issue”, in proceedings: International Colloquium on earth construction technologies appropriate to developing countries, Brussels, p, 10.
11. Dethier, J. [1994],”Down to earth”, Third edition, Thames and Hudson, London, p, 15.
12. Bellal, T. [1987], “The potential of stabilized soil for housing in Algeria”, Unpublished Master thesis, University of Newcastle/Tyne, UK, p, 84-87.
13. MICL 2/85 [1985], Construire review n°3, Algiers, p 47.
14. Tipple, G. [2000], “Extending themselves“, Liverpool University Press, p, 138.
15. Noui Mehidi, K. [1986], in African Environment, Volume II, N° 1-2, Dakar.
16. Bouadi, S. [1985], In Earth construction technologies: Appropriate to developing countries PGC-HS/KU, Leuven, p, 63.
17. Gold, JR. [1975], “Communicating images of the environment, CURDS, Birmingham, paper n° 29, p, 6.